Integrated and Coordinated Relief Logistics Planning Under Uncertainty for Relief Logistics Operations

by

Afshin Kamyabniya

A THESIS SUBMITTED IN PARTIAL FULFILLMENT OF
THE REQUIREMENTS FOR THE DEGREE OF

DOCTOR OF PHILOSOPHY

in

Telfer School of Management

(Management)

THE UNIVERSITY OF OTTAWA
(Ottawa)

September 2022

Abstract

In this thesis, we explore three critical emergency logistics problems faced by healthcare and humanitarian relief service providers for short-term post-disaster management.

In the first manuscript, we investigate various integration mechanisms (fully integrated horizontal-vertical, horizontal, and vertical resource sharing mechanisms) following a natural disaster for a multi-type whole blood-derived platelets, multi-patient logistics network. The goal is to reduce the amount of shortage and wastage of multi-blood-group of platelets in the response phase of relief logistics operations. To solve the logistics model for a large scale problem, we develop a hybrid exact solution approach involving an augmented epsilon-constraint and Lagrangian relaxation algorithms and demonstrate the model's applicability for a case study of an earthquake. Due to uncertainty in the number of injuries needing multi-type blood-derived platelets, we apply a robust optimization version of the proposed model which captures the expected performance of the system. The results show that the performance of the platelets logistics network under coordinated and integrated mechanisms better control the level of shortage and wastage compared with that of a non-integrated network.

In the second manuscript, we propose a two-stage casualty evacuation model that involves routing of patients with different injury levels during wildfires. The first stage deals with field hospital selection and the second stage determines the number of patients that can be transferred to the selected hospitals or shelters via different routes of the evacuation network. The goal of this model is to reduce the evacuation response time, which ultimately increase the number of evacuated people from evacuation assembly points under limited time windows. To solve the model for large-scale problems, we develop a two-step meta-heuristic algorithm. To consider multiple sources of uncertainty, a flexible robust approach considering the worst-case and expected performance of the system simultaneously is applied to handle any realization of the uncertain parameters. The results show that the fully coordinated evacuation model in which the vehicles can freely pick up and off-board the patients at different locations and are allowed to start their next operations without being forced to return to the departure point (evacuation assembly points) outperforms the non-coordinated and non-integrated evacuation models in terms of number of evacuated patients.

In the third manuscript, we propose an integrated transportation and hospital capacity model to optimize the assignment of relevant medical resources to multi-level-injury patients in the time of a Mass Casualty Incident (MCI). We develop a finite-horizon Markov Decision Process (MDP) to

efficiently allocate resources and hospital capacities to injured people in a dynamic fashion under limited time horizon. We solve this model using the linear programming approach to Approximate Dynamic Programming (ADP), and by developing a two-phase heuristics based on column generation algorithm. The results show better policies can be derived for allocating limited resources (i.e., vehicles) and hospital capacities to the injured people compared with the benchmark.

Each paper makes a worthwhile contribution to the humanitarian relief operations literature and can help relief and healthcare providers optimize resource and service logistics by applying the proposed integration and coordination mechanisms.

Table of Contents

List of Tables

List of Figures

Acknowledgements

This thesis would not have been what it is without the encouragement and support from many individuals. First and foremost I am extremely grateful to my supervisors, Prof. Jonathan Patrick and Prof. Antione Sauré, for their invaluable advice, continuous support, and patience during my PhD study. Their immense knowledge and plentiful experience have encouraged me all the time in my academic research and daily life.

I would also like to thank Dr. Noureddine Benichou, my supervisor at the National Reseach Council of Canada, and his great research team for their valuable technical support on my nearly two-year internship with them. Dr. Noureddine is a wonderful researcher and leader that taught me many lessons for my life. Furthermore, thanks to the Government of Ontario for awarding me the Ontario Trillium Scholarship and to the National Research Council of Canada for the NRC small-Teams Initiative, and Mitacs Globalink Organization for their financial support during my studies.

I have also been fortunate enough to have a great team of co-authors and research advisors for my PhD research. Besides Jonathan Patrick and Antoine Sauré, I had the privilege to work with Dr. Kai Huang from McMaster University and Dr. Sibel Salman from Koc University in two papers.

Finally, I would like to express my gratitude to my love and soulmate, Ghazaleh, and to my mother for their unconditional support and love during my PhD life. Without their tremendous understanding and encouragement in the past few years, it would have been impossible for me to complete my studies.

It is their kind help and support that have made my life in the Canada a wonderful time.

To my family

Co-Authorship Statement

Chapter 2 corresponds to a published article co-authored with Zohreh Noormohammadzadeh, Professors Jonathan Patrick, and Antoine Sauré. Chapter 3 corresponds to a manuscript co-authored with Professors Jonathan Patrick, Antoine Sauré, Professor Kai Huang, and Professor Noureddine Benichou. Finally, Chapter 4 corresponds to a manuscript co-authored with Professors Jonathan Patrick and Antoine Sauré.

The identification and design of the research problems in this thesis were carried out jointly with the aforementioned co-authors. The research, analysis and manuscript preparation were performed by the candidate under close supervision from Professors Jonathan Patrick and Antoine Sauré.

1 Introduction

We begin by discussing the motivation for investigating three managerial and practical Disaster Operations Management (DOM) problems; blood logistics, wildfire evacuation and integrated transportation and capacity planning decisions. Then, in Section 1.2, we give an overview of the thesis. Finally, in Section 1.3, we provide a detailed outline of the thesis.

1.1 Motivation

In the past decade, the frequent occurrence of natural disasters (earthquakes, floods, hurricanes, etc.) has caused numerous mass casualty incidents (MCIs) with severe damages to societies [1][10]. In response to the need for effective logistical plans for MCIs resulting from disasters, different stages have been identified in the process of returning to normalcy post-disaster. The stages include collecting, distributing, and producing medical resources, shelter location, evacuation of the trapped population, and the triaging and transportation of the injured.
Figure 1.1 provides a framework for the main humanitarian logistics activities and their associated facilities and flows [2]. As shown, evacuation deals with transportation of casualties, and distribution of relief resources (i.e., blood products). Figure 1.1 indicates the relationships and flows between facilities and disaster or potential disaster sites for pre-disaster and post-disaster operations.

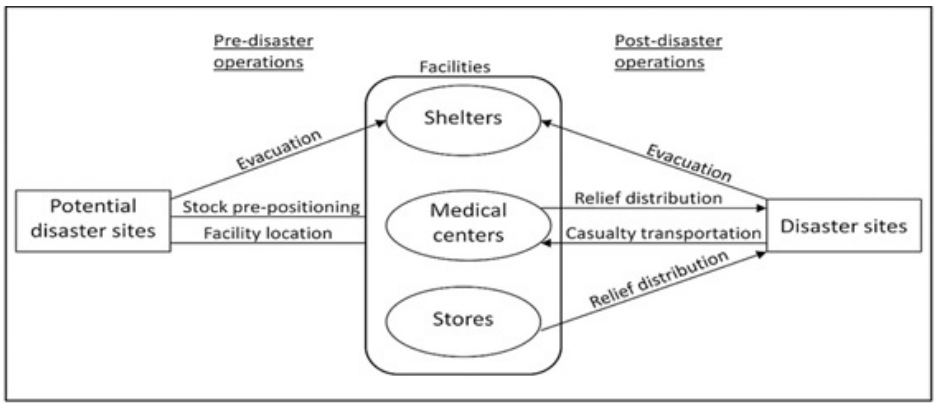

Figure 1.1: Framework for disaster operations and associated facilities and flows

[1] e.g., Indonesia tsunami in 2004, Wenchuan earthquake in 2008, freezing rain in southern China in 2008, Haiti earthquake in 2010, devastating earthquake in Japan in 2011, typhoon Haiyan in 2013, flood disaster in India in 2013, Nepal earthquake in 2015, catastrophic epidemics like the 2014 Ebola pandemic in West Africa

In Humanitarian Relief Operations (HRO), one of the most important tasks is to distribute relief resources to casualties as quickly as possible. Blood-derived platelets are one of the most scarce relief resources with a very short shelf life. Platelets are widely used in blood transfusion centers as a lifesaving treatment [3]. The necessity of platelets is crucial in the aftermath of a disaster to balance the platelets supply through the network and control the wastage and shortage of such products efficiently. The platelet supply chain includes the process of collecting both whole blood and platelets from donors, then testing, producing, and finally delivering platelets to hospitals and medical shelters. In HROs, the main challenges in platelet logistics are the distinction of blood groups (i.e., ABO/Rh(D)-compatibility [2]), the short shelf life of platelets (typically five days), the uncertainty in supply and demand, and finally, the lack of integration and coordination among relief facilities. Consequently, applying resource-sharing integration mechanisms to increase coordination among facilities is highly critical to help mitigate the impact of any shortage and wastage in blood products ([1], [7], [4]).

In addition to efficiently distributing resources such as blood products, the evacuation of injured people from the affected regions is an important part of relief operations. Evacuating injured people can be difficult when the time for transporting the injured people from the affected areas and routes leading to them and medical centers are very limited, particularly in disasters such as wildfires. Wildfires are difficult to control as they propagate rapidly and erratically, threatening human lives and livestock [6]. The economic losses, the number of fatalities, and the number of displaced people resulting from wildfires highlight the need to implement emergency preparedness and response approaches to minimize deaths. Wildfire response is composed of a series of interrelated activities. It involves relief operations ranging from search and rescue to safe transfer of the affected population to shelters. An important problem in wildfire response management is to decide when and where to assign resources and how to evacuate trapped people from burning regions to shelters. It is vital that relief providers efficiently manage their rescue vehicles to save as many of the injured in the minimum possible response time under limited time windows.

Finally, disasters may result in massive MCIs, causing many casualties with different injury seriousness levels. In MCIs, two types of HROs are highlighted: casualty flow and resource allocation planning [8]. Typically, these two operations are not well integrated. One of the unfortunate consequences is that injured patients may arrive to receive medical service at a given location only to find that the required resources are not available. An integrated service-resource-patient-oriented network (i.e., assigning vehicles to patients for receiving treatment service or care at hospitals) for MCIs can prevent shortages of resources and medical services and thus reduce any service delay for injured patients overtime. The integration of casualty transportation network (allocation of

[2] A blood group system that classifies blood types according to the different types of antigens in the red blood cells and antibodies in the plasma.

paramedic vehicles) and patient assignment to the available care capacity of hospitals in a dynamic fashion ensures appropriate utilization of paramedic vehicles and hospital capacities at different decision epochs of a finite time planning horizon.

1.2 Overview of the Thesis

The rest of this thesis is organized in a series of chapters. At the beginning of each chapter, we motivate the problem being addressed and examine the related literature. We then provide the mathematical model and the solution approach followed by our analysis and results. We conclude each chapter with a summary of our main findings. Chapter 5, the final chapter, summarizes the thesis contributions and provides a brief discussion of future research directions.

1.2.1 A Robust Integrated Logistics Model for Platelets in Disaster Relief Operations

In Chapter 2, we study a three-level platelet supply chain consisting of Regional Blood Units (BRU), hospitals, and Special-Needs Medical Shelters (SMS) in disaster zones. The proposed model can be thought of as a multi-injury-level casualty transportation problem with resource sharing among relief facilities. Traditionally, the platelets supply chain has considered separately vertical and horizontal resource sharing for blood logistics. During a disaster, having only vertical or horizontal integration may increase the number of fatalities, the number of wasted resources, the response time of relief operations, and the response cost [5].
This model not only allocates multi-type platelets to patients according to ABO/Rh(d)-compatible blood substitutions but also accounts for the impact of the age of the platelets on the suitability for different types of injuries. To efficiently solve the model and generate a Pareto front for large-scale instances of the problem, we employ Lagrangian relaxation and the augmented ε-constraint method. Finally, to evaluate the performance of the proposed model and solution approach and derive practical insights, we apply it to a case study based on data about a possible earthquake in Tehran, Iran, and conduct some sensitivity analysis. We show that undertaking the matching, substitution, and integration procedures jointly help decision-makers better serve patients in the network.

1.2.2 A Robust Evacuation Model During Wildfires

In chapter 3, we study the effect of different transportation mechanisms on the evacuation of injured people during wildfires. A common transportation strategy for emergency evacuation of casualties during wildfires is that paramedic vehicles managed by hospitals and disaster response relief center must return to the same location they departed from at the end of each trip (i.e.,

transferring patients from one location by a paramedic ambulance to another location is considered a trip). Such a transportation strategy may not be efficient for relief operations under minimal time windows (maximum available time to evacuate people from the evacuation assembly points) with many casualties and with various urgency levels [9]. In this research, instead of assuming that the vehicles must return back to the origin of departure point, we focus on the possibility of multiple trips for vehicles in which a vehicle can on-board injuries from multiple Evacuation Assembly Sites (EAS)s (a split pick-up transportation strategy) and transfer them to multiple medical centers (split delivery transportation strategy).

To address this problem, we develop a two-stage stochastic mixed-integer programming model involving the routing of casualties via less risky routes (routes that the probability of fire reaching them and making them inaccessible is higher than other available routes) and matching them to SMSs or hospitals. To deal with the uncertainty in the model parameters, such as the size of the evacuation time windows of EASs, population in need and accessible routes, we apply a flexible robust approach which considers both worst-case and expected performance of the model under various realizations of the uncertain parameters.

Finally, To solve the proposed model for a case study we develop a two-step meta-heuristic algorithm under different experimental data sets.

1.2.3 A Dynamic Casualty Transportation and Hospital Capacity Planning Model Under Uncertainty

In Chapter 4, we study patient transportation and casualty planning decisions in MCIs. The focus is on effectively transporting patients to different hospitals to receive timely care. Given the sequential of the problem and the existence of multi-group hospitals with different care capabilities, and capacities and significant uncertainty (number of arrivals at the MCI site, number of patients staying at hospitals and number of new demands at each hospital), we develop a MDP model to maximize the expected number of survivals in a finite time-horizon.

To solve the model under various problem sizes, we apply an heuristic approach to efficiently find the solution in a timely fashion.

1.3 Bibliography

[1] Burcu Balcik, Benita M Beamon, Caroline C Krejci, Kyle M Muramatsu, and Magaly Ramirez. Coordination in humanitarian relief chains: Practices, challenges and opportunities. *International Journal of production economics*, 126(1):22–34, 2010.

[2] Aakil M Caunhye, Xiaofeng Nie, and Shaligram Pokharel. Optimization models in emergency logistics: A literature review. *Socio-economic planning sciences*, 46(1):4–13, 2012.

[3] Hamidreza Ensafian and Saeed Yaghoubi. Robust optimization model for integrated procurement, production and distribution in platelet supply chain. *Transportation Research Part E: Logistics and Transportation Review*, 103:32–55, 2017.

[4] Afshin Kamyabniya, Mohammad Mehdi Lotfi, Hassan Hosseini Nasab, and Saeed Yaghoubi. Multiple-organizational coordination planning for humanitarian relief operations. *Journal of Industrial and Systems Engineering*, 11(Special issue: 14th International Industrial Engineering Conference):29–42, 2018.

[5] Anna Nagurney, Amir H Masoumi, and Min Yu. Supply chain network operations management of a blood banking system with cost and risk minimization. *Computational management science*, 9(2):205–231, 2012.

[6] Shahrooz Shahparvari and Babak Abbasi. Robust stochastic vehicle routing and scheduling for bushfire emergency evacuation: An australian case study. *Transportation Research Part A: Policy and Practice*, 104:32–49, 2017.

[7] Jiuh-Biing Sheu and Cheng Pan. Relief supply collaboration for emergency logistics responses to large-scale disasters. *Transportmetrica A: transport science*, 11(3):210–242, 2015.

[8] Inkyung Sung and Taesik Lee. Optimal allocation of emergency medical resources in a mass casualty incident: Patient prioritization by column generation. *European Journal of Operational Research*, 252(2):623–634, 2016.

[9] Haijun Wang, Lijing Du, and Shihua Ma. Multi-objective open location-routing model with split delivery for optimized relief distribution in post-earthquake. *Transportation Research Part E: Logistics and Transportation Review*, 69:160–179, 2014.

[10] Lei Zhou, Xianhua Wu, Zeshui Xu, and Hamido Fujita. Emergency decision making for natural disasters: An overview. *International journal of disaster risk reduction*, 27:567–576, 2018.

2 A Robust Integrated Logistics Model for Age-Based Multi-Group Platelets in Disaster Relief Operations

In this chapter, we consider the problem of evaluating resource-sharing strategies through various forms of integration mechanisms in a multi-patient type and multi-group blood-derived platelets logistics setting. Using robust and stochastic optimization, we show that various integration mechanisms alleviate the shortage and wastage of very short shelf-life products.

2.1 Introduction and Motivation

In disaster relief operations (Disaster Relief Operations (DRO)s), one of the most important tasks of relief facilities is to distribute relief resources, such as blood platelets, to casualties as quickly as possible. Blood-derived platelets are one of the most scarce relief resources with a very short shelf life. Platelets are widely used in blood transfusion centers as a lifesaving treatment [14]. The platelet supply chain includes the process of collecting both whole blood and platelets from donors and testing, producing, and delivering platelets to hospitals and medical shelters. Blood regional units (BRUs) are responsible for managing the operational decisions surrounding blood collection, extraction [1], testing, and delivery of blood products (i.e., plasma, red blood cells, platelets) to hospitals and shelters. Hospitals and special-needs medical shelters (SMSs) serve patients needing multiple types of blood products. In disaster management, the main challenges in platelet logistics are the distinction of blood groups (i.e., ABO/Rh(D)-compatibility), the short shelf life of platelets (typically 5 days), and the uncertainty in demand (the number of injuries).
The motivation for this study is to optimize the use of platelet supply through the integration of platelet logistics with casualty response operations. Through this chapter, we seek to determine optimal platelet-sharing decisions and ABO-Rh(D) substitutions while taking into account the age-differentiated demand from casualties with different levels of injury seriousness.
One of the most significant considerations for platelet logistics is the substitution of blood groups as well as the freshness of platelets in order to match them to casualties with different levels of

[1] Process of separating the whole donated blood into transfusable components: red cells, platelets, and plasma.

injury seriousness. For example, fresh platelets less than 1-day old are superior to older platelets for therapeutic use, especially in the case of patients whose immune systems have been weakened. For platelet transfusion, ABO-incompatible platelets can sometimes cause hemolysis and thus increase the chances of death. To match the multi-age platelets with patients with different levels of injury seriousness, different triage methods are required. Triage helps decide the order of treatment for a large number of casualties. Two of the most widely adopted triage methods are the START (Simple Triage And Rapid Treatment) and SALT (Sort-Assess-Lifesaving Interventions -Treatment/Transport) methods [9]. Both methods classify victims into four broad categories (Minor, Delayed, Immediate, and Deceased) that indicate how quickly a victim should receive care.

In the event of a disaster, there are a number of strategies available to meet the demand for platelets including resource sharing, triaging, ABO/Rh(D)-compatible blood substitutions. These are implemented in an effort to provide faster medical services to the injured and to reduce the shortage of platelets and the number of unserved people.

According to the SALT triage method, triage at the scene or at medical shelters, and off-loading release the burden of serving all types of patients at hospitals so that only type 1 (i.e., high severity or immediate) patients are transported to hospitals, while type 2 and type 3 patients (moderate and mild, respectively) are served in special-needs shelters. Moreover, ABO/Rh(D)-compatible blood substitutions are allowed in cases of blood shortage during emergencies [37]. Thus, blood products of a specific blood group can not only satisfy its own demand but also be used as a substitute for other compatible groups. For example, as shown in Table 2.1, the need for blood group $AB+$ can be fulfilled by all of the other seven blood groups while the first choice is the same blood group (AB+) [59, 41].

Multiple facilities are typically involved in a disaster relief network making resource-sharing coordination highly critical in mitigating the impact of any shortage in resources [3, 61, 34]. Balcik et al. [3] described the term "coordination" as the relationships and interactions among the different actors operating within the disaster relief environment. Vertical integration refers to the extent to which an organization coordinates with the upstream and downstream facilities (e.g., blood regional units and hospitals, respectively). Horizontal integration, on the other hand, refers to the coordination of an organization with others at the same level (e.g., two hospitals) [58]. In this context, integration means that each relief organization has the responsibility to either provide relief vehicles and platelets or distribute platelets to demand zones. Although there have been several attempts to design blood logistics networks considering different types of complexity and challenges [3], integrating blood relief logistics networks while considering the existence of multiple relief entities, the perishability of blood products, and the different injury seriousness levels of casualties has largely been ignored. Therefore, this chapter's principal purpose is to contribute to the literature

Table 2.1: ABO/Rh(D) compatibility for multi-group platelets

Recipient	Priority	Donor	Recipient	Priority	Donor	Recipient	Priority	Donor	Recipient	Priority	Donor
	1st choice	O+		1st choice	O-		1st choice	B+		1st choice	B-
	2nd	O-		2nd	A-		2nd	B-		2nd	AB-
O+	3rd	A+	O-	3rd	B-	B+	3rd	AB+	B-	3rd	A-
	4th	A-		4th	AB-		4th	AB-		4th	O-
	5th	B+		5th	O+		5th	A+		5th	B+
	6th	B-		6th	A+		6th	A-		6th	AB+
	7th	AB+		7th	B+		7th	O+		7th	A+
	8th	AB-		8th	AB+		8th	O-		8th	O+
	1st choice	A+		1st choice	A-		1st choice	AB+		1st choice	AB-
	2nd	A-		2nd	AB-		2nd	AB-		2nd	B-
A+	3rd	AB+	A-	3rd	B-	AB+	3rd	B+	AB-	3rd	A-
	4th	AB-		4th	O-		4th	B-		4th	O-
	5th	B+		5th	A+		5th	A+		5th	AB+
	6th	B-		6th	AB+		6th	A-		6th	B+
	7th	O+		7th	B+		7th	O+		7th	A+
	8th	O-		8th	O+		8th	O-		8th	O+

- For example for a patient with blood group O (Rh+), the most preferred choice (1st choice) for substitution is the same blood group O+ with Rh+, and the next option would be O (Rh-), A (Rh-), B (Rh+), B (Rh-), AB (Rh+), AB (Rh-), respectively.
- Rh+ patients (recipients) may receive Rh+ or Rh- platelets.
- Rh- patients (recipients) should receive Rh- platelets. However, if there is a shortage of Rh- platelets, Rh+ platelets may be given (Lifeservebloodcenter.org)

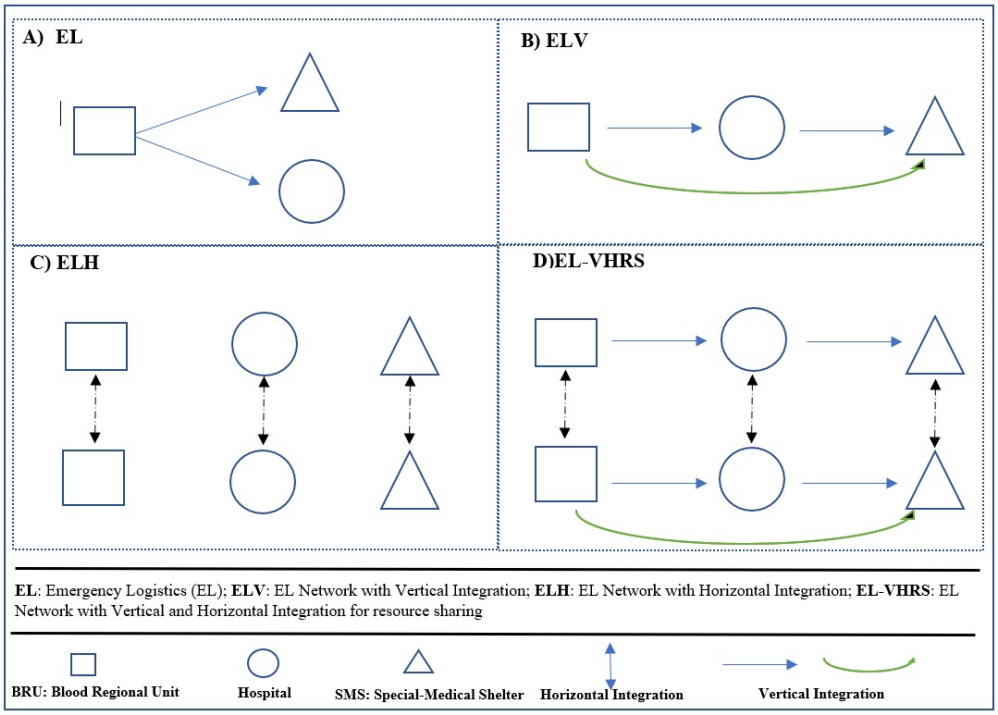

Figure 2.1: Alternative integration mechanisms for platelets logistics

by developing an optimization model for a horizontally and vertically integrated platelets logistics network. Figure 2.1 portrays the individual horizontal and vertical integration mechanisms (ELH and ELV, respectively) and the collective one (EL-VHRS), along with the non-integrated network (EL). For example, the EL-VHRS mechanism (Figure 2.1 D) involves horizontal resource sharing among BRUs, hospitals, and SMSs (vertical dashed bi-directional lines) and vertical resource sharing from BRUs to hospitals, BRUs to SMSs, and hospitals to SMSs (solid horizontal and curved lines).

The remainder of this chapter is organized as follows. In Section 2.2, we discuss the relevant literature on blood logistics in humanitarian relief operations (HROs), integration mechanisms and integrated networks, and casualty flow models. In Section 2.3, we describe what we call the fully integrated emergency logistics planning problem. Then, in Sections 2.4 and 2.5, we describe the proposed model, its formulation, and a hybrid solution method. In Section 2.6, we discuss a number of numerical experiments for a real case study and examine the performance of the approach and the sensitivity of the solution to changes in key parameters. Finally, in Section 2.7, we conclude the chapter and discuss future research directions.

2.2 Related Literature

Given that this work focuses on a fully integrated emergency network for blood logistics for patients with different levels of injury seriousness, we categorize the relevant literature into two main streams which are blood logistics and casualty flow problems. We outline the main research gaps and our contribution to the existing literature.

2.2.1 Blood logistics

Here we present a summary of the most relevant studies on blood logistics under three main categories: general operations, DRO, and integrated blood logistics networks. For each paper, if available, the type of integration mechanism and the included blood characteristics are discussed.

I) General operations : For general or daily blood logistics operations, Zhou et al. [68] analyze an inventory system for perishable platelets under two replenishment modes. They demonstrate the existence and uniqueness of an optimal inventory policy to minimize expected costs under demand uncertainty, lead times, seasonality, and expedited orders. Civelek et al. [8] describe an inventory replenishment and allocation model that takes into account platelet substitution according to a critical-level policy for age-differentiated platelets. To improve the blood supply chain's coordination and encourage blood donations under the risk of network disruptions, Hosseini-Motlagh et al. [24] present a mixed possibilistic-stochastic robust optimization model. Hosseinifard et al. [26] study the donation process in times of a disaster to overcome blood shortages while taking into

account the perishability of blood products and donors' eligibility to give blood. They model the stochastic behavior of both transfusions and blood donations using a Markov Chain.

II) Disaster relief operations: Jabbarzadeh et al. [29] propose a robust model to determine the location for blood collection centers after an earthquake using real data from an Iranian blood transfusion organization. Salehi et al. [55] describe a model for the design of a three-layer blood supply chain network (SCN) including donation areas, collection centers, and transfusion centers under blood demand uncertainty. Fahimnia et al. [16] present a bi-objective stochastic SCN model for efficient blood provision considering the trade-off between cost and delivery time. Ramezanian and Behboodi [51] propose a robust blood logistics model under uncertainty in the demand and supply of blood products that consider social aspects (i.e., fairness and equality) and the impact of blood donors (arrival rate to blood centers, blood donors' experience of the blood donation process, etc.). Habibi-Kouchaksaraei et al. [19] describe a scenario-based robust bi-objective blood logistics model to minimize the costs of temporary and permanent shelters and hospitals and maximize demand satisfaction of injured people for an earthquake. Eskandari-Khanghahi et al. [15] developed a possibilistic multi-objective blood logistics model considering various aspects of sustainability to minimize total costs and environmental effects, and maximize social benefits (equality, fairness, etc.). Cheraghi and Hosseini-Motlagh [6] propose a multi-objective robust blood logistics model incorporating three criteria: casualty urgency, fairness, and disruption risk of facilities. Ma et al. [37] describe a blood allocation model that seeks to minimize the total unmet demand for blood products of multiple groups and lower blood shortage considering optimal ABO/Rh(D)-compatible substitutions. Sharma et al. [60] develop a min-max dynamic location model using integration techniques to locate temporary blood banks to serve hospitals with minimum response time. Fazli-Khalaf et al. [17] present a multi-objective robust possibilistic model for blood logistics during an earthquake. The model seeks to minimize total costs and transportation time while maximizing the reliability (receiving blood with minimum possibility of being outdated) of donated blood. Diabat et al. [12] and Hamdan and Diabat [22] propose a robust two-stage stochastic optimization model to design resilient blood logistics networks after a disaster under possible disruptions of blood facilities and transportation routes. Razavi et al. [52] propose a relief logistics model to distribute multi-type blood products in an equitable way from blood collection points to field hospitals and subsequently between field hospitals. They introduce a multi-objective robust model to minimize, under potential route disruptions, costs and the maximum level of dissatisfaction with unfairness among affected areas.

III)Integrated blood logistics networks : The most relevant studies involving integrated blood logistics networks in either general or relief operations are summarized next.

—Vertically integrated blood logistics networks

Nagurney et al. [45] describes a blood supply chain network for a regionalized blood banking system. The facilities in the network are vertically integrated from collection sites to hospitals. Masoumi et al. [38] analyze a blood logistics model where the synergy of a merger/acquisition as an integration mechanism in the blood banking system is studied. The organizations are vertically integrated from blood collection centers to hospitals. Zahiri and Pishvaee [67] study a regionalized SCN considering perishability as well as group compatibility of blood-derived products in which blood collection centers, temporary medical shelters and lab centers are vertically coordinated. Haeri et al. [20] propose a multi-objective fuzzy programming model involving motivational social aspects (i.e., fairness and equality) to simulate blood donation. In their proposed model, the blood logistics network is vertically integrated from collection centers to demand points (hospitals). Akbarpour et al. [2] describe an integrated robust relief network design problem under uncertainty and a cooperative coverage mechanism for critical and non-critical pharmaceutical perishable items (such as metformin and insulin). They employ an option contract for efficient procurement of supplies and a cooperative mechanism for moving mobile pharmacies post-disaster. Samani et al. [56] propose a two-phase approach to update platelet logistics plans considering disruption risks and lateral transhipment strategies (horizontal resource sharing) between hospitals. Hosseini-Motlagh et al. [25] formulate a two-stage stochastic model to manage a blood supply chain including some crucial features such as perishability, multiple blood groups, ABO-Rh(D) compatibility, and priority rules among compatible groups. They consider a vertical integration among local and regional blood facilities, and hospitals, to reduce the wastage of red blood cells.

—Horizontally integrated blood logistics networks

As stated earlier, horizontal integration (i.e., lateral transhipment) has been considered in the literature as a shortage reduction mechanism to balance inventory levels among facilities in the same echelon. Although various studies have been undertaken to integrate supply chain networks using lateral transshipment policies ([36], [49], [65],[54], [35], [42], [48]), limited research has been done in blood logistics. Wang and Ma [64] proposed an age-based blood logistics model with lateral blood transhipment to reduce the shortage of blood products. Samani et al. [57] propose a mixed fuzzy-stochastic multi-objective model for the design of a blood supply chain network (SCN) involving irregular supply to minimize the shortage of perishable blood products. To integrate the supply network comprised of multiple local and regional blood centers, relief bases, and hospitals, they applied a vertical integration strategy. Kamyabniya et al. [31] describe a two-step resource-sharing coordination mechanism to prevent wastage and shortage of O-type platelets in

a multi-period planning horizon. They present a decentralized bi-level mixed integer model under demand and supply uncertainty for a possible earthquake in Tehran, Iran. Kamyabniya et al. [32] and Kamyabniya et al. [33] describe a bi-objective location-allocation robust fuzzy programming model for multi-type blood-derived platelets. Finally, Dehghani and Abbasi [10] and Dehghani et al. [11] present a deterministic model and a two-stage stochastic model, respectively, for an integrated blood logistics network. They employed a lateral transhipment strategy between hospitals to minimize the shortage and wastage of blood products.

2.2.2 Casualty flow models

In this category, we include papers that consider the transportation of casualties and the distribution of relief commodities to injured people with different urgency levels. With respect to integrated resource allocation and casualty transportation and treatment modelling, Sheu and Pan [61] classify survivors into three groups (normal people, the elderly, and women with young children) to facilitate differentiating the urgency level of relief services needed by survivors. Dean and Nair [9] and Sung and Lee [62] model an ambulance scheduling problem as a patient prioritization problem where different triage methods are considered to provide better responses to the maximum number of patients. They assign differing survival probabilities to patients to represent different levels of injury seriousness. For emergency planning under uncertain demand and supply, approaches such as stochastic programming [43, 47, 28, 67] and dynamic multi-stage planning [27, 1] have been considered a great deal. However, a limited number of studies in the context of disaster relief operations have used robust modelling for worst-case scenarios in terms of demand and supply levels [32, 34, 2, 52, 14].

2.2.3 Gap analysis

Although blood logistics in DROs is receiving increased attention in the literature, the existing models exhibit several drawbacks. Despite the numerous papers published on casualty management and blood supply chain network design in DROs, the joint consideration of these two areas has been limited. Although the vital role of coordination among relief facilities and network integration for blood logistics has been recognized by researchers, only a few studies have addressed it [3, 32, 34, 46].

The two closest studies to our research are those by Kamyabniya et al. [31], Kamyabniya et al. [32] and Samani et al. [56]. However, neither of these studies considers a fully integrated blood logistics network under vertical and horizontal integration mechanisms. Furthermore, both studies by Kamyabniya et al. [31] and Samani et al. [56] apply fuzzy programming as the primary approach to deal with the uncertainties, vagueness and ambiguity due to information deficiency in determin-

ing some of the model parameters. However, their methods rely on expert knowledge in providing some degree of information concerning some of the model's parameters. It may also generate infeasible solutions for some realizations of uncertain parameters. In contrast, we employ a robust programming approach with a known probability distribution, making the model resilient against any uncertain parameter realization, a similar approach as employed by Kamyabniya et al. [32]. The main difference between the work described in this chapter and that in Kamyabniya et al. [32] is the application of multiple mechanisms (blood substitution/matching protocols, integration of multiple entities, etc.) in the model's formulation. Unlike the studies mentioned above, we seek to identify strategies that match multiple platelets types with the needs of casualties. Such a matching strategy is neither considered in the blood logistics nor the logistics management literature.
In summary, compared to the studies described earlier in Section 2.2; First, few studies develop optimization models incorporating the perishability of multi-type scarce resources with a very short shelf life, such as blood-derived products. Second, none of the papers mentioned above considers matching multi-group blood products to patients of different injury levels. Third, only a limited number of studies have explored multi-stage models under uncertainty using robust optimization for multi-group age-differentiated blood logistics in HROs. Fourth, we are aware of no research that jointly considers the compatibility of blood products with patients while also considering the perishability of blood products under various resource-sharing (integration) mechanisms.

2.3 Problem Statement

A three-level platelets supply chain consisting of blood regional units (BRUs), hospitals, and special-needs medical shelters (SMSs) in disaster zones is considered. The proposed model can be thought of as a multi-period (i.e., day) multi-injury-level casualty transportation model involving horizontal and vertical resource sharing among relief facilities. During a disaster, BRUs, hospitals, and SMSs face an unexpected growth in platelets demand from patients. People with different levels of injury seriousness are assumed to need different groups of blood-derived platelets. Hence, we seek to optimize the amount and type of platelets sharing (among BRUs, hospitals, SMSs, hospital-to-hospital, BRU-to-BRU, SMS-to-SMS), the matching of age-differentiated platelets to patients with varying injury levels, and the transportation of platelets in a multi-period setting under demand uncertainty. We formulate a mixed integer bi-objective model that considers age-sensitive blood sharing and matching to multi-level-injury patients. Neglecting the possibility of a full integration among facilities at different or the same echelon results in the co-existence of shortages and wastage for the same platelet product. During a disaster, having only vertical or horizontal integration may increase the number of fatalities, wastage, the response time of relief operations, and the response cost [46].

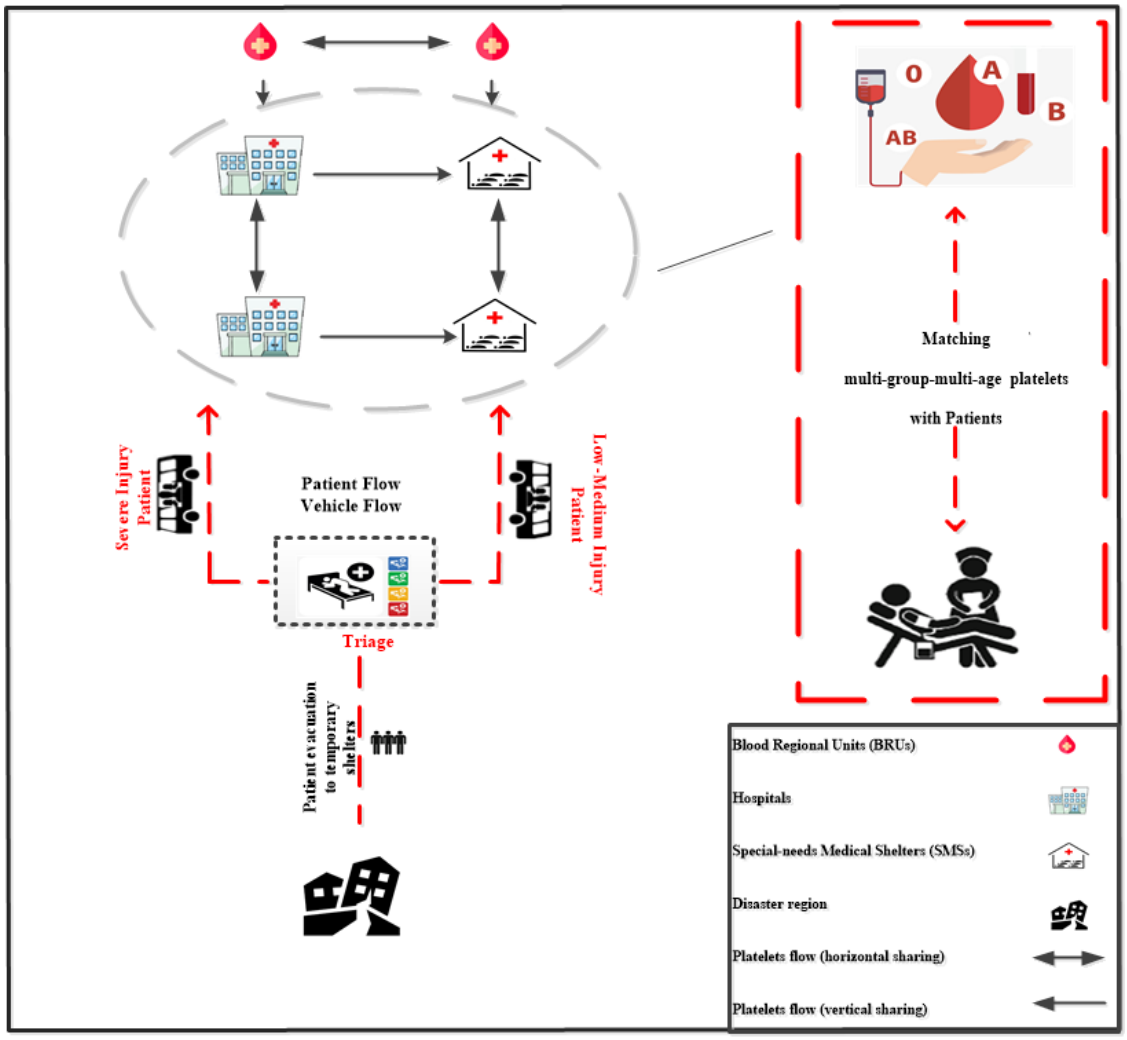

Figure 2.2: A horizontally and vertically blood integrated supply and casualty transportation network.

In Figure 2.2, a horizontally and vertically integrated blood-derived platelets supply chain along with patient matching to hospitals and SMSs having multi-group multi-type platelets are illustrated. Such significance across the relief logistics network is a feature of the fully-coordinated relief model.

2.4 Model formulation

In this section, we outline the main assumptions required for the problem formulation and specify the parameters, variables, objective function and constraints considered in the model. Table 2.2 represents the notation used in the model formulation.

2.4.1 Assumptions

We assume that each day's unmet demand at any hospital or SMS is carried over to the next period (with the further assumption that untreated patients from previous days still need the same amount of platelets), that at the end of each day all vehicles return to their original locations, that the number of vehicles available from each organization at the beginning of each day is known, and that three levels of injury seriousness are considered (severe, moderate, low) [9]. In addition, we consider that each vehicle can make multiple trips during each day. During each trip, a vehicle will only visit one entity on the network.

Also, we do not consider the platelet collection, production, and testing processes. Hence, the facilities only distribute the supplied platelets from regional blood units to other blood centers, hospitals, and special-needs medical shelters. Finally, it is assumed that the available platelets have already gone through the two-day collection, extraction, testing, and production processes, meaning that platelet collection and production are out of the scope of this chapter.

2.4.2 The integrated platelets logistics model

Below we present the mathematical formulation of the problem. We have included superscript s to denote the scenario associated with the number of affected people to avoid having to repeat the constraints in the robust version (Section 2.4.3). The deterministic version can be obtained by simply removing superscript s. We define two objective functions, Z_1^s and Z_2^s, associated with the total unmet demand for platelets and total relief cost, respectively. We minimize both objective functions (Z_1^s and Z_2^s) simultaneously using the hybrid solution approach described in Section 2.5.

$$\min Z_1^s = \sum_{\substack{h,c,t \\ u \in J \cup K}} \eta^h \times USIP_u^{hcts} + \sum_{\substack{l,c,r,t \\ u \in J \cup K}} W_{lc} \times Q_u^{lcrt} \tag{2.1}$$

Table 2.2: Model Notation (Blood Logistics Model)

Sets	
I	Blood regional units
J	Hospitals
K	Special-needs medical shelters
R	Platelet ages
T	Days in the planning horizon
V	Vehicles for platelets transportation
W	Vehicles for injured people transportation
C	Platelet groups
H	Injury levels (type of patients)
S	Scenarios
U	Facilities in the network, $U = I \cup J \cup K$
$U(u)$	Possible facility destinations for origin facility u
$H(u)$	Types of patients that can be transferred to facility u, $u \in J \cup K$
$V(u)$	Vehicles assigned to facility u for back-and-forth trips from facility u only to other facilities
Indices	
i, i'	a blood regional unit, $i, i' \in I$
j, j'	a hospital, $j, j' \in J$
k	a special-needs medical shelter, $k \in K$
r	a platelet age, $r \in R$
t	a day in the planning horizon, $t \in T$
v	a vehicle, $v \in V \cup W$
c, l	a platelet group, $c, l \in C$
h	an injury level, $h \in H$
s	a scenario, $s \in S$
u, u'	a facility in the network, $u, u' \in U$
Parameters	
SL_i^{ct}	Platelet group c stock target level at blood regional unit i on day t [bags]
τ	Number of units of platelets extracted from one donor by apheresis [bags]
η^h	Average number of platelets needed for a patient with an injury of level h [bags]
PDZ_h^{st}	Total number of injured people of injury level h on day t under scenario s
β^{rt}	Proportion of the total demand for platelets on day t that needs to be r days old
π^s	Probability of occurrence of scenario s
W^{lc}	Priority weight associated with substituting platelets of blood group l with platelets of blood group c
ξ^{cl}	1 if platelets of blood group c can be substituted with platelets of blood group l, 0 otherwise
DB_i^{ct}	Number of platelets of blood group c extracted from donated whole-blood at blood regional unit i received on day t [bags]
CI_u^h	Capacity of facility u for accepting people with injuries of level h, $u \in J \cup K$
f^{ht}	Survival probability of a person with an injury of level h on day t
$CC_{uu'}$	Coordination cost between facility u and facility u'
WC_u	Wastage cost at facility u
IC	Blood holding cost
$TC_{uu'v}$	Transportation cost from facility u to facility u' by vehicle v
MUV_v	Maximum daily usage of vehicle v [hours]
$t_{uu'v}$	Transportation time between facility u and facility u' by vehicle v [hours]
VC_v	Platelets load capacity of vehicle v [bags]
UTC	Under-target cost at blood regional units
h_r	Use of platelets of age r by a specific type of patient
$MT_{uu'v}^t$	Maximum number of trips between facility u and other facilities u' by vehicle v on day t
Decision Variables	
$B_{uu'v}^{crts}$	Amount of platelets of type c and age r transported from facility u to facility u' by vehicle v on day t under scenario s, $u' \in U(u)$ [bags]
AP_u^{ct}	Number of platelets of group c extracted by apheresis at facility u on day t, $u \in I \cup J$ [bags]
Q_u^{clrt}	Amount of platelets of group c used to substitute of group l for r days old platelets at facility u on day t, $u \in J \cup K$ [bags]
IN_u^{crts}	Inventory level of platelets of group c and age r at facility u on day t under scenario s [bags]
WA_u^{st}	Total waste of platelets at facility u on day t under scenario s [bags]
$USIP_u^{hcts}$	Number of people with an injury of level h at facility u not served with blood group c on day t under scenario s, $u \in J \cup K$
SIP_u^{hcrts}	Number of people with an injury of level h served with blood group c and age r at facility u on day t under scenario s, $u \in J \cup K$
IP_{uv}^{hcts}	Percentage of people with an injury of level h transferred to facility u by vehicle v to receive platelet type c on day t under scenario s, $u \in J \cup K, v \in W$
UL_i^{cts}	Gap between the inventory level and the minimum stock level for platelet type c at blood regional unit i on day t under scenario s
$NT_{uu'v}^t$	Number of trips between facility u and u' by vehicle v on day t

The first term in Equation (2.1) corresponds to the penalty associated with the total unmet demand (number of patients not served with the required platelet type matched to their blood group; $USIP_u^{hcts}$) for multi-type platelets of different ages at hospitals and SMSs over the DRO planning horizon (on the day t). The second term in Equation (2.1) represents the total penalty associated with $ABO/Rh(D)$-compatible blood substitutions. W_{lc} denotes the penalty incurred when substituting platelets of group c for platelets of group l and Q_u^{lcrt} is a decision variable that represents the amount of platelets of group c used to substitute r-day old platelets from group l at facility u on day t.

$$\min Z_2^s = \sum_{\substack{c,r,t \\ u,u' \in U(u),v}} TC_{uu'v} \times B_{uu'v}^{crts} + \sum_{c,r,t,u} IC \times IN_u^{crts} + \sum_{t,u} WC_u \times WA_u^{st} + \sum_{\substack{c,r,t \\ u,u' \in U(u),v}} CC_{uu'} \times B_{uu'v}^{crts} + \sum_{c,t,i} UTC \times UL_i^{cts} \tag{2.2}$$

Equation (2.2) involves five terms: blood distribution costs between facilities (i.e., BRUs to hospitals, hospitals to SMSs, BRUs to SMSs), inventory costs, wastage costs, coordination costs (hospitals, BRUs, and SMSs), and under stock target penalties at the BRUs. The under-target penalties at BRUs are defined as proportional to the total gap between the inventory level and the minimum stock level required for each platelet group (UL_i^{cts}). The blood distribution costs are a function of the amount of blood transported and the unit transportation cost between facilities. Coordination costs represent the costs associated with maintaining the horizontal flow between facilities.

Constraints (2.3) to (2.5) balance the flow of platelets for each hospital, BRU and SMS on day t. Equation (2.3) represents the general structure of the flow balance constraints for fresh, young, and old blood of type c at the different facilities on the day t. For $r = 1$ (fresh blood) and hospital j, platelet availability on day t includes the platelets transported from all BRUs and other hospitals minus those transported out of hospital j plus the extraction of platelets directly from donors using the apheresis method (not available at SMSs). ξ^{cl} is a binary matrix that represents the possibility of substitution of platelets of a group c for group l. The term $\tau \times AP_j^{ct}$ denotes the number of platelet bags extracted using the apheresis method, where τ is the average number of platelet bags extracted from a donor. This term is only included for fresh platelets and patients with injury level $h = 1$. For patients with injury level $h = 1$, only fresh platelets (r=1) are used. Equation (2.4) is the equivalent constraint for young platelets (r=2 and 3) and old platelets (r=4), and involves only patients with injury levels $h = 2$ and $h = 3$. The first term of the RHS of Constraint (2.3) represents the number of patients of type h receiving platelets of type c (η^h is the average number

of platelets required by patients of type h). The second term is the ending inventory of fresh (r=1) platelets of type c at hospital j. Equation (2.4) has a similar form but for different platelet ages ($r > 1$) and levels of injury seriousness (h_r).

$$\sum_{\substack{u:j\in U(u),\\ v\in V}} B_{ujv}^{c1ts} - \sum_{\substack{u\in U(j),\\ v\in V}} B_{juv}^{c1ts} + \sum_{l} \xi^{lc} \times Q_j^{lc1t} - \sum_{l} \xi^{cl} \times Q_j^{cl1t} + \tau \times AP_j^{ct}$$
$$= \eta^1 \times SIP_j^{1c1ts} + IN_j^{c1ts} \qquad \forall c, t, j \tag{2.3}$$

$$IN_j^{c(r-1)(t-1)s} + \sum_{\substack{u:j\in U(u),\\ v\in V}} B_{ujv}^{crts} - \sum_{\substack{u\in U(j),\\ v\in V}} B_{juv}^{crts} + \sum_{l} \xi^{lc} \times Q_j^{lcrt} - \sum_{l} \xi^{cl} \times Q_j^{clrt}$$
$$= \eta^{h_r} \times SIP_j^{h_r crts} + IN_j^{crts} \qquad \forall c, r > 1, t, j \tag{2.4}$$

Flow balance constraints for all ages of platelets (fresh, young, and old) at the BRUs are explained below. The main differences compared to Equation (2.3) are that BRUs do not treat patients and that there are additional outflows representing the transport of platelets to hospitals and SMSs for each BRU. In Equation (2.3), $\tau \times AP_i^{ct}$ denotes the number of bags of platelets donated through the apheresis method and DB_i^{ct-2} is the number of whole blood-extracted platelets (without using the apheresis method) from two days ago ($t-2$) (due to the 48 hours needed for processing and testing of whole-blood-derived platelets before being made available for transfusion). The expressions on the LHS of Equation (2.4) represent the platelets transferred to BRU i from other BRUs and from BRU i to hospitals, other BRUs, and SMSs. The consideration of under-target stock level in Equation (2.10) at BRUs helps improve supply reliability by balancing inventory levels across BRUs. Thus, if one or more BRUs suddenly become unavailable, the remaining are better prepared to satisfy the demand for different types of platelets. Equation (2.5) is only written for fresh platelets (r=1), while for r-day old platelets ($r = 2, 3$ and 4), only the inventory of the previous day must be added to the LHS of the equation. It should be noted that the term $\tau \times AP_i^{ct}$ only appear in the Equation (2.5) for $r = 1$.

$$\sum_{\substack{u:i\in U(u),\\ v\in V}} B_{uiv}^{c1ts} - \sum_{\substack{u\in U(i),\\ v\in V}} B_{iuv}^{c1ts} + \tau \times AP_i^{ct} + DB_i^{c(t-2)} = IN_i^{c1ts} \qquad \forall c, t, i \tag{2.5}$$

For brevity, the balance constraints for all ages of platelets at SMSs are not repeated. In the case of SMSs, there is no apheresis donation. For each SMS, there are platelet inflows from BRUs and hospitals and outflows to other SMSs. Equations (2.3) to (2.5) allow horizontal integration among hospitals, BRUs, and SMSs, and vertical integration between hospitals and SMSs, BRUs and hospitals, and BRUs and SMSs. Due to the 3-day shelf life of platelets, any 4-day-old platelets

stored in any facility must be discarded. This is captured in Equation (2.6). The ending inventory of platelets of age 4 (maximum age of platelets) is considered as wastage.

$$WA_u^{st} = \sum_c IN_u^{c4ts} \qquad \forall u, t \tag{2.6}$$

On each day t, the platelets transported by a vehicle between facilities must not exceed the vehicle's load capacity (VC_v) multiplied by the number of trips between the facilities. This is captured in Equation (2.7). An upper bound on the number of trips for each vehicle is imposed in Equation (2.9). Note that a vehicle can be loaded more than once. Thus $NT_{uu'v}^t$ represents multiple back-and-forth trips occurring several times on the same day. The LHS of Equation (2.8) is the total transport time where $tt_{uu'v}$ represents the transportation time from facility u to facility u'. In the case where no vehicles are available at facility u, the RHS of Equation (2.8) is zero to prevent any transportation between facilities. However, if one or more vehicles are available at each facility, the total transportation time, i.e., the LHS of Equation (2.8), cannot exceed a maximum daily utilization MUV_v.

$$\sum_{c,r} B_{uu'v}^{crts} \leq VC_v \times NT_{uu'v}^t \qquad \forall t, u, u' \in U(u), v \in V \tag{2.7}$$

$$\sum_{u' \in U(u)} 2 \times t_{uu'v} \times NT_{uu'v}^t \leq MUV_v \qquad \forall t, u, v \in V(u) \tag{2.8}$$

$$NT_{uu'v}^t \leq MT_{uu'v}^t = \left\lceil \frac{MUV_v}{2 \times tt_{uu'v}} \right\rceil \qquad \forall t, u, u' \in U(u), v \in V(u) \tag{2.9}$$

$$UL_i^{cts} = \max\left(SL_i^{ct} - \sum_r IN_i^{crt}, 0 \right) \qquad \forall c, t, i \tag{2.10}$$

Equation (2.10) determines the amount of platelets below-target for each BRU, where SL_i^{ct} is the stock target level at the end of day t at BRU i. For the case study presented later, stock target levels are defined by the Iranian Blood Transfusion Organization (IBTO) for each subordinate blood regional unit to balance the network at the supplier level. The nonlinear term in Equation

(2.10) can be substituted by the equations ($UL_i^{cts} \geq SL_i^{ct} - \sum_r IN_i^{crt}$) and ($UL_i^{cts} \geq 0$).

$$\sum_{j \in J, v \in W} IP_{jv}^{hcts} = 1 \qquad \forall c, h \neq 1, t \tag{2.11}$$

$$\sum_{k \in K, v \in W} IP_{kv}^{1cts} = 1 \qquad \forall c, t \tag{2.12}$$

Equations (2.11) and (2.12) ensure that all injured people of types 2 and 3 (moderate and severe) are transferred to hospitals while those of type 1 (mild) are assigned to shelters.

$$\sum_{v \in W} PDZ_h^{st} \times IP_{uv}^{hcts} \leq CI_u^h \qquad \forall c, t, u \in J \cup K, h \in H(u) \tag{2.13}$$

Equation (2.13) prevents the capacity of each facility for injury level h from being exceeded. It states that the number of the affected population of type h in the disaster region (PDZ_h^{st}) transferred to a facility cannot exceed the available service capacity of that facility for that injury level.

$$USIP_u^{hc(t-1)s} \times f^{h(t-1)} + \sum_{v \in W} PDZ^{st} \times IP_{uv}^{hcts} = \sum_r SIP_u^{hcrts} + USIP_u^{hcts} \qquad \forall c, t, u \in J \cup K, h \in H(u) \tag{2.14}$$

Equation (2.14) specifies the number of injured people not receiving platelets. The parameter f^{ht} denotes the survival probability of people with injury seriousness level h on the day t. In other words, if a patient with an injury of level h cannot be served on the day t, then the patient may die with probability f^{ht}. The first term on the LHS of Equation (2.14) represents the number of patients not served at the facilities (hospitals or shelters) on the day $t-1$ who survived. The second term of the equation is the fraction of total casualties to be served at SMSs and hospitals. The RHS of this equation involves the number of patients treated plus those not treated on the current day t.

$$IP_{uv}^{hcts} \geq 0 \qquad \forall h, c, t, s, u \in J \cup K, v \in W$$

$$B_{uu'v}^{crts}, AP_u^{ct}, Q_u^{clrt}, IN_u^{crts}, WA_u^{st}, USIP_u^{hcts}, SIP_u^{hcrts}, UL_i^{cts}, NT_{uu'v}^{t} \in \mathbb{Z}^+ \qquad \forall c, l, r, t, s, u, u' \in U(u), h \in H(u), v \in V(u) \tag{2.15}$$

Finally, Equation (2.15) guarantees the non-negative and integer nature of the decision variables.

2.4.3 A robust integrated platelets logistics model

To tackle the uncertainty in the demand for platelets during disaster relief operations, we present a robust version of the model described in Section 2.4.2. The robust approach developed by Yu and Li [66] as an extension to that proposed by Mulvey et al. [44] is employed. The goal is to find solutions having the smallest expected performance deviation from the performance of the scenario-specific optimal solutions. The robust optimization methods developed by Yu and Li [66] and Mulvey et al. [44] extend stochastic programming approaches by replacing the traditionally expected cost minimization objective with one that explicitly addresses cost variability. The aforementioned authors developed a robust optimization method capable of tackling the decision-makers favoured risk aversion or service-level function, yielding a series of solutions that are progressively less sensitive to realizations of the data in a scenario set. Yu and Li [66] developed a new formulation which is more computationally effective than that proposed by Mulvey et al. [44], requiring fewer additional variables. An alternative method is the one proposed by Bertsimas and Sim [5], which is suitable for linear programming models with an uncertain coefficient matrix or left-hand side vector. Their method provides solutions with different levels of conservatism that can be adjusted for any constraint violation level using probabilistic limits. This method is best suited for cases searching for robustness with high protection levels for some constraint violations.
The advantage of using Yu and Li [66]'s approach is that it ensures model robustness by minimizing both the expected performance and deviation from expected performance for all possible scenarios. In other words, it considers a trade-off between the expected performance and the standard deviations from the expected performance. It performs well in situations in which the best and worse solutions are close to the model's expected performance which is the case we are looking for in our model.

2.4.3.1 A robust formulation

To minimize the expected shortage and total logistics cost in Equation (2.1) and (2.2) across all scenarios ($\sum_s \pi^s = 1$), the following changes are made to the objective functions. Equations (2.16) and (2.17) below specify the objective functions (2.1) and (2.2) for each scenario $s \in S$, respectively. The last term of Equation (2.17) denotes the demand under-fulfilment penalty, where ϑ is the demand constraint violation penalty (the penalty associated with the shortage of platelets at hospitals and SMSs). A high variance for Υ^s and ζ^s implies high-risk decisions. Because of the uncertainty in the value of PDZ_h^{st} in equations (2.13) and (2.14), the model may be infeasible for some scenarios and needs to be controlled using an infeasibility penalty term denoted as a

constraint violation cost.

$$\Upsilon^s = \sum_{\substack{h,c,t \\ u \in J \cup K}} \eta^h \times USIP_u^{hcts} + \sum_{\substack{l,c,r,t, \\ u \in J \cup K}} W_{lc} \times Q_u^{lcrt} \tag{2.16}$$

$$\begin{aligned} \zeta^s = & \sum_{\substack{c,r,t \\ u,u' \in U(u),v}} TC_{uu'v} \times B_{uu'v}^{crts} + \sum_{c,r,t,u} IC \times IN_u^{crts} + \sum_{t,u} WC_u \times WA_u^{st} + \\ & \sum_{\substack{c,r,t \\ u,u' \in U(u),v}} CC_{uu'} \times B_{uu'v}^{crts} + \sum_{c,t,i} UTC \times UL_i^{cts} + \vartheta \times \left(\sum_{\substack{h,c,t \\ u \in J \cup K}} \eta^h \times USIP_u^{hcts} \right) \end{aligned} \tag{2.17}$$

Having defined equations (2.16) and (2.17) for each scenario, the new objective functions, denoted Z_1^E and Z_2^E, are as follows:

$$Z_1^E = \sum_s \pi^s \times \Upsilon^s + \lambda_1 \times \sum_s \pi^s \times \left[\left(\Upsilon^s - \sum_{s'} \pi^{s'} \times \Upsilon^{s'} \right) + 2 \times \theta_1^s \right] \tag{2.18}$$

$$Z_2^E = \sum_s \pi^s \times \zeta^s + \lambda_2 \times \sum_s \pi^s \times \left[\left(\zeta^s - \sum_{s'} \pi^{s'} \times \zeta^{s'} \right) + 2 \times \theta_2^s \right] \tag{2.19}$$

The first and second terms in equations (2.18) and (2.19) denote the expected value of the original objective function over the set of scenarios and the penalty associated with deviations from the optimal values (variance of the total shortage and cost, respectively). The third term in the objective functions is an infeasibility penalty. Solution robustness is captured by the first term which models the decision maker's desire for lower shortage and costs, while the second term represents the model robustness, penalizing solutions that fail to meet demand. Using the weights λ_1 and λ_2, the trade-off between solution robustness and model robustness can be balanced. λ_i indicates the weight placed on the solution variability for objective i, where the solution is less sensitive to the scenario variability as λ increases.

$$\left[\left(\Upsilon^s - \sum_{s'} \pi^{s'} \times \Upsilon^{s'} \right) + \theta_1^s \right] \geq 0 \qquad \forall s \tag{2.20}$$

$$\left[\left(\zeta^s - \sum_{s'} \pi^{s'} \times \zeta^{s'} \right) + \theta_2^s \right] \geq 0 \qquad \forall s \tag{2.21}$$

Equations (2.20) and (2.21) address potential model infeasibility for each scenario. If the model is feasible, then θ^s will be equal to 0; otherwise, θ^s will be assigned a value according to equations (2.20) and (2.21) to capture the amount of infeasibility. In addition, the last term of Equation (2.17) is used to penalize violations of the control constraints and helps adjust the model in response to changes in the data. As mentioned above for equations (2.20) and (2.21), if ζ^s is greater than

$\sum_s \pi^s \zeta^s$, then $\theta_2^s = 0$, otherwise $\theta_2^s = \sum_s \pi^s \zeta^s - \zeta^s$. Hence, the robust version of the main model is defined by Constraints (2.3)-(2.21).

2.5 A Hybrid solution approach

The robust bi-objective model proposed in Section 2.4.3 is converted into a single-objective model using the augmented ϵ-constraint method. Solving the resulting single-objective model using standard solution methods often takes an extremely long time. For this reason, Lagrangian relaxation is used to solve the resulting model resulting in a computation time of less than one hour for the large-scale case study described later.

Phase 1. Transformation to a single-objective model

The augmented ϵ-constraint method is an improvement on the original ϵ-constraint method first proposed by Haimes and Wismer [21] as a means of deriving a Pareto front for combinatorial optimization problems. In the ϵ-constraint method, all objectives except for one are converted into constraints and an upper bound is set for each constraint. The method works by pre-defining a virtual grid in the objective function space and solving different single-objective problems constrained to each grid cell. Thus, all Pareto optimal solutions can be obtained if this grid is fine enough such that at most one Pareto-optimal solution is contained in each cell [40]. The idea is to overcome the complexity of solving a multi-objective model by minimizing or maximizing one objective at a time and expressing the other objectives in the form of inequality constraints. In this method, the ranges of the objective functions (lower and upper bounds) are computed using a Lexicographic approach. The Pareto efficiency of the solution is assured since the reformulated ϵ-constraint model employs appropriate slack (or surplus) variables. The optimal solution of the problem in the form of inequality constraints is guaranteed to be an efficient solution only if all $(q-1)$ objective function constraints are binding, where q denotes the number of objective functions [13]. Otherwise, if there are alternative optima that may improve one of the non-binding constraints, the obtained optimal solution using inequality constraints is not in fact efficient but only a weakly efficient solution. However, the objective function can be modified as follows to force the formulation to produce efficient solutions only.

$$\min_{\vec{x} \in \rho} \left[F(x) = (f_1(x), f_2(x), ..., f_q(x)) \right], \tag{2.22}$$

where $\vec{x}$ is the vector of decision variables, $F(x)$ is the vector of q objective functions, and ρ is the feasible solution space. The modified objective function is defined as:

$$\min_{\vec{x} \in \rho} \left(f_1(x) - eps \times \left(\frac{sl_2}{r_2} + 10^{-1} \times \frac{sl_3}{r_3} + \cdots + 10^{-(q-2)} \times \frac{sl_q}{r_q} \right) \right) \tag{2.23}$$

where f_1 is the main objective function and *eps* is a very small number (between 10^{-6} and 10^{-3}). Here, r_k and sl_k are the range and the slack variable associated with objective function f_k, respectively. In order to avoid any scaling issues, $\frac{sl_k}{r_k}$ is used instead of sl_k in Equation (2.23). The second term in the objective function of (2.23) drives the search for the best possible alternative optima of Min $f_1(x)$, the one that minimizes the sum. This improved ϵ-constraint method called the augmented ϵ-constraint method greatly reduces the solution time as many redundant iterations are avoided.

Let us consider a multi-objective problem with q objective functions as below:

$$f_k(\rho) + sl_k = \epsilon_k \qquad \forall x \in \rho, sl_k \in \mathbb{R}^+ k = 1, ..., q \tag{2.24}$$

In Equation (2.24), $\epsilon_k = ub_k - i_k \times step_k$, where ϵ_k is the RHS parameter for the specific iteration drawn from the grid points of the objective functions $2, ..., q$. Here, ub_k and i_k denote an upper bound and the grid points for a specific objective function k. As explained by Mavrotas [39] and Mavrotas and Florios [40], to compute $step_k$, first, for each objective function $2, ..., q$, the objective function range r_k must be calculated. In the next step, as illustrated in Algorithm 1, the range of the k^{th} objective function is divided into g_k equally sized intervals using $(g_k - 1)$ equidistant grid points. The discretization step for this objective function is $step_k = \frac{r_k}{g_k}$.

In each iteration, we check the value of the slack variable associated with the innermost objective function. When the slack variable s_k is larger than $step_k$, then, in the next iteration, the same solution will be obtained with the only difference being that the slack variable will be $sl_k - step_k$. This makes the iteration redundant and therefore it can be bypassed as no new Pareto optimal solution is generated. In this chapter, we set the first objective function as the main objective function and transform the second objective function into a constraint. Therefore, the bi-objective model is transformed into a single-objective model as follows. For the case study discussed later, we divide the ranges of the objective functions (r_k) into 10 equal intervals (g_k =10) and use 11 grid points to determine ϵ_k (in our case ϵ_2) in Equation (2.24).

$$\min_{\vec{x}} F_1 = f_1(\vec{x}) - eps \times \left(\frac{sl_2}{r_2}\right)$$

where
$$f_1(x) = \sum_s \pi^s \times \left[\sum_{\substack{h,c,t \\ u\in J\cup K}} \eta^h \times USIP_u^{hcts} + \sum_{\substack{l,c,r,t, \\ u\in J\cup K}} W_{lc} \times Q_u^{lcrt}\right] + \lambda_1 \times \sum_s \left[\left(\sum_{\substack{h,c,t \\ u\in J\cup K}} \eta^h \times USIP_u^{hcts} + \sum_{\substack{l,c,r,t, \\ u\in J\cup K}} W_{lc} \times Q_u^{lcrt}\right) - \sum_{s'} \pi^{s'} \times \Upsilon^{s'}\right) + 2 \times \theta_1^s\right] \quad (2.25)$$

subject to

$$\sum_s \pi^s \times \zeta^s + \lambda_2 \times \sum_s \pi^s \left[\left(\zeta^s - \sum_{s'} \pi^{s'} \times \zeta^{s'}\right) + 2 \times \theta_2^s\right] + sl_2 = \epsilon_2 \quad (2.26)$$

$(2.3) - (2.15), (2.17), (2.20) - (2.21).$

Algorithm 1: The Augmented Epsilon-Constraint Algorithm.

Step1. For $k = 1$ **to** q,

Solve $Min_{x\in\rho}\ f_k(x)$ and set upper bound ub_k for $k = 2, ..., q$

Next k

Step2. Calculate ranges $r_k = f_k^{max} - f_k^{min}$ for $k = 2, ..., q$

Step3. Divide r_k into g_k intervals using $g_k - 1$ equally spaced grid points for $k = 2, ..., q$.

Step4. For $k = 2$ **to** q

For i_k=0 **to** g_k

Compute $\epsilon_k = (ub_k - i_k) \times step_k = ub_k - i_k \times \frac{r_k}{g_k}$

Next $i_k \rightarrow$ **1**

Next k

Set Non-Dominated Set (NDS) = $\emptyset$ and number of Pareto optimal solution $n_q = 0$

Step 5. At the current grid points i_k,

Set the value of ϵ_k for each objective function k in constraints **for** $k = 2, ..., q$

Step.6 Solve the augmented ϵ-constraint model for some combination of ϵ_k **for** $k = 2, ..., q$

Step7. If the augmented ϵ-constraint model is feasible **Then**

Add solution to NDS

Set $b = int(\frac{sl_k}{step_k})$ (bypass coefficient), where int () is the function that returns the integer part of a real number.

Update the current grid point ($i_k = i_k + b$)

Else

$i_k = g_k$

End If

If $i_k \leq g_k$

$i_k = i_k + 1$, go to Step 5.

Else

Break

End If

Note. Our approach starts with the most relaxed value for ϵ_k at the first grid point and strengthens the bound gradually.

Note. The bypass coefficient b indicates how many consecutive iterations we can bypass.

Phase 2. Solving the single-objective problem through Lagrangian relaxation

Lagrangian relaxation is a method that provides upper and lower bounds on the optimal objective value of a constrained optimization problem, allowing a decision maker to determine how far the current best feasible solution is from optimality. The idea behind Lagrangian relaxation is that many hard problems can be viewed as easy problems complicated by a relatively small set of difficult constraints. Dualizing such constraints produces a Lagrangian problem that may be easy to solve and whose optimal value defines a lower bound (for minimization problems) on the optimal value of the original model [18]. The Lagrangian relaxation method described below involves three steps: (1) finding a lower bound for the optimal solution; (2) obtaining an upper bound; and (3) updating the upper and lower bounds if they are not sufficiently close. These steps are repeated iteratively until the lower and upper bounds provide an acceptable optimality gap.

1) Finding a lower bound: A lower bound is achieved by relaxing a select number of constraints in order to make the problem easier to solve even if it causes infeasibility [18]. We relax Constraint (2.3) since it drastically reduced the solution time compared to relaxing other constraints. Relaxing this constraint generates the following Lagrangian dual problem.

$$\min \omega_{LDP} = \sum_s \pi^s \left[\sum_{\substack{h,c,t \\ u \in J \cup K}} \eta^h \times USIP_u^{hcts} + \sum_{\substack{l,c,r,t, \\ u \in J \cup K}} W_{lc} \times Q_u^{lcrt} \right]$$

$$+ \lambda_1 \times \sum_s \left[\left(\sum_{\substack{h,c,t \\ u \in J \cup K}} \eta^h \times USIP_u^{hcts} + (\sum_{\substack{l,c,r,t, \\ u \in J \cup K}} W_{lc} \times Q_u^{lcrt}) - (\sum_{s'} \pi^{s'} \times \Upsilon^{s'}) \right) + 2 \times \theta_1^s \right]$$

$$+ \sum_{u,c,t,s} \Delta_u^{cts} \times (IN_j^{c(r-1)(t-1)s} + \sum_{\substack{u:j \in U(u), \\ v \in V}} B_{ujv}^{crts} - \sum_{\substack{u \in U(j), \\ v \in V}} B_{juv}^{crts} + (\sum_l \xi^{lc} \times Q_j^{lcrt} - \sum_l \xi^{cl} \times Q_j^{clrt})$$

$$- \eta^{h_r} \times SIP_j^{h_r crts} - IN_j^{crts})$$

subject to

$(2.3), (2.5) - (2.15), (2.17), (2.19) - (2.21).$

where Δ_u^{cts} denotes the Lagrange multipliers associated with Constraint (2.4). The optimal objective value of the Lagrangian dual problem ω_{LDP} gives a lower bound on that for the original problem.

2) Finding an upper bound

At each iteration of the Lagrangian Relaxation approach, an upper bound is acquired if the solution is feasible for the original problem. If the upper and lower bounds are the same, the algorithm terminates and an optimal solution has been obtained. However, if the solution is infeasible, a feasible solution is found as follows. We minimize (2.25) subject to constraints (2.3)-(2.15), (2.19)-(2.21) and (2.26) while setting the integer decision variables equal to the optimal values acquired from solving the Lagrangian dual problem. The resulting feasible solution provides an upper bound for the model.

3) Updating lower and upper bounds

At each iteration of the Lagrangian Relaxation procedure, the Lagrange multipliers are updated and new lower and upper bounds are obtained. We employ the subgradient method [18] to update the values of the Lagrange multipliers (ℓ) at each iteration:

$$\ell = \frac{\mu \times (Z_{UB} - Z_{LB})}{GR_e^2} \tag{2.27}$$

where μ is a parameter between 0 and 2 pre-defined by decision-makers. It is recommended that, at first, μ is set to 2. The value of GR_e below is obtained using the optimal solution of the Lagrangian dual:

$$GR_e = IN_j^{c(r-1)(t-1)s} + \sum_{\substack{u:j\in U(u),\\ v\in V}} B_{ujv}^{crts} - \sum_{\substack{u\in U(j),\\ v\in V}} B_{juv}^{crts} + (\sum_l \xi^{lc} \times Q_j^{lcrt} - \sum_l \xi^{cl} \times Q_j^{clrt})$$

$$- \eta^{h_r} \times SIP_j^{h_r crts} - IN_j^{crts}) \tag{2.28}$$

In Equation (2.27), Z_{UB} is the lowest upper bound and Z_{LB} is the lower bound obtained in the latest iteration. The values of the Lagrangian multipliers are updated as follows:

$$\mu^{n+1} = \max(0, \mu^n + \ell^n \times GR_e)$$

At the first iteration $\mu = 2$ and if no improvement is achieved after a predetermined number of iterations then μ can be reduced to half of its previous value. This process continues until one of the following conditions holds: a feasible solution within the acceptable tolerance is found or the minimum value of μ is reached. A pseudo-code of this approach is provided in Algorithm 2.

Algorithm 2: Relaxation Lagrangian Algorithm.

Initial value: $\Delta_k^{c,t,s} = 0.8, \mu = 2, Z_{LB} = -\infty$ and $Z_{UB} = +\infty$

Step 1.

Solve The Lagrangian relaxation model and obtain lower bound (Z_{LB} and the number of trips/day by vehicle v taken from one facility to another one ($NT_{uu'v}^t$),
Obtain a feasible solution.

IF $Z_{LB}^{old} \leq Z_{LB}^{new}$, **then** $Z_{LB} = Z_{LB}^{new}$

Compute GR_e using the optimal values obtained from solving the LDP (Lagrangian Dual Problem).

Step2.

Solve the original model by fixing ($NT_{uu'v}^t$)
and the inventory variables (IN_j^{crt}) to determine an upper bound Z_{UB}.
Obtain a feasible solution.

IF $Z_{UB}^{old} \geq Z_{UB}^{new}$, **then** $Z_{UB} = Z_{UB}^{new}$

Step.3

Compute $\ell = \frac{\mu(Z_{UB} - Z_{LB})}{GR_e^2}$

IF the stopping conditions are met,

then stop and Z_{LB} is the best solution.

ELSE update the Lagrange multipliers as below and $\mu^{n+1} = max(0, \mu^n + \ell^n GR_e)$.

go to step 1 to calculate new lower and upper bounds.

2.6 Implementation and evaluation

To benchmark the performance of the proposed blood logistics model and solution approach, we compare the model's results under various scenarios, taking into account different experimental datasets. To analyze the impact of different integration mechanisms, we evaluate the performance of the proposed solution approach for a real case study based on data from District 3 of Tehran, Iran. The model was solved using GAMS 24.1.2 with CPLEX as the solver on a Core i7-8565U 2.4 GHz PC with 16 GB RAM running Windows 10.

2.6.1 Case study

Tehran, the capital city of Iran, is an earthquake-prone city and one of the largest cities in Western Asia that has not yet experienced a major earthquake. The Tehran Disaster Mitigation and Management Organization (TDMMO), the institution in charge of the coordination and monitoring of the facilities involved in any emergency response in Tehran, coordinate all relief capacities to tackle any possible earthquake in the city. One of its major concerns is the provision of medical resources, specifically platelet products, for the severely injured population. The Iranian Blood Transfusion Organization (IBTO) is responsible for the provision of blood to hospitals and SMSs in the response phase of emergencies. The collection of blood in Tehran is through either temporary mobile blood facilities such as blood donation buses or permanent facilities located in different regions. The required data for our case study was obtained from TDMMO and its subordinate committees. Tehran is located in a region with several earthquake faults including the north fault that lies between the western part of the "Mosha" fault and the city of Tehran, and it is approximately 90 kilometres long. If the north fault becomes active the damage from an earthquake will be severe. Estimates of the number of affected people and the vulnerability associated with each district of Tehran were obtained from the Tehran Earthquake Damage Estimation System (TEDES) based on an earthquake measuring 7 on the Richter scale and a population density of about 10,000 people per square kilometre (District 3 of Tehran City; total population of 300,000 and total area of 3,000 Hectares) (Tehran.ir/district3). This information is displayed in Figure 2.3 [53].

2.6.2 Data

In this section, the information concerning the case under study is provided:

2.6.2.1 Supply and demand

The travel time between facilities, the available storage capacity for platelets, the number of injured people in the affected region and the average number of platelets of type h required per

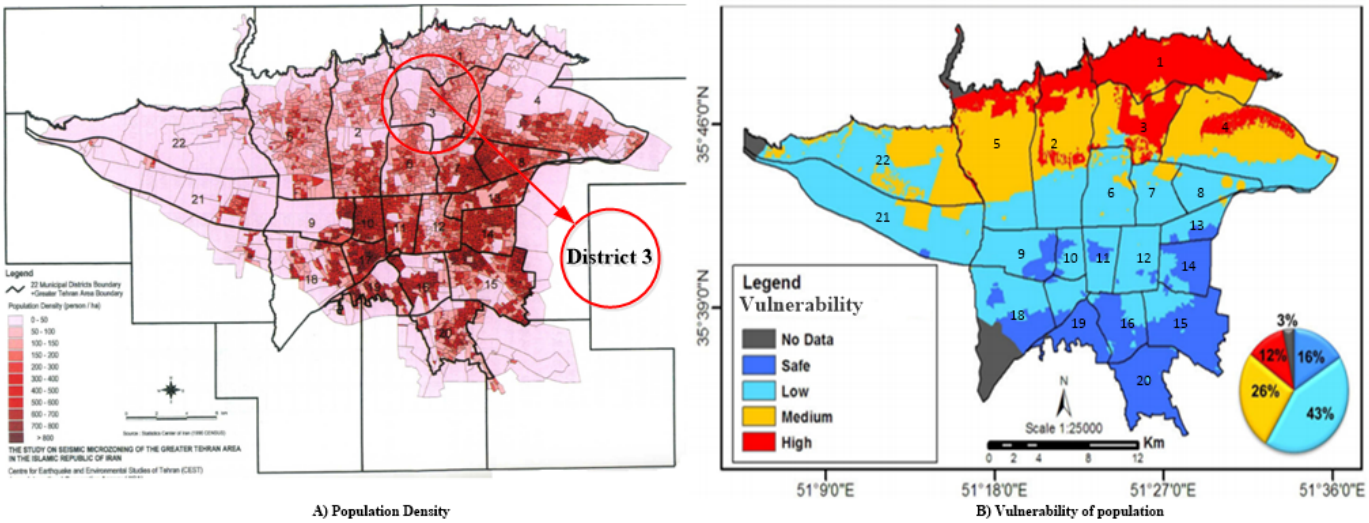

Figure 2.3: Population density around Tehran's north fault and seismic map of vulnerable areas.

injured person were all provided by the IBTO and the TDMMO. The affected population is set to 10 per cent of the total population of District 3, Tehran (3,000 people). The number of affected people of each type (PDZ_h) is considered uncertain following a uniform probability distribution U(450,600). This means that we have finite support as well as equally likely events. The number of platelet donations (each donation is considered to be a bag of platelets) at BRUs is assumed to be 300 per day (the same for all BRUs). We only consider the case where the number of injuries decreases over time whereas the platelet supply increases due to an increased level of donation in response to the disaster. The reason for having a decreasing demand (i.e., fewer people requiring platelets) is that the number of impacted people who may be found and need platelets typically decreases during the first 72 hours of a disaster. Stock levels at all BRUs are considered to be 50 platelet bags per day for a 5-day operation. As regards the apheresis method, the average number of extracted platelet bags per donor (τ) is 7. The number of platelet bags needed by an injured person of type h is determined to be from 3 to 6 [4]. It should be noted that special field transfusion units for SMSs are considered storage containers for multi-type blood products, having a capacity of 150-250 platelet units (www.military-medicine.com/article/3574).

. **A. Cost component**

Table 2.3 provides other inputs obtained from the literature. The coordination costs include not only the administration costs associated with updating, sharing, and analyzing the inventory and demand information but also the costs related to preparing and evaluating the collaboration proposals and acquiring bags of platelets from other facilities. The administration costs are based on TDMMO experts' opinions. The transportation costs are calculated based on transportation times and a unit cost of $100/mile in the case of a special blood bus (SBB) and a unit cost of $120/mile for an ambulance. It should be noted that the transportation costs are assumed to be linear with respect to the number of trips but not the number of platelets bags transported.

Table 2.3: Cost parameters from the literature

Parameters		Value			Unit	Reference
		BRU	**Hospital**	**SMS**		
CC*	**PC***	400	538.72	-	**$/per blood bag**	Pierskalla [50]
	Adm-C*	100	200	-		Toner et al. [63]
Wastage cost		250	150	150	**$/ per blood bag**	Chung et al. [7]
Inventory cost		1.25	1.25	1.25	**$/per blood bag per day**	Hess and Thomas [23]
						Toner et al. [63]
Shortage cost		1000	1500	1500	**$/ per blood bag**	Chung et al. [7]
*Adm-C: administrative cost PC: purchase cost CC: coordination cost *Administration cost occurs when horizontal (e.g., hospital-to-hospital) resource sharing happens.						

B.Survival probability

In our model, we assume that all patients belong to a particular type h and their survival probability f^{ht} depends on the particular injury level. Here, the START triage method is employed to classify injured people into types. According to Jin et al. [30], 95% of patients die if they cannot receive medical treatment before the time at which their survival probability falls below 10%. In this study, only patients with a survival probability between 30% and 80% are considered, with a lower probability for severely injured people and a higher probability for mildly injured cases.

C. Vehicles and travel times

BRUs and hospitals, respectively, use two types of vehicles, SBBs and ambulances. The capacity of SBBs is 100 platelets and the capacity of ambulances is two people. It is assumed that vehicles travel at 80 miles/hour on average.

D. Time scale

The selection of the appropriate time scale is very important [1]. Since the problem is at the tactical level, it is suitable to have longer time periods (e.g., days) compared with very detailed operational-level planning (e.g., seconds, minutes). Typically, a time horizon of 72 hours to one week is considered for short-term disaster response operations (OCHA, 2017). However, since two days are required for the testing and processing of new platelets, the relief response operation time is assumed to be seven days. Notably, although the unmet demand at any hospital or SMS can be carried over to the next period, we consider seven days of relief operations, as it is the typical short-term immediate duration for the response phase of DROs.

2.6.3 Computational Results - Deterministic Models

In this section, the results obtained using the deterministic version of both the proposed model (EL-VHRS) and the emergency logistics model with no resource sharing (EL) are compared in terms of different performance metrics.

2.6.3.1 Trade-off between relief costs and shortage of platelets

In our case study, the under-target penalties and related costs are offset by the coordination costs while in previous models in the literature [16, 47] the coordination costs are not paid and the under-target penalties and related costs are high. Hence, in Figure 2.4, we illustrate the shortage reduction obtained via the EL-VHRS model when compared to the EL, so the reader can observe the value of coordination. Figure 2.4 (A and B), in grey, show the total number of unserved patients for the deterministic EL and EL-VHRS models, respectively, for a 7-day time horizon. As shown in Figure 2.4 (A), hospitals, SMSs and BRUs all perform significantly worse in terms of unmet demand and under target values, respectively, without coordination (see hospital 6 and BRU 4). For example, although no patients are transferred to SMSs 18 and 21 (while receiving platelets from BRUs 5 and 9), these SMSs are unable to share platelets with other shelters. On the other hand, Figure 2.4 (B) shows the improved performance (in terms of unmet demand and under-target values) of the EL-VHRS compared to the EL. The platelets sharing from SMS 21 to SMS 22 and BRU 9 to BRU 4 reduces (by more than 50%) the number of unserved injured people at SMS 22 and under-target inventory levels at BRU 4, respectively. Overall, the results in Figure 2.4 show that the resource sharing among BRUs, hospitals and SMSs decreases the number of unserved injured people and reduces the level of platelets' under-target by a substantial amount. Table 2.4 summarizes the impact of integration (resource sharing) among the facilities for the aforementioned case study (three BRUs, five hospitals, six SMSs, two types of vehicles, and eight blood groups for a 72-hour relief operation) by comparing the output from the deterministic EL-VHRS model to that from the deterministic EL model. In terms of the level of platelets' under-target at BRUs, the EL-VHRS outperforms the EL model by 22%. The EL-VHRS model also serves more patients and reduces significantly the total number of unserved patients at hospitals (50.6 % reduction with respect to the EL model). Using the EL-VHRS model, the total number of unserved patients at SMSs is reduced by 51.3% on average. Although, in the presence of integration (resource sharing), there are extra costs associated with coordination and transportation between facilities, the deterministic version of the EL-VHRS model reduces shortages, which is more costly in relief operations. The net result is a 31% reduction in the total cost.

2.6.4 Computational results - Robust Models

To evaluate the efficiency of the proposed solution hybrid approach for the robust model, we apply it to both the EL-VHRS and the EL models under various problem settings.

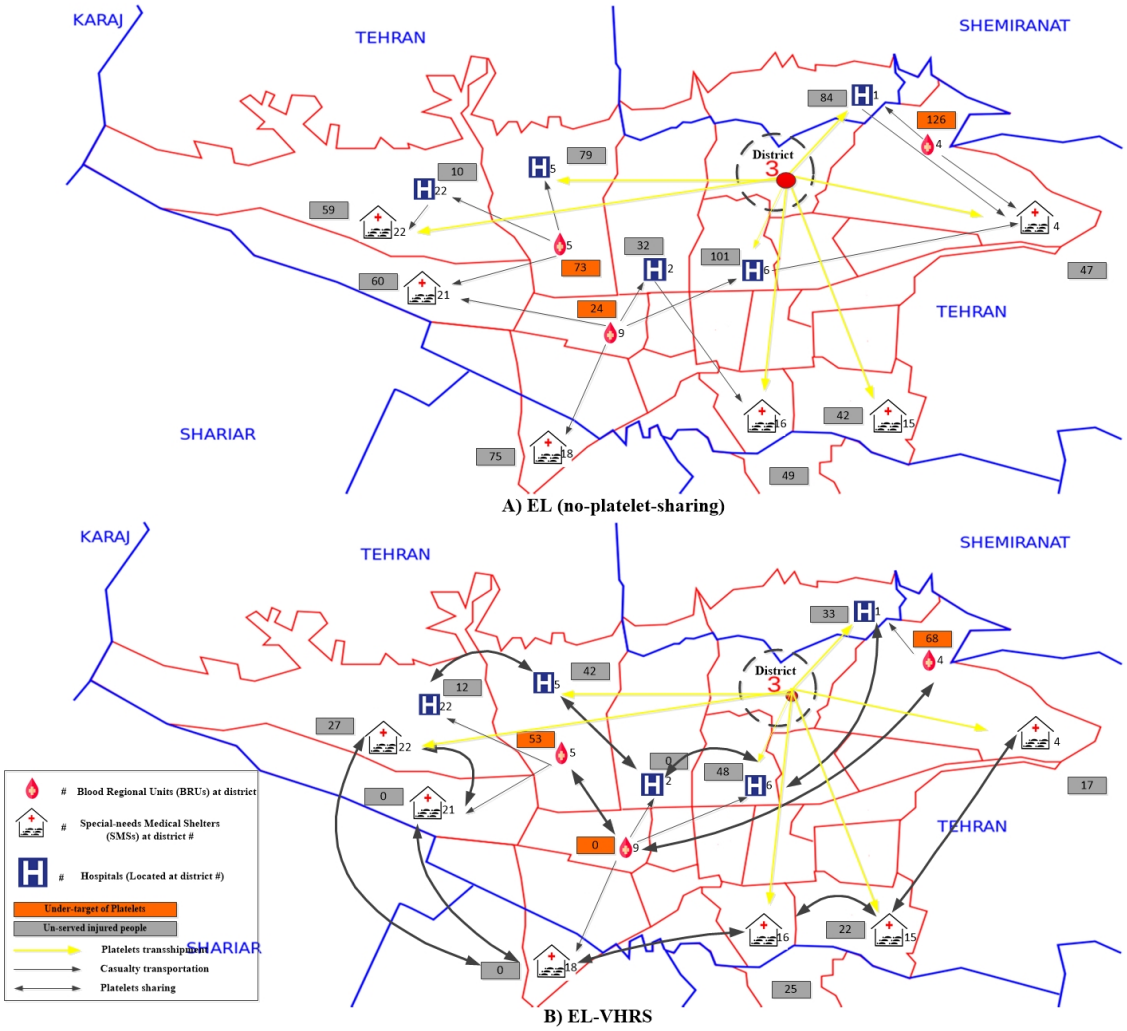

Figure 2.4: Comparison of the solution of the deterministic EL (No-Platelets Sharing) and EL-VHRS models in terms of shortage amount and the number of unserved injuries for District 3 of Tehran.

Table 2.4: Comparison of the solution obtained from the deterministic EL-VHRS and EL models in terms of the total cost, under-target inventory levels, and unserved people by injury type.

Points	Total	EL	EL-VHRS	Decrease/increase
BRU	**PLT-UT**	223	172	-22%
Hospital	**USI h=1**	70	31	-56%
	USI h=2	81	40	-51%
	USI h=3	94	50	-47%
SMS	**USI h=1**	77	39	-49%
	USI h=2	52	28	-46%
	USI h=3	80	33	-59%
Total Cost		4.2 M$	2.9M$	-31%
***PLT-UT=under-target level, USI=Unserved people**				

Table 2.5: Characteristics of the three datasets used to evaluate the performance of the proposed approach

	$\|I\|$	$\|J\|$	$\|K\|$	$\|T\|$	$\|V\|$	$\|C\|$	$\|S\|$
Dataset 1	3	5	6	4	5	8	5
Dataset 2	5	8	12	5	7	8	10
Dataset 3	7	10	15	7	8	8	15

Table 2.6: Summary of the performance of the proposed hybrid solution approach for larger datasets for the EL and EL-VHRS models.

Dataset	El-VHRS			Dataset	EL			***GAP
	(*ϵ ×1000$)	*USI	RunTime		(ϵ ×1000$)	USI	RunTime	
	**B-to-B & H-to-H & S-to-S				**B-to-B & H-to-H & S-to-S			
1	3,200	51	0:02:01	1	6,352	79	1:04:00	1.00
	3,165	53	0:01:54		6,342	84	1:32:56	1.00
	3,120	54	0:01:56		6,340	100	1:59:13	1.00
	3,100	59	0:02:23		6,239	96	1:45:21	1.00
	3,099	61	0:01:49		6,181	95	1:00:44	1.00
2	5,019	74	0:11:43	2	9,189	106	2:10:59	1.00
	5,120	79	0:12:02		9,193	116	3:52:31	1.00
	5,180	81	0:15:01		9,104	125	3:25:34	1.00
	5,365	82	0:16:49		9,099	112	3:01:52	1.00
	5,491	86	0:19:34		9,004	105	4:01:22	1.00
3	7,899	117	0:51:11	3	11,103	129	4:24:52	1.00
	7,921	133	0:59:06		11,126	145	5:25:33	1.00
	8,240	145	0:48:56		11,145	159	5:45:01	1.00
	8,331	130	0:49:41		11,039	149	5:12:59	1.00
	8,478	119	1:05:01		11,001	136	5:11:27	1.00

*ϵ ×1000: **Cost tolerance**, **USI**: unserved injuries

BB:BRU-to-BRU, **HH**:hospital-to-hospital, **SS**: shelter-to-shelter

***GAP**: (UB-LB)/UB)×100

2.6.4.1 Computational experiments

For the robust version of the EL-VHRS model, we designed a set of test experiments to (1) evaluate the performance of the proposed hybrid solution method under different scenarios, (2) identify possible tradeoffs between relief costs and the number of unserved patients, and (3) quantify the benefits of the proposed robust stochastic programming approach by comparing its performance against that of the deterministic EL model. Three random instances were generated with different problem sizes as shown in Table 2.5. For these three datasets, Table 2.6 presents the numerical results obtained using the hybrid solution method for different cost tolerances (upper bound on the second objective function, ϵ_2).

From left to right, the columns "cost tolerance (ϵ ×1000$)" and "the total number of unserved injuries (USI)" provide the outcome from the fully integrated model (EL-VHRS) and from the model without integration (EL). The column labelled "GAP" is the per cent difference between the upper and lower bounds. The model runtime is given in the next column. While the augmented

epsilon constraint method (coded in GAMS) was unable to provide feasible solutions for all datasets within 24 hours, the hybrid solution method was capable of reaching optimal solutions for all instances within a reasonable amount of time. High-quality solutions that are close to optimal could be obtained in a shorter runtime by setting the termination condition at some pre-specified GAP value rather than looking for zero-gap solutions. These results show that it is possible to achieve a significant reduction in the number of unserved injuries with only a minor increase in relief operation costs. For example, for Dataset 1, a minor decrease in the total number of unserved people brings with it an increase from 3,100 to 3,120 of the relief cost tolerance (compare this to the next range of cost tolerance values where ϵ changes from 3,099 to 3,100). On the other hand, for Dataset 1 EL, a decrease in the total number of unserved people from 95 to 72 occurs when the relief cost increases from 6,181 to 6,352 (171×1000 extra cost). As the results in Table 2.6 indicate, EL-VHRS has a better performance in terms of the number of unserved injuries. Thus, platelet sharing among BRUs, Hospitals, and SMSs allows a better distribution of platelets to each facility, which ultimately may increase the survival of injured people. Even though the EL-VHRS has more variables, the proposed hybrid solution approach can reach the optimal solution in a shorter time compared to the EL model. For example, for the largest dataset (Dataset 3), a solution to the EL-VHRS was found within around 1 hour while it took more than five hours for the EL model. Overall, the EL-VHRS model outperforms the EL model in terms of solution time as well as the chosen performance measures.

2.6.4.2 Individual impacts of different integration mechanisms on the platelets supply chain

. In this section, we evaluate and compare three integration mechanisms structures: EL network with horizontal integration (ELH), EL network with vertical integration (ELV), and EL network with no integration. Note that the full integrated scenario was analyzed thoroughly in the previous sections.

The effect of integration mechanisms on wastage and shortage

As mentioned before, horizontal and vertical integration mechanisms are procedures used to reduce high levels of shortage and wastage at different facilities. According to their age and group, received platelet bags in SMSs and hospitals are categorized and stored in blood banks. Upon the arrival of patients, platelets are matched in terms of age and group with patients depending on their injury level. Table 2.7 summarizes the results obtained for each form of integration for that instance(s). Considering that there was inventory available at the beginning of the planning horizon at each facility, the total shortage was 9.92%, 7.77%, and 11.22%, on average, for the ELV, ELH, and EL structures, respectively.

Table 2.7: The effect of integration on shortage and wastage levels

	Platelet group	ELV*						ELH*						EL*	
		B-H**		B-S		H-S		B-B		H-H		S-S			
		*SH****	*WS*	*SH*	*WS*	*SH*	*WS*	*SH*	*WS*	*SH*	*WS*	*SH*	*WS*	*SH*	*WS*
All facilities (BRUs, Hospitals, and SMSs)	**O+**	39	0	38	10	30	5	26	0	15	2	19	0	41	17
	O-	56	14	55	0	41	9	37	0	25	0	29	8	61	29
	B+	18	0	12	32	12	18	10	0	12	0	16	8	19	9
	B-	21	21	18	30	19	21	12	16	12	4	16	11	20	11
	A+	20	16	15	0	19	0	10	15	14	9	22	3	15	8
	A-	8	0	21	19	18	0	16	19	21	14	17	0	20	7
	AB+	15	0	20	20	21	0	24	0	18	6	13	0	17	12
	AB-	6	15	3	3	11	7	10	0	17	4	10	4	9	1
	Total	183	66	182	114	171	60	145	50	134	39	142	34	202	94
	Total substitution	54		61		55		40		41		38		40	
	Total demand	1800						1800						1800	

* ELV: Emergency logistics network with vertical integration; ELH: Emergency logistics network with horizontal integration, EL: Emergency logistics with no integration

** B-H (BRUs to hospitals); B-S (BRUs to SMSs), H-S (hospitals to SMSs), B-B (BRUs to BRUs), H-H (hospitals to hospitals), S-S (SMSs to SMSs)

*** SH (shortage level); WS (wastage level)

Similarly, on average, the total wastage was 4.43%, 2.23%, and 5.2% for the three structures, respectively. An interesting result is the higher demand satisfaction provided by the horizontal (ELH) and vertical (ELV) mechanisms when compared to the non-integrated model (EL). It is important to note that there are a few cases showing both wastage and shortage for a platelet group. Overall, the results show a satisfactory performance of the ELV mechanism in terms of platelet wastage and shortage.

The effect of integration mechanisms on platelets substitution

Figure 2.5 shows the total number of substitutions among different blood groups considering ABO/Rh(D)-compatible platelet substitution priority values (Table 2.1). According to Figure 2.5, as expected, the platelets consumption for each blood group is in descending order O+, A+, B+, O-, A-, B-, AB+ and AB- for the three mechanisms. Generally speaking, it is a good result since approximately 70 % of the total population have blood group O+ or A+. Due to high shortage levels during disasters, a common strategy is to employ substitutions among blood groups to satisfy demand. It should be noted that substitution is not recommended these days due to possible severe transfusion-related reactions. For example, haemolysis and circulating immune complexes are possible if a recipient with platelets in the ABO group A receives platelets from the ABO group O. It is an interesting result to see that the ELH and ELV mechanisms handle substitutions better. For example, for the ELH mechanism, the blood group O- has the highest substitution rate for the demand for blood group O+, while the blood group B- is the most often used to meet the demand for blood group O-.

2.6.4.3 Solution robustness versus model robustness

As mentioned in Subsection 2.4.3, we considered a penalty value (ϑ) associated with the violation of Equation (2.4) which corresponds to the cost of constraint violation for unserved patients in

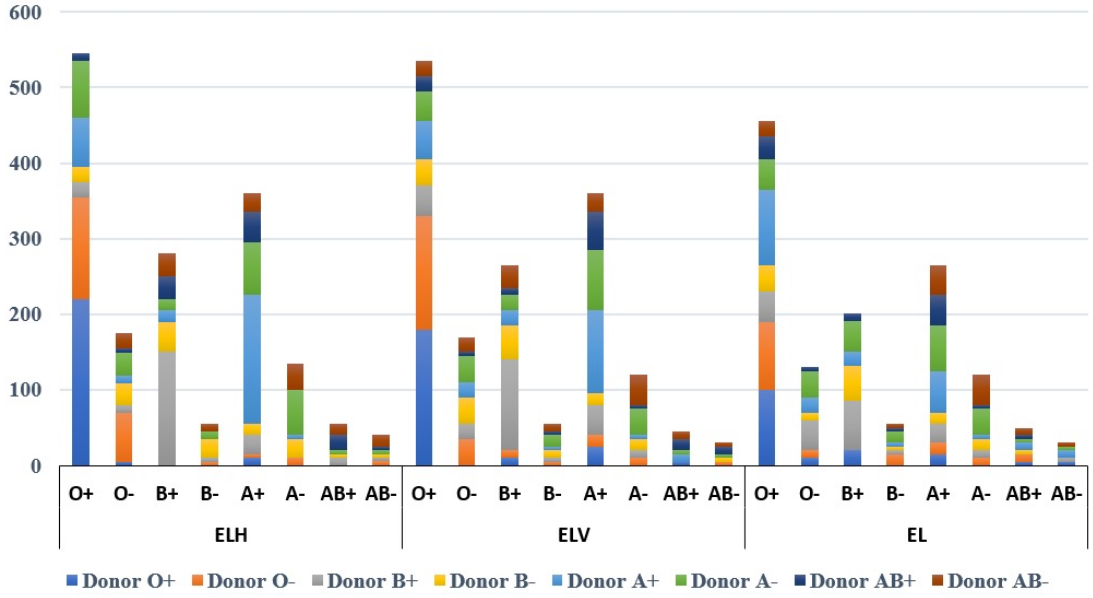

Figure 2.5: The effect of integration mechanisms on the platelets substitution.

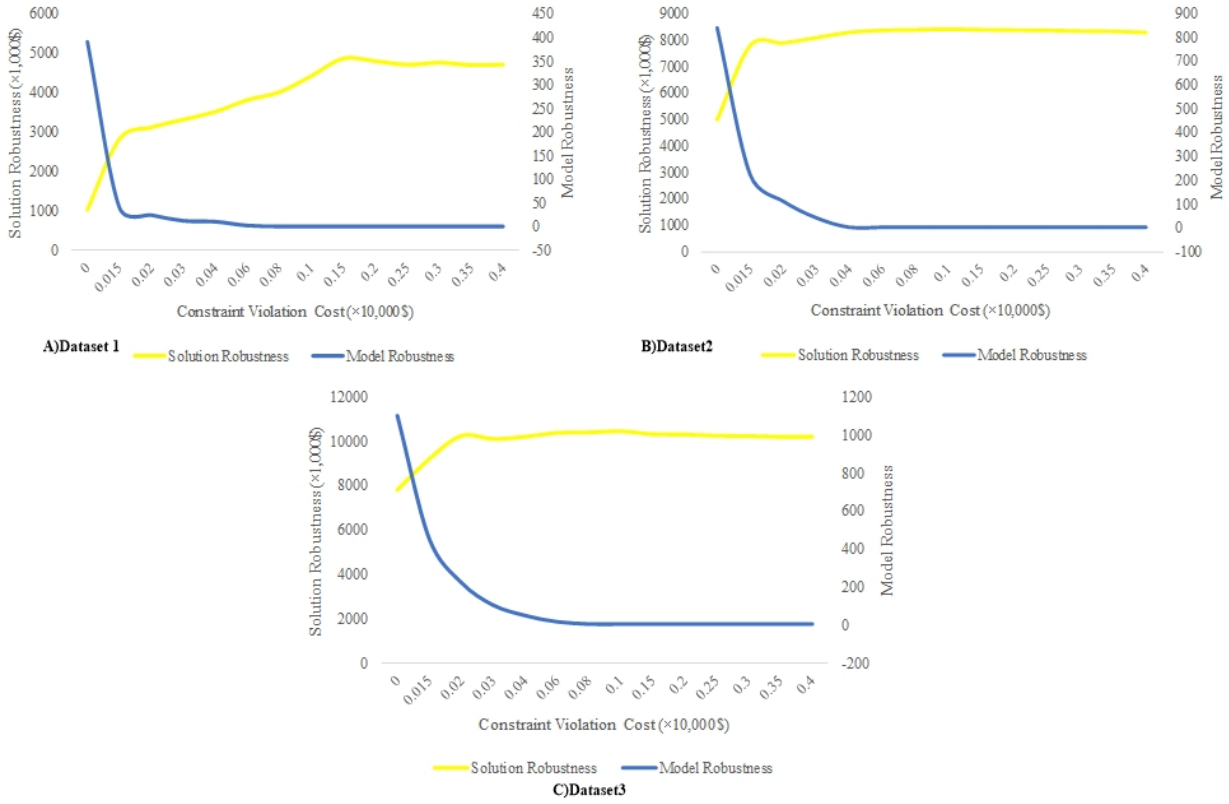

Figure 2.6: Tradeoff between relief cost and platelets shortage amount for Datasets 1 to 3

period t. This penalty is placed in the objective function (2.17) to find an optimal or near-optimal solution (solution robustness) and a feasible or near-feasible solution (model robustness). The tradeoff between solution and model robustness is a challenging area in the robust optimization literature [29]. A risk-taker may set small values for any penalties associated with the number of unserved patients that reduce the total relief cost by focusing decisions on the cost minimization objective. On the other hand, to reduce the level of unserved injured people in SMSs and hospitals for each age group, a risk-averse decision maker may choose higher values for these penalties yielding higher total costs but reducing the number of unserved patients. By changing the constraint violation penalty, a decision maker can determine the trade-off between the total expected cost and the number of unserved patients for each scenario. Figure 2.6 shows the trade-off between solution robustness and model robustness for different constraint violation costs for all three datasets provided in Table 2.5. We can see that the total relief cost, which represents solution robustness, increases as the violation cost increases, but the number of unserved patients, representing model robustness, decreases. Setting up a robust optimization problem with no unserved patients will require a large penalty value to avoid constraint violation. For instance, for Dataset 1 at ϑ=1,500, a robust objective function incurs a cost of \$4,857 ($\times 10^3$) but ensures that no unserved patients are present under any scenario.

Moreover, the robust optimization approach can also be adjusted for different weights (λ). As already mentioned, λ indicates the weight placed on the solution variance. The solution is less sensitive to uncertainty as λ increases. The influence of this weight (λ) on the expected number of unserved injuries is illustrated in Figure 2.7. For Dataset 1, Figure 2.7 shows that an increase in this weight decreases the expected number of unserved injured people. At $\lambda = 9$, the expected number of injured people reaches a minimum, after which the expected number of unserved remains constant.

2.6.5 Managerial insights

The results demonstrate that the performance of emergency logistics operations for platelets logistics with the coordinated structure is significantly improved in terms of unserved injured people and total cost compared to the non-integrated and non-coordinated logistics network. Overall, the following managerial insights are demonstrated from implementing the robust EL-VHRS approach: **(1)** Those managing and controlling the logistics of resources among the facilities in times of disaster can benefit from different forms of integration to help balance the relief network and guard against potential shortage and wastage of platelets. Even if having a fully integrated network is not possible, even partial integration can reduce the number of unserved injuries and wastage of platelets significantly compared with a non-integrated relief network. It is recommended that

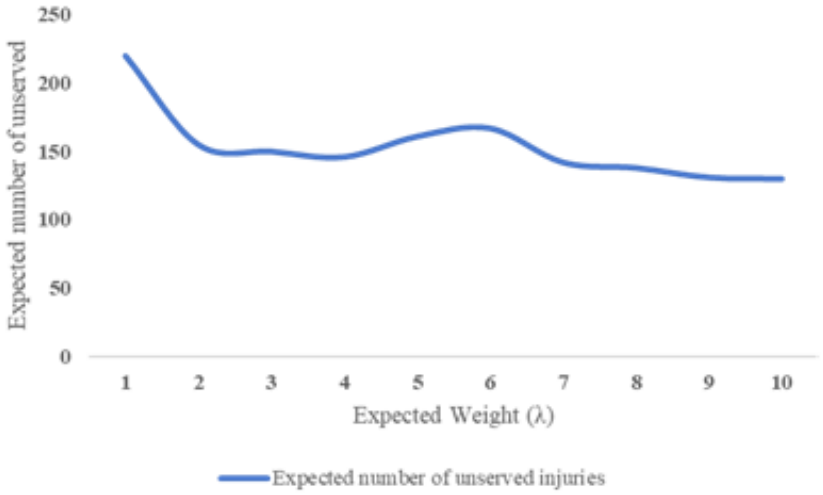

Figure 2.7: Impact of weight λ on the expected shortage (corresponding to the number of unserved injured people) for Dataset 1

decision-makers apply the fully integrated mechanism first, or if not possible, then the ELH rather than the ELV;

(2) By considering the multi-group platelets substitution procedure along with integration mechanisms, the relief logistics managers can better control the inventory and flow of platelets within the network under a range of potential situations (e.g., an increase in new donations (supply) or a more prolonged disaster relief operation). Although the substitution procedure is a common practice to reduce platelet shortages, the results demonstrate that the integration mechanisms can reduce the substitution rates among blood groups. As stated before, substitution is discouraged due to severe potential reactions. However, in disasters, due to the high demand for platelets from the affected people, the application of both blood substitution and integration is recommended for satisfactory outcomes;

(3) Matching fresh, young, and old platelets with injury levels can be an excellent strategy to reduce shortage and wastage. A matching policy enables platelets of specific blood groups to be shipped to hospitals and SMSs serving casualties and needing the particular blood group.

2.7 Conclusions and recommendations

With a significant number of natural disasters happening globally, the need for better planning of disaster relief operations is becoming increasingly relevant. Challenges to the proper management of disasters include the existence of several response facilities with limited transport and storage capacity, patients with varying urgency levels, and perishable supplies. In this chapter, an optimization model involving BRUs, hospitals, and SMSs was developed to efficiently manage one of the most limited and perishable resources, platelets, during DROs which aims to decrease the

total cost and unfulfilled demand for platelets from the affected population. To better manage the relief logistics network, we proposed an integrated robust bi-objective model that considers resource sharing and demand uncertainty for each relief organization. To demonstrate the effectiveness of the proposed robust bi-objective model, an illustrative example including six hospitals, four blood regional units and eight special-needs medical shelters was solved by a hybrid method using both Lagrangian relaxation and the epsilon-constraint approach. In addition, sensitivity analysis was performed to ascertain the impact of a number of key parameters such as shortage and wastage levels of platelets. Future research in this area will model the interaction between relief organizations with different levels of responsibility, and undependable different resources and capacity levels which is more complex than the centralized problem setting analyzed here. Furthermore, since each agent (BRU, Hospital, or SMS) may have its own budget/cost considerations, a future research endeavour would be to look at the coordination problem that would come into play when each agent tries to minimize their cost as opposed to a central authority minimizing the total cost. Since platelet collection, production, and testing processes at the clinical stage were not studied here, we also plan to integrate these processes into the proposed logistics network.

2.8 Bibliography

[1] Abbas Afshar and Ali Haghani. Modeling integrated supply chain logistics in real-time large-scale disaster relief operations. *Socio-Economic Planning Sciences*, 46(4):327–338, 2012.

[2] Mina Akbarpour, S Ali Torabi, and Ali Ghavamifar. Designing an integrated pharmaceutical relief chain network under demand uncertainty. *Transportation Research Part E: Logistics and Transportation Review*, 136:101867, 2020.

[3] Burcu Balcik, Benita M Beamon, Caroline C Krejci, Kyle M Muramatsu, and Magaly Ramirez. Coordination in humanitarian relief chains: Practices, challenges and opportunities. *International Journal of Production Economics*, 126(1):22–34, 2010.

[4] Richard J. Benjamin, Louis Katz, Richard.R Gammon, Susan L. Stramer, and Eva Quinley. The argument(s) for lowering the us minimum required content of apheresis platelet components. *Transfusion*, 59:779–788, 2019.

[5] Dimitris Bertsimas and Melvyn Sim. The price of robustness. *Operations research*, 52(1): 35–53, 2004.

[6] Sara Cheraghi and Seyyed-Mahdi Hosseini-Motlagh. Responsive and reliable injured-oriented blood supply chain for disaster relief: a real case study. *Annals of Operations Research*, 291 (1):129–167, 2020.

[7] Koo-Whang Chung, Sridhar Basavaraju, and et al. Mu, Yi. Declining blood collection and utilization in the united states. *Transfusion*, 56(9):2184–2192, 2016.

[8] Ismail Civelek, Itir Karaesmen, and Alan Scheller-Wolf. Blood platelet inventory management with protection levels. *European Journal of Operational Research*, 243(3):826–838, 2015.

[9] Matthew D. Dean and Suresh K. Nair. Mass-casualty triage: Distribution of victims to multiple hospitals using the save model. *European Journal of Operational Research*, 238(1): 363–373, 2014.

[10] Maryam Dehghani and Babak Abbasi. An age-based lateral-transshipment policy for perishable items. *International Journal of Production Economics*, 198:93–103, 2018.

[11] Maryam Dehghani, Babak Abbasi, and Fabricio Oliveira. Proactive transshipment in the blood supply chain: A stochastic programming approach. *Omega*, 98:102112, 2021.

[12] Ali Diabat, Armin Jabbarzadeh, and Amir Khosrojerdi. A perishable product supply chain network design problem with reliability and disruption considerations. *International Journal of Production Economics*, 212:125–138, 2019.

[13] Matthias Ehrgott and Margaret M Wiecek. Saddle points and pareto points in multiple objective programming. *Journal of Global Optimization*, 32(1):11–33, 2005.

[14] Hamidreza Ensafian and Saeed Yaghoubi. Robust optimization model for integrated procurement, production and distribution in platelet supply chain. *Transportation Research Part E: Logistics and Transportation Review*, 103:32–55, 2017.

[15] Marzieh Eskandari-Khanghahi, Reza Tavakkoli-Moghaddam, Ata Allah Taleizadeh, and Saman Hassanzadeh Amin. Designing and optimizing a sustainable supply chain network for a blood platelet bank under uncertainty. *Engineering Applications of Artificial Intelligence*, 71:236–250, 2018.

[16] Behnam Fahimnia, Armin Jabbarzadeh, Ali Ghavamifar, and Michael Bell. Supply chain design for efficient and effective blood supply in disasters. *International Journal of Production Economics*, 183:700–709, 2017.

[17] Mohamadreza Fazli-Khalaf, Soheyl Khalilpourazari, and Mohammad Mohammadi. Mixed robust possibilistic flexible chance constraint optimization model for emergency blood supply chain network design. *Annals of Operations Research*, 283(1):1079–1109, 2019.

[18] Marshall L Fisher. The lagrangian relaxation method for solving integer programming problems. *Management science*, 50:1861–1871, 2004.

[19] Mitra Habibi-Kouchaksaraei, Mohammad Mahdi Paydar, and Ebrahim Asadi-Gangraj. Designing a bi-objective multi-echelon robust blood supply chain in a disaster. *Applied Mathematical Modelling*, 55:583–599, 2018.

[20] Abdorrahman Haeri, Seyyed-Mahdi Hosseini-Motlagh, Mohammad Reza Ghatreh Samani, and Marziehsadat Rezaei. A mixed resilient-efficient approach toward blood supply chain network design. *International Transactions in Operational Research*, 27(4):1962–2001, 2020.

[21] L. Haimes and L. Wismer. On a bicriterion formulation of the problem of integrated systems identification and system optimization. *IEEE-SMC, SMC-1*, 1:296–297, 1971.

[22] Bayan Hamdan and Ali Diabat. Robust design of blood supply chains under risk of disruptions using lagrangian relaxation. *Transportation Research Part E: Logistics and Transportation Review*, 134:101764, 2020.

[23] JR Hess and MJG Thomas. Blood use in war and disaster: lessons from the past century. *Transfusion*, 43(11):1622–1633, 2003.

[24] Seyyed-Mahdi Hosseini-Motlagh, Mohammad Reza Ghatreh Samani, and Sara Cheraghi. Robust and stable flexible blood supply chain network design under motivational initiatives. *Socio-Economic Planning Sciences*, 70:100725, 2020.

[25] Seyyed-Mahdi Hosseini-Motlagh, Mohammad Reza Ghatreh Samani, and Shamim Homaei. Blood supply chain management: robust optimization, disruption risk, and blood group compatibility (a real-life case). *Journal of Ambient Intelligence and Humanized Computing*, 11(3): 1085–1104, 2020.

[26] Zahra Hosseinifard, Babak Abbasi, Masih Fadaki, and Nigel M Clay. Postdisaster volatility of blood donations in an unsteady blood supply chain. *Decision Sciences*, 51(2):255–281, 2020.

[27] Kai Huang, Yiping Jiang, Yufei Yuan, and Lindu Zhao. Modeling multiple humanitarian objectives in emergency response to large-scale disasters. *Transportation Research Part E: Logistics and Transportation Review*, 75:1–17, 2015.

[28] Maqsood I. and Huang G.H. A dual two-stage stochastic model for flood management with inexact-integer analysis under multiple uncertainties. *Stochastic Environmental Research and Risk Assessment*, 27(3):643–657, 2013.

[29] Armin Jabbarzadeh, Behnam Fahimnia, and Stefan Seuring. Dynamic supply chain network design for the supply of blood in disasters: A robust model with real world application. *Transportation Research Part E: Logistics and Transportation Review*, 70:225–244, 2014.

[30] Sukho Jin, Sukjae Jeong, Jangyeop Kim, and Kim Kyungsup. A logistics model for the transport of disaster victims with various injuries and survival probabilities. *Annals of Operations Research*, 230:17–33, 2015.

[31] Afshin Kamyabniya, MM Lotfi, Hua Cai, Hasan Hosseininasab, Saeed Yaghoubi, and Yuehwern Yih. A two-phase coordinated logistics planning approach to platelets provision in humanitarian relief operations. *IISE Transactions*, 51(1):1–21, 2019.

[32] Afshin Kamyabniya, MM Lotfi, Mohsen Naderpour, and Yuehwern Yih. Robust platelet logistics planning in disaster relief operations under uncertainty: a coordinated approach. *Information Systems Frontiers*, 20(4):759–782, 2018.

[33] Afshin Kamyabniya, Mohammad Mehdi Lotfi, Hassan Hosseini Nasab, and Saeed Yaghoubi. Multiple-organizational coordination planning for humanitarian relief operations. *Journal of Industrial and Systems Engineering*, 11(Special issue: 14th International Industrial Engineering Conference):29–42, 2018.

[34] Afshin Kamyabniya, Zohre Noormohammadzadeh, Antoine Sauré, and Jonathan Patrick. A robust integrated logistics model for age-based multi-group platelets in disaster relief operations. *Transportation Research Part E: Logistics and Transportation Review*, 152:102371, 2021.

[35] Xiaohong Li, Linyan Sun, and Jie Gao. Coordinating preventive lateral transshipment between two locations. *Computers & Industrial Engineering*, 66(4):933–943, 2013.

[36] Chao Liang, Suresh P Sethi, Ruixia Shi, and Jun Zhang. Inventory sharing with transshipment: Impacts of demand distribution shapes and setup costs. *Production and Operations Management*, 23(10):1779–1794, 2014.

[37] Zu-Jun Ma, Ke-Ming Wang, and Ying Dai. An emergency blood allocation approach considering blood group compatibility in disaster relief operations. *International Journal of Disaster Risk Science*, 10(1):74–88, 2019.

[38] Amir H Masoumi, Min Yu, and Anna Nagurney. Mergers and acquisitions in blood banking systems: A supply chain network approach. *International Journal of Production Economics*, 193:406–421, 2017.

[39] George Mavrotas. Effective implementation of the ε-constraint method in multi-objective mathematical programming problems. *Applied mathematics and computation*, 213(2):455–465, 2009.

[40] George Mavrotas and Kostas Florios. An improved version of the augmented ε-constraint method (augmecon2) for finding the exact pareto set in multi-objective integer programming problems. *Applied Mathematics and Computation*, 219(18):9652–9669, 2013.

[41] MedicalNewsToday. Everything you need to know about blood types, 2020. URL `https://www.medicalnewstoday.com/articles/218285`.

[42] Joern Meissner and Olga V Senicheva. Approximate dynamic programming for lateral transshipment problems in multi-location inventory systems. *European Journal of Operational Research*, 265(1):49–64, 2018.

[43] Huseyin Onur Mete and Zelda B Zabinsky. Stochastic optimization of medical supply location and distribution in disaster management. *International Journal of Production Economics*, 126 (1):76–84, 2010.

[44] John M Mulvey, Robert J Vanderbei, and Stavros A Zenios. Robust optimization of large-scale systems. *Operations research*, 43(2):264–281, 1995.

[45] Anna Nagurney, Amir H Masoumi, and Min Yu. Supply chain network operations management of a blood banking system with cost and risk minimization. *Computational management science*, 9(2):205–231, 2012.

[46] Anna Nagurney, Amir H Masoumi, and Min Yu. Supply chain network operations management of a blood banking system with cost and risk minimization. *Computational Management Science*, 9(2):205–231, 2012.

[47] Mehdi Najafi, Kourosh Eshghi, and Sander de Leeuw. A dynamic dispatching and routing model to plan/re-plan logistics activities in response to an earthquake. *OR spectrum*, 36(2): 323–356, 2014.

[48] Dilupa Nakandala, Henry Lau, and Paul KC Shum. A lateral transshipment model for perishable inventory management. *International Journal of Production Research*, 55(18):5341–5354, 2017.

[49] Seung Jae Park, Guoming Lai, and Sridhar Seshadri. Inventory sharing in the presence of commodity markets. *Production and Operations Management*, 25(7):1245–1260, 2016.

[50] William P Pierskalla. *Supply chain management of blood banks*, pages 103–145. Springer, 2005.

[51] Reza Ramezanian and Zahra Behboodi. Blood supply chain network design under uncertainties in supply and demand considering social aspects. *Transportation Research Part E: Logistics and Transportation Review*, 104:69–82, 2017.

[52] Niloufar Razavi, Hadi Gholizadeh, Sina Nayeria, and Tannaz Alizadeh Ashrafi. A robust optimization model of the field hospitals in the sustainable blood supply chain in crisis logistics. *Journal of the Operational Research Society*, pages 1–26, 2020.

[53] F Rezaie and M Panahi. Gis modeling of seismic vulnerability of residential fabrics considering geotechnical, structural, social and physical distance indicators in tehran using multi-criteria decision-making techniques. *Natural Hazards and Earth System Sciences*, 15(3):461–474, 2015.

[54] Ying Rong, Lawrence V Snyder, and Yang Sun. Inventory sharing under decentralized preventive transshipments. *Naval Research Logistics (NRL)*, 57(6):540–562, 2010.

[55] Faraz Salehi, Masoud Mahootchi, and Seyed Mohammad Moattar Husseini. Developing a robust stochastic model for designing a blood supply chain network in a crisis: A possible earthquake in tehran. *Annals of Operations Research*, pages 1–25, 2017.

[56] Mohammad Reza Ghatreh Samani, Seyyed-Mahdi Hosseini-Motlagh, and Shamim Homaei. A reactive phase against disruptions for designing a proactive platelet supply network. *Transportation Research Part E: Logistics and Transportation Review*, 140:102008, 2020.

[57] Mohammad Reza Ghatreh Samani, S Ali Torabi, and Seyyed-Mahdi Hosseini-Motlagh. Integrated blood supply chain planning for disaster relief. *International journal of disaster risk reduction*, 27:168–188, 2018.

[58] Sabine F Schulz and Alexander Blecken. Horizontal cooperation in disaster relief logistics: benefits and impediments. *International Journal of Physical Distribution & Logistics Management*, 40(8/9):636–656, 2010.

[59] Canadian Blood Services. Abo/rh(d) compatibility for multi-group platelets, 2020. URL `https://www.blood.ca/en/blood/donating-blood/what-my-blood-type`.

[60] Bhuvnesh Sharma, Maria Ramkumar, Nachiappan Subramanian, and Bharat Malhotra. Dynamic temporary blood facility location-allocation during and post-disaster periods. *Annals of Operations Research*, 283(1):705–736, 2019.

[61] Jiuh-Biing Sheu and Cheng Pan. Relief supply collaboration for emergency logistics responses to large-scale disasters. *Transportmetrica A: transport science*, 11(3):210–242, 2015.

[62] Inkyung Sung and Taesik Lee. Optimal allocation of emergency medical resources in a mass casualty incident: Patient prioritization by column generation. *European Journal of Operational Research*, 252(2):623–634, 2016.

[63] Richard W Toner, Laura Pizzi, Brian Leas, Quigley Alyson Ballas, Samir K, and Neil I Goldfarb. Costs to hospitals of acquiring and processing blood in the us: a survey of hospital-based blood banks and transfusion services. *Appl Health Econ Health Policy*, 9(1):29–37, 2011.

[64] Ke-Ming Wang and Zu-Jun Ma. Age-based policy for blood transshipment during blood shortage. *Transportation Research Part E: Logistics and Transportation Review*, 80:166–183, 2015.

[65] David D Yao, Sean X Zhou, and Weifen Zhuang. Joint initial stocking and transshipment—asymptotics and bounds. *Production and Operations Management*, 25(2):273–289, 2016.

[66] Chian-Son Yu and Han-Lin Li. A robust optimization model for stochastic logistic problems. *International Journal of Production Economics*, 64:385–397, 2000.

[67] Behzad Zahiri and Mir Saman Pishvaee. Blood supply chain network design considering blood group compatibility under uncertainty. *International Journal of Production Research*, 55(7): 2013–2033, 2017.

[68] Deming Zhou, Lawrence C Leung, and William P Pierskalla. Inventory management of platelets in hospitals: Optimal inventory policy for perishable products with regular and optional expedited replenishments. *Manufacturing & Service Operations Management*, 13(4): 420–438, 2011.

3 A Robust Heterogeneous Vehicle Routing Problem with Split pickup and Delivery for Casualty Evacuation in Wildfires

We consider the problem of transporting patients of multiple levels of injury seriousness using heterogeneous vehicles (vehicles with different capacities and costs) to different medical centers (i.e., hospitals) through less risky routes by using various forms of vehicle routing mechanisms. A detailed description of the problem under study in this chapter is given in Section 3.3. Using optimization, robust and stochastic modelling, and statistics, we show that using various vehicle routing mechanisms such as split pickup and delivery improves casualty evacuation operations when considering limited time windows for evacuation assembly points (EASs), where patients are waiting to be transferred by different paramedic vehicles to medical centers with limited capacity (SMSs and hospitals).

3.1 Introduction and Motivation

Wildfires are difficult to control as they propagate rapidly and erratically. They threaten human lives and livestock [28]. The economic losses, the number of fatalities, the number of displaced people, and other socio-economic factors resulting from wildfires highlight the need to implement emergency preparedness and response approaches. Due to the frequency and intensity of wildfires affecting residential areas, people are often exposed to life-threatening risks. As a result, they need to be evacuated to medical centers, hospitals, or special-need medical shelters (SMS). During a wildfire, the affected population either go themselves to evacuation assembly areas (EASs) or is transferred by rescue and relief teams to the EASs. Once the triage process is complete, the evacuees have transferred via emergency medical services (EMS) vehicles to other EASs to pick up more injured (if the vehicle capacity allows it) or medical centers (hospitals or SMSs). However, due to EMS vehicles' limited capacity, it is often challenging to transport all evacuees from different geographical regions in a timely fashion. This, in turn, may further decrease the chance of survival for the evacuees needing immediate care [18, 30]. A common transportation strategy in the literature is to direct EMS vehicles managed by each relief facility (i.e., hospitals, SMSs, EASs) to return to

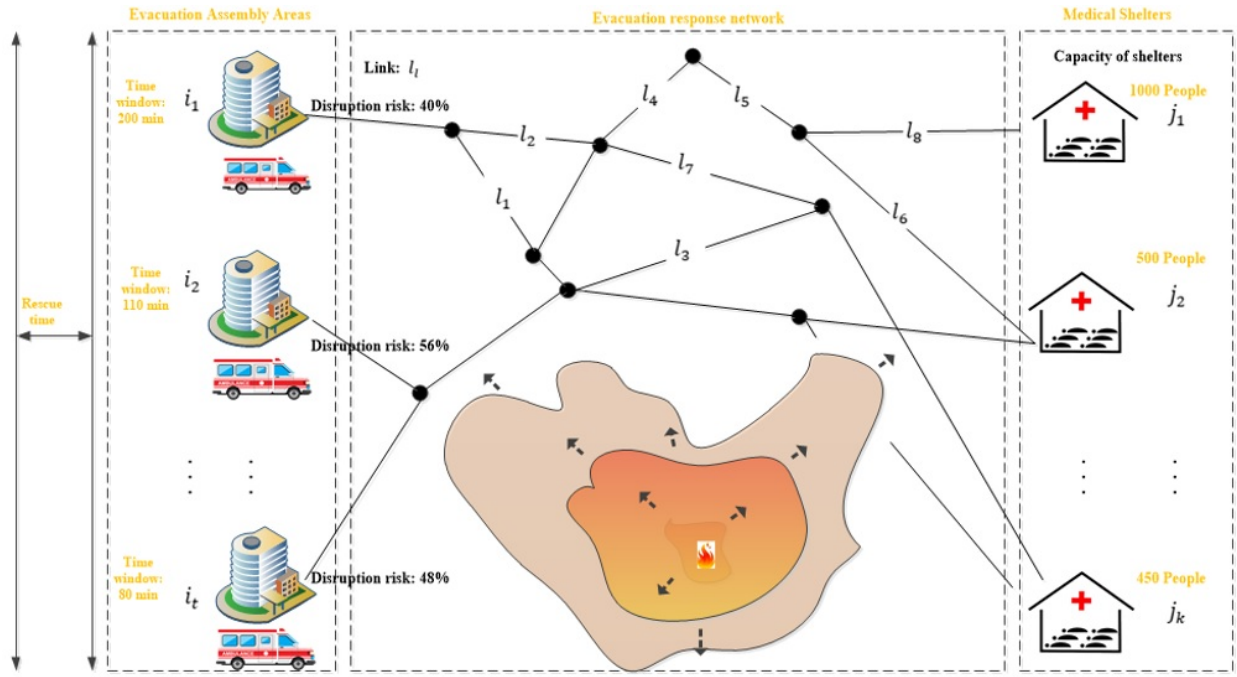

Figure 3.1: Wildfire Evacuation Network.

the same location from which they departed at the end of each period (i.e., on an hourly or daily basis). The description of periods in our case is provided in Section 3.3. Such a transportation strategy may not be efficient for relief operations under time windows with many casualties with various urgency levels [40]. In addition to the possibility of multiple trips per vehicle, a vehicle can also collect injured from multiple EASs (a split pick-up transportation strategy) and transfer them to multiple medical centers (split delivery transportation strategy). In effectively managing such emergency evacuation operations, the key decisions are (1) when paramedic vehicles should transport evacuees from each EAS and (2) to which hospitals or SMSs they should be transported. The problem corresponds to a multi-destination multi-trip network flow problem where the emergency evacuation network is a two-echelon network consisting of evacuation assembly areas, hospitals and SMS, with roads and segments connecting the EASs to medical centers (SMSs and hospitals), as shown in Figure 3.1. It should be noted that the routes depicted in in this figure are considered to be virtual roads between locations, not physical ones. For each EAS on the left-hand side, there is a limited time window (for casualty evacuation due to fire spread), representing the maximum time the EAS is available. As the fire spreads through the region based on different elements such as fire intensity and wind direction, some EASs and routes become riskier for casualty transportation and may become unavailable/inaccessible.

In this thesis, decisions are made considering a short (maximum 8 hours) planning horizon (immediate response phase of disaster relief operations). We formulate a two-stage stochastic mixed-integer programming model to capture the idea of routing casualties via less risky routes and matching them to relevant vehicles and SMSs or hospitals based on their level of urgency.

A fully coordinated evacuation strategy under split pick-up and delivery transportation strategies has not been used in wildfire evacuation models to date. We posit that a casualty transportation model under a fully coordinated evacuation strategy can potentially increase the number of survivors. Employing such a strategy across the emergency evacuation network is a feature of an integrated relief network. Moreover, during a wildfire, EAS may face an unexpected growth in the number of injured needing to be transported to hospitals and SMSs. Hence, we seek to maximize the number of people with varying injury seriousness via safe routes using two paramedic vehicle types under uncertainty.

It should be noted that there is no difference between affected people's evacuation and pushing patients toward the shelters in this research. Both refer to transporting patients to medical locations (SMSs and hospitals).

The motivation for this study is to optimize the use of available paramedic vehicles through the integration of vehicle logistics with casualty transportation operations. Throughout this chapter, we seek to determine optimal vehicle routing and medical center selection decisions while taking into account casualties with different levels of injury seriousness under limited evacuation time windows, risky routes, and limited capacity of vehicles and medical centers.

The remainder of this chapter is organized as follows. In Section 3.2, we discuss the relevant literature on casualty transportation models, vehicle routing models in HROs, and wildfire preparedness and response planning. In Section 3.3, we describe in detail the problem under study, the coordinated vehicle routing problem, and develop the proposed model. Then in Section 3.4, a hybrid meta-heuristic solution method is proposed. In Section 3.5, we discuss a number of numerical experiments from a case study and in Section 3.6, we examine the performance of the approach and the sensitivity of the solution to changes in key parameters. Finally, in Section 3.7, we conclude the study and discuss future research directions.

3.2 Related Literature

Emergency evacuation, in a disaster situation, refers to transferring evacuees from disaster-affected areas to safer, protected shelters. The Australian Evacuation Framework simplifies the evacuation process by identifying five-decoupling points: decision, warning, withdrawal, shelter, and return [39]. These decisions require issuing warning messages or, in some cases, a mandatory evacuation order, setting up assembly points, and transferring evacuees to established evacuation shelters. There is an extensive body of literature on emergency evacuation, which incorporates various interconnected components of an emergency risk management framework such as prevention or mitigation, preparedness, response, and recovery. Evacuation relates to the emergency response which operationalizes the safe relocation of evacuees to protected shelters within a restricted time

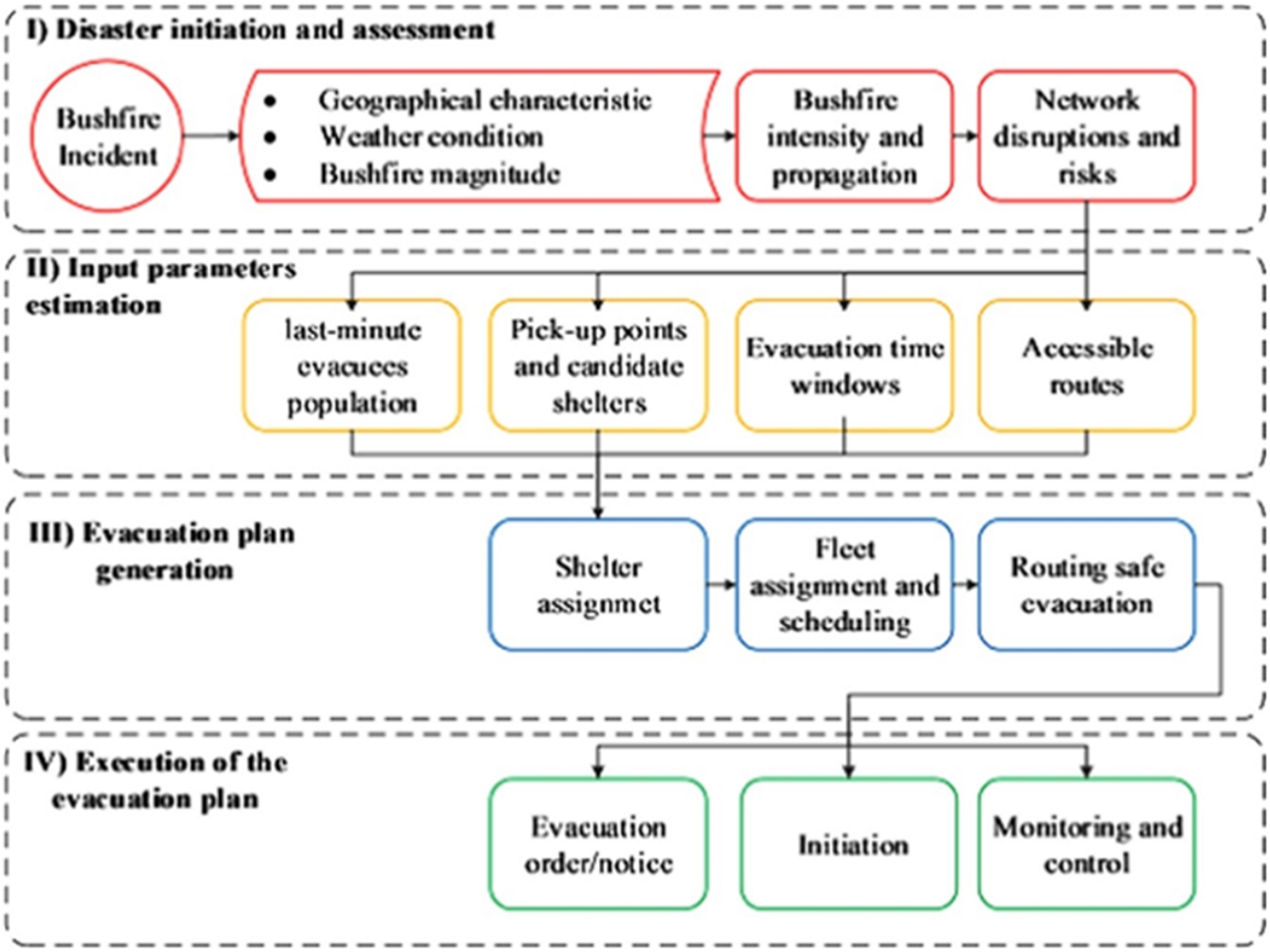

Figure 3.2: Interdependent and interlocking components of the short-notice emergency evacuation process

.

window. The response to a short-notice evacuation is dependent on various operations such as an emergency declaration, warning messages, registration and tracing, resource mobilization, and search and rescue. Figure 3.2 illustrates the interrelated and interlocking sequences and procedures involved in a typical emergency response [29]. The process comprises four major stages: (I) disaster (wildfire) initiation (i.e., the time when the wildfire started) and assessment, (II) input parameters (i.e., number of injured people) estimation, (III) evacuation plan generation and (IV) execution of the evacuation plan. In the stage I, the scale, intensity and magnitude of the wildfires are assessed. This stage requires some initial inputs (e.g. affected areas, bushfire direction, and transportation network data) to evaluate the potential threat. Stage II estimates the operational inputs, which include the number of late evacuees, the number and location of candidate shelters (based on capacity, accessibility and other risk factors), accessibility of routes, and most importantly the time windows. Stage III generates evacuation plans and actions, including tasks such as assigning rescue vehicles, allocating shelters, and identifying the safest and shortest routes. Generated plans

are re-assessed in terms of feasibility and soundness in responding to real-world situations. Finally, in Stage IV, the generated evacuation plans are implemented by emergency service agencies. These include broadcasting an evacuation notice or order, initiating evacuation by the transportation of evacuees to shelters, assignment of vehicles, delineation of routes, and finally monitoring and control of the mission.

Safe transfer of evacuees from designated assembly points located within the affected areas to safe shelters may appear to be a simple operation. However, it is complicated because it involves assigning shelters and transferring evacuees through safe routes from location to location without forcing the vehicles to return to their main depot (departure) at each period within a restricted time window and the existence of multiple sources of uncertainty. Another aspect of the model's complexity is that multiple pick up and delivery at each period is possible for each vehicle. In this regard, keeping track of the location of vehicles and the arrival time of each vehicle at the destination would make the problem challenging. Given that this thesis studies a coordinated evacuation network for the transportation of patients with different levels of injury seriousness, we categorize the relevant literature into two main streams: vehicle routing and casualty transportation under uncertainty. In the following subsections, the main research gaps and our contribution to the existing literature are presented.

3.2.1 Vehicle routing problems and casualty flow models

The vehicle routing problem (VRP) is a widely studied problem in the literature [22, 33, 24, 9], with applications in many fields including emergency evacuation. VRP models seek to use a fleet of vehicles to transfer resources or the affected population between locations. The majority of the recent research in this area involves the application of VRP variations to a range of fields using either heuristic solution algorithms or exact solution approaches. There are four common variants of classic VRPs: capacitated VRP (CVRP), dynamic VRP (DVRP), VRP with time windows (VRPTW), and multi-destination VRP (MDVRP). In CVRPs, vehicles have a predefined limited capacity. In DVRPs some elements, such as the availability of a link in the road network, could vary over time. VRP-TW is the traditional VRP problem with the addition of time windows for serving demand. Finally, MDVRPs include multiple visits to a single destination or a series of collection points. Although many variants of the classic VRP model exist, there are still some new approaches that have not been applied in the wildfire domain, such as a variant of the VRP-TW called Open VRP-TW (OVRP-TW). Consider an evacuation assembly point from which several patients have to be transported to a set of medical centers (e.g., hospitals and shelters) in a relatively short time. In this type of routing approach (OVRP-TW), rescue vehicles do not return to their main location or assembly point at the end of each trip. Instead, they can start the next trip

from the same location where the last trip ended. For such models, the vehicles can employ various routing strategies for split pick-up and split the delivery of resources or patients. One of the few studies in the wildfire evacuation domain involving the specific OVRP-TW structure can be found in Shahparvari et al. [31]. Shahparvari et al. [31] developed a bi-objective transportation model to determine optimal evacuation plans for "late" evacuees. Late evacuees are those who choose to stay and defend their properties instead of leaving early or those who arrive late to evacuation areas for various reasons. The model seeks to maximize the number of people evacuated to the nearest shelters using the most reliable routes and under hard time windows. To transfer people through the safest and most reliable routes, the authors computed route passage capabilities and route resistance functions based on wildfire propagation to determine the risk associated with each relief route. To solve the model, they applied an ϵ-constraint approach. Zhou and Erdogan [47] introduce a bi-objective two-stage emergency evacuation optimization model that seeks to minimize the total relief costs and maximize the number of at-risk people evacuated under various fire scenarios. Their model takes into account different wildfire-spread scenarios and their impact on high-risk areas. To determine the probability of different wildfire scenarios, they considered the impact of wind direction and fire speed for a case study of a wildfire in Santa Clara County, California. They used a goal programming approach to solve the bi-objective problem under conflicting objectives. Shahparvari et al. [30] proposed a bi-objective optimization model to support the transportation of late evacuees from multiple townships to functioning shelters via the safest and nearest routes under road disruption risk and limited time windows. They employed a weighted average method to calculate the cumulative disruption risk of routes based on three risk levels. To deal with the uncertainty in the parameters of the model (i.e., disruption risks of routes, and time windows), they applied a heuristic solution technique and fuzzy optimization to optimize emergency delivery service. The model is applied to a real case study of the 2009 Black Saturday bushfires in Victoria, Australia.

Cova et al. [10] develop an optimization model to evacuate trapped people within wildfire regions instead of pushing them toward shelters. They proposed a new method to delimit wildfire evacuation trigger points using fire spread modelling and geographical information systems. To solve the model, they used a simple greedy algorithm (i.e., take the option that most increases the objective function at each iterative step), where for each household, the approach identifies the protective option that offers the highest level of (life) protection (relative to its expected fire threat level) that meets the time constraints. Yang et al. [43] develop a two-layer emergency logistics system with a single depot and multiple demand sites for wildfire response. In the first stage, fire propagation behaviour is predicted. In the second stage, a resource allocation and vehicle routing problem is developed to minimize the resource delivery travel times and costs. For this purpose, they devel-

oped a multi-objective VRP model and a heuristic algorithm to provide the associated solutions of the VRP model.

In summary, in the domain of wildfire evacuation, the application of OVRP-TW where vehicles can collaboratively transport patients to various locations in the network has not been studied extensively. Most models in this context assume vehicles must return to their main depot at the end of evacuation or trip, which may not be practical for many relief operations with limited time windows, various sources of uncertainty, limited resources, etc.

3.2.2 Casualty Evacuation under uncertainty

In wildfire evacuation, there are only a few studies that develop evacuation models in the presence of multiple sources of uncertainty. For VRP models, uncertainty can exist in the travel times and locations, as well as in the number of available vehicles and number of customers [41]. There has seen considerable research done on Stochastic VRPs (SVRPs), where it is assumed that the source of uncertainty follows a known probability distribution [7]. One alternative to SVRP is to incorporate uncertainty as fuzzy values. Lai and Hwang [20] were the first to consider fuzzy VRP models and the approach has been subsequently explored by many researchers. Considering various solution approaches to derive robust solutions against multiple realizations of the uncertain parameters is essential for wildfire evacuation operations where an infeasible solution can result in loss of lives. Hence, the incorporation of the uncertainty associated with bushfire propagation, available evacuation time windows and travel times should be considered critical in emergency evacuation modelling. For emergency evacuation planning under multiple sources of uncertainty, approaches such as stochastic programming [23, 26, 16, 45] and dynamic multi-stage planning [15, 1] have been proven useful. A limited number of studies in the context of disaster relief operations have used robust modelling for worst-case scenarios taking into account uncertainties, for example, in the number of evacuees in the fire-affected regions, time windows for assembly points, and travel times among multiple locations in the evacuation network. For further information and a comprehensive review of robust optimization approaches in DROs refer to Kamyabniya et al. [18] and Ben-Tal et al. [4]. In the context of wildfire evacuation, only one study considers a robust optimization approach. Shahparvari and Abbasi [28] propose an innovative formulation and decision support system to maximize the number of late evacuees transported to EASs under limited time windows. To guarantee the robustness of the proposed model, they consider an LP model with an uncertain right-hand side, a similar approach to Bertsimas and Sim [8]. The proposed model also considers road availability and disruptions. Shahparvari and Abbasi [28] develop a greedy solution method to cope with the complex nature of their VRP model.

Ntaimo et al. [27] combine fire behaviour simulation and a two-stage stochastic integer program-

ming model to optimize the mix of resources sent to multiple fires in each fire day scenario following an outbreak. The authors seek to minimize a combination of the fire's spread, resource deployment cost, and expected suppression cost. They implement the proposed combined simulation-optimization (an integer programming model) model in a commercial solver; however, for a large number of scenarios, they employed the sample approximation approach as a sampling approach to reduce the size of the approximate problem.

3.2.3 Research gap

Although evacuation planning has received increased attention in the literature, the existing models exhibit a number of drawbacks, as outlined below. The closest study to our work is the paper by Shahparvari et al. [31]. However, their research does not consider matching medical resources and services available at field hospitals to the needs of the affected population (injury levels). Moreover, the routing strategies they consider do not allow vehicles to freely travel through different locations in the network without having to return to the main depot at the end of each trip. They develop a multi-objective integer programming model for such a VRP problem and apply an ϵ-constraint approach to solve the problem without uncertainty in the parameters of the model. In contrast, we develop a two-stage stochastic optimization approach to capture uncertainty in the parameters of the model. Although both models utilize robust optimization, we use different methods for modelling the robustness.

In summary, first, employing optimization-based approaches under uncertainty to determine optimal evacuation plans has rarely been developed for wildfires. Inaccessibility or limited availability of evacuation routes, the possibility of the rapid spread of the fire due to intense winds, and the lack of wildfire response resources make wildfire evacuation planning very unique. These factors result in a highly limited response time that in turn makes evacuation planning very demanding. Second, only a few studies in emergency planning in the event of a wildfire have been conducted for heterogeneous casualty evacuation. The majority of the studies are focused on resource deployment to burning regions and on how to search for the affected population. Third, the majority of the existing models are single-stage planning models, ignoring the multi-stage multi-period characteristics of emergency evacuation plans. Fourth, there is only one study that considers a robust approach to emergency evacuation planning during wildfires. The majority of the studies in this area consider the expected value of the objective function, which fails to account for the presence of significant uncertainty in terms of the extent and impact of any wildfire. Fifth, the majority of studies in this area assume that evacuation vehicles must return to their starting point at the end of each planning period. To deal with the shortcomings above, in this chapter, we develop a multi-period robust emergency evacuation model that considers routing strategies and various

sources of uncertainty to address the aforementioned research gaps.

3.3 Problem Description

We model an evacuation logistics network consisting of evacuation assembly points (EASs), hospitals, and special-needs medical shelters (SMSs) in fire-affected zones. The proposed model, called 2MCVRP-TW, can be thought of as a multi-destination multi-depot coordinated capacitated VRP model with time windows for the transportation of patients of various injury seriousness via multiple types of vehicles. During a wildfire, people with different levels of injury seriousness need different vehicles to be transported via safe (less risky) routes to available medical centers (SMSs and hospitals). Note that transportation is always via a safe route, what changes here is the time it takes to (find) travel the safe route, which is one of the sources of uncertainty in your model. In our model, the riskiness of routes is measured probabilistically. For each origin-destination pair, we consider two potential routes - a shorter, more direct route versus a longer, detour route. A risky route corresponds to one where the probability of needing to take the detour is higher. Thus, we account for uncertainty in travel times among facilities (locations in the network), time windows of EASs, and the number of people at EASs.

Decisions are made on a minute-to-minute basis over a very short planning horizon corresponding to the response phase of a wildfire. We formulate the problem as a mixed integer two-stage stochastic model that matches the type of vehicle and medical center to the needs of patients. In uncoordinated evacuation networks, the number of evacuees at a specific geographical location (EAS) is served only by the rescue vehicles assigned to that EAS while in coordinated evacuation networks vehicles are shared across the network. In this research, three vehicle routing strategies are compared with respect to the survival rate of evacuees and evacuation time. The first routing strategy, the 2MCVRP-TW with split pick-up routing, allows sending vehicles from one EAS to another to pick up patients till they reach their maximum capacity. The second strategy, the 2MCVRP-TW with split delivery, allows delivering patients boarded on the same vehicle to different medical centers. The third strategy, the 2MCVRP-TW with split pick up and delivery, combines the two strategies above and allows vehicles to travel to different locations in the network without any restrictions on returning to their main depot at the end of each trip.

As stated earlier, no fully coordinated routing mechanism has been used in wildfire evacuation models or incorporated into patient allocation models. We posit that a fully coordinated casualty evacuation model (2MCVRP-TW) that considers both split-pickup and split-delivery mechanisms can potentially help balance patient transportation and assignment across the medical centers.

We assume a higher level organization (e.g., the disaster mitigation command centre and chief fire agency (CFA) in the case study introduced later) is responsible for ensuring information is shared

among EASs, hospitals, and SMSs to ensure the provision of vehicles. Finally, to tackle multiple sources of uncertainty, we present a robust counterpart of the proposed deterministic model. Since the deterministic model cannot capture different sources of the uncertainty mentioned above, we develop a robust model that can generate resilient evacuation plans against various realizations of the uncertain parameters of the model.

3.3.1 Model Formulation

In this section, we outline the main assumptions required for the problem formulation, and specify the parameters, variables, objective function and constraints considered in the two models. Table 3.1 represents the notation used in the model formulation.

3.3.1.1 Assumptions

We assume that the location of hospitals is pre-designated by the CFA mentioned in Section 3.3 and that the capacity and number of paramedic vehicles and medical centers are finite and known. The availability of evacuation assembly areas is subject to time windows, the capacity of ambulances and buses is limited, and that the capacity of routes is unlimited.
The SMSs, hospitals, routes, and evacuation assembly areas can be served by several vehicles. The ambulances and paramedic buses are present at the evacuation assembly areas to transport the victims at the beginning of the evacuation process. Moreover, we consider that the SMSs and hospitals are not identical, differing in their capacity and treatment capabilities and that the number of casualties assembled at EASs is not the same and is uncertain. Similarly, the route's availability is subject to uncertainty that may make a route unavailable for transporting patients from the EASs to the SMSs and hospitals. We consider three types of injured patients: severe (type 1), moderate (type 2), and mild (type 3). In our model formulation, elements such as when to take the patients from EASs (based on their triage levels), where to transport them (type of facility needed for the specific patient type) and how to take them (transportation mode for a specific patient) are taken into account as decisions. Finally, we consider that a vehicle can make single or multiple trips and the vehicles do not need to return to their departure locations.

3.3.1.2 The proposed model

As stated earlier, we first develop a two-stage stochastic optimization model for casualty evacuation in wildfires. The chosen approach is capable of modelling a problem where decisions are required to be made sequentially and can capture the uncertainty in the parameters of the model. In the first stage of the two-stage optimization model, the location of SMSs is selected. Accordingly, based on the decisions made in the first stage, the second stage determines the optimal routes for

Table 3.1: Model Notation (Wildfire Evacuation Model)

Sets	
N	Locations in the evacuation network = $K \cup D$
D	Evacuation assembly shelters, $D = \{1, 2, ..., \|D\|\}$
K	Medical centers, $K = \{1, 2, ..., \|K\|\} = K_1 \cup K_2$
K_1	Hospitals, $K_1 \subseteq K$
K_2	SMSs, $K_2 \subseteq K$
X	Trips any vehicle makes , $x \in X$
H	Injury levels, $H = \{1, 2, ..., \|H\|\}$
V	Vehicles for injured people transportation, $V = \{1, 2, ..., \|V\|\} = V_A \cup V_B$
V_A	Ambulances, $V_A \subseteq V$
V_B	Special Paramedic Buses, $V_B \subseteq V$
Indices	
i, j	A location, $i, j \in N$
x	A trip, $x \in X$
v	A vehicle, $v \in V$
h	An injury level, $h \in H$
Parameters	
Ψ	Maximum number of SMSs
π_s	Probability of occurrence of scenario s
TW_i	Available evacuation time [minutes] for evacuation assembly shelter i
SC_jh	Capacity of medical center j [the number of people] for accepting injured people of injury seriousness level h, $j \in K$, $h \in H$
OC_j	Operational cost [dollar] for setting up a location j, $j \in K_2$
CW_1	First Objective function weight
CW_2	Second Objective function weight
t_{ij}^v	Transportation time between location i and location j [minutes] by vehicle v, $i, j \in N$, $v \in V$
VC_v	Capacity of vehicle v [the number of people] for injured people transportation, $v \in V$
P_{ih}	Total number of injured people at evacuation assembly shelter i of injury seriousness of type h, $i \in D$, $h \in H$
Decision Variables	
IPH_{ijvh}^{xs}	Number of people of injury seriousness of type h who travel to location j from location i by vehicle v in trip x, $i, j \in N$, $v \in V$, $x \in X$, $h \in H$
UD_{ih}^{s}	Number of people of injury seriousness type h at evacuation assembly shelter i that are not moved within time window, $i \in D$, $h \in H$
γ_i	1 if a location i is active to receive casualties, $i \in K_2$
Y_{ijv}^{xs}	1 if vehicle v in trip x travels from location i to location j , 0 otherwise, $i, j \in N$, $v \in V$, $x \in X$
ST_{vxs}	Time when vehicle v starts its trip x, $v \in V$, $x \in X$
ET_{vxs}	Time when vehicle v finishes its trip x, $v \in V$, $x \in X$
TT_{ivx}^{s}	Time when vehicle v in trip x arrives at node i, $i \in N$, $v \in V$, $x \in X$
SP_{iv}^{xs}	1 if vehicle v starts evacuation from location i in its trip x, 0 otherwise, $i \in N$, $v \in V$, $x \in X$
EP_{iv}^{xs}	1 if vehicle v finishes evacuation at location i in its trip x, 0 otherwise, $i \in N$, $v \in V$, $x \in X$

vehicles to transfer casualties to the SMSs and hospitals from the EASs. The application of robust optimization, explained in Section 3.3.2, is justified in our study since we need to generate robust evacuation plans under any realization of various sources of the uncertainty mentioned earlier.

Below we present the mathematical formulation of the problem. The deterministic version can be obtained by simply removing sub/superscript s. We define a two-stage single objective function, Z^E, associated involving the operational cost to set up an SMS, unmet demand and the number of injured people transferred. The realistic basis for employing the cost term at the first stage is its importance for the decision-makers leading relief operations under a limited budget. Although relying solely on minimizing logistics costs might be appropriate for non-relief operations, it is undoubtedly not sufficient for modelling disaster relief operations. Thus, the second term of the objective function minimizes a weighted sum of unmet demand and ensures that the less lengthy routes are selected to transport the patients from the EASs to the SMSs and hospitals.

$$\min Z^E = \sum_{j \in K_2} OC_j \times \gamma_j + \sum_s \pi_s \left(CW_1 \times \sum_{i \in D,h} UD_{ih}^s + CW_2 \times \sum_{i,j,x,v} Y_{i,j,v}^{x,s} \right) \tag{3.1}$$

The first term of Equation (3.1) captures the decisions regarding the first stage of the problem which is the selection of SMSs. It incorporates the total cost of operating the SMSs. The second term represents the objective function of the second-stage problem, which determines the routing plan of vehicles to transfer casualties through the evacuation network. The second term is the expected total unmet demand related to the number of patients not evacuated from EASs $i \in D$. Another term, $CW_2 \times Y_{i,j,v}^{x,s}$, reflects the expected penalty associated with transporting evacuees through unsafe routes. As the different terms in the objective function are non-commensurate, they are converted to each other by the penalty method, which results in a normalized objective function. As the second term regarding the number of evacuated patients is highly critical, more penalty (CW_1) is assigned to it compared to the cost associated with SMS location (OC_j). To make the objective function dimensionless, we optimize each of the objectives individually first, then divide each objective by those optimum values before summing all normalized terms as one objective. It is important to note that the criteria for selecting the shelters include their capacity, their distance from other medical centers, and EASs, and the operational cost/penalty that is incorporated in the objective function (Equation 3.1).

$$\sum_{j \in K_2} \gamma_j \leq \Psi \tag{3.2}$$

Constraint (3.2) restricts the number of allocated shelters to be less than or equal to the maximum number available.

$$\sum_{i\in N,s,x,v} Y_{ijv}^{xs} \leq \gamma_j \qquad \forall j \in K_2 \tag{3.3}$$

Constraint (3.3) ensures that only trips to available SMSs happen.

$$\sum_{\substack{i\in N\\ v,x}} IPH_{ijvh}^{xs} - \sum_{\substack{j':j'\neq j\in K_2\\ v,x}} IPH_{jj'vh}^{xs} \leq SC_{jh} \times \gamma_j \qquad \forall j \in K_2, h = 2,3, s \tag{3.4}$$

$$\sum_{\substack{i\in N\\ v\in V_A,x}} IPH_{ijvh}^{xs} \leq SC_{jh} \qquad \forall j \in K_1, h = 1, s \tag{3.5}$$

$$\sum_{\substack{j':j'\neq j\in K_2\\ v,x}} IPH_{jj'vh}^{xs} = 0 \qquad \forall j \in K_2, h = 1, s \tag{3.5a}$$

$$\sum_{\substack{i\in N\\ v\in V,x}} IPH_{ijvh}^{xs} = 0 \qquad \forall j \in K_1, h = 2,3, s \tag{3.5b}$$

Constraints (3.4) and (3.5) impose that the number of casualties transported to each SMS or hospital be within their capacity. Notably, according to Equation (3.4), there is not any patient transfer from SMSs and hospitals, respectively, as it is assumed the SMSs are capable of providing the patients with relevant medical needs. It should be noted that, based on Equation (3.5), only severely injured patients ($h = 1$) are sent to hospitals and only by ambulance. Equations (3.5a) and (3.5b) prevent other types of patients from being sent to hospitals or patients of type 1 to SMSs.

$$UD_{ih}^{s} + (\sum_{\substack{j\in N\\ v,x}} IPH_{ijvh}^{xs} - \sum_{\substack{i':i'\neq i\in D\\ v,x}} IPH_{i'ivh}^{xs}) = P_{ih}^{s} \qquad \forall i \in D, h, s \tag{3.6}$$

Constraint (3.6) ensures that the number of casualties to be transported from/to each EAS to/from other locations plus the number of evacuees who are not evacuated from the EAS equals the injured population at the area that each EAS represents.

$$IPH_{ijvh}^{xs} \leq VC_v \times Y_{ijv}^{xs} \qquad \forall i, j, x, v, h, s \tag{3.7}$$

Constraint (3.7) restricts the number of boarding patients in each trip to the capacity of the corresponding vehicle. This equation also does not allow any boarding if a vehicle does not leave an EAS.

$$SP_{jv}^{xs} + \sum_{i \in N} Y_{ijv}^{xs} = \sum_{i \in N} Y_{jiv}^{xs} + EP_{jv}^{xs} \qquad \forall v, x, j \in N, s \tag{3.8}$$

$$\sum_{j \in N} Y_{ijv}^{xs} + EP_{iv}^{xs} \leq 1 \qquad \forall i \in N, v, x, s \tag{3.9}$$

Constraint (3.8) states the flow conservation for the evacuation network. For each vehicle, the number of people who arrive at a location must be equal to the number of people who depart. Simply put, Constraint (3.8) determines the location of each vehicle on each trip. In other words, this constraint specifies that a vehicle might start its trip from a location j or end its trip at a location j, meaning that starting and finishing points of a vehicle should be the same for the vehicle at a specific trip. According to constraint (3.9), it is possible that a vehicle does not leave an EAS and finishes its trip at location j (EP_{iv}^{xs}). Hence, if a vehicle at trip x moves from a location j to i, it ends its trip there or starts its trip from the same location j to move to another location.

$$EP_{jv}^{xs} = SP_{jv}^{x+1,s} \qquad \forall v, x \in \{1, 2, ..., |X| - 1\}, j \in N, s \tag{3.10}$$

Constraint (3.10) guarantees that, for each trip, a vehicle starts from the same point that it finished its previous trip. This constraint keeps track of the location of each vehicle on each trip and is used as a complement constraint to the constraints (3.8) and (3.9) to determine the connectivity of trips for a specific vehicle through the network.

$$\sum_{i \in N} EP_{iv}^{xs} = 1 \qquad \forall v, x \geq 1, s \tag{3.11}$$

Constraint (3.11) determines the final location of each trip for each vehicle. It guarantees that a vehicle must end its trip at a location which is not met twice a specific trip. In other words, it avoids any sub-tour for a vehicle on a specific trip.

$$TT_{jvx}^{s} \geq TT_{ivx}^{s} + t_{ij}^{vs} - M \times (1 - Y_{ijv}^{xs}) \qquad \forall i \in N, j \in N, x, v, s \tag{3.12}$$

Constraint (3.12) determines the time a vehicle arrives at an EAS or medical centre. On the LHS of this constraint, the time it takes a vehicle to arrive at location j should be equal to or greater than the arrival time of that vehicle at location i, a precedent location before location j, plus the

time it takes to travel from location i to j. This constraint guarantees that no sub-tour exists for a specific vehicle to move from location i to j, and location j is scheduled to be visited after location i by a vehicle. The term $M \times (1 - Y_{ijv}^{xs})$ on the RHS of this constraint prevents any trip to location j if no routes are available between location j and i ($Y_{ijv}^{xs} = 0$).

$$ST_{vxs} = 0 \qquad \forall x = 1, v \in V, s \tag{3.13}$$

Constraint (3.13) sets the start time of a vehicle's first trip at zero. At each trip, the start time of each trip of a specific vehicle should be computed to keep track of the time each vehicle starts its trip, and the time it ends (ET_{vxs} variable in (3.15)) each trip and the end of each vehicle's operations.

$$ET_{v,x-1,s} = ST_{vxs} \qquad \forall x > 1, v \in V, s \tag{3.14}$$

$$ET_{vxs} = ST_{vxs} + \sum_{ij \in N} t_{ij}^{vs} \times Y_{ijv}^{xs} \qquad \forall x, v \in V, s \tag{3.15}$$

$$TT_{ivx}^{s} \leq TW_{i}^{s} \qquad \forall i \in D, x, v \in V, s \tag{3.16}$$

Constraint (3.14) defines the start time of the subsequent trip of a vehicle as the time when the previous trip ends, and Constraint (3.15) calculates the end time of a trip of a vehicle as the time when it starts its trip plus the travel time between location i to j. Constraint (3.14) ensures the connectivity of trip schedules for a specific vehicle and the time it takes to start and finish a trip of a specific vehicle. While constraint (3.14) ensures the connectivity of trip schedules for each vehicle's trips, constraint (3.15) takes control of such a schedule for a specific trip for that vehicle. Constraint (3.16) links the time a vehicle arrives at a location with the corresponding time window. Simply put, a vehicle can not take another trip to evacuate more casualties from the EASs if the time window of the EAS i is *zero* or the fire has already reached that EAS.

$$TT_{jvx}^{s} \geq ET_{v,x-1,s} + t_{ij}^{vs} - M \times (1 - EP_{iv}^{x-1,s}) \qquad \forall i \in N, x > 1, v, s \tag{3.17}$$

Constraint (3.17) ensures that the arrival time of a vehicle at a location is feasible given the last location of the vehicle. Feasibility means that the arrival time of a vehicle at a location j cannot be regarded as a feasible trip schedule if the vehicle did not finish its previous trip at a precedent location i that is not linked to location j. As specified in this constraint, if the final location of a vehicle in its previous trip is not location i ($EP_{iv}^{x-1,s} = 0$), the vehicle would not travel to location

j at all. On the contrary, if the vehicle ended its previous trip at location i ($EP_{iv}^{x-1,s} = 1$), the visit time of location j for that vehicle start from the time when it ended it previous trip plus the travel time between location i to j for that vehicle.

$$\sum_{j:j\neq i\in N} Y_{ijv}^{xs} \geq SP_{iv}^{xs} \qquad \forall i, x, v \in V, s \tag{3.18}$$

$$\sum_{j:j\neq i\in N} Y_{jiv}^{xs} \geq EP_{iv}^{xs} \qquad \forall i, x, v \in V, s \tag{3.19}$$

Constraints (3.18) and (3.19) avoid location i to be the start and end location of any vehicles if there is no trip from i to any other locations and from other locations to location i, respectively. Hence, if the LHS of constraints (3.18) and (3.19) are zero for a specific vehicle on specific trips, that vehicle cannot visit location i for any of all its trips.

$$SP_{iv}^{xs} \leq \gamma_j \qquad \forall i, j \in K_2, i = j, x, v \in V, s \tag{3.20}$$

$$EP_{iv}^{xs} \leq \gamma_j \qquad \forall i, j \in K_2, i = j, x, v \in V, s \tag{3.21}$$

Constraints (3.20) and (3.21) guarantee that no vehicle can start or end a trip at a non-existing shelter. These two constraints have defined a complement to constraints (3.18) and (3.19) to ensure the feasible start and end location of trips for a vehicle across all the locations in the network. In other words, these constraints guarantee the trip schedules are defined from feasible locations in the network; otherwise, sub-tours (any trip that ends up at a location not valid for a trip schedule of a vehicle) might prevent the connectivity of trip schedules for a vehicle.

$$\begin{aligned} &IPH_{ijvh}^{xs} \geq 0 \ \ and \ \ integer && \forall i, j, v, x, h, s \\ &ET_{vxs}, ST_{vxs}, TT_{ivx}^{s} \geq 0 && \forall i, v, x, s \\ &Y_{ijv}^{xs}, \gamma_j, SP_{jv}^{xs}, EP_{jv}^{xs} \in \{0, 1\} && \forall i, j, v, x, s \end{aligned} \tag{3.22}$$

Finally, constraint (3.22) defines variables as being non-negative and binary.

3.3.2 The robust evacuation model

Successful evacuation planning depends on the best possible configuration (building an evacuation network with fundamental elements such as the design of routes, routing strategies, the link among locations, etc.) and performance, which depends on several uncertain factors. Uncertainty

in patient evacuation is related to fluctuations in travel times between locations (regarded as the availability of routes), time windows for EASs and the number of evacuees at each EAS. The first step to incorporating such uncertainties in evacuation modelling is to choose an appropriate method to deal with the different sources of uncertainty. Common methodologies for dealing with uncertainty are stochastic programming (probability models, recourse models and robust stochastic programming), fuzzy techniques in cases where interval or fuzzy information (flexible and possibilistic programming) is involved [21], stochastic dynamic programming and robust optimization. When a researcher models a real-world problem with noisy, incomplete or erroneous data, robust optimization techniques are beneficial to generate robust policies against any realizations of various sources of uncertainty under the problem setting [25]. In this section, the robust approach developed by Aghezzaf et al. [2] as an extension of that of Mulvey et al. [25] is employed for the proposed model. The main objective of the robust approach proposed by Mulvey et al. [25] is to find a solution having the smallest deviation from the performance of the scenario-specific optimal solutions.

In the context of robust optimization, Yu and Li [44] and Mulvey et al. [25] describe stochastic programming approaches developed by replacing the expected cost minimization objective with one that explicitly addresses cost variability. They propose a robust optimization model capable of tackling the decision makers' favoured risk-aversion or service-level function, yielding a series of solutions that are progressively less sensitive to realizations of the data in a scenario set. Yu and Li [44] developed a new formulation which is more effective than the model proposed by Mulvey et al. [25] requiring fewer additional variables.

However, the approaches by Mulvey et al. [25] and Yu and Li [44] do not consider the maximum variability imposed by the scenarios (worst-case scenario) and instead only incorporate the expected performance into the objective function. Hence, such approaches are not appropriate for various applications in practice or problem settings and can result in high costs or delays to the system (i.e., evacuation response efforts) and a heavy computational burden. An alternative approach is the one proposed by Bertsimas and Sim [8]. They consider a linear programming model with an uncertain coefficient matrix on the left-hand side. Their method provides a solution with different levels of conservatism that can be adjusted for any constraint violation using probabilistic limits. This model is best suited to cases searching for robustness against constraint violation.

Concerning the robust approaches that could be fitted with our model, the approach proposed by Aghezzaf et al. [2] has the advantage of generating solutions that are less sensitive to the data in the scenario set. The advantage of Aghezzaf's approach [2] is that it takes care of model and optimality robustness by minimizing both the expected performance and the maximum deviation (under worst-case scenario) of the model for all possible scenarios generated. As the robust method

applied in this chapter is a scenario-based one, I generated the required scenarios through several meetings and scenario assessment sessions with practitioners from the National Research Council of Canada. Thus the uncertainty sets (upper and lower bounds) related to each uncertain parameter in our model were determined based on expert opinion based on a similar situation that happened in the 2009 Black Saturday Australian Bushfire case which will be explained later in Section 3.5. Note that different parameters in our model that define a scenario are not independent. Therefore, scenarios cannot be defined based on independent uncertainty sets. The opinion of the aforementioned experts was required to define each particular scenario and not only the bounds of uncertainty sets.

However, new robust methodologies exist for dealing with various sources of uncertainty in the input parameters. Worst-case optimization is one of the most popular branches of robust optimization focusing on the extreme values of an uncertainty set (bounds) associated with each uncertain parameter [11]. There exists approaches in the literature for dealing with uncertainty in the LHS of constraints [6], RHS of constraints [48, 26], in the objective function [4, 8]. Such approaches are proven to perform well for different problem settings; however, the approach used here performs well for problems for which flexibility between the expected performance and the worst-case scenario is essential. The reader is referred to [6, 5, 11, 4] for comprehensive surveys of robust optimization approaches.

- **The robust formulation**

In this section, the robust version of the model in Section 3.3.1 is presented. To minimize the total operational cost and unmet demand under both the expected and the worst-case scenarios across all scenarios, the following changes are made to the objective function of the model in Section 3.3.1.

$$\min Z^R = \eta \times max_{s \in S}(\xi_s - \xi_s^*) + \lambda \times \sum_s \pi_s \times \xi_s \tag{3.23}$$

$$\xi_s = \sum_{j \in K_2} OC_j \times \gamma_j + \left(CW_1 \times \sum_{i \in D,h} UD_{ih}^s + CW_2 \times \sum_{i,j,x,v} Y_{i,j,v}^{xs} \right) \tag{3.24}$$

$$(3.2) - (3.5), (3.7) - (3.22). \tag{3.25}$$

The first term in the objective function in Equation (3.23) is the maximum variability while the second term is the expected weighted operational costs, travel duration and unmet demand ($\sum_s \pi_s \times \xi_s$). The parameters η (variability weight) and λ (expected cost weight) can be set by the wildfire response manager to reflect their preferences. Hence, to produce evacuation plans with higher objective variability but lower expected response time and shortage, the weight of η should

be increased and vice versa. In expression (3.23), ξ_s^* is the optimal value obtained by solving the deterministic model under the realization of the $sth, s \in S$ uncertain parameters (P_{ih}^s, t_{ij}^{vs}, and TW_i^s). Simply put, ξ_s^* is the optimal performance of the model resulting from the occurrence of scenario $s \in S$ in which UD_{ih}^s is the variable defined in constraint (3.6), related to operational costs, the under-fulfilment of demand for evacuation (number unserved people) and unnecessary trips, respectively.

To prevent any constraint violation (3.6) related to the under-fulfilment of demand (number unserved people), a penalty of constraint violation is considered (CW_1). This penalty cost is placed in the objective function in Equation (3.24) to find an optimal or near-optimal solution (solution robustness) and a feasible or near-feasible solution (model robustness).

- **Linearization**

Due to the non-linearity term of the $max_{s\in S}(\xi_s - \xi_s^*)$ in Equation (3.23), this term is replaced with the corresponding using the auxiliar variable Λ and the set of inequality constraints (3.27):

$$\min Z^R = \eta \times \Lambda + \lambda \times \sum_s \pi_s \times \xi_s \tag{3.26}$$

$$\xi_s - \xi_s^* \leq \Lambda \tag{3.27}$$
$$(3.2) - (3.5), (3.7) - (3.22), \Lambda \geq 0.$$

3.4 A Hybrid solution approach

Finding an optimal solution for the proposed evacuation model is not an easy task and the use of traditional linear and non-linear programming methods is accompanied by a heavy computational burden. Exact solutions (optimal) for large instances of the problem are impractical due to the complexity of the problem. VRP models are NP-hard problems. To ensure the applicability of the model to real-world instances of the problem, a hybrid heuristic solution algorithm method is required. In this chapter, we develop a combined two-phase solution methodology involving the Harris Hawks [13] and the Imperialist Competitive meta-heuristic algorithms [3] (HHO and ICA, respectively) to solve our NP-hard problem in a reasonable amount of time (less than one hour for the case study described later in this chapter). The reasons why these two algorithms are applied in our study compared to many other meta-heuristics algorithms are explained in the next paragraphs. Next, each algorithm is briefly required and then the combination of both is presented.

In general, meta-heuristics are classified into two types: single-solution based (e.g., Simulated

Annealing) and population-based (e.g., genetic algorithms) [13]. In the former, only one solution is processed during the optimization process, while in the latter, a set of solutions (i.e., a population) evolve during each iteration of the optimization process. Population-based techniques can often find an optimal or suboptimal solution that may be the same as the exact optimum or located in its neighbourhood. Regardless of the variety of these algorithms, there is a common feature: the search steps have two phases: exploration (diversification) and exploitation (intensification) which will be explained later. A well-organized optimizer should be capable of making a reasonable, fine balance between exploration and exploitation tendencies. Otherwise, the possibility of being trapped in local optima (LO) and immature convergence drawbacks increases. These are the main disadvantages of other meta-heuristic algorithms compared to population-based ones. One of the advantages of population-based algorithms such as the ones we use as the combination of HHO and ICA algorithms is their successful, inexpensive, and efficient application in recent years. As stated by Wolpert and Macready [42] based on the No Free Lunch (NFL) theorem, all optimization algorithms proposed so far show an equivalent performance on average if we apply them to all possible optimization tasks. However, according to NFL, we cannot theoretically consider an algorithm as a general-purpose universally-best optimizer. As a result, new optimizers with specific global and local searching strategies should be developed to apply to various forms of optimization tasks.

Overall, the algorithms used in this research are categorized as human-social (the ICA) and nature-inspired (the HHO) evolutionary optimization techniques and belong to a class of population-based algorithms. The main advantage of our combined HHO and ICA algorithm is its fast convergence rate. Moreover, its novel strategies prevent the algorithm from being trapped in local optima. In contrast, other algorithms, such as the Genetic algorithm, are computationally expensive (time-consuming) and face other challenges such as determining the right mutation rate that may results in the algorithm not converging.

Next, in sections 3.4.1 and 3.4.2, we describe the ICA and HHO algorithms in their general forms. Then, in Section 3.4.3, we introduce the hybrid ICAHHO algorithm, its steps, operators, and tuning parameters. We also provide a detailed pseudocode and explain how the algorithm is applied to the proposed evacuation model.

3.4.1 The Imperialist Competitive Optimization Algorithm (ICA)

This is a novel optimization method developed based on a socio-politically motivating strategy. The ICA is a multi-agent algorithm in which each agent is a country and can be either a colony or an imperialist. The countries form empires in the solution search space [3, 34]. Imperialistic competition is key, hopefully causing the colonies to converge to the global minimum of the cost

function.

Initial colonies are divided among the imperialists based on their "power". The power of each country is inversely proportional to its cost. The imperialist states together with their colonies form "empires". After forming initial empires, the colonies in each empire start moving toward their relevant imperialist country. This movement is a simple model of assimilation pursued by some of the imperialist states. The total power of an empire depends on both the power of the imperialist country and the power of its colonies. This fact is modelled by defining the total power of an empire as the power of the imperialist country plus a percentage of the mean power of its colonies. Subsequently, imperialistic competition begins among all the empires. Any empire that is not able to succeed in this competition and cannot increase its power (or at least prevent losing its power) is eliminated from the competition. The imperialistic competition gradually results in an increase in the power of successful empires and a decrease in the power of weaker ones. Weak empires will lose their power and ultimately collapse. The movement of colonies toward their relevant imperialist states along with competition among empires, and also the collapse mechanism, cause all the countries to converge to a state in which there exists just one empire and all other countries are colonies of that empire. In this new world, colonies will have the same position and power as the imperialist. Figure 3.3 summarized the ICA algorithm. The role of the ICA algorithm within the proposed solution approach will be explained later. The main advantage of ICA algorithms is their exploration feature, which allows them to explore various regions of the solution space. This feature, for instance, picks the weakest colony from the weakest empire and gives it to the empire with the most likelihood of possessing it. Such a colony-empire substitution or movement results in exploring regions of the solution space that include optimal or near-optimal solutions.

3.4.2 The Harris Hawks Optimization Algorithm (HHO)

The Harris Hawks Optimization (HHO) algorithm is a novel population-based, nature-inspired, and gradient-free optimization algorithm [13] that represents the cooperative behaviour and chasing style of a Harris hawk to catch prey. In this algorithm, several hawks cooperatively pounce prey from different directions in an attempt to surprise it. Harris hawks show a variety of chasing patterns and cooperative techniques based on the dynamic nature of scenarios (explained later) and escaping patterns of the prey. The HHO mathematically mimics such dynamic patterns and behaviours through the optimization process.

All HHO algorithms feature two phases: exploration (diversification) and exploitation (intensification). In the former, the algorithm utilizes and applies its randomized operators (selection of scenarios of Harris Hawks' movement) to explore various regions of the solution space. The exploratory behaviour of a well-designed optimizer should be able to explore randomly-generated

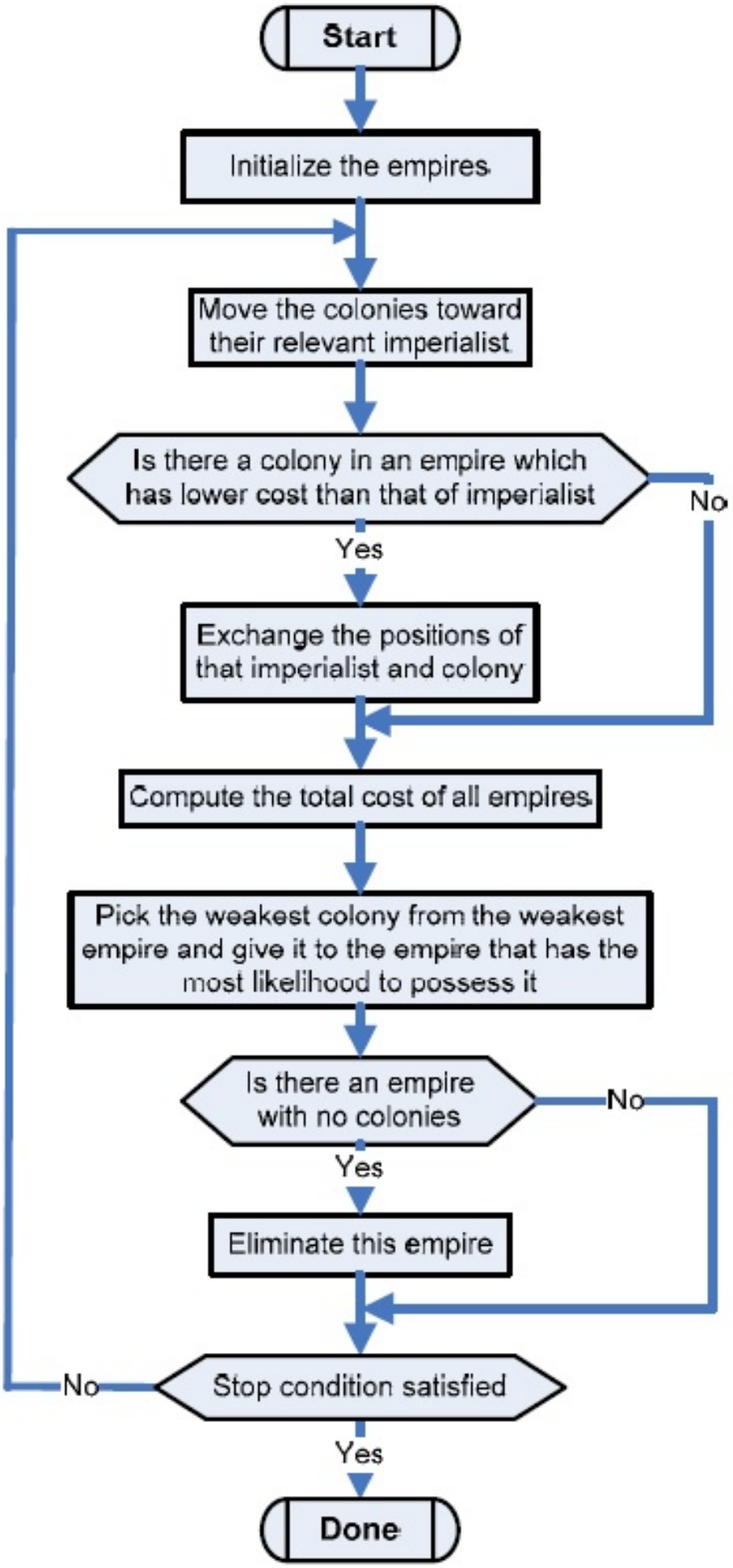

Figure 3.3: The ICA algorithm

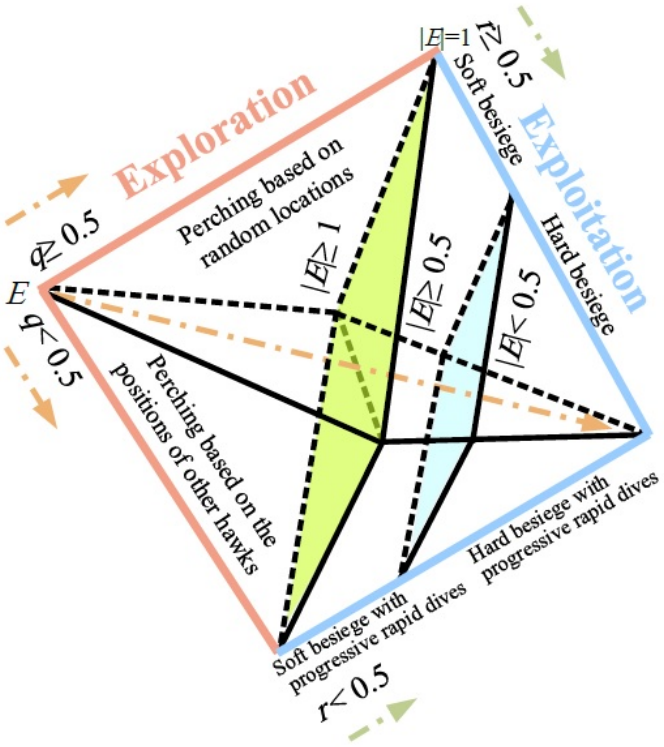

Figure 3.4: The HHO algorithm

solutions from different areas of the solution space during the early stages of the search process [12]. In the latter, the optimizer focuses on the neighbourhood of better-quality solutions located inside the solution space. Overall, the main idea behind the implementation of such an algorithm is to achieve a reasonable balance between the exploration and exploitation tendencies so as to prevent the algorithm from getting trapped in local optima.

A detailed description of the main steps of the HHO algorithm is presented in the following subsections. Also, an overall description of the HHO algorithm is depicted in Figure 3.4.

1- Exploration phase:

In the HHO algorithm, Harris's hawks perch randomly in some locations and wait to detect prey (rabbit) based on various strategies. If we consider an equal chance of occurrence q for each perching strategy, they perch based on the positions of other Hawks (to be close enough to them when attacking) and the prey (rabbit).

$$X(t+1) = \begin{cases} X_{rand}(t) - r_1|X_{rand}(t) - 2r_2X(t)| & q >= 0.5 \\ \Big(X_{rabbit}(t) - X_m(t)\Big)r_3\Big(LB + r_4(UB - LB)\Big) & q < 0.5 \end{cases} \tag{3.28}$$

where $X(t+1)$ is the position vector of the hawks in the next iteration t, $X_{rabbit}(t)$ is the position of the prey (rabbit), $X(t)$ is the current position vector of the hawks, r_1, r_2, r_3, r_4, and q are

random numbers with interval $(0, 1)$, which are updated in each iteration. LB and UB are the upper and lower bounds of the decision variables, $X_{rand}(t)$ is a randomly selected hawk from the current population, and X_m is the average position of the current population of hawks. The average position of the hawks is computed using Equation (3.29):

$$X_m(t) = \frac{1}{N} \sum_{i=1}^{N} X_i(t) \tag{3.29}$$

where $X_i(t)$ indicates the location of hawk i in iteration t and N denotes the total number of hawks.

2- Transition from exploration to exploitation:

The transition between the exploration phase and the exploitation phase depends on the implementation of different cooperative behaviours based on the escaping energy of the prey. Reasonably, the energy of prey decreases over time. Typically the energy of a rabbit is modelled as:

$$E_t = 2E_0(1 - \frac{t}{T}) \tag{3.30}$$

where E_t indicates the escaping energy of the prey, T is the maximum number of iterations, and E_0 is the rabbit's initial energy.

When the escaping energy $E \geq 1$, the hawks search different regions to explore a location (exploration phase) and then when $E \leq 1$, the algorithm exploits the neighbourhoods of the best solutions.

3- Exploitation phase:

In the exploitation phase, Harris's hawks perform a surprise pounce by attacking the intended prey detected in the exploration phase. However, prey often attempts to escape from dangerous situations. Hence, different chasing styles are considered. Suppose that $r < 0.5$ is the chance of a prey successfully escaping before the surprise pounce. Whatever the prey does, the hawks will perform a hard or soft besiege to catch the prey. It means that they will encircle the prey from different directions softly or hard depending on the retained energy of the prey. To model this strategy and enable the HHO algorithm to switch between soft and hard besiege processes, the E function is utilized. In this regard, when $E \geq 0.5$, a soft besiege happens, and when $E < 0.5$, a hard besiege occurs.

3.1. Soft besiege: This behavior is modeled by the following rules:

$$X(t+1) = \Delta X(t) - E|JX_{rabbit}(t) - X(t)| \tag{3.31}$$

$$\Delta X(t) = X_{rabbit}(t) - X(t) \tag{3.32}$$

where $\Delta X(t)$ is the difference between the position vector of the rabbit and the current location of hawks in iteration t, r_5 is a random number in the interval $(0, 1)$, and $J = 2(1 - r_5)$ represents the random jump strength of the rabbit throughout the escaping procedure. The J value changes randomly in each iteration to simulate the nature of rabbit motions.

3.2. Hard besiege: In this situation, the current positions are updated using Equation (3.33):

$$X(t+1) = X_{rabbit}(t) - E|\Delta X(t)| \tag{3.33}$$

Algorithm #1: The HHO Algorithm

Step 1. the population number ($POP_{n=1,2,...,N}$) and the number of iterations T as stopping condition are selected.

Step 2. Each hawk (1 to n) is randomly assigned to a location Λ (part of the solution space in terms of its direction and distance to the prey).

Step 3. Set the hunting position L to 0 and the rabbit's escape energy E to ∞ and set X_{rabbit} as the location of the rabbit (best location).

Step 4. Perform the following steps until the stopping condition is satisfied.

Step 5. For each hawk (1 to n) and rabbits (1 to m), check their location Λ_m and Λ_n compared to other Hawks and the prey. For each hawk, update the initial energy E_0 and jump strength J.

Step 6. Update E using Equation (3.30).

Step 7. If $|E| > 1$ (exploration phase) update the location vector using Equation (3.28).

Step 8. If $|E| < 1$ (exploitation phase), then if ($r >= 0.5$ and $|E| >= 0.5$), update the location vector using Equation (3.31), else if ($r \geq 0.5$ and $|E| \leq 0.5$), update the location vector using Equation (3.33).

Step 9. Evaluate the objective function for all hawks Z_n and set $\min Z_n$ equal to $|E|$ and update the rabbit's position X_{rabbit}.

3.4.3 A Hybrid Meta-Heuristic Algorithm for the 2MCVRP-TW Model

To reach the optimal or near-optimal solution faster for large instances and achieve a promising strategy, we combine the HHO [13] and the ICA algorithms [34]. The HHO is a robust algorithm in the exploitation phase, but it has poor performance during the exploration phase. The ICA, on the other hand, has a better performance (searching the solution space faster) in terms of exploration [19]. Although combining these two population-based algorithms enhances the search capabilities, this does not guarantee a global optimum.

The combined hybrid algorithm, called ICAHHO, can pursue several potentially optimal solutions as the result of the diversification power of the ICA. Moreover, the randomized time-varying nature of the HHO algorithm helps avoid local minima. The combination of the HHO and the ICA algorithms helps avoid premature convergence. Simultaneously, the promising regions are carefully examined, which are prevalent issues (i.e., getting stuck in local minima, premature convergence of the algorithms) arising in applying meta-heuristics to complex solution spaces. It should be noted that the operators used in the ICAHHO algorithm (Algorithm #2) are explained in detail after introducing the steps of the algorithm. Furthermore, some of the tuning parameters for the ICAHHO algorithm are presented below:

N_{pop} = 500, Number of empires: $\frac{N_{pop}}{10}$, Assimilation rate=2, Probability of revolution (Prevolve)=0.5, Uniting threshold (The percent of Search Space Size, which enables the uniting process of two Empires)=0.45, Search space size= $upperbound - lowerbound$ of the independent decision variables, Number of iterations= 500.

The main steps of the algorithm are summarized in the following. It is important to note that in the ICAHHO algorithm (Algorithm 2), the colonies are denoted as the routes with higher cost compared to their empire or the solution or routes with the lowest cost (the objective function value (Equation 3.1). To link algorithms 2 and 3 to the characteristic of our proposed model, we will explain in detail the various operators used in the algorithms.

In Algorithm 2, various operators based on those of the HHO and the ICA algorithms are employed. Such operators are called by the ICAHHO algorithm to compute the objective function of the main model (Equation 3.1) within the bounds of the independent decision variables (Y^x_{ijv} and IPH^x_{ijv}). At each stage, a set of solutions (various routes defined by Y^x_{ijv} and the number of transported patients to multiple locations, given by IPH^x_{ijv}) is generated that costs less. Gradually, we keep the solutions that cost less and produce new solutions and compare them with the previous ones. If the solution was better, we will accept the new solution. In the first iteration, a set of solutions is produced, the solutions with minimum cost define the empires and the higher cost ones, the colonies.

Algorithm #2: The ICAHHO Algorithm

Step 1. Initialization

Step 1.1. the population number ($Npop$), number of iterations, number of empires, assimilation factor, and the algorithm's revolution rate (probability of revolution) are selected.

Step 1.2. Select a few random points in the solution space ($upperbound - lowerbound$ of the

routing variables; Y_{ijv}^{x} and IPH_{ijv}^{x}) and form initial groups (generating initial countries randomly).

Step 2. Evaluate the fitness of each country.

Step 3. Form initial empires.

Step 3.1. Choice power countries as imperialists.

Step 3.2. Assign other countries (colonies) to imperialists based on their power.

Step 4. Move the colonies of an empire toward the imperialist based on HHO rules (Implementation of HHO).

Step 4.1. For each empire, the position of the empire defines the position of the prey and the position of the colonies, those of the hawks.

Step 4.2. Consider the cost of each empire as the cost of the prey.

Step 4.3. Update the positions of each empire and colony.

Step 5. Revolution among colonies and imperialist.

Step 6. If the cost of a colony is lower than that of the imperialist, exchange positions.

Step 7. Calculate the total power of the empires.

Step 8. Select the weakest colony of the weakest empire and assign it to one of the strange empires (Imperialistic competition step).

Step 9. Eliminate the powerless empires (the imperialist with no colony).

Step 10. Uniting similar empires.

Step 11. If there is only one group left, stop. Otherwise return to **Step 2**.

When the HHO algorithm is applied in the ICA algorithm, the positions of colonies and empire define those of hawks and prey to move toward better solutions, improved Y_{ijv}^{x} and IPH_{ijv}^{x} variable values resulting in a lower cost.

The applied operators are briefly explained below:

- **Create-initial-population** operator: **Steps 1-3** are performed using this operator. such an operator not only creates the initial value of parameters or population (number of population, number of imperialists, assimilation rate, etc.), but it also sorts the population based on their cost. The empire that has the minimum cost (Equation 3.1) is chosen as the best solution. To find the empire with the minimum cost (Equation 3.1), the following operators are executed.

- **Assimilation** operator: In **Step 3.2**, the assimilation operator has the duty assigning colonies to empires or routing variables (Y_{ijv}^{xs} and IPH_{ijv}^{xs}) of higher costs to the one with the lowest cost. In our hybrid algorithm, the assimilation process is done based on the HHO rules. In other words, all the operators at each iteration are computed using the bounds (lower bound, lb and upper bound ub) of the routing variables of the main model. The IC-AHHO algorithm continues iterating until there is no improvement in the objective function

in Equation 3.1 using the Y_{ijv}^{xs} and IPH_{ijv}^{xs} variables.

- In **Step 4**, various strategies based on the values of E and q (refer to the HHO algorithm) are determined. The HHO algorithm is used here to move the colonies toward the solutions (Y_{ijv}^{x} and IPH_{ijv}^{x}) with fewer costs (Equation 3.1). In the basic steps of the HHO algorithm, a hawk is trying to catch prey while, by combining the HHO and the ICA algorithms, we consider a group of hawks and a prey. The prey in the HHO algorithm is positioned itself as an empire in the ICA algorithm and the group of hawks as the colonies. It should be noted that the empire and colonies in Algorithm 2 represent the solutions of independent decision variables (Y_{ijv}^{x} and IPH_{ijv}^{x}) with minimum cost and the higher cost ones, respectively. In other words, at each iteration of the algorithm, new routes are generated to improve the model's objective function (Equation 3.1).

- **Calculated-total-cost** operator: In **Step 4.3**, the operator computes the total cost for an empire (equivalent to the value of the objective function in Equation 3.1 for the derived solution or the current empire) based on the cost of colonies and imperialists. In other words, by searching through the solution space, better routes are computed to minimize the objective function related to the total operational cost and unmet demand.

- Further in **Step 5**, to change randomly some of the variables to see their impact on the objective function cost, the **Revolution** operator at colonies or routes with higher costs should be used. If the random value assigned to a variable is lower than the probability of revolution, for all the colonies i to k, their position is updated:
$lowerbound(k)$+ random parameter $\times\big(upperbound(k) - lowerbound(k)\big)$. The revolution happens when the position of colonies or routes with higher costs moves toward a better position or lower costs. When the routes with lower costs are generated at the current run compared to the values of routing variables in the previous run, the revolution with the probability mentioned above occurs to find a solution with a lower objective function value (lower unmet demand and operational cost).

- In this algorithm in **Steps 6 and 7**, when one of the routes in an empire or the route with minimum cost becomes more powerful than the empire, then their positions are exchanged using the **exchange-operator**. Thus, if the value of a specific route compared to its empire or the route with the lowest cost is lower, that route becomes the new best route or empire with the minimum cost.

- **Imperialistic-competition** operator: In **Steps 8 and 9**, the operator combines colonies or routes (solutions with the lowest cost) while the weakest colony or routes with higher costs in the weakest empire (having the lowest cost compared to other routes in its empire) is

separated from that empire and randomly assigned to another empire. In other words, this operator combines Y_{ijv}^{x} and IPH_{ijv}^{x} with higher costs and moves them to the solution space where the routes with lower costs exist.

- When a colony or route with the higher cost is separated from an empire, we need to apply another operator, called **roulette-wheel** that assigns a random number to combine a colony or route with higher cost with another empire or route with minimum cost. This operator uses the fitness function that assigns to every routing variable value (solution) in the population of all other routes. The probability function of the selection of a solution where f_i represents the fitness of solution i, N represents the size of the population of all possible routes and the probability function p_i is given by $P_i = \frac{f_i}{\sum_{j=1}^{N} f_i}$

- According to the **Step 10**, if two routes or empires with the lowest cost are very similar, they are merged using the **uniting-similar-empires** operator. Two routes are merged if they take more than 0.4 of the solution space. The value of 0.4 is obtained by performing several trial-and-error experiments. In this operator, for different routes or empires resulting in lower costs compared to weaker solutions or colonies, the distance of the values of the two routes is computed. The distance is computed by finding the difference between the position of two solutions (routing values with the lowest costs). If the distance is lower than 0.4 $\times$ search space size and if one solution or empire i is lower than another solution or empire j, the solution i is regarded as the best and another solution j the worst. Finally, the solution or the route which is chosen as the best, the total cost of the objective function (Equation 3.1) is updated based on the value of the new best route or solution.

- Finally, in **Step 11**, the stopping criterion is introduced. The stopping condition for the algorithm is the number of iterations based on a trial and error approach and if there exists no solution better than the solution or the routes that are generated. For the case study described later, we run the ICAHHO algorithm five times, each run with 1,000 iterations. The stopping criterion is checked, if the convergence (stopping) plot becomes unchanged under a pre-specified number of iterations (e.g. 1000 iterations), then the algorithm stops, otherwise, we need to increase the number of runs and iterations to reach convergence.

In summary, for each run, after producing an initial population or the number of possible routes and sorting them based on the cost of each empire, the aforementioned operators are employed. Out of the different runs, the one which results in the lowest expected total cost associated with the operation of the SMSs, the number of unserved evacuees and the length of routes must be chosen as the best run. It should be noted that, after computing the value of the independent routing variables (Y_{ijv}^{x} and IPH_{ijv}^{x}) of the proposed evacuation model using the ICAHHO algorithm in

Algorithm #3: The ICAHHO Algorithm

Inputs: algorithm and problem parameters
Outputs: The location of the rabbit and its fitness value
Generate the population randomly $X_i(i = 1{:}N)$
While (stopping condition is not met) **do**
Initialized the empires:
For (each country (X_i)) **do**
    Compute the evolution cost C_i
    Sort the compute cost C_i in descending order for the entire population
    Select N_{imp} (number of imperialist countries) out of N_{pop}
    Normalize the cost of each imperialist C_n
    Compute the normalized power of each imperialist P_n
    Assign N_{col}remained countries to the imperialist
End
Assimilation, Revolution, Imperialist Competition Processes:
For j=1 to N_{imp} **do**
    Move the colony toward the relevant imperialist (assimilation)
    Compute the costs of assimilated countries
    Perform revolution on the new colony
    If the cost of the new colony is less than the cost of imperialist, **Then**
        Exchange the position of colony and imperialist
    Pick the weakest colony (colonies) from the weakest empire and assign it (them) to the empire that has the most likely to possess it
    End
End
Elimination process:
If there is imperialist with no colonies, **Then**
    Eliminate the imperialist
End
Return X_{min}

Figure 3.5: The ICAHHO algorithm

each run, the $fitness$ function in our code for Equations (3.1) to (3.27), uses such values as inputs to calculate the objective function of the main model. In other words, at each run, the ICAHHO algorithm saves the best solution (the best values of the Y^x_{ijv} and the IPH^x_{ijv} resulting in a minimum cost) which allows us to plot the convergence curve and compute the objective function of the robust evacuation model (Equation 3.26). The pseudocode of the algorithm is presented in Figure 3.5.

3.5 Implementation and evaluation

To benchmark the performance of the solutions obtained via the proposed approach, we compare the deterministic and robust models' results with those from other potential policies, taking into account different experimental datasets. To evaluate the models' performance for a real-world case study, we use data from the Murrindindi region of Victoria, Australia. The models were coded in GAMS with CPLEX as the solver, and Matlab was used to code the hybrid meta-heuristic algorithm (ICAHHO). All results in this chapter were obtained using a windows 10 pro PC with a Core i7-8565U 2.4 GHz processor and 16 Gb.

3.5.1 Case problem

This section begins with a detailed description of the case study in Victoria, Australia, which is used to evaluate the proposed solution approach. The data was gathered from different sources in the literature [29, 31, 36, 38, 37].

The Shire of Murrindindi is a region located approximately 100 kilometres northeast of Melbourne in Victoria, Australia. It has a population of 41,860 with a population density of 3.5 people per square kilometre. Around 46 % of the total land area of the municipality is forest (1,788 square kilometres), including state forests, parks, reserves, and other public lands. A large proportion of this land is mountainous and densely forested (Figure 3.7). This region has been classified as a high-risk bushfire-prone area and has experienced various massive and minor bushfires resulting in significant losses of wildlife, infrastructure and human lives [35].

A series of severe bushfires hit Murrindindi on and around Saturday, February 7 2009, a date which is now known as Black Saturday. The initial phase of the fire commenced near a sawmill on Wilhelmina Falls Road around 3:00 pm. The bushfire spread rapidly and by 4:30 pm had reached the town of Narbethong, more than 50 km away. Due to a change in wind direction, the fire swept through the towns of Marysville, Buxton, and Taggerty. The fire burnt approximately 168,000 hectares of land and resulted in massive disruption and damage to some crucial infrastructure. The Black Saturday Murrindindi wildfire resulted in the deaths of 40 people, 71 injured people, and the dislocation of more than 500 households (Figure 3.6). Figure 3.6 indicates the affected region, the location of the fire source, the wind direction from north to west at the beginning of the

Table 3.2: The information data of the case study area.

	EAS i	Population* (evacuees) (P)	Time Windows (minute)** i	#	Shelters $\in k$	Capacity (evacuees) (SC_{k2})	#	Hospital $\in k$	Capacity (evacuees) (SC_{k1})***
1	Narbethong	40	200	1	Alexandra	50	6	Yea District Memorial Hospital	10
2	Marysville	20	190	2	Thornton	40	7	Healesville Hospital Yarra Valley Health	20
3	Taggerty	50	240	3	Eildon	50			
4	Buxton	30	300	4	Yea	30			
5	Cambarville	30	360	5	Yarra Glen	50			
6	Rubicon	50	400						

*population refers to the number of evacuees located at EASs.
**time windows for each township is computed in section 3.5.2.3.
***only capacity related to patients with medical needs is given here.

evacuation response operation and later from south to west, and the location of townships (EASs) SMSs and hospitals.

3.5.2 Data

The geographical region for this study are shown in Figures 3.6 and 3.7. According to Figure 3.7 [38], the geographical region consists of the six main towns (EASs) that are at high risk of frequent wildfires (Narbethong, Marysville, Taggerty, Buxton, Cambarville, and Rubicon) [28]. According to the Chief Fire Agency (CFA) research data, around 2,160 people in total lived in the area and only 1,100 persons were required to be evacuated by evacuation teams [29]. Furthermore, out of the 1,100 evacuees, only around 220 people needed immediate medical care at medical centers. We consider approximately the same number of evacuees (around 20 % of the total number) who require medical care at different levels and must be transferred to medical centers. According to the CFA [35], five potential locations (Goughs Bay's fire station in Alexandra, a recreation reserve oval in Thornton, a basketball court in Eildon, a skate park in Yea, and a race track in Yarra Glen) are considered as the potential location of shelters in adjacent towns to locate the evacuees of injury types (triage levels) 2 and 3. Also, for patients of injury type 1, we considered two hospitals: District Memorial Hospital in Yea and Healesville Hospital in Yarra Valley. It should be noted that the location of SMSs is pre-specified by the CFA and, in this research, we only decide which specific SMSs to select. The decision concerning the potential locations of potential SMSs and hospitals is out of the scope of this study.

Table 3.2 outlines the finite service capacity of each shelter and hospital. Travel times and vehicle capacity are critical factors in emergency evacuations, having an impact on the evacuation plan. Vehicle capacity and travel time between any two locations of the evacuation network are derived from actual geographical data and travel speed zones [36], for available EASs. The time windows, wildfire spread direction and road disruption data were all derived from the recorded figures for the 2009 Murrindindi Black Saturday bushfire [37]. As stated earlier in Section 3.3.2, we consider three sources of uncertainty in our model which are characterized in detail in the following.

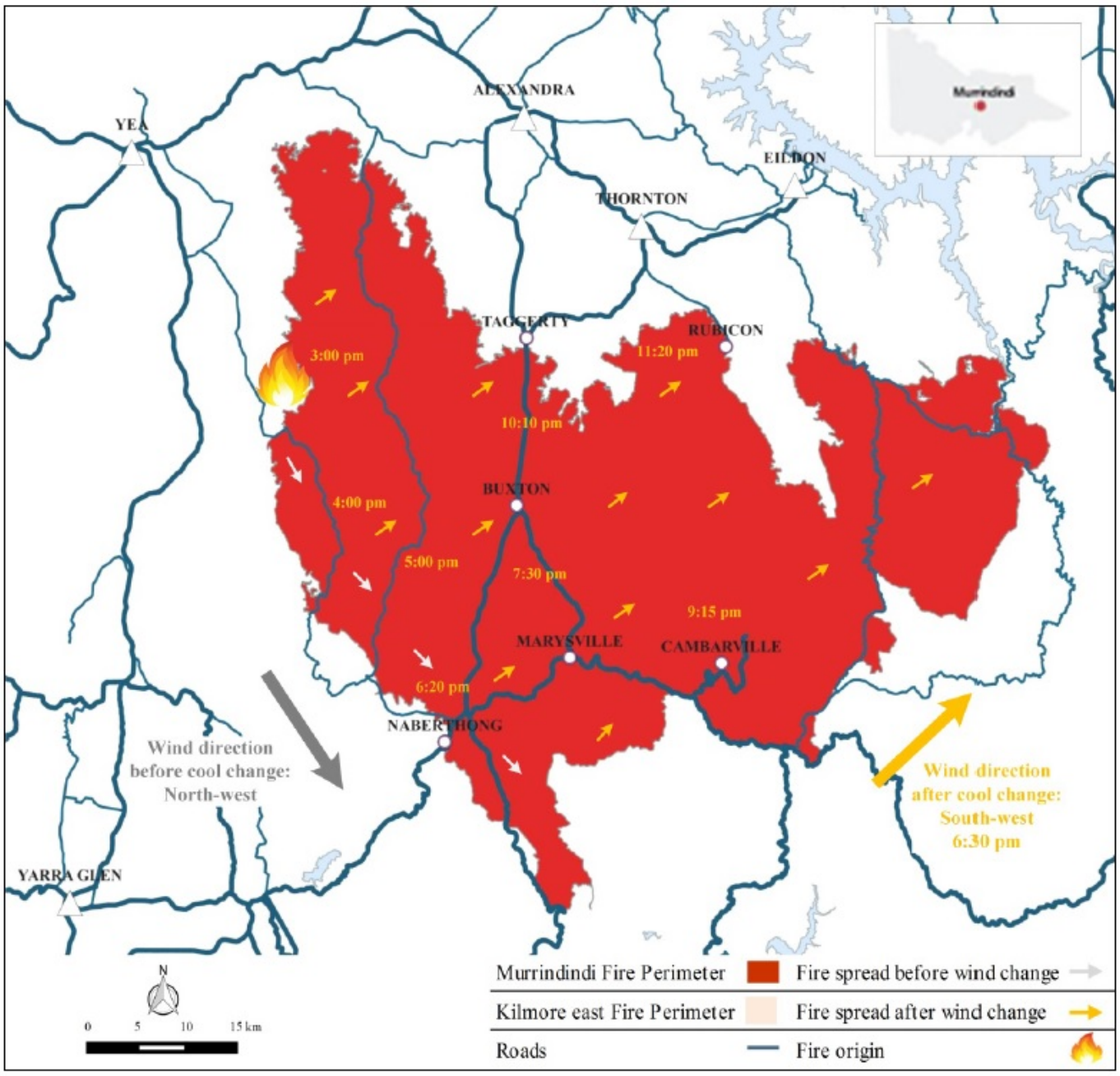

Figure 3.6: 2009 Murrindindi Black Saturday bushfire propagation map. The fire commenced in an area near the Murrindindi Sawmill at approximately 3:00 pm. The blue and red arcs show the wind direction on Black Saturday. The white and yellow arrows, respectively, show the bushfire direction before and after a 6:30 pm wind direction change. The fire reached the nearby town of Rubicon after 9 hours.

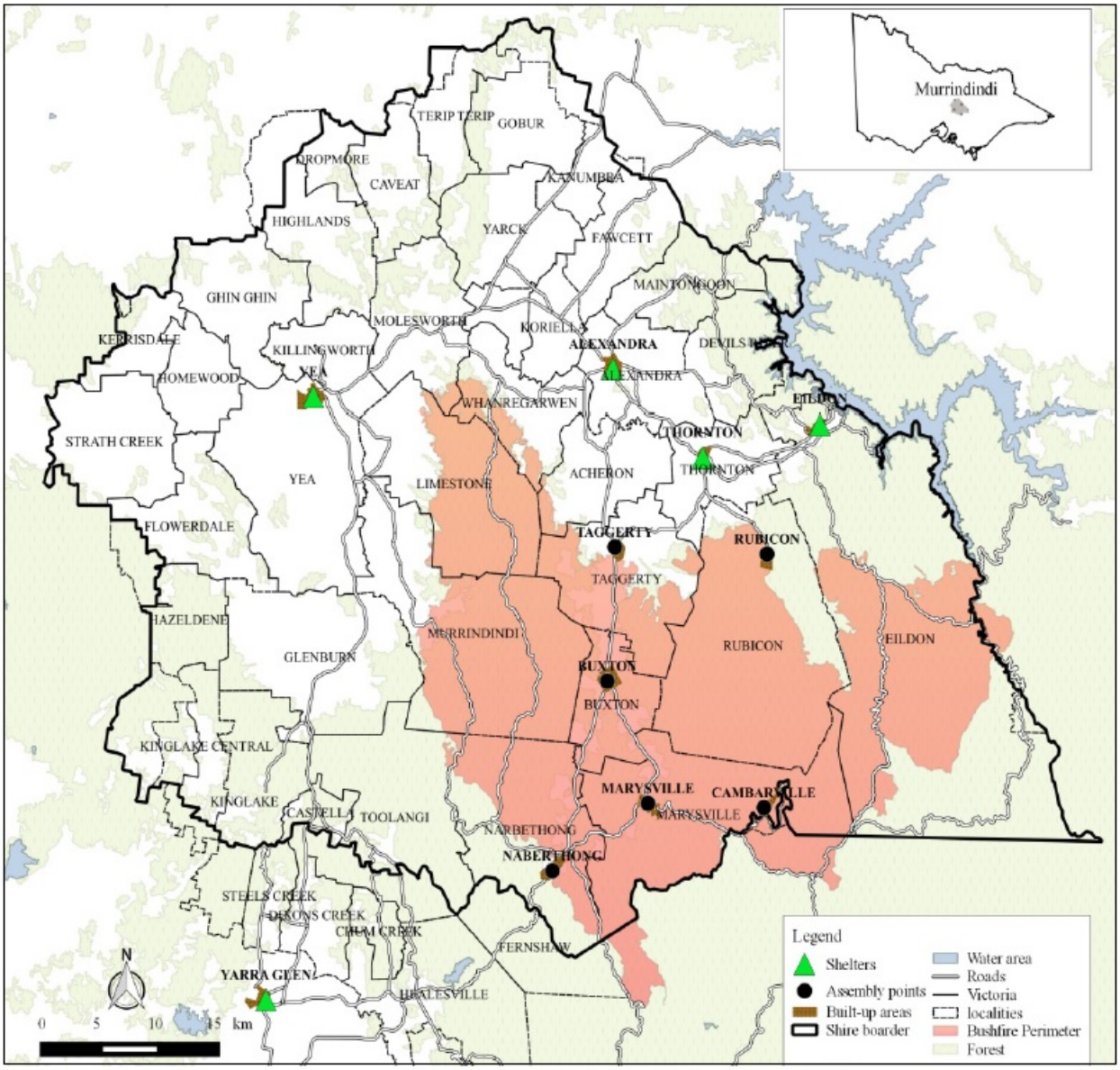

Figure 3.7: Case-study region - Murrindindi Shire, Victoria, Australia.

3.5.2.1 Number of evacuees at EASs

The first source of uncertainty is the number of people (P_{ih}) waiting at each EAS. In real wildfire evacuation settings, it is very complicated to predict the behavioural patterns of evacuees. Therefore, in this chapter, we assume P_{ih} follows a uniform probability distribution $U(10, 50)$ no matter the distance of an EAS i from the fire. The reason is that no historical data exists showing which EAS the evacuees selected.

3.5.2.2 Vehicles capacity and travel times

In this study, the facilities (EASs, SMSs, and hospitals) use two types of vehicles, paramedic buses (capacity of 10) and ambulances (capacity of one). The speed zones [36] suggest that the travel speed for all the areas in the study is 100 km/h without congestion. However, it should be noted that the travel time between geographical locations for ambulances is less than that of paramedic buses (lower by 20 %).

During emergencies, timing is known to be the most crucial issue. During an evacuation, traffic increases which increase the travel times accordingly [46]. There is a wide range of road congestion algorithms which can be utilised (for example see [32]) to adjust travel times. An appropriate route resistance function, for instance, should reflect how various transit components may directly or indirectly impact evacuation times. The following expression is therefore used to adjust travel times:

$$t_{ij}^{v} \times (1 + TMF) + DT$$

where t_{ij}^{v} denotes travel time of vehicle v between location i and location j, TMF is percent travel time inflation due to road congestion (time impedance factor), and DT represents the dwell time. The latter (DT) represents the time the vehicle is boarding/alighting evacuees [39]. On average, the dwell time is no longer than 12.5 seconds/person in emergency evacuation [31]. In this chapter, it is therefore assumed that the DT and TMF values are known and are set to 10 minutes and 10%, respectively. Transportation times between facilities are considered to be uniform. During wildfires, the closer the location of a route is to the source of the fire, the riskier that route for patient transportation is. Travel times are inevitably impacted by two main elements: the risk of a route (based on historical data on the frequency and impact of wildfire on that route), and other vehicle-related and road congestion factors (TMF and DT). Assuming a distribution for the travel time parameter t_{ij}^{v} without considering the risk element may not be wise, as it may result in wrong estimates for routes located closer or further from the source of the fire. For instance, if the route between locations i and j is closer to the source of the fire compared to the route between i

Table 3.3: Wildfire routes risk assessment module (RR_{ij}) for the studied area.

Risk 100% : $\text{RR}_{ij} = (\text{IP}_{ij} \times PP_{ij}) \times (RRC_{ij} \times LC_{ij})$	Probability ($\text{IP}_{ij} \times PP_{ij}$)	50%	IP_{ij} (Ignition Probability)	45%	Ignition potential	50%
					Fuel on road reserve	20%
					Ignition history	30%
			PP_{ij} (Propagation Probability)	55%	Fire Behaviour	50%
					Propagation ability	50%
	Consequence ($\text{RRC}_{ij} \times LC_{ij}$)	50%	RRC_{ij} (Road Reserve Consequence)	10%	Economic assets	40%
					Cultural assets	5%
					Environmental assets	5%
					CFA precincts	5%
			LC_{ij} (Landscape Consequence)	90%	Economic assets	40%
					Cultural assets	10%
					Environmental assets	10%
					Human assets	50%

and j', the distribution based on travel times may not differentiate the risk of such routes and may assign lower travel time to ij compared to ij'. Clearly, the route of ij is riskier than route ij' due to disruption that may require a longer re-route. As a result, we consider travel times as uncertain and following a uniform distribution, where t_{ij}^v is the uncertain term in the following distribution:

$$t_{ij}^v + U\Big(t_{ij}^v \times (1 + TMF) + DT,\ \ t_{ij}^v \times (1 + RR_{ij})\Big)$$

Where RR_{ij} denotes the risk of the route between i and j. We use the wildfire risk assessment approach provided in Table 3.3 [38] as the source for determining the disruption risk for each route. The reason for using RR_{ij} in the above distribution is the advantage of getting less bias and more reliable distribution for the uncertain parameter t_{ij}^v. As clearly stated, this formulation of the travel time can capture the risk of the routes and the road congestion factor which can delay the evacuation process. The RR_{ij} factor for each connection between locations i and j can be computed using the Table 3.3. In this table, the RR_{ij} is computed based on two main elements: probability and consequence of fire on each route. Each element has an equal impact (50%) on the risk level of each route. As the route disruption and the way the fire spreads or propagates toward the routes in the evacuation network are more critical for casualty transportation compared to other elements, higher weights are considered for each. Overall, the travel times and associated risk for each link in the evacuation network are given in tables 3.4, 3.5 and 3.6.

3.5.2.3 Times windows for EASs

The impact of a wildfire varies depending on various factors such as the intensity and direction of the fire and the vulnerability of the EASs [31, 29]. Since the risk level of routes can be captured by the travel time parameter t_{ij}^v, here we only focus on the availability of EASs. Once a wildfire

Table 3.4: Travel times and disruption risk for trips between EASs and medical centers (hospitals and SMSs)

From	To	Travel time (min)	Disruption risk	From	To	Travel time (min)	Disruption risk
Narbethong	Yea	63	0.54	Marysville	Yea	65	0.5
	Alexandra	34	0.55		Alexandra	42	0.5
	Thornton	30	0.55		Thornton	33	0.49
	Eildon	41	0.56		Eildon	46	0.52
	Yarra	36	0.48		Yarra	47	0.51
	Yea and District Memorial Hospital	35	0.41		Yea and District Memorial Hospital	44	0.4
	Healesville Hospital and Yarra Valley Health	20	0.39		Healesville Hospital and Yarra Valley Health	39	0.33
Buxton	Yea	59	0.5	Taggerty	Yea	37	0.51
	Alexandra	30	0.51		Alexandra	14	0.52
	Thornton	21	0.49		Thornton	10	0.5
	Eildon	34	0.53		Eildon	21	0.62
	Yarra	53	0.53		Yarra	56	0.52
	Yea and District Memorial Hospital	15	0.48		Yea and District Memorial Hospital	15	0.49
	Healesville Hospital and Yarra Valley Health	28	0.29		Healesville Hospital and Yarra Valley Health	25	0.36
Cambarville Yea	Yea	76	0.49	Rubicon	Yea	47	0.55
	Alexandra	53	0.48		Alexandra	26	0.58
	Thornton	49	0.46		Thornton	15	0.63
	Eildon	60	0.49		Eildon	147	0.42
	Yarra	65	0.48		Yarra	81	0.54
	Yea and District Memorial Hospital	45	0.32		Yea and District Memorial Hospital	55	0.38
	Healesville Hospital and Yarra Valley Health	20	0.30		Healesville Hospital and Yarra Valley Health	50	0.31

hits a region, the EASs within the region will no longer be accessible, creating a time window for each EAS.

The propagation of a wildfire across a geographic area is highly unpredictable. Generally, the wildfire spread rate (BSR) is influenced by three fundamental factors: fuel, topography, and weather. More importantly, changes in each of these elements can significantly alter its impact. The historical data provided by the Victorian Bushfire Royal Commission related to time windows for each EAS in the region being considered is provided in Table 3.2.

3.5.2.4 Time scale

Since the problem is at the operational level, it is suitable to have a shorter continuous time scale (e.g., minutes). As the evacuation of patients must be undertaken within a limited amount of time (the time windows) for each EAS, the proposed evacuation VRP model (2MCVRP-TW) deals with a very short-term relief operation.

3.6 Results and analysis

To test the ability of the deterministic and robust models with/without using the hybrid solution approach to generate good evacuation plans, it is important to consider realistic wildfire scenarios.

Table 3.5: Travel times and disruption risk for trips between EASs

From	To	Travel time (min)	Disruption risk	From	To	Travel time (min)	Disruption risk
Nabethong	Marysville	10	0.55	Marysville	Nabethong	10	0.55
	Buxton	15	0.51		Buxton	10	0.54
	Taggerty	25	0.55		Taggerty	20	0.59
	Cambarville	20	0.49		Cambarville	8	0.41
	Rubicon	30	0.61		Rubicon	25	0.46
Buxton	Marysville	10	0.54	Taggerty	Marysville	20	0.59
	Nabethong	15	0.51		Nabethong	25	0.55
	Taggerty	10	0.41		Buxton	10	0.41
	Cambarville	20	0.39		Cambarville	30	0.59
	Rubicon	20	0.44		Rubicon	15	0.35
Cambarville	Marysville	8	0.41	Rubicon	Marysville	25	0.46
	Nabethong	20	0.49		Nabethong	30	0.61
	Taggerty	30	0.59		Taggerty	15	0.35
	Buxton	20	0.41		Cambarville	40	0.61
	Rubicon	40	0.61		Buxton	20	0.44

Table 3.6: Travel times and disruption risk for trips between medical centers (SMSs and hospitals)

	From/To	Yea	Alexandra	Thornton	Eildon	Yarra	Yea and District Memorial Hospital	Healesville Hospital and Yarra Valley Health
Travel time (min)	Yea	-	15	20	30	30	5	35
Disruption risk		-	0.22	0.15	0.26	0.30	0.25	0.25
Travel time (min)	Alexandra	15	-	10	20	35	15	30
Disruption risk		0.22	-	0.25	0.19	0.22	0.22	0.31
Travel time (min)	Thornton	20	10	-	10	35	18	30
Disruption risk		0.15	0.25	-	0.22	0.19	0.29	0.34
Travel time (min)	Eildon	30	20	10	-	40	27	34
Disruption risk		0.26	0.19	0.19	-	0.34	0.21	0.35
Travel time (min)	Yarra	30	35	35	40	-	30	10
Disruption risk		0.30	0.22	0.19	0.34	-	0.36	0.29
Travel time (min)	Yea and District Memorial Hospital	5	15	18	27	30	-	25
Disruption risk		0.25	0.22	0.29	0.21	0.36	-	0.39
Travel time (min)	Healesville Hospital and Yarra Valley Health	35	30	30	34	10	25	-
Disruption risk		0.25	0.31	0.34	0.35	0.29	0.39	-

Two scenarios were developed to reflect alternative levels of disruption and uncertainty. Additionally, sensitivity analyses were undertaken to evaluate the performance of the proposed coordinated 2MCVRP-TW deterministic and robust models, i.e., the split delivery and split pickup transportation strategy, compared with that of the non-fully coordinated transportation approaches. Furthermore, the efficiency of the proposed hybrid algorithm is analyzed under different settings and compared with the solution obtained with the Cplex solver. It should be noted that such a comparison is undertaken only for the data size associated with the case study for both deterministic and robust models; however, for larger data sets only the hybrid algorithm is employed to get the results. Finally, a sensitivity analysis regarding key problem parameters is provided to obtain insights into how such changes may affect emergency evacuation plans.

This section is organized as follows. First, in Section 3.6.1 we estimate the value of the corresponding coordinated strategy under the proposed robust approach. Second, in Section 3.6.2 we estimate the value of corresponding uncertainty by comparing the robust approach vs. the deterministic one for both the coordinated and the un-coordinated strategies. Third, in Section 3.6.3 we estimate the value of using the proposed hybrid algorithm with reference to exact solutions under various cases for both the coordinated and the un-coordinated strategies. Fourth, in Section 3.6.4 we perform a sensitivity analysis regarding key problem parameters, and finally, in Section 3.6.5 we analyze the model and the solution robustness.

3.6.1 Value of the coordinated evacuation strategy under the robust approach

In this section, the results obtained for the 2MCVRP-TW model are compared under the following two scenarios.

Scenario I: Baseline. It reflects the actual series of events that occurred during the 2009 Black Saturday wildfires. All the parameters of the deterministic and robust models are based on the derived data described in Section 3.5. Origins, destinations, and regional road data are input to both models mentioned above. The dynamics of the wildfire, the travel times among various locations and the time windows for evacuation are all set based on the historical records [38].

Scenario II: Disruption in a high capacity shelter. It is created to investigate the ability of the models to generate routing plans under the disruption of a high-capacity shelter. The shelter that accommodates the largest number of evacuees is disrupted to capture the impact of this situation on the evacuation plans, including vehicle scheduling and utilisation, and routing.

The purpose of this section is to investigate the capability of the aforementioned models to generate valid emergency evacuation plans that optimize the utilisation of available resources such as vehicles and shelters while transferring the maximum number of the affected populations to the relevant medical centers via the safest routes. Notably, the plans obtained using the proposed algorithm

are optimal for the deterministic and robust models.

Under Scenario I (baseline), the evacuation plan uses six paramedic buses and two ambulances to transport evacuees to six SMSs. Bus 1 starts its operation at Buxton, transporting its first passengers to the closest available SMS in Thornton, via the safest route. Due to the short travel time and evacuation time window, Bus 1 is unable to return to Buxton to pick up further evacuees from that township. Instead, Bus 1 leaves Thornton to pick up evacuees from Taggerty. Taggerty has the third shortest evacuation time window behind Narbethong and Marysville. Table 3.7 illustrates that multiple trips via the lowest risk routes are necessary in order to rescue all 30 evacuees of types 2 and 3 from Buxton by Buses 1,3, and 4 prior to the wildfire engulfing the town. After delivering 20 evacuees to Buxton and Taggerty, Bus 1 travels to Rubicon (the nearest EAS) from Thornton to pick up all 50 people from that EAS, delivering them to Eildon until it reaches its capacity. Table 3.7 demonstrates that Bus 1 could transport 70 evacuees of triage levels of types 2 and 3 from Buxton, Taggerty, and Rubicon to the closest available SMSs of Eildon and Thornton via seven trips, within the predefined wildfire evacuation time window. However, other non-transferred evacuees at other wildfire-affected townships also need to be safely evacuated within their respective time windows. Hence, the model assigns Bus 2 to start its evacuation operation from Narbethong. Given that the Eildon has already reached full capacity due to evacuees delivered by Bus 1, and it is also far from the Narbethong, Bus 2 evacuates 20 evacuees of triage level 3 to the closest available SMS at Yarra Glen. Two ambulances are employed to take 10 evacuees of type 1 to a designated hospital at Healsville. Table 3.7 outlines the schedule for each designated paramedic bus and ambulance and the evacuation process for the other EASs.

The results for the previous scenario show that the shelters in Alexandra and Thornton, due to their proximity to the townships and high capacity, are vital to the evacuation of patients from EASs. In Scenario II, it is assumed that Thornton is not available as a safe shelter. The results in Table 3.8 show that the model re-routes the available paramedic buses and ambulances to enable the safe transport of all evacuees to the remaining SMSs. Compared to Scenario I, more ambulances and paramedic buses are employed to transport all the evacuees to the available SMSs. Bus 1 starts its evacuation operation by transferring all the evacuees from Buxton to the SMS located at Alexandra. Bus 2 performs multiple pickups from Rubicon to safely transport evacuees to the shelter in Eildon until the latter reaches its capacity. Buses 3 to 7 transfer the remaining evacuees from the remaining wildfire-affected EASs. Under this scenario, since the whole affected population cannot be transferred within the time windows of the EASs, 7 ambulances are employed. As it takes less time to transfer patients with ambulances than with buses, thus, ambulances transfer the remaining 30 patients (out of a population of 220) with different levels of injury seriousness. Overall, with the shelter in Thornton unavailable, the model uses more ambulance and paramedic

Table 3.7: The evacuation plan under Scenario I (baseline).

Vehicle	Trip #	From	To	Transferred EAS	# Transferred Patient	
					Type 2	*Type 3*
Bus1	1	Buxton	Thornton	***Rubicon***	30	20
	2	Thornton	Taggerty	***Taggerty***	-	10
		Taggery	Thornton	***Buxton***	10	-
	3	Thornton	Rubicon			
		Rubicon	Eildon			
	4	Eildon	Rubicon	**Transferred EAS**	**# Non-Transferred Patient**	
		Rubicon	Eildon		*Type 2*	*Type 3*
	5	Eildon	Rubicon	***Narbethong***	10	20
		Rubicon	Eildon	***Marysville***	5	15
	6	Eildon	Rubicon	***Buxton***	14	-
		Rubicon	Eildon	***Taggerty***	15	25
	7	Eildon	Rubicon	***Cambarville***	-	30
		Rubicon	Eildon			
Bus 2	1	Narbethong	Yarra Glen	**Transferred EAS**	**# Transferred Patient**	
	2	Yarra Glen	Narbethong		*Type 2*	*Type 3*
		Narbethong	Yarra Glen	***Narbethong***	-	20
	3	Yarra Glen	Narbethong	**Transferred EAS**	**# Non-Transferred Patient**	
		Narbethong	Yarra Glen		*Type 2*	*Type 3*
				Narbethong	10	-
				Marysville	5	15
				Buxton	20	-
				Taggerty	15	25
				Cambarville	-	30
Bus 3	1	Marysville	Narbethong	***Transferred EAS***	**# Transferred Patient**	
		Narbethong	Yarra Glen		*Type 2*	*Type 3*
	2	Yarra Glen	Buxton	***Marrysville***	5	-
				Narbethong	5	-
		Buxton	Alexandra	***Buxton***	10	-
				Taggerty	-	10
	3	Alexandra	Taggerty	***Transferred EAS***	**# Non-Transferred Patient**	
		Taggerty	Alexandra		*Type 2*	*Type 3*
				Marrysville	-	15
				Narbethong	5	-
				Taggerty	15	15
				Buxton	10	-
				Cambarville	-	30
Bus 4	1	Cambarville	Narbethong	***Transferred EAS***	**# Transferred Patient**	
		Narbethong	Yarra Glen		*Type 2*	*Type 3*
	2	Yarra Glen	Cambarville	***Cambarville***	-	5
				Narbethong	5	-
				Buxton	10	-
		Cambarville	Thornton	***Transferred EAS***	**# Non-Transferred Patient**	
	3	Thornton	Buxton		*Type 2*	*Type 3*
		Buxton	Thornton	***Marrysville***	-	15
				Taggerty	15	15
				Cambarville	-	25
Bus 5	1	Cambarville	Marrysville	***Transferred EAS***	**# Transferred Patient**	
		Marrysville	Alexandra		*Type 2*	*Type 3*
	2	Alexandra	Taggerty	***Marrysville***	-	5
				Taggerty	20	10
				Cambarville	-	5
		Taggerty	Yea	***Transferred EAS***	**# Non-Transferred Patient**	
	3	Yea	Taggerty		*Type 2*	*Type 3*
		Taggerty	Yea	***Marrysville***	-	10
				Cambarville	-	20
	4	Yea	Taggerty			
		Taggerty	Alexandra			
		Alexandra	Yea			
Bus 6	1	Cambarville	Alexandra	***Transferred EAS***	**# Transferred Patient**	
	2	Alexandra	Cambarville		**Type 2**	***Type 3***
		Cambarville	Alexandra	***Marrysville***	-	10
				Cambarville	-	20
		Alexandra	Yea	***Transferred EAS***	**# Non-Transferred Patient**	
	3	Yea	Marysville		**Type 2**	*Type 3*
		Marysville	Yea	***Marrysville***	-	-
				Cambarville	-	-
Total					210	

Vehicle	Trip #	From	To	Transferred EAS	# Transferred Patient
					Type 1
Amb 1	1	Narbethong	Healsville Hospital	***Narbethong***	6
	2	Healsville Hospital	Narbethong	**Transferred EAS**	**# Non-Transferred Patient**
		Narbethong	Healsville Hospital		*Type 1*
	3	Healsville Hospital	Narbethong	***Narbethong***	4
		Narbethong	Healsville Hospital		
	4	Healsville Hospital	Narbethong		
		Narbethong	Healsville Hospital		
	5	Healsville Hospital	Narbethong		
		Narbethong	Healsville Hospital		
	6	Healsville Hospital	Narbethong		
		Narbethong	Healsville Hospital		
Amb2	1	Narbethong	Healsville Hospital	**Transferred EAS**	**# Transferred Patient**
	2	Healsville Hospital	Narbethong		*Type 1*
		Narbethong	Healsville Hospital	***Narbethong***	4
	3	Healsville Hospital	Narbethong	**Transferred EAS**	**# Non-Transferred Patient**
		Narbethong	Healsville Hospital		*Type 1*
	4	Healsville Hospital	Narbethong	***Narbethong***	4
		Narbethong	Healsville Hospital		
Total					10

buses to evacuate the entire affected population to the remaining SMSs.

3.6.2 Value of the robust approach vs. the deterministic one under coordinated and uncoordinated strategies

In this section, the results obtained using the deterministic and robust models under coordinated and uncoordinated evacuation strategies are compared in terms of different performance metrics (i.e., the number of vehicles used, and the number of non-evacuated patients).
Table 3.9 summarizes the impact of coordinated and uncoordinated vehicle routing strategies for the aforementioned case study involving six EASs, two hospitals, five SMSs, two types of vehicles, and limited time windows. It allows us to compare the solution from the deterministic model to that from the robust model under three different scenarios. Scenarios I and II are as explained earlier. Here we consider a new scenario, scenario 3, to study the total evacuation time when all the evacuees are to be transported by the rescue vehicles.

As depicted in Table 3.9 for the robust model, it is interesting to see that no patients remained at the EASs under the CR strategy while under the UCR strategy we observed 43 evacuees not transported away from the townships. More importantly, under the UCR routing strategy, the total number of non-evacuated patients for the robust model is roughly 34% less than the deterministic model under the same strategy. In summary, our results show that the robust model under both the CR and UCR routing strategies reduces significantly the total number of non-evacuated patients from EASs.
In terms of the total evacuation time, the solution from the robust model under the CR routing strategy evaluates everyone within the maximum time window of 6.6 hours (400 minutes). However, under scenarios 2 and 3, the same model under the UCR strategy fails to evacuate 18 and 25 patients, respectively. For Scenario 3, we released the upper bound of the time windows to determine how long it takes to evacuate the whole affected population from the EASs. As clearly shown, for the robust model under CR there is no change compared to Scenario 1 while for Scenario 3 for the UCR strategy around 1.7 extra hours were required to evacuate 220 people from the wildfire-affected townships. The evacuation time results demonstrate that the robust model under either strategy, CR or UCR, outperforms its deterministic version under the same scenarios.
Finally, due to restricting factors such as the lack of coordination in the network and the limited time windows, the utilization of vehicles for the robust model is inevitably lower than that for the deterministic model across all scenarios for the UCR strategy. As in the proposed robust model under the CR strategy, vehicles can freely travel to different locations without being forced to return to their EAS, the network is more coordinated and more patients can be served using fewer vehicles.

Table 3.8: The evacuation plan under Scenario II (shelter disruption).

Vehicle	Trip #	From	To	Transferred EAS	# Transferred Patient		Vehicle	Trip #	From	To	Transferred EAS	# Transferred Patient
					Type 2	*Type 3*						*Type 3*
Bus 1	1	Buxton	Alexandra	***Taggerty***	10	10	Amb 1	1	Narbethong	Healsville Hospital	***Narbethong***	6
	2	Alexandra	Buxton	***Buxton***	10	20		2	Healsville Hospital	Narbethong		
		Buxton	Alexandra						Narbethong	Healsville Hospital		
	3	Alexandra	Buxton	**Transferred EAS**	**# Non-Transferred Patient**			3	Healsville Hospital	Narbethong		
		Buxton	Alexandra		*Type 2*	*Type 3*			Narbethong	Healsville Hospital		
	4	Alexandra	Taggerty	***Narbethong***	10	20		4	Healsville Hospital	Narbethong		
		Taggerty	Alexandra	***Marysville***	*5*	*15*			Narbethong	Healsville Hospital		
	5	Alexandra	Taggerty	***Taggerty***	10	20		5	Healsville Hospital	Narbethong		
		Taggerty	Alexandra	***Cambarville***	-	30			Narbethong	Healsville Hospital		
				Rubicon	30	20						
Bus 2	1	Eildon	Rubicon					6	Healsville Hospital	Narbethong		
		Rubicon	Eildon	***Transferred EAS***	**# Transferred Patient**				Narbethong	Healsville Hospital		
	2	Eildon	Rubicon		*Type 2*	*Type 3*	Amb2	1	Narbethong	Healsville Hospital	**Transferred EAS**	**# Transferred Patient**
		Rubicon	Eildon	***Rubicon***	30	20		2	Healsville Hospital	Narbethong		*Type 3*
	3	Eildon	Rubicon	***Transferred EAS***	**# Non-Transferred Patient**				Narbethong	Healsville Hospital	***Narbethong***	4
		Rubicon	Eildon		***Type 2***	*Type 3*		3	Healsville Hospital	Narbethong		
	4	Eildon	Rubicon	***Narbethong***	10	20			Narbethong	Healsville Hospital		
		Rubicon	Eildon	***Marysville***	*5*	*15*		4	Healsville Hospital	Narbethong		
	5	Eildon	Rubicon	***Taggerty***	10	20			Narbethong	Healsville Hospital		
		Rubicon	Eildon	***Cambarville***	-	30	Amb3	1	Taggerty	Yea Memorial Hospital	**Transferred EAS**	**# Transferred Patient**
Bus 3	1	Narbethong	Yarra Glen	**Transferred EAS**	**# Transferred Patient**			2	Yea Memorial Hospital	Taggerty		***Type 3***
	2	Yarra Glen	Narbethong		*Type 2*	*Type 3*			Taggerty	Yea Memorial Hospital	***Taggerty***	*5*
		Narbethong	Yarra Glen	***Narbethong***	10	10		3	Yea Memorial Hospital	Taggerty		
				Transferred EAS	**# Non-Transferred Patient**				Taggerty	Yea Memorial Hospital		
					Type 2	*Type 3*		4	Yea Memorial Hospital	Taggerty		
				Narbethong	-	10			Taggerty	Yea Memorial Hospital		
				Marysville	5	15						
				Taggerty	10	20		5	Yea Memorial Hospital	Taggerty		
				Cambarville	-	30						
Bus 4	1	Marrysville	Yarra Glen	***Transferred EAS***	**# Transferred Patient**				Taggerty	Yea Memorial Hospital		
	2	Yarra Glen	Marrysville		*Type 2*	*Type 3*	Amb4	1	Taggerty	Yea Memorial Hospital	**Transferred EAS**	**# Transferred Patient**
		Marrysville	Yarra Glen	***Marysville***	5	15		2	Yea Memorial Hospital	Taggerty		*Type 3*
	3	Yarra Glen	Marrysville	***Transferred EAS***	**# Non-Transferred Patient**				Taggerty	Yea Memorial Hospital	***Taggerty***	*5*
		Marrysville	Yarra Glen		*Type 2*	*Type 3*		3	Yea Memorial Hospital	Taggerty		
				Narbethong	-	*10*			Taggerty	Yea Memorial Hospital		
				Taggerty	*10*	*20*						
				Cambarville	-	30		4	Yea Memorial Hospital	Taggerty		
Bus 5	1	Cambarville	Yarra Glen	***Transferred EAS***	**# Transferred Patient**				Taggerty	Yea Memorial Hospital		
	2	Yarra Glen	Cambarville		*Type 2*	*Type 3*		5	Yea Memorial Hospital	Taggerty		
		Cambarville	Yea	***Cambarville***	-	20			Taggerty	Yea Memorial Hospital		
				Transferred EAS	**# Non-Transferred Patient**		Amb5	1	Buxton	Yea Memorial Hospital	**Transferred EAS**	**# Transferred Patient**
					Type 2	*Type 3*		2	Yea Memorial Hospital	Buxton		Type 1
				Narbethong	-	10			Buxton	*Yea Memorial Hospital*	***Buxton***	*4*
				Taggerty	10	20						
				Cambarville	-	10						
Bus 6	1	Cambarville	Yea	***Transferred EAS***	**# Transferred Patient**			3	Yea Memorial Hospital	Buxton		
					Type 2	*Type 3*			Buxton	*Yea Memorial Hospital*		
				Cambarville	-	10		4	Yea Memorial Hospital	Buxton		
				Transferred EAS	**# Non-Transferred Patient**				Buxton	*Yea Memorial Hospital*		
					Type 2	*Type 3*	Amb6	1	Naberthong	Healsville Hospital	**Transferred EAS**	**# Transferred Patient**
				Narbethong	-	10		2	Healsville Hospital	Naberthong		*Type 1*
				Taggerty	10	20						
Bus 7	1	Taggerty	Yea	***Transferred EAS***	**# Transferred Patient**				Naberthong	Healsville Hospital	***Naberthong***	*3*
	2	Yea	Taggerty		*Type 2*	*Type 3*		3	Healsville Hospital	Naberthong		
		Taggerty	Yea	***Taggerty***	10	10			Naberthong	Healsville Hospital		
				Transferred EAS	**# Non-Transferred Patient**		Amb7	1	Naberthong	Healsville Hospital	**Transferred EAS**	**# Transferred Patient**
					Type 2	***Type 3***		2	Healsville Hospital	Naberthong		*Type 1*
				Taggerty	-	10			Naberthong	Healsville Hospital	***Naberthong***	*3*
				Narbethong	-	10						
								3	Healsville Hospital	Naberthong		
									Naberthong	Healsville Hospital		
Total					190		Total					30

Table 3.9: Comparison of the solution obtained via the robust and deterministic models under coordinated and uncoordinated routing strategies for three scenarios

Performance Metric		**Robust Model**						**Deterministic Model**					
		Sc1		*Sc2*		*Sc3*		*Sc1*		*Sc2*		*Sc3*	
		CR	UCR	CR	UCR	CR	UCR	CR	UCR	CR	UCR	CR	UCR
# Non-Evacuated Patients (UD)	***Type 1***	-	3	-	5	-	-	2	6	7	8	-	-
	Type 2	-	6	-	10	-	-	2	9	9	12	-	-
	Type 3	-	9	-	10	-	-	6	11	9	12	-	-
Total		**-**	**18**	**-**	**25**	**-**	**-**	**10**	**26**	**25**	**32**	**-**	**-**
Total Evacuation Time (hours)		5.7	6.6	5.9	6.6	5.7	8.3	6.6	6.6	6.6	6.6	5.7	9.5
# vehicles used	***Bus***	6	4	7	3	6	10	5	3	6	2	6	12
	Amb	2	-	7	1	2	9	1	1	3	4	2	13
	Total	**8**	**4**	**14**	**4**	**8**	**19**	**6**	**4**	**9**	**6**	**8**	**25**

CR: the proposed coordinated CVRP-TW model; UCR: uncoordinated VRP model; Sc: scenario
Amb: Ambulance

To evaluate the efficiency of the proposed hybrid approach, in Section 3.6.5 we apply it to both the coordinated and uncoordinated models under different problem settings.

3.6.3 Value of hybrid algorithm under coordinated and uncoordinated strategies

For the robust version of the 2MCVRP-TW model, we designed a set of experiments to (1) evaluate the performance of the proposed hybrid solution method under different scenarios, (2) identify the impact of various vehicle routing strategies on the number of non-evacuated patients, and (3) quantify the benefits of the proposed robust stochastic programming approach by comparing its performance against that of the deterministic model under coordinated and uncoordinated routing strategies. In this regard, 10 random instances were generated of different problem sizes. Input data for these experiments are given in Table 3.10. For all the experiments, we used the following algorithm parameters: population size of 500, the assimilation rate of 0.2, uniting threshold (the percentage of search space size) of 0.45, and the number of imperialists equal to the number of the population divided by 10, and probability of revolution of 0.5. The selection of values for all the algorithm parameters and their definition were previously explained in Section 3.4.3.

For these ten datasets, Table 3.11 presents the numerical results obtained using the hybrid approach and exact solutions. In order to provide an acceptable result for our case, the hybrid algorithm (ICAHHO) is run five times for each dataset. In Table 3.11, the best solution, the average solution and the average percentage deviation ($\overline{RPD}$) are used to provide a comprehensive comparison of the results. The purpose of computing RPD is to measure the degree of deviation

Table 3.10: Numerical experiments parameters.

Parameter description	Applied values
Number of EASs (D)	Random $\sim uniform\{4, 7\}$
Number of medical centers (K)	Random $\sim uniform\{5, 9\}$
Travel time (t_{ij}^v)	Random $\sim uniform\{15, 60\}$
Time windows (TW_i)	Random $\sim uniform\{150, 450\}$
Capacity of medical centers (SC_{ih})	Random $\sim uniform\{15, 50\}$
Risk of disruption (RR_{ij})	Random $\sim uniform\{0.25, 0.6\}$

Table 3.11: Hybrid solution algorithm results for the robust model (Avg-Average, p.t(s) - processing time (seconds), RPD - Related Percentage Deviation).

Dataset	I	J	Coordinated CVRP-TW								uncoordinated CVRP-TW							
			Exact solution				Hybrid				Exact Solution				Hybrid			
			Best*	Avg**	p.t(s)	RPD	Best	Avg	p.t(s)	RPD	Best	Avg	p.t(s)	RPD	Best	Avg	p.t(s)	RPD
1	6	5	0.632	0.632	5578.5	0	0.632	0.632	1132	0	0.779	0.779	6700	0	0.779	0.779	1450	0
2	9	6	-				0.655	0.634	1190	0.265	-				0.701	0.689	1488	0.389
3	12	10	-				0.721	0.702	1280	0.135	-				0.811	0.801	1502	0.231
4	18	10	-				0.734	0.705	1295	0.156	-				0.823	0.826	1681	0.203
5	20	12	-				0.811	0.802	1310	0.190	-				0.841	0.819	1893	0.295
6	14	5	-				0.856	0.801	1265	0.126	-				0.902	0.899	1601	0.199
7	14	7	-				0.875	0.855	1301	0.18	-				0.910	0.908	1610	0.201
8	11	8	-				0.596	0.600	1110	0.201	-				0.699	0.710	1520	0.246
9	23	11	-				0.718	0.688	1540	0.078	-				0.893	0.866	2100	0.101
10	25	5	-				0.712	0.676	1610	0.089	-				0.901	0.902	2058	0.1
Avg						0		0.142								0.196		

*Best: the best result of the normalized objective function
**Avg: average of the results across five runs

of the individual results with respect to the average measurement. The following equation defines how the RPD is calculated:

$$\overline{RPD} = \sum_{i=1}^{R} \frac{(\frac{B-U_i}{B})}{R} \times 100 \tag{3.34}$$

where R, B, and U_i represent the number of iterations for each dataset, the best result across all runs, and the solution from the algorithm in the ith run, respectively.

As Table 3.11 shows, the exact method is only capable of solving the smallest problem. The proposed hybrid algorithm has a lower $\overline{RPD}$ and a shorter computational time under the coordinated routing strategy than the uncoordinated strategy in most cases. The maximum value for the RPD using the hybrid algorithm is 0.265 with an average of 0.142 (average result across the five runs for each individual dataset) for the coordinated model, while it is 0.389 with an average of 0.196 for the uncoordinated one. This means that the coordinated approach using the hybrid algorithm can find solutions in a shorter computation time.

Also, by increasing the size of datasets, the hybrid approach provides better results under the coordinated strategy (best solution and average solution) than under the uncoordinated model. Regarding processing times, under both coordinated and uncoordinated routing strategies, the hybrid solution performed five times faster than the exact solution. As clearly shown, the difference

Table 3.12: The impact of various routing strategies on the number of non-evacuated patients, vehicle utilization and total evacuation time.

Type of Problem	**Scenario I**			**Scenario II**		
	Total Unmet Demand	*Total Evacuation Time (hours)*	*Vehicles Used*	*Total Unmet Demand*	*Total Evacuation Time*	*Vehicles Used*
Full coordination (split pickup split delivery)	**0**	**5.7**	**8**	**0**	**5.9**	**14**
Split pickup only	16	7.2	12	19	8.6	13
Split delivery only	14	6.9	12	18	7.3	13
No coordination	18	8.8	4	25	9.5	19

in execution times between the commercial solver and our hybrid solution approach is evident. It is important to note that the computational time is not the main point here since the model and solution approach are meant to be used as a planning tool.

3.6.4 Sensitivity analysis of model key parameters

3.6.4.1 Individual effects of routing strategies on casualty evacuation

In this section, we evaluate and compare four routing strategies: full coordination (split delivery and split pickup), only split pickup, only split delivery, and no coordination.

Table 3.12 summarizes the results for each routing strategy for the first two scenarios explained earlier. The results show that full coordination outperforms the other strategies in terms of unmet demand, total evacuation time and vehicle utilization. Under full coordination, no patients remain at EASs for both scenarios while under no coordination, 18 and 25 people were not evacuated for Scenario I and Scenario II, respectively. Similarly, approximately 35% less evacuation time is required under full coordination when compared to the no coordination strategy. In this regard, the split delivery and split pickup strategies performed much better than the no coordination strategy. However, considering the same number of vehicles, the split-delivery strategy outperforms the split-pickup one in terms of total evacuation time and total unmet demand. This result shows that transferring patients to different locations during each trip results in better evacuation outcomes. Overall, the results in Table 3.12 show that different levels of coordination provides better results than those obtained via a model which requires vehicles to return to their EAS at the end of each trip. Although under Scenario I and II, the number of people who remained unevacuated at EASs for split pickup and split delivery strategies is not satisfactory, it is still lower than that of the no coordination strategy. Hence, a full coordination strategy is recommended to be applied compared to all the other strategies.

3.6.4.2 The effect of shelters location on the number of patients evacuated

The total number of candidate shelters (SMSs) for the Black Saturday case study was five ($\Psi = 5$). However, the optimal location of shelters clearly influences the evacuation routes and

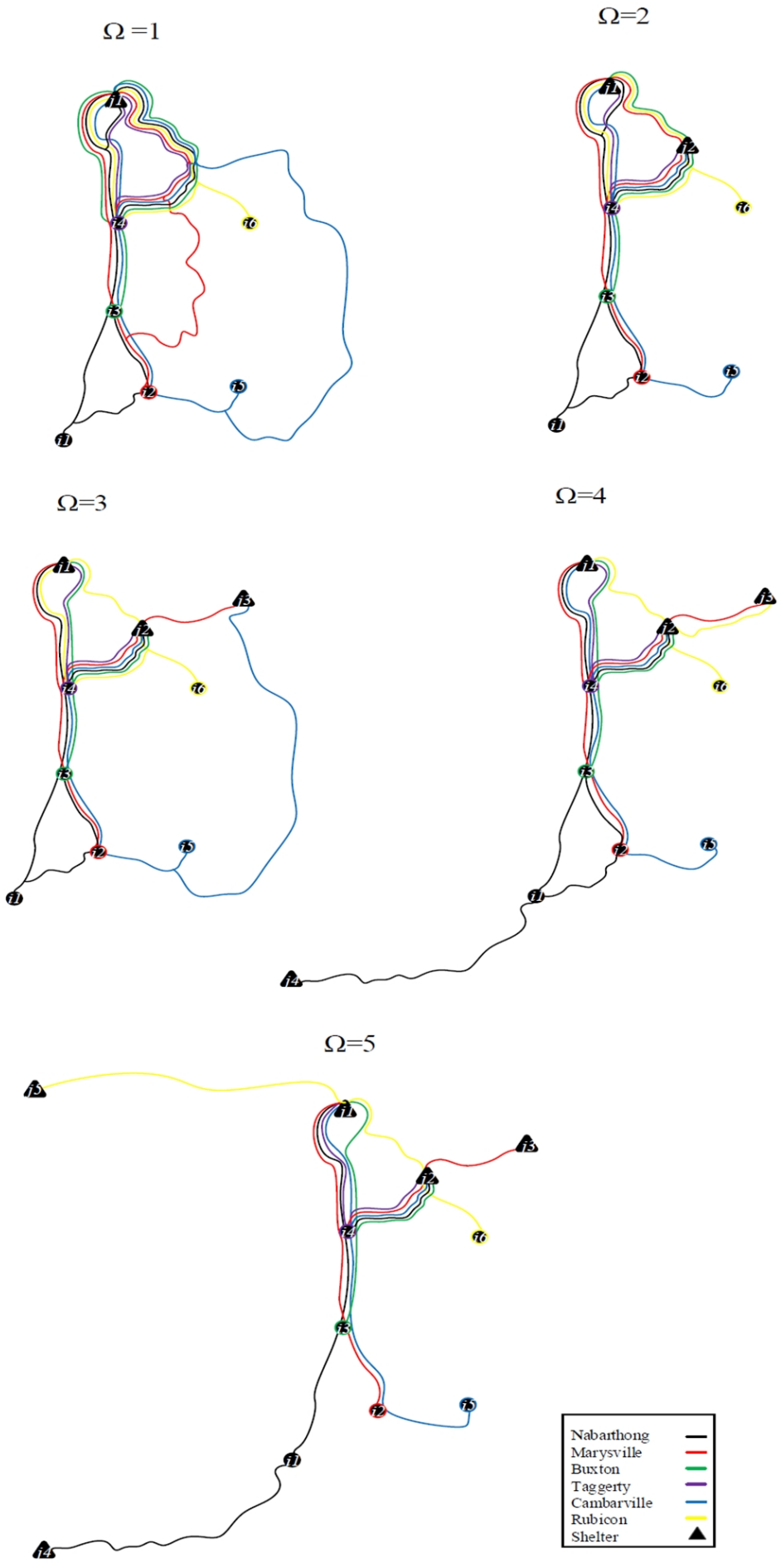

Figure 3.8: Optimal routes depending on the number of shelters available.

thus the total evacuation time and number of people evacuated. Hence, a sensitivity analysis in relation to the maximum number of available shelters Ψ is shown in Figures 3.8 and 3.9. As depicted by Figure 3.8, it is interesting to see that increasing the number of shelters does not drastically increase vehicle assignment. This indicates that the model can control the disruption of transferring injured people by increasing the number of shelters (which, of course, increases the expected number of required trips). In Figure 3.8, different colours are utilised for different vehicles to show the evacuation paths for each township. In each scenario, the evacuation process is limited to the number of available shelters which are considered for evacuation of patient types 2 and 3 only. It is important to note that the model tends to decrease the number of assigned vehicles depending on the time windows (which, of course, decreases the objective function). For example, in the case of $\Psi = 4$, Rubicon evacuees are moved by only one bus travelling seven times between Rubicon and Eildon due to sufficient time being available.

Results in Figure 3.9 indicate that due to the evacuation time windows, distances and capacities, at least 5 and 7 shelters for the coordinated and uncoordinated routing strategies respectively are required under the scenario I to evacuate all patients from the fire-affected EASs.

However, under scenario II, only four shelters are needed using the coordinated strategy while the same number of shelters as in Scenario II is required for the no coordination strategy. Overall, the results indicate that the no coordination strategy requires more shelters to evacuate the affected population than the full coordination strategy, which ultimately increases the evacuation operation's cost.

3.6.4.3 The effect of time impedance on the number of patients evacuated under the full coordination strategy

An analysis was also carried out about the effect of the TMF on the optimal evacuation plan. Figure 3.10 shows that under Scenario I the minimum number of paramedic buses required to evacuate all patients from the EASs is increasing in the time impedance factor. In the case of no traffic in the network ($TMF = 0$), a minimum of 8 vehicles (paramedic buses) are needed while for a trip of 80% at least 15 vehicles are required. However, by referring to the results provided in Table 3.12 at least 19 vehicles are required for the no-coordination strategy to transfer all the patients from the EASs within the time windows, showing that even under the worst-case scenario (highest $TMF = 80\%$), the coordinated model performs better.

3.6.5 Solution robustness versus model robustness

As mentioned in Section 3.3.2, we consider a penalty (CW_1) associated with the violation of constraint (3.24), which was also referred to as the weight of the second term of the objective

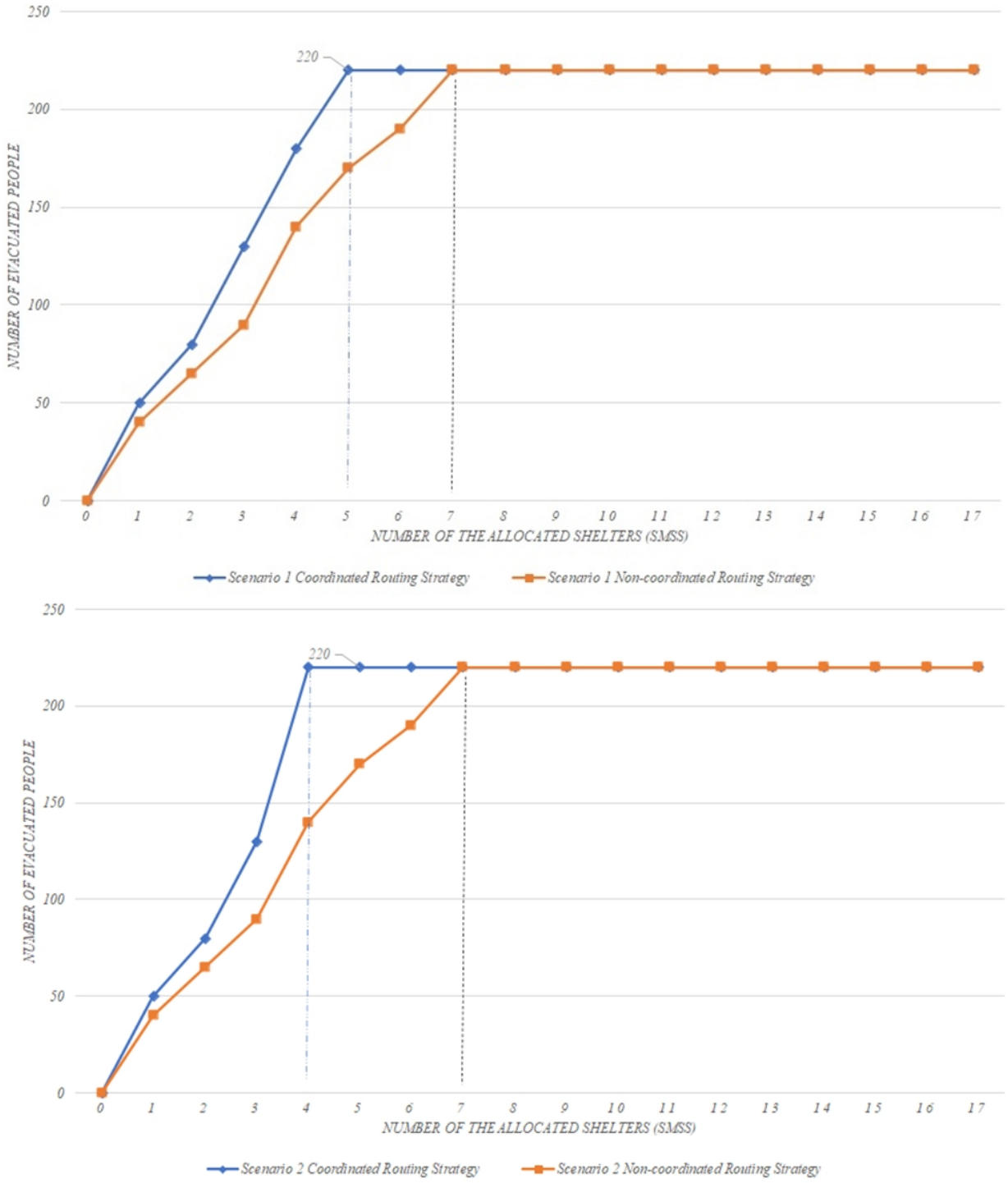

Figure 3.9: Number of required shelters under the coordinated and uncoordinated routing strategies for scenarios 1 and 2

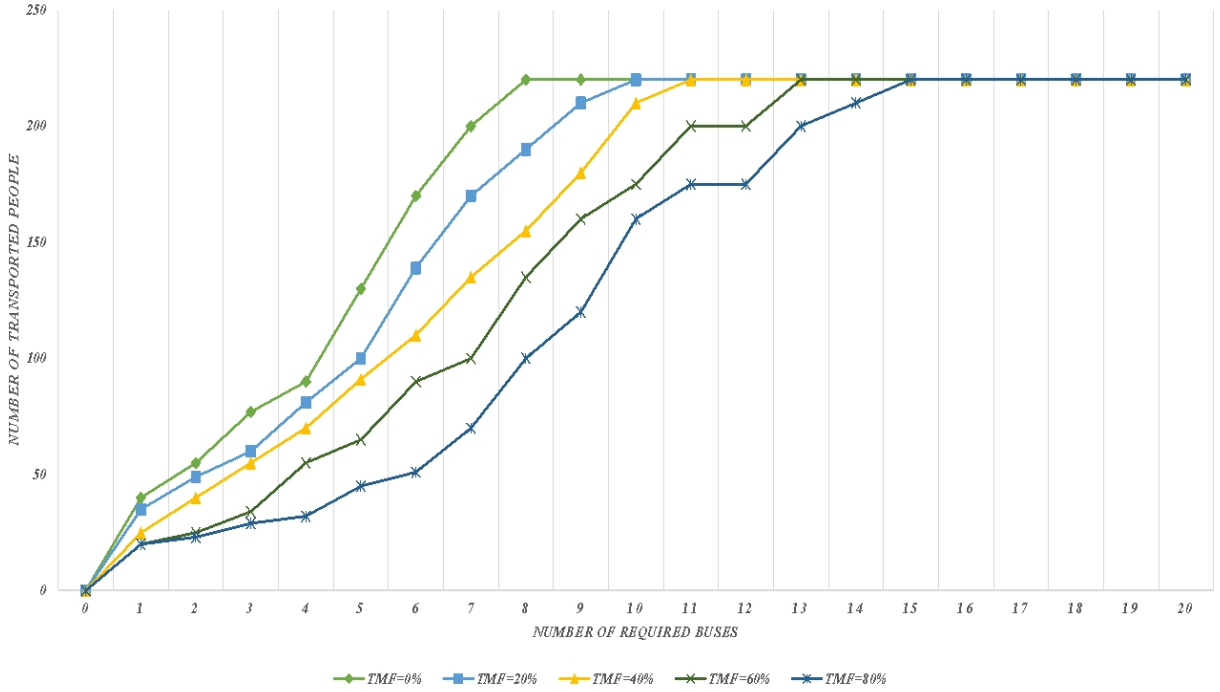

Figure 3.10: Impact of the time impedance factor on the total number of vehicles required to evacuate all the affected population.

function of the main model. This penalty cost is used in Equation 3.24 to find an optimal or near-optimal solution (solution robustness) and a feasible or near-feasible solution (model robustness). The tradeoff between solution robustness and model robustness is a challenging area in the robust optimization literature [17].

A risk-taker may set small values for the penalties associated with the number of unserved patients that reduce the total relief time and cost by focusing on the weighted shelter selection cost and travel length minimization objective. On the other hand, to reduce the level of unserved evacuees, a risk-averse decision maker may choose high values for this penalty yielding higher total costs or penalties but reducing the number of unserved patients. Therefore, we can analyse the tradeoff between solution robustness and model robustness for different constraint violation penalties, as shown in Figure 3.11. As the violation penalty increases, the total cost representing the solution robustness increases, but the under-fulfilment of evacuees' demand representing model robustness decreases. A robust optimization problem with no under-fulfilment of demand incurs a large penalty cost to avoid constraint violation. For instance, at $CW_1 = \$1,800$, the robust objective function value is \$13,100 $\times 1,000$ but ensures that no unserved patients are present under any scenario.

The robust optimization approach can be run using two different variability weights (η) and expected cost weights (λ). Their impact on the expected cost and variability is illustrated in Figure 3.12. To investigate the impact of λ on the expected cost and variability, η was set to 1 and the model was run for different weights of λ. This procedure was also used to determine the effect

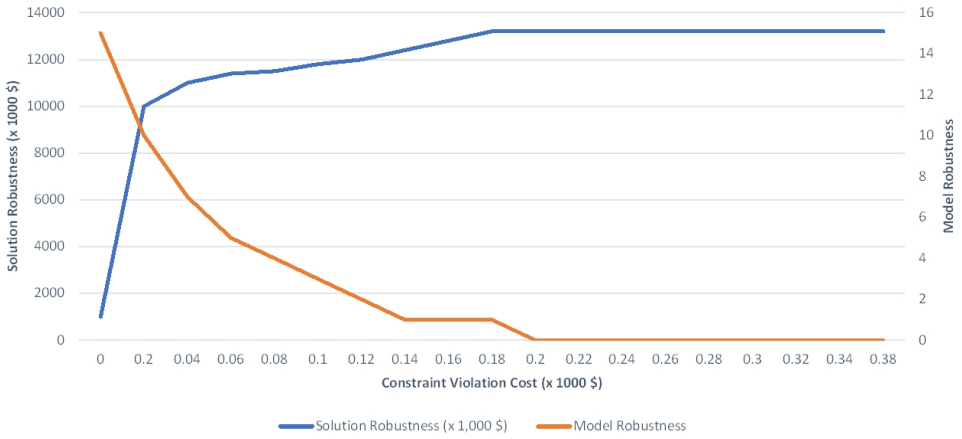

Figure 3.11: Tradeoff between evacuation cost and evacuees' under-fulfilment.

of η on expected cost and variability. Figure 3.12 shows that an increase in the expected cost weight decreases the expected cost and variability when η is fixed at 1. At $(\eta = 1, \lambda = 9)$ and $(\eta = 6, \lambda = 1)$, the expected cost and the maximum variability reach their minima, after which the expected cost and variability remain constant.

3.6.6 Managerial insights

Different solution approaches and evacuation routing strategies are considered in this study to make casualty evacuation resilient to uncertainty in wildfire propagation. The results demonstrate that the performance of the proposed vehicle routing model under the full coordination strategy significantly improved the evacuation plan, in terms of patient unevacuated and total cost for multiple scenarios. It would be beneficial for relief and wildfire response managers to use fully coordinated split pickup and split delivery and even its subordinate strategies (only split pickup and only split delivery) when compared with the no coordination strategy. The proposed model enhances casualty evacuation resiliency against time windows, risky routes, and the unavailability of shelters through a robust approach.

The robust model with a coordinated routing strategy may allow relief managers to analyze and assess their critical decisions on the network configuration from both a cost and a service perspective. Specifically, due to the unexpected nature of disasters, various sources of uncertainty, and lack of coordination, the proposed robust model could become a practical approach for dealing with uncertainty in wildfire propagation and affected populations. Overall, the following managerial insights have been obtained from the results in this chapter:

(1) Decision makers managing and controlling the fleet of evacuation vehicles can benefit from faster vehicle routing mechanisms to coordinate the relief network for potential under-fulfilment of evacuation demand. Even if implementing a full coordination strategy is not possible, the other routing strategies (either split pickup or split delivery) could reduce the number of unserved pop-

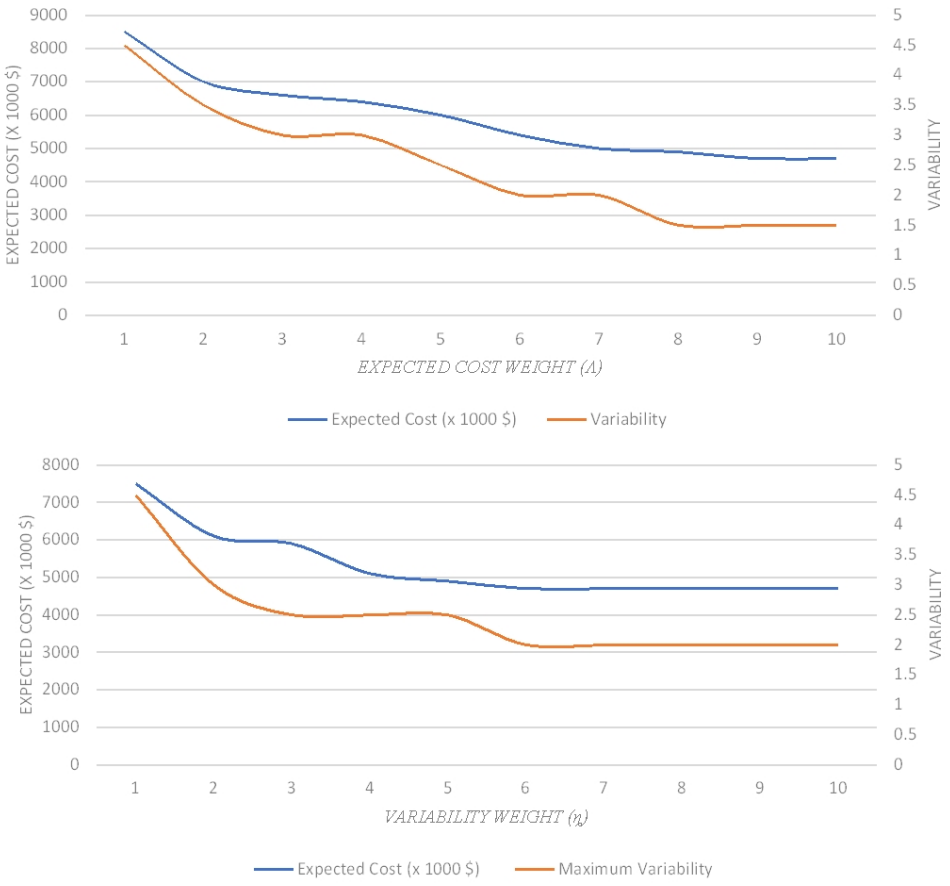

Figure 3.12: Impact of the expected cost weight (λ) on variability and expected cost and impact of the variability weight (η) on the maximum variability and expected cost.

ulations significantly when compared with the no coordination strategy. It is recommended to consider full coordination first, followed by the split delivery strategy and then by the split pickup one.

(2) The proposed model and solution approach are capable of assigning the minimum number of safe shelters to be transferred to each one within the time windows to efficiently serve wildfire-affected areas. The models also show the importance of backup shelters during bushfires. It is highly beneficial to have backup shelters for the evacuation network when the number of vehicles is limited but capable of travelling to all the locations under the full coordination strategy. As the results showed for the full coordination strategy, by increasing the number of shelters, the same number of vehicles were used compared to that of the no coordination strategy, but more people were evacuated. Hence, it is recommended to have the possibility of increasing the number of shelters as backup shelters to assign a sufficient number of shelters to the evacuees. Most evacuees could be transferred to safe shelters within their close vicinity, but this would increase the risk of over-utilisation in case of a disruption. Overall, the model and solution approach described in this chapter seek to generate fleet scheduling plans whereby the timing, shelter and routes are assigned to multiple vehicles. The fleet schedules can be regenerated based on changing management objectives to help plan future scenarios of resource allocation in terms of establishing new shelters or assembly points.

3.7 Conclusions and recommendations

With a significant number of wildfires happening globally, the need for better wildfire evacuation plans is becoming increasingly relevant. Challenges to proper evacuation management include the existence of several response facilities (e.g., assembly points, and medical centers), patients with varying urgency levels limited transport capacity and route accessibility, and time windows. In this research, an optimization model was developed to efficiently manage evacuees' transportation via safe routes, and to decrease total operational cost, and unfulfilled demand for the affected population in this type of situation. To better define evacuation plans, we proposed a robust two-stage stochastic model under multiple sources of uncertainty regarding time windows for EASs, travel times among locations and affected population (to be transferred to safe shelters and hospitals). To demonstrate the effectiveness of the proposed robust model, we solved an illustrative example including five SMSs, six evacuation assembly points and two regional hospitals by off-the-shelf software (GAMS with Cplex solver) and compared with a hybrid method using both the Imperative Competitive and the Harris Hawks Optimization approach algorithms combined. However, only the proposed hybrid algorithms were used for larger instances to solve the robust model for various problem sizes. Finally, sensitivity analyses were performed to evaluate the impact of several key

parameters, such as the number of unmet demands and vehicles utilized. Future research in this area will seek to incorporate evacuees' behaviour which influences the effectiveness of the evacuation process. Other sources of uncertainty such as reduction in road capacity due to flooding or avalanche along with the uncertain evacuee's behaviour could be considered in the future. With appropriate model calibration and adjustment, this model and solution approach could also be applied to other natural disasters such as flooding and cyclones, which are also widely prevalent in Australia and other countries. Furthermore, many people rely on their own vehicles to leave affected areas for safer places. This flow of evacuees increases the background traffic and may cause network congestion that in turn affects the evacuation process. Developing dynamic optimization evacuation models that can update the status of the network at each period may prevent any delays in joining late evacuees or those who leave affected areas by their vehicles. Additionally, there are other modes of evacuation such as helicopters and personal automobiles, that could be integrated into a single evacuation framework. Finally, as argued by Holguín-Veras et al. [14], the development and incorporation of more welfare economic principles such as social costs (the summation of logistics and deprivation costs) linked to human suffering levels for post-disaster humanitarian logistics models must be undertaken. An interesting extension of our work would be to incorporate vehicle availability as a first-stage decision variable.

3.8 Bibliography

[1] Abbas Afshar and Ali Haghani. Modeling integrated supply chain logistics in real-time large-scale disaster relief operations. *Socio-Economic Planning Sciences*, 46(4):327–338, 2012.

[2] El-Houssaine Aghezzaf, Carles Sitompul, and Najib M Najid. Models for robust tactical planning in multi-stage production systems with uncertain demands. *Computers & Operations Research*, 37(5):880–889, 2010.

[3] Esmaeil Atashpaz-Gargari and Caro Lucas. Imperialist competitive algorithm: an algorithm for optimization inspired by imperialistic competition. In *2007 IEEE congress on evolutionary computation*, pages 4661–4667. Ieee, 2007.

[4] Aharon Ben-Tal, Laurent El Ghaoui, and Arkadi Nemirovski. *Robust optimization*, volume 28. Princeton University Press, 2009.

[5] Aharon Ben-Tal and Arkadi Nemirovski. Selected topics in robust convex optimization. *Mathematical Programming*, 112(1):125–158, 2008.

[6] Dimitris Bertsimas, David B Brown, and Constantine Caramanis. Theory and applications of robust optimization. *SIAM review*, 53(3):464–501, 2011.

[7] Dimitris Bertsimas, Philippe Chervi, and Michael Peterson. Computational approaches to stochastic vehicle routing problems. *Transportation science*, 29(4):342–352, 1995.

[8] Dimitris Bertsimas and Melvyn Sim. The price of robustness. *Operations research*, 52(1): 35–53, 2004.

[9] Kris Braekers, Katrien Ramaekers, and Inneke Van Nieuwenhuyse. The vehicle routing problem: State of the art classification and review. *Computers & Industrial Engineering*, 99: 300–313, 2016.

[10] Thomas J Cova, Philip E Dennison, and Frank A Drews. Modeling evacuate versus shelter-in-place decisions in wildfires. *Sustainability*, 3(10):1662–1687, 2011.

[11] Virginie Gabrel, Cécile Murat, and Aurélie Thiele. Recent advances in robust optimization: An overview. *European journal of operational research*, 235(3):471–483, 2014.

[12] Ali Asghar Heidari, Ibrahim Aljarah, Hossam Faris, Huiling Chen, Jie Luo, and Seyedali Mirjalili. An enhanced associative learning-based exploratory whale optimizer for global optimization. *Neural Computing and Applications*, pages 1–27, 2019.

[13] Ali Asghar Heidari, Seyedali Mirjalili, Hossam Faris, Ibrahim Aljarah, Majdi Mafarja, and Huiling Chen. Harris hawks optimization: Algorithm and applications. *Future generation computer systems*, 97:849–872, 2019.

[14] José Holguín-Veras, Noel Pérez, Miguel Jaller, Luk N Van Wassenhove, and Felipe Aros-Vera. On the appropriate objective function for post-disaster humanitarian logistics models. *Journal of Operations Management*, 31(5):262–280, 2013.

[15] Kai Huang, Yiping Jiang, Yufei Yuan, and Lindu Zhao. Modeling multiple humanitarian objectives in emergency response to large-scale disasters. *Transportation Research Part E: Logistics and Transportation Review*, 75:1–17, 2015.

[16] Maqsood I. and Huang G.H. A dual two-stage stochastic model for flood management with inexact-integer analysis under multiple uncertainties. *Stochastic Environmental Research and Risk Assessment*, 27(3):643–657, 2013.

[17] Armin Jabbarzadeh, Behnam Fahimnia, and Stefan Seuring. Dynamic supply chain network design for the supply of blood in disasters: A robust model with real world application. *Transportation Research Part E: Logistics and Transportation Review*, 70:225–244, 2014.

[18] Afshin Kamyabniya, MM Lotfi, Mohsen Naderpour, and Yuehwern Yih. Robust platelet logistics planning in disaster relief operations under uncertainty: a coordinated approach. *Information Systems Frontiers*, 20(4):759–782, 2018.

[19] A Kaveh, P Rahmani, and A Dadras Eslamlou. An efficient hybrid approach based on harris hawks optimization and imperialist competitive algorithm for structural optimization. *Engineering with Computers*, pages 1–29, 2021.

[20] Young-Jou Lai and Ching-Lai Hwang. A new approach to some possibilistic linear programming problems. *Fuzzy sets and systems*, 49(2):121–133, 1992.

[21] Ming Li, Zheng Wang, and Felix TS Chan. A robust inventory routing policy under inventory inaccuracy and replenishment lead-time. *Transportation Research Part E: Logistics and Transportation Review*, 91:290–305, 2016.

[22] Chang-Shi Liu and Ming-Yong Lai. Retracted: The vehicle routing problem with uncertain demand at nodes, 2009.

[23] Huseyin Onur Mete and Zelda B Zabinsky. Stochastic optimization of medical supply location and distribution in disaster management. *International Journal of Production Economics*, 126 (1):76–84, 2010.

[24] Jairo R Montoya-Torres, Julián López Franco, Santiago Nieto Isaza, Heriberto Felizzola Jiménez, and Nilson Herazo-Padilla. A literature review on the vehicle routing problem with multiple depots. *Computers & Industrial Engineering*, 79:115–129, 2015.

[25] John M Mulvey, Robert J Vanderbei, and Stavros A Zenios. Robust optimization of large-scale systems. *Operations research*, 43(2):264–281, 1995.

[26] Mehdi Najafi, Kourosh Eshghi, and Sander de Leeuw. A dynamic dispatching and routing model to plan/re-plan logistics activities in response to an earthquake. *OR spectrum*, 36(2): 323–356, 2014.

[27] Lewis Ntaimo, Julian A Gallego-Arrubla, Jianbang Gan, Curt Stripling, Joshua Young, and Thomas Spencer. A simulation and stochastic integer programming approach to wildfire initial attack planning. *Forest Science*, 59(1):105–117, 2013.

[28] Shahrooz Shahparvari and Babak Abbasi. Robust stochastic vehicle routing and scheduling for bushfire emergency evacuation: An australian case study. *Transportation Research Part A: Policy and Practice*, 104:32–49, 2017.

[29] Shahrooz Shahparvari, Babak Abbasi, and Prem Chhetri. Possibilistic scheduling routing for short-notice bushfire emergency evacuation under uncertainties: An australian case study. *Omega*, 72:96–117, 2017.

[30] Shahrooz Shahparvari, Babak Abbasi, Prem Chhetri, and Ahmad Abareshi. Fleet routing and scheduling in bushfire emergency evacuation: A regional case study of the black saturday bushfires in australia. *Transportation Research Part D: Transport and Environment*, 67:703–722, 2019.

[31] Shahrooz Shahparvari, Prem Chhetri, Babak Abbasi, and Ahmad Abareshi. Enhancing emergency evacuation response of late evacuees: Revisiting the case of australian black saturday bushfire. *Transportation research part E: logistics and transportation review*, 93:148–176, 2016.

[32] Virginia P Sisiopiku, Steven L Jones Jr, Andrew J Sullivan, Sameer S Patharkar, Xiaohong Tang, et al. Regional traffic simulation for emergency preparedness. Technical report, University Transportation Center for Alabama, 2004.

[33] Marius M Solomon. Algorithms for the vehicle routing and scheduling problems with time window constraints. *Operations research*, 35(2):254–265, 1987.

[34] S Talatahari, B Farahmand Azar, R Sheikholeslami, and AH Gandomi. Imperialist competitive algorithm combined with chaos for global optimization. *Communications in Nonlinear Science and Numerical Simulation*, 17(3):1312–1319, 2012.

[35] Bernard Teague, Ronald McLeod, and Susan Pascoe. Interim report: 2009 victorian bushfires royal commission. 2009.

[36] VICROADS. Vicroads, speed zone maps. *URL: < http://www.data.vic.edu.au/>*, ; v.u.(ed.). 2014.

[37] VICROADS. Victorian bushfires royal commission. *Interim Report, Section 7.*, 2009.

[38] VICROADS. Road bushfire risk assessment guideline and risk mapping methodology. *URL: https://www.vicroads.vic.gov.au/ /media/files/technical documents/guidelines/bushfire risk guidelines- web.pdf?la=en.*, 2013.

[39] Vukan R Vuchic. *Urban transit: operations, planning, and economics*. John Wiley & Sons, 2017.

[40] Haijun Wang, Lijing Du, and Shihua Ma. Multi-objective open location-routing model with split delivery for optimized relief distribution in post-earthquake. *Transportation Research Part E: Logistics and Transportation Review*, 69:160–179, 2014.

[41] C Donald J Waters. Vehicle-scheduling problems with uncertainty and omitted customers. *Journal of the Operational Research Society*, 40(12):1099–1108, 1989.

[42] David H Wolpert and William G Macready. No free lunch theorems for optimization. *IEEE transactions on evolutionary computation*, 1(1):67–82, 1997.

[43] Zhongzhen Yang, Liquan Guo, and Zaili Yang. Emergency logistics for wildfire suppression based on forecasted disaster evolution. *Annals of Operations Research*, 283(1):917–937, 2019.

[44] Chian-Son Yu and Han-Lin Li. A robust optimization model for stochastic logistic problems. *International Journal of Production Economics*, 64:385–397, 2000.

[45] Behzad Zahiri and Mir Saman Pishvaee. Blood supply chain network design considering blood group compatibility under uncertainty. *International Journal of Production Research*, 55(7): 2013–2033, 2017.

[46] Fang Zhao, Keqiang Xing, Shanshan Yang, Chenxi Lu, and Soon Chung. Hurricane evacuation planning for special needs populations. *FTA-FL-04-7104-2010.04, LCTR-TRANSPO-Year2-P3*, 2010.

[47] Siqiong Zhou and Ayca Erdogan. A spatial optimization model for resource allocation for wildfire suppression and resident evacuation. *Computers & Industrial Engineering*, 138:106101, 2019.

[48] Shiva Zokaee, Ali Bozorgi-Amiri, and Seyed Jafar Sadjadi. A robust optimization model for humanitarian relief chain design under uncertainty. *Applied Mathematical Modelling*, 40 (17-18):7996–8016, 2016.

4 A Dynamic Capacity Planning Model in Mass Casualty Incidents Under Uncertainty

This research focuses on the response to a Mass Casualty Incident (MCI) involving patients with varying degrees of injury severity and multiple potential treatment destinations. Two decisions are considered. First, we look to determine the optimal destination for each patient at the MCI and second we look to determine the timing and size of capacity increases at the various hospitals in the network. We assume that each hospital has a number of potential strategies designed to increase capacity such as early discharges (relatively low cost), patient transfers or cancellations of elective admissions (higher cost). The goal of this research is therefore to determine the destination of each MCI patient and the timing of a multi-echelon capacity increase response.

This problem that will be explained later (Section 4.3) and such a situation can be modelled as a sequential decision-making problem and thus fits naturally into a Markov Decision Process (MDP). As is the case with many applications, the potential size of the problem leads to issues of tractability which we address later in Section 4.4 by using the linear programming approach to Approximate Dynamic Programming (ADP).

4.1 Introduction and Motivation

Mass casualty incidents (MCIs) cause many casualties with various levels of injury severity. To respond effectively in the aftermath of an MCI, multiple stages in humanitarian relief operations (HROs) seek to reduce any adverse impacts on the affected population. During the initial response, injured people are assessed, triaged, and subsequently transferred from the MCI site via ambulances to hospitals with available capacity providing the appropriate level of care.
Responding to an MCI requires both patient transportation decisions and capacity planning for healthcare centres (i.e. hospitals) [35]. In times of an MCI, hospitals may face increasing wait times and severe shortages for a wide range of medical services. In most cases, the influx of MCI patients leads to a severe disruption in the ability of the hospital to respond to regular demand. It is well known that delays in care provision in emergency departments (EDs) negatively affect patient outcomes [3, 30]. Sub-optimal decision surrounding the response to the MCI (such as overloading a single hospital) may exacerbate such delays.

Thus, MCI response managers must balance the needs of the MCI demand with the relative capacity at each hospital and the relative cost of increasing capacity. One key element for effective capacity planning of hospitals is improved patient transportation from the MCI site to the various hospitals with different service capabilities particularly when patients have varying types and severity of injury. For example, some patients may require urgent, immediate treatment and must be transferred to the nearest hospital that can provide the appropriate care. More flexibility is possible with less-urgent patients. Triangulating patients and prioritizing them for EMS provision is called triage. In a triage process, patients are classified into several groups based on the severity of their injuries. The most widely practised triage system is "Simple Triage And Rapid Treatment (START)", where patients are grouped into four classes – expectant, immediate, delayed, and minor [34].

MCI management is complicated by significant uncertainty both in terms of the demand at the MCI site and regular demand arriving to the ED of each hospital. MCI managers will generally have little prior knowledge of the extent of the arriving demand. Under such uncertainty, managers must plan for many potential future scenarios to avoid being caught unprepared. Thus, transportation decisions must consider various characteristics of the available hospitals including their location, capacity, service rate, and care capability [7, 30, 35, 22].

Figure 4.1 provides a general structure of a MCI response network. The strong likelihood that demand will tax the available capacity in a disaster management setting heightens the critical nature of the resource allocation problem. During minor or moderate surges, when resources are typically adequate, strategies such as discharging patients early and/or cancelling elective operations may be sufficient to redirect adequate resources to the surge event. As the size of the surge increases, more drastic measures are required to mitigate the disaster's impact - typically involving much higher costs.

The motivation behind the current research is the lack of an existing model that incorporates both patient transportation and resource capacity planning in the event of an MCI; the development of an algorithm to solve these types of models faster compared to the existing algorithms in the literature, and the analysis of different strategies for allocating resources to the injured in an integrated relief network. We argue that this is most appropriately modeled through a finite-horizon MDP allowing for non-stationary demand arriving to the MCI site (typically a MCI has a high initial demand tapering off fairly quickly). We seek to determine optimal vehicle assignment and hospital capacity planning decisions while taking into account patients with different levels of injury severity, the limited capacity of vehicles and hospitals and multiple sources of uncertainty - the arrival of daily demand at the hospitals, the number of new arrivals at the MCI site and the number of patients discharged from the hospital.

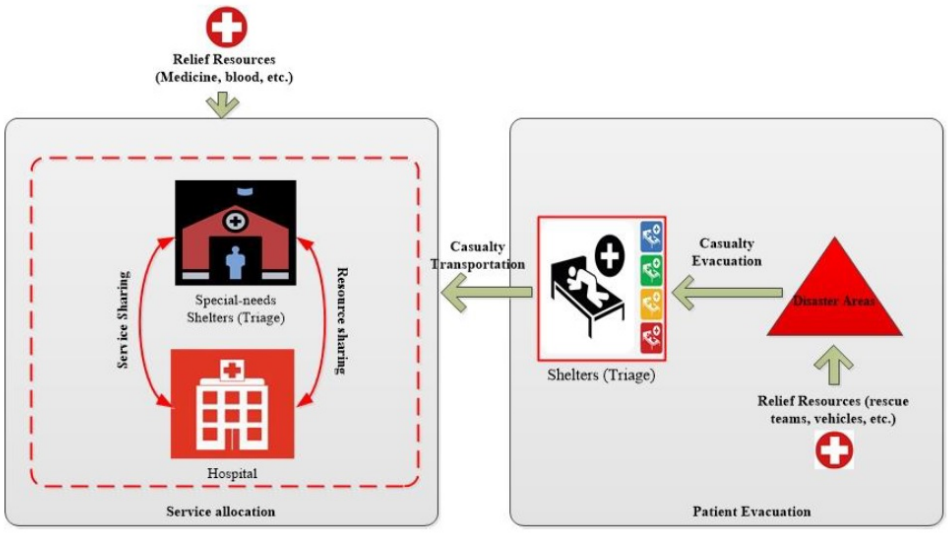

Figure 4.1: Current relief logistics for casualty flow and resource allocation operations

Decisions are made under a short planning horizon with 15-minute intervals between periods, for a planning horizon of up to six hours (immediate response MCI operations). The reason for incorporating very short time intervals is that the ambulances need sufficient time to finish at least one trip from the MCI site to the hospitals. Hence, after a 15-minute interval, we can get new updates concerning the location of the ambulances for the next decision epoch. Furthermore, for the finite-horizon MDP, as the model should be resolved for each decision epoch, making the time intervals shorter than the one considered in this study increases the state space drastically with many time indices, resulting in a considerable algorithm run time. It is important to note that the average ambulance response time for MCIs differs from country to country. The average response time of ambulances is, for instance, 10 to 18 minutes in Canada, 11.4 minutes in Australia, etc. However, it should be noted that the average time does not include the time it takes to board and alight the injured.

We formulate a Markov decision process (MDP) under the finite-time horizon and non-stationary condition for modelling an integrated transportation and capacity planning model during an MCI under multiple sources of uncertainty. We first study the policy impact of various parameters in the model (particularly the uncertainty). Second, we solve the proposed finite-horizon MDP model (through the LP approach to ADP) for a large-scale instance.

The proposed model can be used by the practitioners for pre-planning (preparedness) phase of MCIs in order to ensure adequate capacity is available at hospitals with various care capabilities for multi-type injured population. In other words, the proposed model is not intended to be employed for the real-time planning (during the MCI or the response phase of MCI).

This research makes the following contributions. First, we develop a finite horizong Markov Decision Process (MDP) model for patient transportation and hospital capacity planning that makes

best use of the available resources to provide timely access to care for all patients (both MCI and regular). We demonstrate that the proposed model yields a better outcome than a myopic approach for both congested and non-congested systems. To overcome the practical challenges of implementing the proposed model, we develop an equivalent approximate linear formulation of the proposed MDP model which we solve through column generation.

The remainder of this chapter is organized as follows. In Section 4.2, we discuss the relevant literature on casualty flow models with/without considering uncertainty and various modelling approaches for dealing with uncertainty. In Section 4.3, we describe what we call the dynamic integrated vehicle assignment and capacity planning problem and develop the proposed model. In Section 4.4, we provide the equivalent approximate linear formulation (ALP) of the proposed MDP model. In section 4.5, we propose a two-phase heuristic solution method to solve the equivalent ALP model in a timely fashion. In Section 4.6, we examine the performance of the approach and the sensitivity of the solution to changes in key parameters. Finally, in Section 4.7, we conclude the study and discuss future research directions.

4.2 Related Literature

This section reviews previous studies on operations management of MCIs including casualty flow models and relevant solution methodologies and modelling approaches. A comparative analysis of some of the relevant studies is provided in Tables 4.1 and 4.2.

4.2.1 Casualty flow models

A number of researchers have studied casualty transportation to/and from shelters and hospitals [30, 31, 37]. Wilson et al. [37] model the transportation of casualties to hospitals as a single-period scheduling problem where they consider a set of sequential tasks, such as pre-transport treatment, transportation to the hospital, and treatment. Dean and Nair [7] and Sung and Lee [35] model the patient prioritization problem as an ambulance scheduling problem and propose different triage methods to provide better and more timely treatment. Dean and Nair [7] formulate a resource-constraint triage problem as a mixed-integer problem with the goal of effectively evacuating victims to the different area hospitals in order to provide the greatest good to the greatest number of patients while not overwhelming any single hospital. Similarly, to ration the emergency medical resources based on prioritization, Sung and Lee [35] model a resource-constraint triage problem as a set partitioning problem, and apply a column generation approach to efficiently handle a large number of feasible ambulance schedules. Jin et al. [15] propose an optimization model as a mixed integer programming model for patient delivery and medical resource allocation with capacity restrictions. They formulate the model to maximize the number of affected people

whose survival probability exceeds a given threshold (below this level the patient's health condition severely decreases). They divide all affected people into several categories with differentiated survival probabilities depending on each victim's injury level. They apply their model in a case study with data from a department store collapse in South Korea.

Zhu et al. [41] seeks to optimize the transportation strategy using two optimization models where the relative deprivation cost[1] is proposed as one of the decision-making objectives. To emphasize equity and highlight rescue priority, they incorporate the deprivation cost and the in-transit tolerable suffering duration as a time window constraint into their model. Their first model as a mixed-integer model deals with optimal path selection with vehicles' capacities and victims' tolerable time windows, and the second one considers the same model with diverse injury degrees. To solve the model, they apply the ant colony optimization as an efficient method for routing problems.

4.2.1.1 Casualty flow models under uncertainty

Different approaches are present in the literature to tackle the uncertainty associated with demand, supply, and travel times etc. Dynamic multi-stage planning allows the researcher to model a situation where uncertain information is revealed in stages as the MCI event unfolds [26]. Zhang et al. [40] propose a three-stage single-objective model based on fuzzy logic. Additionally, they employ an approximate two-stage stochastic programming approach for large-scale problems to mitigate the worst-case scenario. Yu et al. [38] propose a dynamic programming model for a multi-period resource allocation problem, with special attention paid to the human suffering resulting from any delivery delay. To improve the efficiency, effectiveness and equity of the allocation, their study simultaneously seeks to minimize accessibility costs, the starting state-based deprivation costs and terminal penalty costs. They propose a dynamic programming model to solve the resulting nonlinear problem to optimality.

Using a Markov decision process formulation, Mills et al. [22] develop two heuristic policies that use limited information such as mean travel times and congestion levels to determine (1) how to allocate ambulances to patient locations and (2) which medical facility should be the destination for those ambulances. In a simulation study, they incorporate patient survival rates and service times for different types of traumatic injuries. They propose heuristics that can substantially improve the expected number of survivors compared to the common practice of transporting to the nearest facility, even when the decision maker has only limited up-to-date information about the system state. In particular, a myopic approach that considers what is best for the next patient increases the expected number of survivors in almost all scenarios. Using a more sophisticated one-step

[1] As defined by Holguín-Veras et al. [11], the deprivation cost is an economic valuation of human sufferings associated with a lack of access to the emergency relief service.

policy improvement approach provides further improvement when the event involves patients who do not deteriorate rapidly and especially when the transportation is not the bottleneck and the casualties are spread over many locations.

4.2.2 Modeling and solution approaches

For situations with high levels of uncertainty such as MCIs, stochastic and fuzzy programming [27, 12, 21, 23, 8, 26, 40] and robust optimization [36, 12, 17, 20, 42] are the most common approaches. Only a few studies apply Markov decision processes or model decision making in situations (i.e., MCIs) where information is revealed over time in a dynamic fashion [22, 38, 18, 9]. As an example of a study that employed the MDP approach for MCIs, Zayas-Cabán et al. [39] develop policies to mobilize ambulances from surrounding areas in response to a mass-casualty incident and allocate this additional capacity among affected regions. The objective is to clear the system as quickly as possible while keeping the cost of moving vehicles under a certain budget.
Mills et al. [22] demonstrate the benefit of sharing information about the congestion in the emergency department and inpatient wards when assigning patients to hospitals and accounting for the probabilistic need for inpatient resources. Jotshi et al. [16] consider congestion at the receiving facilities but they assume that this (and other system state information) is exogenous and independent of the decision on where to send patients. Li and Glazebrook [19] propose a semi-Markov decision process model and solved this model with approximate dynamic programming. Their solution demonstrates that patients in the highest medical severity class should not always be given the highest transport priority. Jacobson et al. [13] solve a similar scheduling problem under various MCI conditions and find that the optimal policy provides higher priority to low triage class patients when this lower priority class represents a larger portion of the total number of patients.

—Infinite horizon MDP models

Most MDP approaches develop an infinite-horizon MDP model. Such an MDP approach does not take into account the impact of the initial state. Ramirez-Nafarrate et al. [29] present an infinite horizon MDP to determine emergency department (ED) policies that minimizes the long-run average tardiness per patient for a single ED. Such an MDP formulation minimizes the average time that patients wait beyond their recommended safety time threshold. The model considers two treatment areas, differentiated by patient severity, and assumes the availability of (some) information on the time to start treatment in a neighbouring hospital if an ambulance patient is diverted. DuBois and Albert [9] present an infinite horizon MDP model for ambulance dispatching with prioritized patients. The results suggest that delaying service to low-priority patients when the system is congested enables ambulances to immediately respond to future high-priority patients who may need care and whose conditions may deteriorate.

Table 4.1: The most relevant studies (methodologies)

Reference	Year	Objective Function	Decision	Methodology	Solution Algorithm
Mete & Zabinsky	2010	TT	FS, VA	MIP (two-stage stochastic)	Exact
Salmeron & Apte	2010	UD, UIP	VF, PA, RA	MIP (two-stage stochastic)	Exact
Ben-Tal et al.	2011	TC	VF	Robust stochastic multi-type dynamic routing	Min-max criterion /Affinely Adjustable Robust Couterpart
Jabbarzadeh et al.	2012	TC	RF, FL	MINP (Robust allocation)	Exact
Ozdamar and Demir	2012	TT, VU	RF	MINP	Multi-level clustering
Afshar& Haghani	2012	UD	RF, FL, VF	MIP (Dynamic allocation & multi-period routing)	Exact
Edrissi et al.	2013	CCR, ELAP, FCR	RF, VPR	Multi-agent multi-period allocation	Huerisitc
Najafi et al.	2013	UIP, TVU, UD	RF, VF, PF	MO-MIP(Robust stochastic dynamic multi-period)	Heuristic hierarchical
Bozorgi-Amiri et al.	2013	TC, UD, SL	RF	MO-MINP (Robust stochastic)	Compromise approach
Davis et al.	2013	TC	RA	MIP (single-period two-stage stochastic)	Exact
Abounacer et al.	2014	TT, UD, FS	RA, FL	MO-MIP (Single period deterministic allocation)	Exact (Epsilon-constraint)
Liberatore et al.	2014	DS	RF, VF	MO-MINP (Robust allocation)	Lexicographic/ RecHADS algorithm
Najafi et al.	2014	UIP, UD	PF, VF, RF	MIP (Multi-period dynamic allocation/routing)	Heuristic
Dean &Nair	2014	PT	PF, VF	MIP (multi-period allocation)	Exact

Table 4.1 continued from previous page

Sheu	2014	CRS	RA, VF	MIP (multi-period deterministic)	Structural equational modeling
Huang et al.	2015	LSU, DC, FA	RF	MO-MIP (Dynamic multi-period allocation)	Weighted sum &Variational Inequalities
Wang et al.	2015	TT, TC, RR	VF, RF	MINP	NSGA/NGDA
Sheu&Pan	2015	TD, TC	PF	MIP	Exact
Camacho-Vallejo et al.	2015	RT, TC	RF	MIBNP (Single period deterministic allocation)	Exact
Sung & Lee	2016	SP	VF, PF	MIP (Multi-period routing)	Column Generation
Repoussis et al.	2016	PTT	VF, PF	MIP (Multi-period routing)	Heuristic / Local search / Valid inequalities
Tofighi et al.	2016	TT, TC	FS, RA	MIP (Possibilistic-stochastic)	Differential evolution
Pradhananga	2016	TC	FS, RA	MIP (Single-period stochastic allocation)	Exact
Zokaee et la.	2016	TC	RF, FL	MIP (Robust stochastic)	Exact
Ransikarbum & Mason	2016	TC, UD, EC	RF	MO-MIP (single-period deterministic)	Goal programming
Kamyabniya	2017	UD, TC	RF	BMIP (Robust possibilistic, multi-period mutli-commodity allocation)	Exact (epsilon-constraint)
Sharma et al.	2017	TC	RA, FL	Bayesian belief network (shelters ranking)	Tabu-search
Rezaei-Malek et al.	2017	RT, TC	RF, FL	MIP (Robust stochastic)	The reservation level driven Tchebycheff procedure (RLTP)
Fahimnia et al.	2017	TC, DT	RA, FL	BMIP (Scenario stochastic)	Epsilon-constraint & Lagrangian relaxation
Fazli-Khalaf et al.	2017	TC, TT, TRB	RF	MO-MIP (Robust possibilistic flexible chance constraint)	Exact
Shahparvari et al.	2017	TTE	VF	MIP(Multi-destination dynamic vehicle routing)	Interactive fuzzy – Genetic

Table 4.1 continued from previous page

Zhou et al.	2017	TR, UD	RA	MO-MIP (multi-period dynamic scheduling)	NSGA-II
Fereiduni and Shahanghi	2017	TC	RF, FL	MIP (Multi-period scenrio-based robust)	Exact
Swamy et al.	2017	TD, SL	FL, SL, VF	MIP (Multi-period routing)	Heuristic
Zhu et a.	2018	DC, TC	PF, VF	MIP (Multi-period routing)	Ant-Colony
Kamyabniya	2018	TT, TC	RF	MIBP (Fuzzy bi-level, multi-period allocation)	Fuzzy Kth-Best
Cheraghi & Motlagh	2018	UD, TC	PA, FS, RA	MO-MIP (Multi-period robust stochastic)	Fuzzy-VIKOR
Ma et al.	2018	UD	RA	MIP (multi-group single period allocation)	Greedy heuristic
Habibi et al.	2018	UD, TC	FL, RF	BMIP (Scenario-based Robust)	Exact (goal programming)
Samani et al.	2018	TC, UD	RF, FL	BMIP (two-stage robust possibilistic)	Three-phase fuzzy approach
Mills et al.	2018	TTE	PF, VF, FS	Multi-dimentional Markov process	Hueristic approach
Liu et al.	2018	UD	RF, PF, VF	MIP (Multi-period dynamic robust predictive control) /rolling horizon	Real-time exact
Mejia-Argueta et al.	2018	TT, RT, TC	FL, RF, PF, VF	MO-MIP (single period deterministic)	Exact (Epsilon-constraint)
Mollah et al.	2018	TC	VF, FL	MIP (single-period deterministic)	Genetic
Rodriguez et al.	2018	TC, UD	PA, RA, VA, PA	BMIP (single-period deterministic)	Weighted sum & Epsilon constraint
Tavana et al.	2018	TC, RT	RF, FL	MO-MIP (Multi-period routing)	NSGA-II
Elci & Noyan	2018	TC	RA, FL	MIP(Two-stage stochastic / CvaR)	Benders decomposition-based branch & cut
Sabouhi et al.	2018	TT	RF, PF	MIP (Robust possibilistic)	Exact

Table 4.1 continued from previous page

Yu et al.	2018	TC	RA	NIP (Approximate multi-period dynamic allocation)	Rollout algorithm
Moreno et al.	2018	TC, PS	FL, VF, RF	MIP (Two-stage multi-period stochastic scheduling)	Fix-and-Optimize Heuristic
Doan & Shawn	2019	PSH, TC	PA, EA	BMIP (Two-stage multi-period stochastic)	Exact
Paul & Zhang	2019	TC	RA	MIP(Two-stage stochastic)	Exact
Zhang et al.	2019	TC, UD, TT	RA	MO-MIP (Three-stage fuzzy-stochastic/Approximate single-stage)	Exact

Abbreviation:
UD: Unsatisfied demand; RF: Resource flow; FL: Facility location; VF: Vehicular flow; RA: Resource allocation; TT: Transportation time; PF: Patient flow; TC: total cost; TD: travel distance; RT: response time; DT: delivery time; TRB: Total reliability tested blood; TTE: total transferred evacuees; FS: facility selection; TR: total risk; TVU: total vehicle utilized; UIP: unserved injured people; PTT: patient treatment time; PT: patient treatment; NIP: non-linear integer programming; EC: Equality coverage; PS: Patient suffering; DS: demand satisfaction; CRS: collective resilience survivors; RR: route reliability; SL: satisfaction level; VU: Vehicle utilized; CCR: Casualty chance removal; FCR: Failure chance removal; ELAP: Emergency location/allocation problem; VPR: vulnerability population ratio

They address the issue by formulating and studying an infinite horizon Markov decision process model (under average reward conditions) that determines which type of ambulances (servers) to send to patients in real-time. Jenkins et al. [14] examine the management of military aeromedical evacuation assets. They present a discounted, infinite-horizon MDP model and solve it using approximate dynamic programming to attain high-quality dispatching, preemption-rerouting, and redeployment policies that improve the performance of the military emergency system.

—Finite-horizon MDP models and their applications

As stated earlier, the applications of finite-horizon MDP models using approximate dynamic programming (ADP) have not been investigated in the context of MCI response management. Bhattacharya and Kharoufeh [4] present an LP approach to solving non-stationary, finite-horizon MDP models that can potentially overcome the computational challenges of standard MDP solution procedures. Their model is solved using an ADP solution approach with significantly fewer decision variables. This is one of the first studies in the literature that shows the application of LP and ADP modelling and solution methods for finite-horizon MDP models from the theoretical points of view. They demonstrate that solving the LP formulations can provide computational advantages over the standard value and policy iteration algorithms. Perhaps most importantly, these formulations naturally facilitate the use of approximate LP procedures for finite-horizon MDP models. From the application point of view for the MCI networks modelled in a dynamic fashion, the paper by Najafi et al. [24] focus on the transport of both commodity towards affected areas and injured people to hospitals. Their proposed model is capable of receiving updated information at any time and adjusting plans accordingly. They propose a dynamic model that is focused on assisting disaster managers in planning/re-plan the logistical activities during the response phase after an earthquake at each decision epoch. Their results show that locating a relatively large number of hospitals and suppliers with small capacities is preferred over locating a few hospitals and suppliers with large capacities because this leads to shorter waiting times for serving injured people and better satisfying needs. They solve the dynamic network using a heuristic algorithm that updates the information at each decision epoch.

To the best of our knowledge, there is no work in the literature that studies the integrated resource-service (casualty-transportation and hospital capacity planning) problem in MCIs. However, in terms of modeling and solution approach, two papers by Najafi et al. [24] and Bhattacharya and Kharoufeh [4] are the closest ones to our research, respectively. Unlike the work by Najafi et al. [24], we make decisions regarding hospitals' capacity and match resources and services based on the urgency levels of patients.

Table 4.2: The most relevant studies (MCI management)

Reference	Year	Model Features								Uncertainty modeling		
		Period		Resource		Parameters		Objectives		Stochastic/Fuzzy	Dynamic	Robust
		Single	Multiple	Single	Multiple	Certain	Uncertain	Single	Multiple			
Salmeron & Apte	2010	*		*			*		*	*		
Mete & Zabinsky	2010	*		*			*	*		*		
Ben-Tal et al.	2011		*	*			*	*		*		*
Jabbarzadeh et al.	2012		*	*			*	*		*		*
Ozadamar and Demir	2012	*			*	*		*				
Afshar& Haghani	2012		*		*	*		*				
Davis et al.	2013	*		*			*	*		*		
Edrissi et al.	2013		*	*		*			*			
Bozorgi-Amiri et al.	2013	*			*		*		*	*		*
Najafi et al.	2013		*		*		*		*			*
Abounacer et al.	2014	*			*	*			*			
Liberatore et al.	2014	*		*		*			*			
Najafi et al.	2014		*		*	*			*			
Dean &Nair	2014		*		*	*		*				
Sheu	2014		*		*	*		*				
Sheu&Pan	2015	*			*	*		*				
Wang et al.	2015		*		*		*	*				*
Huang et al.	2015		*	*		*			*			
Camacho-Vallejo et al.	2015	*			*	*			*			

Table 4.2 continued from previous page

Paul & MacDonald	2016		*	*			*	*		*		
Sung & Lee	2016	*			*	*		*				
Repoussis et al.	2016	*			*	*		*				
Tofighi et al.	2016	*			*		*		*	*	*	
Pradhananga	2016	*			*		*					
Zokaee et la.	2016	*			*		*	*				*
Ransikarbum & Mason	2016	*		*		*			*			
Moreno et al.	2016		*		*		*		*	*		
Kamyabniya	2017		*		*		*		*			*
Sharma et al.	2017	*		*		*		*			*	
Rezaei-Malek et al.	2017		*		*		*		*			*
Fahimnia et al.	2017		*	*			*		*	*		
Fazli-Khalaf et al.	2017		*	*			*		*			*
Shahparvari et al.	2017		*	*			*	*		*		
Zhou et al.	2017		*		*	*			*			
Swamy et al.	2017	*		*		*			*			
Zhu et a.	2018	*			*	*			*			
Niessner et al.	2018		*		*	*		*				
Kamyabniya	2018		*		*		*		*			*
Cheraghi & Motlagh	2018		*		*		*		*			*
Ma et al.	2018	*			*	*		*				
Habibi et al.	2018		*	*			*		*			*

Table 4.2 continued from previous page

Samani et al.	2018		*		*		*		*	*		
Mills et al.	2018		*		*	*		*			*	
Liu et al.	2018		*		*	*		*				*
Mejia-Argueta et al.	2018	*		*		*			*			
Mollah et al.	2018	*		*		*		*				
Rodriguez et al.	2018	*			*	*			*			
Tavana et al.	2018		*		*	*			*			
Elci & Noyan	2018	*		*		*		*				
Sabouhi et al.	2018	*		*			*		*	*		*
Yu et al.	2018		*	*		*			*		*	
Moreno et al.	2018		*		*		*		*	*		
Zhang et al.	2019		*		*		*		*	*		
Doan & Shawn	2019		*		*		*		*	*		
Paul & Zhang	2019	*		*			*	*		*		

Although their work does consider a sequential decision-making structure, meaning that they assume the network information are updated, the decision are not taken based on the various network states at each decision epoch. Furthermore, their model assume the information updating mechanism can deal with uncertainty exists in the relief operations; hence, no sources of uncertainty is defined in their study. On the contrary, in our study, we apply a finite-time horizon MDP modelling approach to capture the evolving uncertainty in MCI response plans and the sequential nature of decision making. Finally, our proposed model considers patient transfers among hospitals in times of congestion or due to the unavailability of services. Although the study by Bhattacharya and Kharoufeh [4] is similar to our approach in terms of application of an ADP solution approach to our finite-horizon MDP model, the complexity of our proposed model with large state-action space and the solution approach is not comparable. They present the approximate linear formulation of the finite-horizon MDP model, but they assume the complicated derived formulation can be solved using the off-shelf solvers. In contrast, we develop a two-phase heuristic algorithm to overcome the computational issues of finite-horizon MDP models with huge state-action space.

We conclude this section by returning to the patient distribution problem in the aftermath of an MCI. If transportation and hospital treatment resources are not limited, prior mass casualty incident response models could be appropriate (non-integrated models). On the other hand, if transportation and hospital resources are limited, we submit that the proposed integrated model has the potential to improve MCI response management and thereby increase patient survival.

4.2.3 Research gap

While patient transportation and capacity planning during MCIs is receiving increased attention in the literature, the problem integrating resource-service (i.e. vehicle-hospital capacity) allocation to multi-level-injury patients has not been extensively studied.

A few studies focus on simultaneously integrating casualty transportation and hospital capacity allocation to minimize the transit and waiting times for transporting injured people and allocating hospital services to the affected population. However, none of these studies address the problem in a dynamic setting where decisions must be made within a limited time window (finite-horizon) and when at each period of the planning horizon, a complex model must be solved for many state-action pairs. Second, most existing models only consider a single resource type or medical service or make no distinction between severity of patients' condition when planning relief operations in MCIs. Third, approaches such as approximate dynamic programming have rarely been applied to the above mentioned problems. This lack of application of MDP has less to do with fit and more to do with tractability. MCI relief operations are a natural fit for MDPs as they involve a sequential decision problem with evolving uncertain information. Decisions made early in the

planning horizon impact what decisions are possible in the future. For instance, a failure to proactively increase capacity may lead to downstream congestion that in turn leads to high waiting times and poor care. The application of ADP allows us to overcome the computational challenges that come with applying MDP to a problem as complex as MCI relief planning.

4.3 Problem statement

During MCIs, central emergency preparedness units, such as the Hospital Emergency Preparedness Committee of Ottawa (HEPCO), are responsible for coordinating hospitals to ensure a rapid response to the disaster. It is a significant challenge for HEPCO and other relief agencies to determine how best to respond to a mass casualty event while still supporting the regular demand arriving at the various general-care hospitals. Without proper planning, it is easy for patients to be transferred to facilities that are not adequately prepared in terms of resources for the arrival of such a influx of patients. This mismatching of resources and services to patients can result in a shortage of capacity at hospitals, increased waiting times and lengthened response times. The goal is to ensure that hospitals have sufficient capacity to treat patients transported to them by the optimized casualty transportation policy. As stated earlier, in MCIs involving many injuries or deaths, two types of relief operations are highlighted: casualty flow and service allocation planning. Typically, these two operations are not well integrated. One of the unfortunate consequences is that injured patients may arrive at a given location only to find that the required resources are not available. We believe that an integrated service-resource-patient-oriented network for MCIs can prevent shortages of resources (ambulances) and medical services (hospital capacity) and thus reduce any service delay for injured patients. In general, hospitals do not have similar trauma centers and care capabilities. Consequently, patient transfers between hospitals is considered as a strategy to release capacity at a hospital and assign that capacity to more urgent patients. The overall nature of the problem comes from discussions with the HEPCO that highlighted the challenges mentioned above.

Figure 4.2 depicts the flows of patients and resources in the event of a major disaster. As shown in the first layer, affected populations are transferred from the MCI region to different hospitals after triage. While the majority of demand is likely known at the onset or soon after, it is reasonable to assume that new demand may arrive in the ensuing time following the initial MCI event. We assume that the network of hospitals has a fleet of ambulances available that must accommodate both the demand at the MCI site and the regular demand occurring in the region. Given the available resources, a decision must be made as to the allocation of each ambulance (i.e. what patient an ambulance transports and to what destination). Patients are assumed to be categorized based on severity and resource requirements.

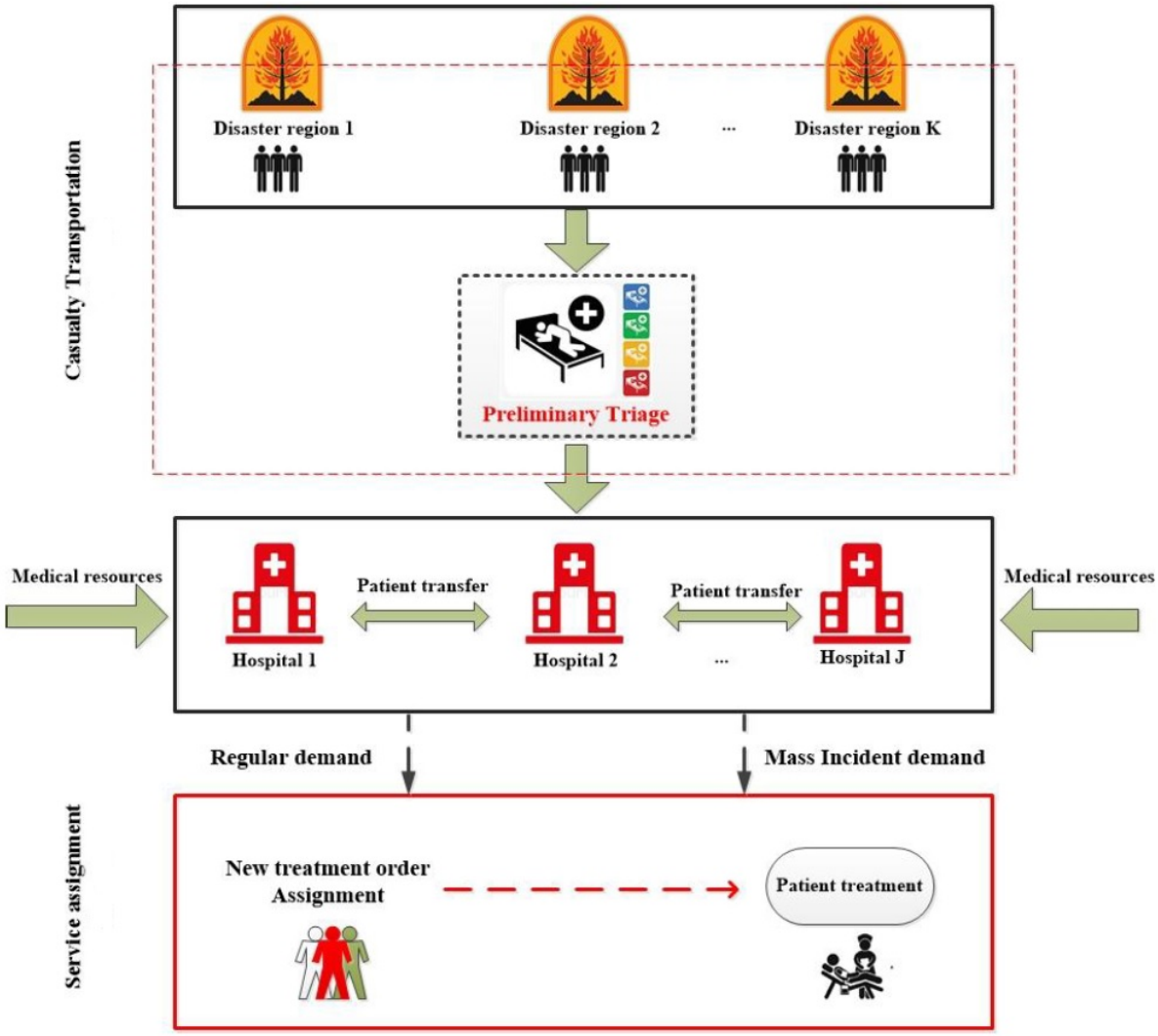

Figure 4.2: The proposed integrated casualty transportation and hospital capacity logistics planning structure

Simultaneously the level of capacity at each hospital is assessed. If capacity is insufficient, additional measures must be taken (e.g., off-loading less severe patients to other hospitals, cancelling elective surgery, etc.). We assume that there are a number of potential measures that can be taken to create capacity and that these measures can be ranked based on their costliness. Thus our setting combines the transportation decisions of multi-type patients using a limit ambulance capacity from one MCI to a network of hospitals and the capacity planning operations available to the hospitals. Thus, we develop an integrated casualty transportation and hospital capacity planning model to capture the dynamic behaviour of the system due to various sources of uncertainty and maximize the expected number of survivals (number of transferred patients of varying severity to relevant hospitals) in a finite planning horizon. The overall output of the current research focuses on effectively transporting patients to different hospitals to provide timely care to the those at the MCI site while not overwhelming any hospital.

4.3.1 Proposed Finite-horizon MDP Model

We formulate a finite time-horizon MDP model. We consider a system with R locations - an MCI site and multiple hospitals. We assume that we are dealing with a short planning horizon that is divided into discrete time intervals to create decision epochs. While it is true that decisions are in fact made in continuous time, this is not much of a simplification provided the time interval between the discrete epochs is kept small. At each decision epoch, the decision maker observes the capacity of treatment services at each hospital, the current amount and location of patients and the position of each ambulance in order to determine where to send each ambulance and whether or not to increase capacity at any hospital. Below, we outline the four components of an MDP model. As will be stated later, the patients waiting at the MCI site are assumed to be already triaged; hence, in this research, the injured people are classified into different injury seriousness classes ranging from minor, moderate, serious, severe, and critical.

The reason why we use the finite-horizon MDP approach for our case is that finite horizon MDPs are sensitive to the initial state. They attempt to be optimal in the sense that the policy is optimal for all given allowable initial states. whereas infinite horizon formulations provide a steady state policy. In the case of the MCI event it is clearly important that one reacts to the initial conditions of the event. Moreover, the length of the horizon is finite since the MCI recovery is completed once all patients from the MCI are transported to a hospital.

4.3.1.1 Assumptions

The detailed routing of patients to hospitals through multiple potential routes is not considered in this study. Nor is the potential uncertainty around travel time. It is assumed that the location

of the MCI and each hospital is known so that travel times can be reasonably anticipated. It is also assumed that patients waiting at the MCI site are already triaged. Hospitals are presumed to differ in treatment capability, capacity and anticipated regular demand. Hospitals can expand their capacity at each decision epoch according to the congestion state of the system or lack of capacity at other hospitals but only at a certain rate and to a max capacity. Also, the utilization of hospital capacity is assumed to be divided into patient types. The purpose of this assumption is to decrease the state space for ease of computation. Moreover, when the injured people are triaged at the MCI site, a relevant treatment service for a specific patient type is chosen before being transferred to any hospital. Also, the arrival of patients at the MCI site, the length of stay at each hospital, and the daily arrivals of patients at hospitals are unknown and follow different probability distributions.

Although the decision concerns allocation of patients to ambulances and not specific routing decisions, the location of vehicles is captured by the state variables as important information when deciding on capacity and allocation. Hence, patient allocation-related decisions are taken based on the state of the vehicles (empty or transporting a patient) and their location/distance in time units from different locations in the network.

Finally, an important assumption in our study is that it is possible to move/discharge patients that are already at the hospital within the planning horizon of our study. This is aligned with the reality as the Ottawa Hospital had to free up the capacity of ED rooms during the bus crash incident described later by sending the existing patients to other hospitals and institutions. Patients in the waiting room were triaged and those who could be safely moved were advised to go to another emergency room. Thus, we are assuming that the hospitals have the potential to free up capacity and the cost is well-captured by our stepwise function that will be explained in Section 4.3.1.2.

4.3.1.2 Mathematical formulation

In this section, Table (4.3) presents the sets, parameters, actions, and system state sets, followed by a detailed description of the main components of an MDP.

The System State. In the proposed model, the system state is defined as $S^t = (n^t, P^t, AC^t, B^t)$. We define $n^t = n_i^t$, where n_i^t represents the number of patients of type i at the MCI site at time t. $B^t = B_{ijc}^t$ represents the number of ambulances transporting a patient of type i to site j that is c decision epochs away. We let $i = 0$ represent an empty ambulance. The state information for hospitals is represented by P_{ij}^t and AC_{ij}^t where P_{ij}^t represents the number of type i patients at hospital j at decision epoch t and AC_{ij}^t represents the capacity at hospital j to service type i patients at time t.

The Actions. The actions determine where to send the ambulances and with whom (type of

patient) and whether to increase the hospital's capacity by either expanding the capacity available at that hospital or transferring specific types of patients to other hospitals. Thus, a vector of possible actions can be written as $(\vec{a^1}, \vec{a^2})=\{a_{ij}^{1t}, a_{ijj'}^{2t}\}$, where a_{ij}^{1t} represents the increase in the amount of the capacity for patients of type i at hospital j at decision epoch t and $a_{ijj'}^{2t}$ is the decision to transport a type i patient to location j from locations j'. These actions are constrained by a number of factors as outlined below.

$$a_{ij}^{1t} \leq AC_{ij}^{t} \times \delta \qquad \forall t, j \in H, i \neq 0 \tag{4.1}$$

Equation (4.1) imposes an upper bound on the capacity increase at a given hospital from one decision epoch to the next. δ represents the percent increase in total capacity allowed per decision epoch (expansion rate).

$$\sum_{j' \in H} a_{iDj'}^{2t} \leq n_i^t \qquad \forall t, i \neq 0 \tag{4.2}$$

$$\sum_{\substack{j' \in H \\ j' \neq j}} a_{ijj'}^{2t} \leq p_{ij}^{t} \qquad \forall t, i \leq 3, i \notin \{0\}, j \in H \tag{4.3}$$

$$\sum_{\substack{j' \in R \\ j' \neq j}} a_{ijj'}^{2t} = 0 \qquad \forall t, i \geq 4, j \in H \tag{4.4}$$

$$AC_{ij}^{t} \leq M_{ij} \qquad \forall i \neq 0, j \in H, t \tag{4.5}$$

Equations (4.2)-(4.5) present bounds on the transportation decisions in each decision epoch. Equation (4.2) ensures that one cannot transport more patients from the MCI site than are currently waiting. Similarly, Equation (4.3) prevents a hospital from transferring more patients than its current patient population. Notably, this equation only allows transportation of moderately injured patients ($i \leq 3$). Equation (4.4) prevents hospitals from transferring patients of high severity ($i > 3$) to other hospitals. These constraints can obviously be relaxed if the setting permits. Equation (4.5) imposes an upper bound for assigning the capacity of hospital j to a patient of type i. If a hospital j cannot treat patients of type i then $M_{ij} = 0$. Otherwise, M_{ij} represents an upper

bound on the amount of capacity that can be provided for patients of type i.

$$\sum_{\substack{i \cup \{0\}, j \in R \\ c}} B_{ijc}^{t} = TV \qquad \forall t \tag{4.6}$$

$$\sum_{\substack{j' : j' \neq j \in R \\ i}} a_{ijj'}^{2t} \leq B_{0j0}^{t} \qquad \forall t, j \in R \tag{4.7}$$

Equation (4.6) guarantees that the number of patients transferred at each decision epoch cannot exceed the available number of ambulances (TV) and Equation (4.7) guarantees that the number of patients transferred from hospital j is less than the number of available ambulances currently at hospital j.

Table 4.3: Model notation (Dynamic Capacity Planning Model)

Sets	
R	Locations in the MCI network
D	MCI site, $D \subseteq R$
H	Hospital, $H \subseteq R$
t	Time periods, $t \subseteq T$
c	Distance of ambulances (in time units) from a destination, $c \subseteq C$
I	Type of patient, $i \subseteq I$
Indices	
j, j'	A location, $j, j' \in R$
i	Injury level of a patient, $i \in I$
c, t	A distance of vehicles (in time units) and a time period, respectively
System State	
$S^t = (n_i^t, P_{ij}^t, AC_{ij}^t, B_{ijc}^t)$, $A^t = (a_{ij}^{1t}, a_{ijj'}^{2t})$	
Parameters	
δ	Capacity expansion percentage of hospitals
λ_i^t	New arrivals of patients of type i at MCI site at decision epoch t
M_{ij}	Zero-one parameter representing the ability of hospital j to accept a patient of type i
μ_{ij}^t	New demand for patients of type i at hospital j at decision epoch t
$dist(j, j')$	Distance between location j and j' measured in time units
TV	Total number of ambulances in the network
$\Gamma(i, t)$	Penalty for each patient waiting at the MCI site (Equation 13)
$\theta(j, i, t)$	Penalty for each patient waiting at a hospital (Equation 13)
$W_{q,i,j}^t$	Cost of increasing capacity for a patient of type i at hospital j at level q (Equation 13)

Table 4.3 continued from previous page

$f_{c,j,j'}$	1, if the distance between j and j' is equal to c, 0 otherwise
$PE1_i^t$	Penalty for each patient remaining at the MCI site at last decision epoch (T)
BC_{iH}	Basic Capacity of hospital j for patients of type i
BLC_{1ij}, BLC_{2ij}	1st and 2nd Levels of capacity of hospital j for patients of type i
$Prob_{iH}^t$	Probability of patient type i being discharged from the hospital at decision epoch t
Action variables	
a_{ij}^{1t}	Increase amount of the capacity for treating patients of type i at hospital j at decision epoch t
$a_{ijj'}^{2t}$	Number of patients of type i transferred to location j' from location j at decision epoch t. If $i = 0$, it represents an empty ambulance travelling from j to j'
Other transitions-related variables	
B_{ijc}^t	If $s \geq 0$ represents the number of patients of type i heading to destination j who are c time units away. If $i = 0$, this represents an empty ambulance
AC_{ij}^t	Actual capacity for a patient of type i at hospital j at decision epoch t
n_i^t	Number of patients of type i waiting at the MCI site to be transferred to hospitals at decision epoch t
P_{ij}^t	Number of patients of type i located at hospital j at decision epoch t

State Transitions Once a decision is made at each decision epoch, new information, $Q^t = (\mu^t, \lambda^t)$, is realized where μ^t and λ^t denote the new demand (new patients) at hospitals and the MCI site, respectively. We assume that the distributions of each is known and that the probability for each patient type is independent of the others. The third source of uncertainty considered here is the number of patients who remain in the hospital by the next decision epoch. We assume this follows a binomial distribution: Binomial $\sim (min\{AC^t_{i,h}, P^t_{i,h}\}, 1 - prob^t_{i,h})$ where $prob^t_{i,h}$ represents the probability of discharge. Since μ^t, λ^t, $\hat{p}^t_{i,h}$ are independent events the joint probability $P\ (\lambda^t, \mu^t, \hat{p}^t)$ equals to $\Pi_{i,j,h}\ p(\lambda^t_i) \times p(\mu^t_{ij}) \times p(\hat{p}^t_{i,h})$. Below we define the transition of each state component.

—Patient waiting at the MCI site

$$n^{t+1}_i = n^t_i - \sum_{j'} a^{2t}_{iDj'} + \lambda^t_i \qquad \forall i \notin \{0\}, t \tag{4.8}$$

Equation (4.8) computes the number of new patients at the next decision epoch based on the number of patients remaining at period t ($n^t_i - \sum_{j'} a^{2t}_{iDj'}$) plus the new arrivals of patients of type i (λ^t_i).

—Patient Information at each hospital

$$P^{t+1}_{ij} = \hat{P}^t_{ij} + \mu^t_{ij} + B^t_{ij1} - \sum_{j':j'\neq j\in H} a^{2t}_{ijj'} \qquad \forall j \in H, t, i \tag{4.9}$$

$\hat{P}^t_{lj}$ represents a random variable following the binomial distribution explained earlier. According to Equation (4.9), the number of patients waiting to receive care at period $t+1$ is obtained based on the number of patients who remain at hospital $j \in H$ at period t plus new exogenous arrivals plus new patients who in period t were one period away from hospital j minus those patients transferred out of hospital j to other hospitals in the region in period t.

— The capacity of each Hospital

$$AC^{t+1}_{ij} = AC^t_{ij} + a^{1t}_{ij} \qquad \forall j \in H, t, i \tag{4.10}$$

On the RHS of Equation (4.10), a^{1t}_{ij} represents the amount of increase in capacity for a specific type of patient enacted in period t at hospital j.

—Patient transportation

$$B^{t+1}_{0j0} = B^t_{0j0} + \sum_i B^t_{ij1} - \sum_{i,j':j'\neq j\in R} a^{2t}_{i,j,j'} + \sum_{i,j':j'\neq j\in R} f(1,j,j') \times a^{2t}_{i,j',j} \qquad \forall t, j \in R \qquad (4.11)$$

Equation (4.11) controls the flow of available ambulances at each location. The number of empty ambulances at location j at time $t+1$ is determined by the number available at time t, (B^t_{0j0}), plus the number one time-unit distant from j at time t minus the number of ambulances sent from j to another location at time t. The last term represents the unlikely scenario where the distance between site j' and j is one unit and thus the decision to send an ambulance to j at time t results in an arrival to j at time unit $t+1$.

$$B^{t+1}_{ijc} = B^t_{ij,c+1} + \sum_{j':j'\neq j\in R} a^{2t}_{i,j',j} \times f(c+1,j,j') \qquad \forall c > 0, t, j \in R, i \qquad (4.12)$$

The number of ambulances moving through the network that are c time units away from their destination is computed by the Equation (4.12). The number of ambulances carrying a patient of type i that are c units away and heading toward site j at time $t+1$ is equal to the number of such vehicles that were $c+1$ units away in period t plus any ambulances dispatched at time t from j' to j and where the distance between j and j' is $c+1$.

The Reward/Cost Function. There are four components to our cost function - the cost associated with patients waiting at the MCI site, the cost associated with patients waiting for service at the hospitals, the cost of increasing the capacity and the cost associated with patients who remain unserved at the MCI region in the last decision epoch. Our cost function is defined by a non-linear cost function that captures the reality that increasing capacity is based on different strategies resulting in different costs to the system. We write the costs as

$$R_t(\vec{s^t}, \vec{a^{1t}}, \vec{a^{2t}}) =$$

$$\sum_{i,t}(n^t_i - \sum_{j'\in H} a^{2t}_{iDj'}) \times \Gamma(i,t) + \sum_{ji}(P^t_{ij} - \sum_{j':j'\neq j\in H} a^{2t}_{ijj'} - AC^t_{ij} - a^{1t}_{ij}) \times \theta(j,i,t)$$
$$+ \sum_{q=1,i,j}^{3} (w^t_{q,i,j} \times X^t_{q,i,j}) + \sum_i PE1^T_i \times n^T_i \qquad (4.13)$$

The first term penalizes the number of patients of type i who remain at the MCI site using a weight $\Gamma(i,t)$ while the second penalizes the number of patients waiting to receive treatment service at each hospital. If the difference between the number of patients at the hospital p^t_{ij} is greater than the sum of the number of patients leaving the hospital j and the amount of capacity increase at hospital j $(AC^t_{ij} + a^{1t}_{ij})$, a penalty of $\theta(i,j,t)$ is applied per patient. The third term in

(4.13) captures the cost related to the increase in capacity for a specific patient type i at hospital j. We impose a non-decreasing piece-wise linear function (W^t_{qij}) that imputes a cost depending on how much above the base capacity the current increase lies. To implement this we need to impose additional constraints:

$$\begin{aligned} AC^t_{ij} + a^{1t}_{ij} - BC_{ij} &= X^t_{1,ij} + X^t_{2,ij} + X^t_{3,ij} \\ X^t_{1,ij} &\leq BLC_{1,ij} \\ X^t_{2,ij} &\leq BLC_{2,ij} - BLC_{1,ij} \\ X^t_{3,ij} &\leq M_{ij} - BLC_{2,ij} \\ \forall i, j, t & \end{aligned} \tag{4.14}$$

where BC_{ij} is the base capacity at hospital j, M_{ij} is upper-bound capacity for each type of patient and $BLC_{1,ij},\ BLC_{2,ij}$ represent the levels of capacity that result in a different cost. For any value of $(AC^t_{ij} + a^{1t}_{ij} - BC_{ij} > 0)$, there is a non-decreasing cost w^t_{qij} associated with the increase for each level. Finally, the last term in our cost function penalizes if any patients are still at the MCI site and are not transferred to other hospitals at time t.

The Bellman Equation. The value function v_t of the proposed MDP specifies the minimum cost over the finite horizon for each state and satisfies the following optimality equations for all $(\vec{n}, \vec{p}, \vec{AC}, \vec{B}) \in S$:

$$v_t(S_t) = \min_{(a^{1t}, a^{2t})} \left(R_t(a^{1t}, a^{2t}) + \gamma \sum_{\vec{\lambda}', \vec{\mu}', \vec{\hat{p}}'} \left(p(\vec{\lambda}') \times p(\vec{\mu}') \times p(\vec{\hat{p}}') \right) \times v_{t+1}(s') \right) \qquad \forall t \backslash \{T\} \tag{4.15}$$

$$v_T(s) \leq R_T(s) \qquad \forall s \tag{4.16}$$

$$s.t. \quad (4.1) - (4.13) \quad and \quad (4.15)$$

where γ is the discount factor and s' indicates the future state $s' \in S_t$. Based on the constraints provided earlier, the future state can be written in terms of the current state and action to yield:

$$v_{t+1}(s') = v_{t+1}\left(n^t_i - \sum_{j'} a^{2t}_{iDj'} + \lambda^t_i, \hat{p}^t_{ij} + \mu^t_{ij} + B^t_{ij1} - \sum_{j'} a^{2t}_{ijj'}, AC^t_{ij} + a^{1t}_{ij}, \psi_s \right)$$

where

$$\psi_s = \begin{cases} B^t_{0j0} + \sum_i B^t_{ij1} - \sum_{i,j':j' \neq j \in R} a^{2t}_{i,j,j'} + \sum_{i,j':j' \neq j \in R} f(1,j,j') \times a^{2t}_{i,j',j} & \text{if } c = 0 \\ B^t_{ij,c+1} + \sum_{j':j' \neq j \in R} a^{2t}_{i,j',j} \times f(c+1,j,j') & \text{if } c > 0. \end{cases} \tag{4.17}$$

4.4 Approximate Dynamic Programming

One of the well-known and developing methods for addressing the curse of dimensionality in the MDP literature is approximate dynamic programming (ADP). The curse of dimensionality refers to the common challenge that as the number of state-action pairs increases, solving the model and deriving good policies becomes computationally more challenging. ADP restricts the value function to a specified class of functions and then seeks to find the optimal value function within this class. Employing such an approach does have its challenges, including determining the best class of functions to use for a given problem, determining the optimal approximation within a chosen class of functions and bounding the gap between the cost of the policy determined by the approximate solution and the true cost had we been able to determine the optimal policy.

While we adopt the LP approach to ADP, other approaches to tackling the curse of dimensionality include both simulation and analytical approaches. Simulation-based solutions generate sample paths of the problem and seek to iteratively update the parameters that determine the chosen class of functions. Such methods suffer from the fact that not only is the true value function approximated but an additional source of approximation is introduced through sampling error. Furthermore, as stated by Sauré et al. [32], each solution approach has its advantages and disadvantages. These approaches differ in speed of convergence and their suitability for different problems. For instance, the slow speed of simulation is its main drawback while the linear programming approaches are mostly limited to afine approximation architectures. The main advantage of the latter is that they avoid the need for iterative learning and often provide good results. In their study, Sauré et al. [32] presented a list of ADP applications classified by type of problem and approach (simulation-based and linear programming).

In this research, we focus on an analytical solution developed by several authors [1, 33, 5, 6, 25]. However, the developed approaches are more suitable to infinite-horizon MDP models. As our model is a finite-horizon MDP, we draw from the recent work by Bhattacharya and Kharoufeh [4]. Bhattacharya and Kharoufeh [4] establish lower and upper bounds of the value functions to formulate the primal LP model. The solution of this LP model is the value function of the MDP model, while the solution of its dual problem recovers the optimal policy. They assert that although the LP approach does not (in and of itself) overcome the curses of dimensionality, it lays the groundwork for implementing ALP procedures to solve computationally intractable finite-horizon models. They also suggest an ALP formulation that utilizes parametric or affine basis functions to approximate the value functions at each decision epoch. In light of recent advances in LP solvers, the ALP approach offers computational advantages over traditional MDP solution procedures (such as the value and policy iteration algorithms) for solving high-dimensional finite horizon problems.

—Transforming MDP into its equivalent Approximate linear formulation

The solution approach proceeds as follows:

1. Transform the MDP into its equivalent LP.
2. Approximate the value function by assuming a specific parameterized form.
3. Use the chosen approximation in the LP to create the ALP.
4. Solve the ALP to obtain the optimal linear value function approximation, v_{ALP}.
5. Use v_{ALP} to determine the "best" action for any visited state.

As highlighted by Bhattacharya and Kharoufeh [4], solving the optimality Equations (4.15), (4.16), and (4.17) is equivalent to solving the following LP for any strictly positive α_t:

$$\max_{\vec{v_t}} \sum_{(\vec{n},\vec{p},\vec{AC},\vec{B})\in S} \alpha_t(S) v_t(S)$$

$$R_t(a^{1t}, a^{2t}) + \gamma \sum_{\vec{\lambda}',\vec{\mu}',\vec{\hat{p}}'} \big(p(\vec{\lambda}') \times p(\vec{\mu}') \times p(\vec{\hat{p}}')\big) v_{t+1}\Bigg(n_i^t - \sum_{j'} a_{iDj'}^{2t} + \lambda_i^t, \quad \hat{p}_{ij}^t + \mu_{ij}^t + B_{ij1}^t - \sum_{j'} a_{ijj'}^{2t},$$

$$AC_{ij}^t + a_{ij}^{1t}, B_{0j0}^t + \sum_i B_{ij1}^t - \sum_{i,j':j'\neq j\in R} a_{i,j,j'}^{2t} + \sum_{i,j':j'\neq j\in R} f(1,j,j') \times a_{i,j',j}^{2t},$$

$$B_{ij,c+1}^t + \sum_{j':j'\neq j\in R} a_{i,j',j}^{2t} \times f(c+1,j,j')\Bigg) \geq v_t(S)$$

$$\forall(\vec{a^{1t}}, \vec{a^{2t}}) \in A \ \ and \ \ (\vec{n},\vec{p},\vec{AC},\vec{B}) \in S \ \ and \ \ t\backslash\{T\}$$

$$v_T(s) \leq R_T(s) \qquad \forall s \tag{4.18}$$

As theorized and demonstrated by Bhattacharya and Kharoufeh [4] for a finite-horizon MDP model, we assume that α_t is any positive, bounded vector of real values for different decision epochs $t \in T$ and states $s \in S_t$. Solving the LP however may be impossible given the number of states and actions. A possible solution is to approximate the value function, v, with a linear combination of

basis functions. A reasonable starting point in our model is the following affine approximation.

$$
\begin{aligned}
v_t(S) = W^t_{(0)} + \sum_i n^t_i \times W^t_{(1)i} + \sum_{ij} P^t_{ij} \times W^t_{(2)ij} + \sum_{ij} AC^t_{ij} \times W^t_{(3)ij} + \\
\sum_j B^t_{0j0} \times W^t_{(4)0j0} + \sum_{ij,c>0} B^t_{ijc} \times W^t_{(4)ijc} \qquad \forall t \backslash \{T\} \\
v_T(S) = W^T_{(0)} + \sum_i n^T_i \times W^T_{(1)i} + \sum_{ij} P^T_{ij} \times W^T_{(2)ij} + \sum_{ij} AC^T_{ij} \times W^T_{(3)ij} + \\
\sum_{0j} B^T_{0j0} \times W^T_{(4)0j0} + \sum_{ij,c>0} B^T_{ijc} \times W^T_{(4)ijc} \qquad (4.19)
\end{aligned}
$$

where $W^t_{(0)}, W^t_{(1)i}, W^t_{(2)ij}, W^t_{(3)ij}, W^t_{(4)ij0}$ are marginal costs and we impose restrictions that $W^t_{(1)i}$, $W^t_{(2)ij}$, $W^t_{(3)ij}$ are nonnegative, whereas $W^t_{(0)}$ and $W^t_{(4)ij0}$ are unconstrained. They are marginal costs on the state variables n^t_i, P^t_{ij}, AC^t_{ij}, and B^t_{ijc}, respectively. The reason for making the $W^t_{(4)ij0}$ unconstrained comes from the fact that the marginal cost of an empty vehicle returning to the MCI is likely negative, meaning there is a net benefit to having an ambulance return to retrieve more patients. Therefore, it is clear why we impose restrictions on the other three approximation parameters to be positive since it does not benefit the system to have any patient remain unserved at the MCI site and hospitals over time. Reformulating the LP in terms of this approximate value function yields the following ALP:

$$
\begin{aligned}
&\max_{\vec{W}} \sum_{(\vec{n},\vec{p},\vec{AC},\vec{B}) \in S} \alpha_t(S) \Bigg(W^t_{(0)} + \sum_i n^t_i \times W^t_{(1)i} + \sum_{ij} P^t_{ij} \times W^t_{(2)ij} + \\
&\sum_{ij} AC^t_{ij} \times W^t_{(3)ij} + \sum_{ij} B^t_{0j0} \times W^t_{(4)0j0} + \sum_{ij,c>0} B^t_{ijc} \times W^t_{(4)ijc} \Bigg)
\end{aligned}
$$

$$
\begin{aligned}
&R_t(a^{1t}, a^{2t}) \geq \Bigg(W^t_{(0)} + \sum_i n^t_i \times W^t_{(1)i} + \sum_{ij} P^t_{ij} \times W^t_{(2)ij} + \sum_{ij} AC^t_{ij} \times W^t_{(3)ij} + \\
&\sum_j B^t_{0j0} \times W^t_{(4)0j0} + \sum_{ij,c>0} B^t_{ijc} \times W^t_{(4)ijc} \Bigg) -
\end{aligned}
$$

$$\gamma \sum_{\vec{\lambda}',\vec{\mu}',\vec{p}'} (p(\vec{\lambda}')p(\vec{\mu}')\vec{p}') \left(W_{(0)}^{t+1} + \sum_i \left(n_i^t - \sum_{j'} a_{iDj'}^{2t} + \lambda_i^t \right) \times W_{(1)i}^{t+1} \; + \right.$$
$$\sum_{ij} \left(\hat{p}_{ij}^t + \mu_{ij}^t + B_{ij1}^t - \sum_j a_{ijj'}^{2t} \right) \times W_{(2)ij}^{t+1} \; +$$
$$\sum_{ij} \left(AC_{ij}^t + a_{ij}^{1t} \right) \times W_{(3)ij}^{t+1} \; +$$
$$\sum_j \left(B_{0j0}^t + \sum_i B_{ij1}^t - \sum_{i,j':j'\neq j\in R} a_{i,j,j'}^{2t} + \sum_{i,j':j'\neq j\in R} f(1,j,j') \times a_{i,j',j}^{2t} \right) \times W_{(4)0j0}^{t+1} +$$
$$\left. \sum_{ij,c>0} \left(B_{ij,c+1}^t + \sum_{j':j'\neq j\in R} a_{i,j',j}^{2t} \times f(c+1,j,j') \right) \times W_{(4)ijc}^{t+1} \right)$$

$$\forall (a^{\vec{1}t}, a^{\vec{2}t}) \in A \;\; and \;\; (\vec{n},\vec{p},\vec{AC},\vec{B}) \in S, \vec{W}, t\backslash\{T\}$$

$$W_{(0)}^T + \sum_i n_i^T \times W_{(1)i}^T + \sum_{ij} P_{ij}^T \times W_{(2)ij}^T + \sum_{ij} AC_{ij}^T \times W_{(3)ij}^T + \sum_j B_{0j0}^T \times W_{(4)0j0}^T +$$
$$\sum_{ij,c>0} B_{ijc}^T \times W_{(4)ijc}^T \leq R_T(s) \qquad \forall \;\; s \tag{4.20}$$

Rearranging terms and using the assumption that α_t is a probability distribution transforms the ALP into:

$$\max_{\vec{W}} \left(W_{(0)}^t + \sum_i E_\alpha[n_i^t] \times W_{(1)i}^t + \sum_{ij} E_\alpha[P_{ij}^t] \times W_{(2)ij}^t + \right.$$
$$\left. \sum_{ij} E_\alpha[AC_{ij}^t] \times W_{(3)ij}^t + \sum_j E_\alpha[B_{0j0}^t] \times W_{(4)0j0}^t + \sum_{ij,c>0} E_\alpha[B_{ijc}^t] \times W_{(4)ijc}^t \right)$$

$$(W_{(0)}^t - \gamma W_{(0)}^{t+1}) + \sum_i \left(n_i^t \times W_{(1)i}^t - \gamma \left[n_i^t - \sum_{j'} a_{iDj'}^{2t} + E(\lambda_i^t) \right] \times W_{(1)i}^{t+1} \right)$$
$$+ \sum_{ij} \left(P_{ij}^t \times W_{(2)ij}^t - \gamma \left[\hat{p}_{ij}^t + \mu_{ij}^t + B_{ij1}^t - \sum_j a_{ijj'}^{2t} \right] \times W_{(2)ij}^{t+1} \right)$$
$$+ \sum_{ij} \left(AC_{ij}^t \times W_{(3)ij}^t - \gamma \left[AC_{ij}^t + a_{ij}^{1t} \right] \times W_{(3)ij}^{t+1} \right)$$
$$+ \sum_j \left(B_{0j0}^t \times W_{(4)0j0}^t - \gamma \left[B_{0j0}^t + \sum_i B_{ij1}^t - \sum_{i,j':j'\neq j\in R} a_{i,j,j'}^{2t} + \sum_{i,j':j'\neq j\in R} f(1,j,j') \times a_{i,j',j}^{2t} \right] \times W_{(4)0j0}^{t+1} \right)$$
$$+ \sum_{ij,c>0} \left(B_{ijc}^t \times W_{(4)ijc}^t - \gamma \left[B_{ij,c+1}^t + \sum_{j':j'\neq j\in R} a_{i,j',j}^{2t} \times f(c+1,j,j') \right] \times W_{(4)ijc}^{t+1} \right) \leq R_t(a^{1t}, a^{2t})$$
$$\forall t\backslash\{T\}, W \geq 0$$

$$W^T_{(0)} + \sum_i n^T_i \times W^T_{(1)i} + \sum_{ij} P^T_{ij} \times W^T_{(2)ij} + \sum_{ij} AC^T_{ij} \times W^T_{(3)ij} + \sum_{ij} B^T_{ij0} \times W^T_{(4)ij0} +$$
$$\sum_{ij,c>0} B^T_{ijc} \times W^T_{(4)ijc} \leq R_T(s)$$
$$\forall s \tag{4.21}$$

4.5 Proposed two-phase solution algorithm

Although the ALP has around $1 + I(1 + J(2 + C))$ variables for each decision epoch, the number of constraints remains intractable. Thus, to employ step five of the proposed solution method (Section 4.5), we use a two-phase algorithm applying column generation to solve the dual. We, therefore, formulate the dual of the ALP:

$$\min_{\vec{\phi}} \sum_{(S,A)} \phi^t(S,A) R_t(\vec{a^{1t}}, \vec{a^{2t}})$$
$$\sum_{(S,A)} \phi^1(S,A) = 1$$
$$\sum_{(S,A)} \phi^1(S,A) \times n_{i,1} \geq E_\alpha[n^1_i]$$
$$\sum_{(S,A)} \phi^1(S,A) \times P^1_{ij} \geq E_\alpha[P^1_{ij}]$$
$$\sum_{(S,A)} \phi^1(S,A) \times AC^1_{ij} \geq E_\alpha[AC^1_{ij}]$$
$$\sum_{(S,A)} \phi^1(S,A) \times B^1_{ijc} \geq E_\alpha[B^1_{ijc}]$$
$$\forall t = 1 \tag{4.22}$$

$$\sum_{(S,A)} \phi^t(S,A) - \gamma \times \sum_{(S,A)} \phi^{t-1}(S,A) = 1$$
$$\sum_{(S,A)} \left(\phi^t(S,A) \times n^t_i - \phi^{t-1}(S,A) \left[\gamma \times \left(n^{t-1}_i + E(\lambda^{t-1}_i) - \sum_{j'} a^{2,t-1}_{iDj'} \right) \right] \right) \geq E_\alpha[n^t_i]$$
$$\sum_{(S,A)} \left(\phi^t(S,A) \times P^t_{ij} - \phi^{t-1}(S,A) \left[\gamma \times \left(\hat{p}^{t-1}_{ij} + \mu^{t-1}_{ij} + B^{t-1}_{ij1} - \sum_{j} a^{2,t-1}_{ijj'} \right) \right] \right)$$
$$\geq E_\alpha[P^t_{ij}]$$
$$\sum_{(S,A)} \left(\phi^t(S,A) \times AC^t_{ij} - \phi^{t-1}(S,A) \left[\gamma \times \left(AC^{t-1}_{ij} + a^{1,t-1}_{ij} \right) \right] \right) \geq E_\alpha[AC^t_{ij}]$$

$$\sum_{(S,A)}\left(\phi^t(S,A)\times B^t_{0j0}-\phi^{t-1}(S,A)\left[\gamma\times\left(B^{t-1}_{0j0}+\sum_i B^{t-1}_{ij1}-\sum_{\substack{j':j'\neq j\in R\\ i}} a^{2,t-1}_{i,j,j'}+\sum_{\substack{j':j'\neq j\in R\\ i}} f(1,j,j')\times a^{2,t-1}_{i,j',j}\right)\right]\right)$$

$$\geq E_\alpha[B^t_{0j0}]$$

$$\sum_{(S,A)}\left(\phi^t(S,A)\times B^t_{ijc}-\phi^{t-1}(S,A)\left[\gamma\times\left(B^{t-1}_{ij,c+1}+\sum_{j':j'\neq j\in R} a^{2,t-1}_{i,j',j}\times f(c+1,j,j')\right)\right]\right)\geq E_\alpha[B^t_{ijc}]$$

$$\forall\phi\geq 0, i, j, c, t>1 \tag{4.23}$$

where ϕ denotes the dual variable.

Column generation solves this problem by starting with a small set $S^{'}$ of state-action pairs to the dual and then (using dual prices as estimates for $W^t_{(0)}, W^t_{(1)i}, W^t_{(2)ij}, W^t_{(3)ij}$, and $W^t_{(4)ij0}$) finding one or more violated constraints in the primal. It then adds the state-action pair(s) associated with these violated constraints into the set $S^{'}$ before re-solving the dual. The process iterates until no primal constraint is violated or one is "close enough" to optimality to quit. In general, it may be challenging to find an initial feasible set $S^{'}$ and to find a violated primal constraint. Finding a most violated primal constraint involves solving the following integer program (the subproblem):

$$\begin{aligned}
Z(\vec{W}) = \min_{\vec{n},\vec{p},\vec{AC},\vec{B},a^{1t},a^{2t}} \Bigg[& R_t(a^{1t},a^{2t})- \\
& \left(W^{t=1}_{(0)}\right)-\sum_i\left(n^{t=1}_i\times W^{t=1}_{(1)i}\right)-\sum_{ij}\left(P^{t=1}_{ij}\times W^{t=1}_{(2)ij}\right)-\sum_{ij}\left(AC^{t=1}_{ij}\times W^{t=1}_{(3)ij}\right)- \\
& \sum_j\left(B^{t=1}_{0j0}\times W^{t=1}_{(4)0j0}\right)-\sum_{ij,c>0}\left(B^{t=1}_{ijc}\times W^{t=1}_{(4)ijc}\right)-
\end{aligned} \tag{4.24}$$

$$\begin{aligned}
& \sum_i\left(n^t_i\times W^t_{(1)i}-\gamma\left[n^t_i-\sum_{j'}a^{2t}_{iDj'}+E(\lambda^t_i)\right]\times W^{t+1}_{(1)i}\right)- \\
& \sum_{ij}\left(P^t_{ij}\times W^t_{(2)ij}-\gamma\left[\hat{p}^t_{ij}+\mu^t_{ij}+B^t_{ij1}-\sum_j a^{2t}_{ijj'})\right]\times W^{t+1}_{(2)ij}\right)- \\
& \sum_{ij}\left(AC^t_{ij}\times W^t_{(3)ij}-\gamma\left[AC^t_{ij}+a^{1t}_{ij}\right]\times W^{t+1}_{(3)ij}\right)- \\
& \sum_j\left(B^t_{0j0}\times W^t_{(4)0j0}-\gamma\left[B^t_{0j0}+\sum_i B^t_{ij1}-\sum_{\substack{j':j'\neq j\in R\\ i}} a^{2t}_{i,j,j'}+\sum_{\substack{j':j'\neq j\in R\\ i}} f(1,j,j')\times a^{2t}_{i,j',j}\right]\times W^{t+1}_{(4)0j0}\right)- \\
& \sum_{ij,c>0}\left(B^t_{ijc}\times W^t_{(4)ijc}-\gamma\left[B^t_{ij,c+1}+\sum_{j':j'\neq j\in R} a^{2t}_{i,j',j}\times f(c+1,j,j')\right)\right]\times W^{t+1}_{(4)ijc}\Bigg)- \\
& \left(W^t_{(0)}-\gamma W^{t+1}_{(0)}\right)
\end{aligned}$$

$$\forall t>1\backslash\{T\}$$

$$- \left(W_{(0)}^{t=T} \right) - \sum_{i} \left(n_i^{t=T} \times W_{(1)i}^{t=T} \right) - \sum_{ij} \left(P_{ij}^{t=T} \times W_{(2)ij}^{t=T} \right) - \sum_{ij} \left(AC_{ij}^{t=T} \times W_{(3)ij}^{t=T} \right) -$$

$$\sum_{j} \left(B_{0j0}^{t=T} \times W_{(4)0j0}^{t=T} \right) - \sum_{ij,c>0} \left(B_{ijc}^{t=T} \times W_{(4)ijc}^{t=T} \right) \tag{4.25}$$

$$s.t. \quad (1) - (13) \quad and \quad (15). \tag{4.26}$$

As indicated in Equations (4.24), (4.25), and (4.26), due to non-dependency of the initial state for $t = 1$ and $t = T$ to action variables, the sub-problem is divided into four parts: reward function, approximation parameters for $t = 1$, $t > 1$ and $t < T$, and the last period $t = T$ only, respectively. In the following, the steps of the proposed two-step solution algorithm are described.

Description of the proposed two-phase Algorithm

We start the algorithm by solving the dual of Equation (4.21), shown in Equation (4.22), using the column generation, where $\phi^t(S, A)$ represents the dual variable associated with the state-action pair $(\vec{s_t}, \vec{a_t})$. The corresponding pseudo-code is provided below in Algorithm 1. To determine the next state-action pair to include in the formulation of (4.22) in each iteration of the column generation algorithm, the linear programming model (4.23) is solved.

Algorithm 1 Column generation.

1: Obtain an initial set of feasible state-action pairs $\rho = 1, ..., P$ using the proposed phase 1 approach described in Algorithm 2.
2: Define variables $Sol(t)$ and $r = min_t Sol(t)$ and set the variable $Sol(t) = 0$.
3: **While** $r < 10^{-4} \ \ \forall t \in T$ **do**
4: Solve $Z_{masterproblem}$(4.23), that only considers the current set of columns P.
5: Determine $W_{(0)}^t, W_{(1)i}^t, W_{(2)ij}^t, W_{(3)ij}^t, W_{(4)ij0}^t$ as the shadow prices of the corresponding dual constraints.
6: **For** t**=1 to** T
7: Solve $Z_t subproblem$(4.26) using current shadow prices and store the optimum objective in $Sol(t) = Z_t subproblem$.
8: **If** $Sol(t) < 10^{-4}$ **then**
9: Compute the state-action pair that generates $Sol(t)$.
10: Compute $R_t(\vec{s}, \vec{a})$ and coefficients of $\phi^t(S, A)$ (4.23), and consider it a column.
11: Update P by adding the column just obtained.
12: **end if**
13: **end while**

The first step of the column generation algorithm is to obtain an initial set of feasible state-action pairs ρ using the phase 1 approach described in Algorithm 2. This approach involves a similar iterative process, but with models (4.27) and (4.29) instead, until a feasible solution to (4.22) is found. In other words, the phase 1 algorithm iterates until all the slack variables $\zeta_i^{2,t}, \zeta_{ij}^{3,t}, \zeta_{ij}^{4,t}, \zeta_{ijc}^{5,t}$ in (4.27) are equal to zero.

$$\min_{\phi \vec{\geq} 0, sl \vec{\geq} 0} \sum_{i,t} \zeta_i^{2,t} + \sum_{i,j,t} \zeta_{ij}^{3,t} + \sum_{i,j,t} \zeta_{ij}^{4,t} + \sum_{i,j,c,t} \zeta_{ijc}^{5,t}$$

$$\sum_{(S,A)} \phi^1(S,A) = 1$$

$$\sum_{(S,A)} \phi^1(S,A) \times n_{i,1} + \zeta_i^{2,t} \geq E_\alpha[n_i^1]$$

$$\sum_{(S,A)} \phi^1(S,A) \times P_{ij}^1 + \zeta_{ij}^{3,t} \geq E_\alpha[P_{ij}^1]$$

$$\sum_{(S,A)} \phi^1(S,A) \times AC_{ij}^1 + \zeta_{ij}^{4,t} \geq E_\alpha[AC_{ij}^1]$$

$$\sum_{(S,A)} \phi^1(S,A) \times B_{ij0}^1 + \zeta_{ij0}^{5,t} - \zeta_{ij0}^{5,t} \geq E_\alpha[B_{ij0}^1]$$

$$\sum_{(S,A)} \phi^1(S,A) \times B_{ij,c>1}^1 + \zeta_{ij,c>1}^{5,t} \geq E_\alpha[B_{ij,c>1}^1]$$

$$\forall \phi \geq 0, t = 1, i, j, c$$

$$\sum_{(S,A)} \phi^t(S,A) - \gamma \times \sum_{(S,A)} \phi^{t-1}(S,A) = 1$$

$$\sum_{(S,A)} \left(\phi^t(S,A) \times n_i^t - \phi^{t-1}(S,A) \left[\gamma \times \left(n_i^{t-1} + E(\lambda_i^{t-1}) - \sum_{j'} a_{iDj'}^{2,t-1} \right) \right] \right) + \zeta_i^{2,t} \geq E_\alpha[n_i^t]$$

$$\sum_{(S,A)} \left(\phi^t(S,A) \times P_{ij}^t - \phi^{t-1}(S,A) \left[\gamma \times \left(\hat{p}_{ij}^{t-1} + \mu_{ij}^{t-1} + B_{ij1}^{t-1} - \sum_{j} a_{ijj'}^{2,t-1} \right) \right] \right)$$

$$+ \zeta_{ij}^{3,t} \geq E_\alpha[P_{ij}^t]$$

$$\sum_{(S,A)} \left(\phi^t(S,A) \times AC_{ij}^t - \phi^{t-1}(S,A) \left[\gamma \times \left(AC_{ij}^{t-1} + a_{ij}^{1,t-1} \right) \right] \right) + \zeta_{ij}^{4,t} \geq E_\alpha[AC_{ij}^t]$$

$$\sum_{(S,A)} \left(\phi^t(S,A) \times B_{0j0}^t - \phi^{t-1}(S,A) \left[\gamma \times \left(B_{0j0}^{t-1} + \sum_i B_{ij1}^{t-1} - \sum_{\substack{j':j' \neq j \in R \\ i}} a_{i,j,j'}^{2,t-1} + \sum_{\substack{j':j' \neq j \in R \\ i}} f(1,j,j') \times a_{i,j',j}^{2,t-1} \right) \right] \right)$$

$$+ \zeta_{0j0}^{5,t} - \zeta_{0j0}^{5,t} \geq E_\alpha[B_{0j0}^t]$$

$$\sum_{(S,A)} \left(\phi^t(S,A) \times B_{ijc}^t - \phi^{t-1}(S,A) \left[\gamma \times \left(B_{ij,c+1}^{t-1} + \sum_{j':j' \neq j \in R} a_{i,j',j}^{2,t-1} \times f(c+1,j,j') \right) \right] \right) + \zeta_{ij,c>1}^{5,t} \geq E_\alpha[B_{ijc}^t]$$

$$\forall \phi \geq 0, i, j, c, t > 1 \tag{4.27}$$

Algorithm 2 Phase 1 approach for obtaining a small set of initial columns.

1: Start with the set of state-action pairs as $\rho = \emptyset$

2: **While** $z_{masterPhase1} > 0$ **do**

3: Solve (4.27) and store the optimum objective value in z_{master}.

4: Determine $W^t_{(0)}, W^t_{(1)i}, W^t_{(2)ij}, W^t_{(3)ij}, W^t_{(4)ij0}$ as the shadow prices of the corresponding dual constraints.

5: **If** $z_{masterPhase1} = 0$ **then**

6: **Go to the Step 1, Algorithm 1.**

7: **Else**

8: **For** t**=1 to** T

9: Solve (4.29) using the current shadow prices..

10: Compute the state-action pair obtained as the optimal solution.

11: Compute $R_t(\vec{s}, \vec{a})$ and coefficients of $\phi^t(S, A)$ (4.23), and consider it a column.

12: Update P by adding the column just obtained.

13 Solve (4.27), and store the optimum value of that solved in z_{master}.

14: **end while**

$$
\begin{aligned}
Z(\vec{W}) = \max_{\vec{n},\vec{p},\vec{AC},\vec{B},a^{1t},a^{2t}} \;
&\left(W^{t=1}_{(0)}\right) + \sum_i \left(n^{t=1}_i \times W^{t=1}_{(1)i}\right) + \sum_{ij} \left(P^{t=1}_{ij} \times W^{t=1}_{(2)ij}\right) + \sum_{ij} \left(AC^{t=1}_{ij} \times W^{t=1}_{(3)ij}\right) + \\
&\sum_j \left(B^{t=1}_{0j0} \times W^{t=1}_{(4)0j0}\right) + \sum_{ij,c>0} \left(B^{t=1}_{ijc} \times W^{t=1}_{(4)ijc}\right) + \\
&\sum_i \left(n^t_i \times W^t_{(1)i} - \gamma\left[n^t_i - \sum_{j'} a^{2t}_{iDj'} + E(\lambda^t_i)\right] \times W^{t+1}_{(1)i}\right) + \\
&\sum_{ij} \left(P^t_{ij} \times W^t_{(2)ij} - \gamma\left[\hat{p}^t_{ij} + \mu^t_{ij} + B^t_{ij1} - \sum_j a^{2t}_{ijj'})\right] \times W^{t+1}_{(2)ij}\right) + \\
&\sum_{ij} \left(AC^t_{ij} \times W^t_{(3)ij} - \gamma\left[AC^t_{ij} + a^{1t}_{ij}\right] \times W^{t+1}_{(3)ij}\right) + \\
&\sum_j \left(B^t_{0j0} \times W^t_{(4)0j0} - \gamma\left[B^t_{0j0} + \sum_i B^t_{ij1} - \sum_{\substack{j':j'\neq j\in R \\ i}} a^{2t}_{i,j,j'} + \sum_{\substack{j':j'\neq j\in R \\ i}} f(1,j,j') \times a^{2t}_{i,j',j}\right] \times W^{t+1}_{(4)0j0}\right) + \\
&\sum_{ij,c>0} \left(B^t_{ijc} \times W^t_{(4)ijc} - \gamma\left[B^t_{ij,c+1} + \sum_{j':j'\neq j\in R} a^{2t}_{i,j',j} \times f(c+1,j,j')\right)\right] \times W^{t+1}_{(4)ijc}\Bigg) + \\
&\left(W^t_{(0)} - \gamma W^{t+1}_{(0)}\right) \\
&\forall t > 1 \backslash \{T\}
\end{aligned}
$$

$$+\left(W_{(0)}^{t=T}\right)+\sum_{i}\left(n_{i}^{t=T}\times W_{(1)i}^{t=T}\right)+\sum_{ij}\left(P_{ij}^{t=T}\times W_{(2)ij}^{t=T}\right)+\sum_{ij}\left(AC_{ij}^{t=T}\times W_{(3)ij}^{t=T}\right)+$$

$$\sum_{j}\left(B_{0j0}^{t=T}\times W_{(4)0j0}^{t=T}\right)+\sum_{ij,c>0}\left(B_{ijc}^{t=T}\times W_{(4)ijc}^{t=T}\right) \tag{4.28}$$

$$s.t. \quad (1)-(13) \quad and \quad (15). \tag{4.29}$$

4.6 Implementation and evaluation

To benchmark the performance of the proposed model, we compare the model's results in different scenarios. In addition, we evaluate the model's performance for a real case study based on data from the Bus Crash in 2019 in Ottawa, Canada. The study seeks to evaluate the performance of the integrated casualty transportation and hospital capacity planning model and solution approach under low and fully congested systems and with multiple sources of uncertainty. The model was coded in GAMS 24.1.2 with CPLEX as Solver. The coded model is executed on a system with windows 10 pro 64-bit Core i7-8565U 2.4 GHz PC with 16 G.

4.6.1 Case Problem

This section begins with a description of a recent MCI event that we use to help frame our numerical analysis. The data is gathered from different sources in the literature [10, 28] and experts' opinions.

At 3:50 pm EST, on January 11, 2019, an OC Transpo bus operating on route 269 to Kanata crashed on approach to Westboro Station in the city of Ottawa, leaving 18 patients with severe and critical injuries. Additional injuries came to light after a few hours of relief operations. As a result, the Ottawa Hospital declared a Code Orange—a code reserved for disasters and other major events with a significant number of serious injuries. The last Code Orange occurred in September 2013 when a VIA Rail train collided with an OC Transpo bus. There are four main hospitals in the city of Ottawa, the Ottawa hospital (General, Civic and Riverside campuses), Children Hospital of Eastern Ontario (CHEO), Queensway-Carleton Hospital, and Montfort Hospital. As the Ottawa Hospital serves as the regional trauma centre for Eastern Ontario, all the injured people in the bus crash were transferred to either the General or Civic campuses of the Ottawa Hospital. The emergency department of the Ottawa Hospital organized eight trauma teams, each of which featured two or three nurses, a respiratory therapist, an anaesthetist, an emergency physician, a trauma resident, an orthopaedic surgeon, a vascular surgeon and a trauma team leader. The General campus typically has one such trauma team in operation. A typical Trauma Center at the Civic campus handles about three to four seriously injured patients at any given moment. The Ottawa Hospital confirmed shortly after 8 p.m. that it received 12 patients at its Civic Campus

Table 4.4: The distance (in minutes) between the MCI site and the Ottawa Hospital General and Civic Campuses.

Location	MCI site	General Campus	Civic Campus
MCI site	-	30	20
General Campus	30	-	20
Civic Campus	20	20	-

and six patients at the General Campus following the crash [2].

4.6.1.1 Data

Here, we separate the data into two parts, the first part comes from the historical data, and the second part is estimated as the actual data was unavailable.

Historical data - Real data

This study consists of one MCI site (Westboro Bus Station in Ottawa) and two Ottawa Hospital campuses; General and Civic. To be aligned with the real bus crash event, the other hospitals in the Ottawa region are not included in this study since the patients were only transferred to only the aforementioned campuses. The City of Ottawa Disaster Operations Center employed five paramedic ambulances with a capacity of one patient on each trip. As it took the paramedic response team approximately five hours to respond to the Westboro event, the planning horizon is set at 5 hours or 30 periods of 10-minute intervals. As reported by the Ottawa Hospital, there were two types of injured people in the bus crash case in Ottawa; hence, we consider two types of patients (severely injured, type 1, and moderately injured, type 2).

Estimated data - Other resources

The data here is gathered and estimated from various sources such as similar MCI events, experts' opinions, etc.

Regarding travel times, the actual distances in time units based on Google Maps are provided in Table 4.4. It should be noted that the travel times here consider the boarding/alighting, dwell time, and time impedance factors too which is why the values given in Table 4.4 are higher than the real Google Map travel times. We assume the base capacity of each campus is ten trauma care unit beds for each type of patient. Two capacity increases of 5 are assumed to be possible (from 10 to 15 and from 15 to 20). The capacity increase function is assumed to be a piece-wise linear function in which the system incurs a fixed cost for each increase level from the base capacity of each campus. Unfortunately no information was available on capacity increase costs at the Ottawa Hospital. We assume an average arrival rate of new demand to each hospital of two patients of types 1 and 2 per decision epoch. The capacity expansion rate of each hospital campus is assumed to be 20 %, with a probability of patient discharge [2] of 10 %.

[3]Hospital discharge rates measure the number of patients who leave a hospital after receiving care.

Table 4.5: Multiple sources of costs (penalties in dollar units) for the case study.

Source of cost		General Campus	Civic Campus
Capacity increase cost ($w^t_{q,i,j}$)	1st level of capacity increase	5	5
	2nd level of capacity increase	25	50
Patient waiting at each hospital ($\theta(j,i,t)$)		20	20
Patient waiting at the MCI site ($\Gamma(i,t)$)		100	100

As stated earlier, the various costs incurred to the system arise from multiple sources: the number of patients waiting to receive care at each hospital, the number of patients waiting at the MCI site, and the amount of capacity increase at each hospital. The details of such costs are given in Table 4.5. Recall that the RHS values (the expected parameters over α_t distribution) used in the master problem in Equations (4.22) and (4.23) are arbitrary and must be chosen by the user. We carefully tuned them for each decision epoch. For the number of patients waiting at the MCI, the expected value is set to 18 initially for period $t = 1$; however, it decreases over time as more injured people are transferred to the hospitals at the following decision epochs. For the average value related to the actual capacity of hospitals and the number of patients waiting at the hospitals, we fix them to a constant (i.e., 10 and 0.5 or 1, respectively). This is justified by the fact that the hospitals have a specific level of capacity to serve patients. Finally, there are a lot of indices related to the location of vehicles so tuning them is very challenging. As a result, we set it to a small constant (i.e., 0.05) to force the model to give values to the relevant approximation parameters. Note that while these values are arbitrary, past experiences suggests that a good choice is one that represents an initial system that is quite congested.

Later, in Section 4.6.4, we study the performance of the model under various scenarios reflecting a full and low-congested system.

4.6.2 Results and Sensitivity analysis

To test the ability of the proposed integrated casualty transportation and hospital capacity planning model to generate good policies, we develop realistic MCI scenarios based on the bus crash case study. The scenarios are developed to reflect varying levels of possible congestion from a low-congested to a fully-congested system in different parts of the emergency network (the MCI site and hospitals) under various sources of uncertainty (the number of new arrivals of injured people at the MCI site, arrival of daily patients at each hospital, and the number of patients staying at hospitals). This enables us to derive insights into how each parameter affects MCI planning.

4.6.3 Computational results (the case study) - ADP vs. Myopic policy

In this section, we compare the results of the proposed model (ADP policy) solved using the column generation algorithm with a myopic policy (based on the data provided in Section 4.6.1) over 30 runs. The myopic policy resembles a system where the information concerning the future status of the system is not taken into account, and a rule is used that represents the patients who follow a higher-priority-in first-serve policy. According to this policy, the seriously injured patients (type 1) must be transferred to the nearest hospitals (Civic campus). In contrast, other patients (type 2) must be sent only to the farthest hospital (General campus). In other words, no type 2 patients can be served until the higher priority casualties (type 1) have been transferred from the MCI site. Under this policy, the remaining capacity of the closest hospital is checked per decision epoch. If there are still some patients of type 1 remaining at the MCI site, the actions require the type 1 patients to be transferred to the nearest hospital. If not patients of type 1 remain at the MCI site, the action would be to send the type 2 patients to the farthest hospital. In summary, for this policy, two important elements are checked to take action: distance between each hospital and the MCI site, remaining number of patients of both types, and the remaining capacity at hospitals. In the following sub-sections we compare the results of the ADP policy to that of the Myopic policy under the case study setting.

4.6.3.1 Low-congested and fully congested systems

The low-congested system resembles the case study where the λ and μ values are zero. In other words, we assume that the total demand at the MCI site is known at the outset and that the hospitals do not receive new arrivals due to the emergency (orange code) declared by the hospital. In contrast, for the fully-congested system, we assume a positive λ in the initial time periods and a positive μ. A system is declared fully-congested when the difference between the hospital's base capacity is entirely occupied. In contrast, a low-congested system has some available capacity to assign incoming patients due to a limited number of people waiting at the hospital to receive care and does not overload the base capacity of the hospital. Below we describe the low-congested and fully-congested systems in detail. The number of periods is considered to be 30 periods.

Fully-congested system:

- Number of people at the MCI site (n_i^1) at first period = 18.
- Number of empty vehicles at the MCI site (B_{ij0}^1) at first period = 5.
- Number of patients at each hospital (P_{ij}^1) at first period = 10.
- Base capacity (BC_{ij}^1) for each campus at first period = 10.

- Expected values of for the RHS of dual constraints: $E(n_i^t) = 18$, $E(B_{ij0}^t) = 0.05$, $E(P_{ij}^t) = 0.5$, $E(AC_{ij}^t) = 10$.
- $\lambda_i^t = 5$ (decreases overtime by one per period) and $\mu_{ij}^t = 3$.

Low-congested system:

- Number of people at the MCI site (n_i^1) at first period = 18.
- Number of empty vehicles at the MCI site (B_{ij0}^1) at first period = 5.
- Number of patients at the hospitals (P_{ij}^1) at first period = 0.
- Base capacity (BC_{ij}^t) for both campuses at first period = 10.
- Expected values of for the RHS of dual constraints: $E(n_i^t) = 18$, $E(B_{ij0}^t) = 0.05$, $E(P_{ij}^t) = 0$, $E(AC_{ij}^t) = 10$.
- $\lambda_i^t = 0$ and $\mu_{ij}^t = 0$.

Table 4.6: The results of the case study under ADP and Myopic policies for low-congested and fully-congested systems.

Level of System Congestion	Policy	Strategies		State variables		Solution Time *
		Total Capacity Increase	Total Patient Transfer	Total Patient Waiting at the MCI (last period)	Total Patients Waiting at the Hospital (last period)	
Low-congested (no new arrivals at the MCI site and hospitals)	ADP	2	4	0 patient type 1 0 patient type 2	2 patient type 1 1 patient type 2	8.91 minutes
	Myopic	5	0	3 patient type 1 2 patient type 2	3 patient type 1 4 patient type 2	14.1 minutes
Fully-congested (new arrivals at MCI site and hospitals)	ADP	6±2.01	7±1.83	1.9±1.46 patient type 1 2.89±1.39 patient type 2	2.12±0.86 patient type 1 4±2.43 patient type 2	20.1 minutes
	Myopic	15±1.31	0	8±0.13 patient type 1 9±1.77 patient type 2	11.5±1.40 patient type 1 11±0.81 patient type 2	30.9 minutes

*Total solution time = the amount of time it takes for the two-phase column generation algorithm plus the solution time for simulation algorithm.

As shown in Table 4.6, when the MCI network is a low-congested system, the ADP policy derived from the proposed MDP model outperforms the myopic policy across a number of metrics such as the number of patients waiting to receive care or to be transferred from the MCI site, solution time, etc. In moving from the low-congested system to the fully-congested system, the relative value of the ADP policy over the Myopic only increases. Under the ADP policy, more patients are transferred between the Civic and General campuses while using the Myopic policy, capacity is increased instead. For both the low-congested and fully-congested systems, the system incurs more transfer costs under the ADP policy while reducing the costs associated with increased capacity and patient waiting.

It is important to note that the ADP and myopic policies are derived from the proposed two-phase algorithm and a simulation rule respectively. We used the two-phase column generation algorithm to generate values for the approximation parameters which are then used to derive the ADP policies. However, for the myopic policy, the policy is obtained using a previously defined rule over 30 simulation runs. As for each run, many lines of the rule must be checked, and numerous state-actions exist; it is reasonable to see a slow convergence speed for the simulation rule associated with the myopic policy compared to the ADP one. Thus the results show that first sending the seriously injured patients to the Civic hospital and then sending the ambulances to the MCI site to transfer the rest to the General campus once no type 1 patients remain is not an optimal policy (myopic policy). It increases the amount of waiting and system-based costs (i.e., capacity increase cost) through the MCI network.

4.6.3.2 The impact of the available number of ambulances on the response time and number of unserved patients

Inevitably, the availability of paramedic vehicles positively impacts the MCI relief operations allowing for faster response times and fewer unserved patients. We define the response time as the amount of time (number of periods) required to send all injured people from the MCI site to hospitals.

As illustrated in Figure 4.3, under the ADP policy and in the low-congested scenario, there exists no patients left unserved ($n = 0$ at the end of the planning horizon $t = 30$) even with the current availability of vehicles ($TV = 5$). In contrast, under the Myopic policy, the MCI network for the same system (low-congested) requires 10 vehicles to satisfy the same demand within the same planning horizon. Similarly, for the congested scenario, the number of paramedic ambulances required to transfer all patients from the MCI site is approximately 35% lower (14 vehicles for the ADP and 19 for the myopic) for the ADP policy compared to the Myopic.

Computing the response time under various levels of vehicles' availability would allow the

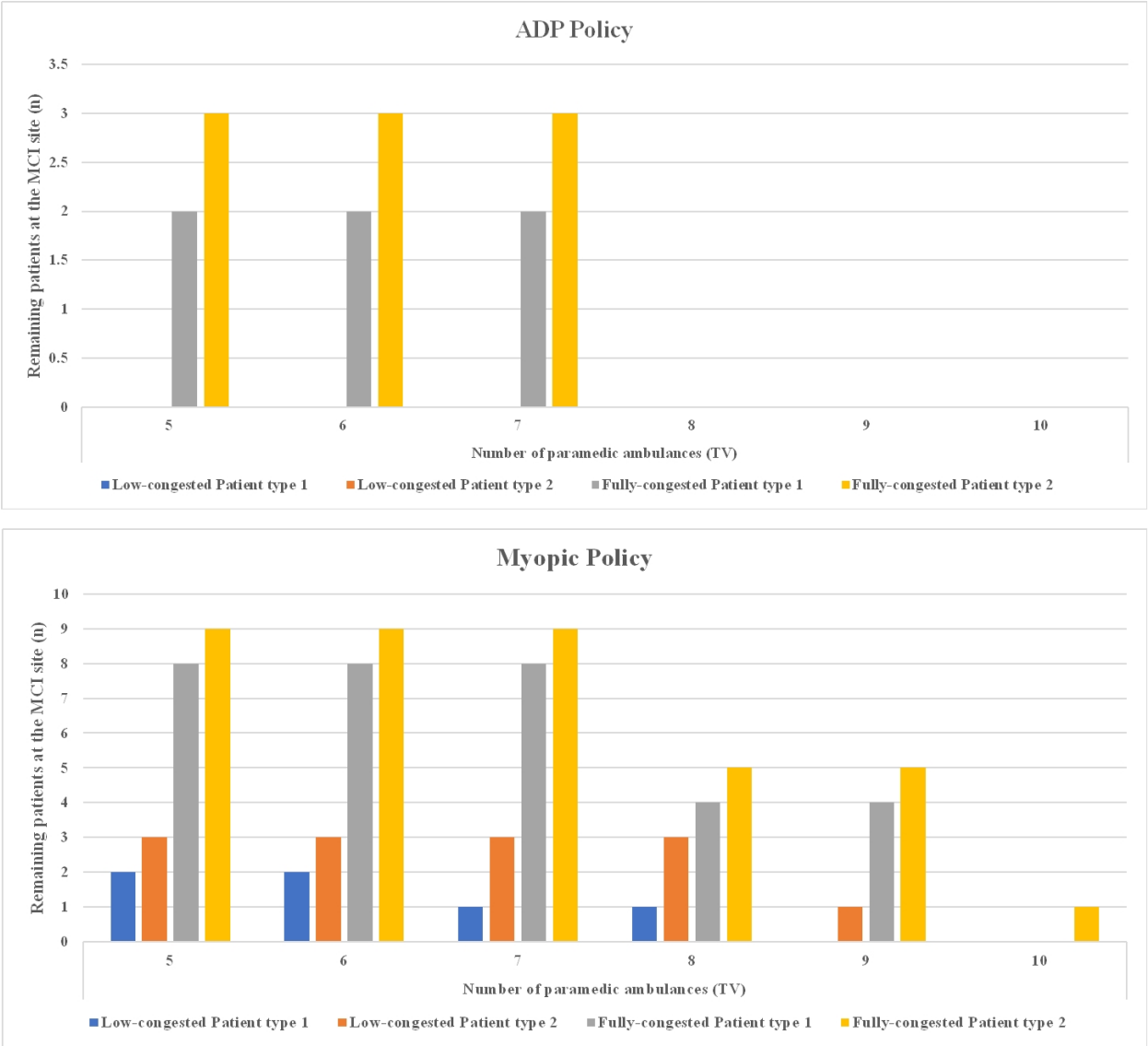

Figure 4.3: The effect of the number of available ambulances on the remaining patients at the MCI site

MCI network decision makers to determine the necessary capacity for future similar incidents. As indicated in Figure 4.4, under the ADP policy, we need at least 19, 25, and 30 periods respectively, to evacuate all patients from the MCI site using only 10, 7 and 5 ambulances respectively. Although a similar declining trend is seen for the myopic policy, in the last period ($t = 30$), around 11 and 15 patients were not evacuated with 5 and 7 paramedic ambulances, respectively. However, allocating ten ambulances allowed all the patients to be transferred from the MCI site within 30 periods. For this analysis, we considered 40 patients compared to the real bus crash to evaluate the performance of the system when the number of patients is more than the real case number.

In summary, under the ADP policy (Figures 4.3 and 4.4), fewer patients are unserved and fewer vehicles are required to fully evacuate all patients with any given target response time. It is not surprising to see such a trend as the myopic policy does not take into account the congestion at the receiving hospital. Such a policy incurs more cost to the system since it requires the Civic hospital to increase more capacity for patients of type 1 while leaving the General hospital idle until the transportation of all patients of type 1 is complete.

4.6.3.3 Form of the optimal approximation parameters

The values of approximation parameters, $W^t_{(1)i}, W^t_{(2)ij}, W^t_{(3)ij}, W^t_{(4)ij0}$ together with the immediate costs determine the optimal action at each decision epoch. Here we study the impact of the approximation parameters derived from the fully-congested scenario. For simplicity, we show the plot for a patient of type 1 and two hospitals. The $W^t_{(1)i}, W^t_{(2)ij}, W^t_{(3)ij}$, and $W^t_{(4)ijc}$ represent the marginal cost of an additional patient/vehicle assigned to the state variables $n^t_i, P^t_{ij}, AC^t_{ij}, B^t_{ijc}$, respectively. As Figure 4.5 indicates there is a nice form for each approximation parameter. For $W^t_{(1)i}$, the marginal cost related to the state variable n^t_i decreases over time, indicating the lower (future) cost as you get closer to the end of the horizon. The approximate parameter $W^t_{(2)ij}$ represents the marginal cost of a patient waiting. The marginal cost related to the state variable p^t_{ij} decreases over time indicating the lower (future) cost as you get closer to the end of the horizon. Since the cost related to waiting is the same at both hospitals ($\theta_{hospital1} = \theta_{hospital2} = 20$), marginal costs are the same, except for the first decision epoch. For $W^t_{(3)ij}$, the system can benefit more from not transferring injured people to the General campus compared to the Civic campus as the cost of increasing capacity for the Civic campus is lower across all decision epochs. Furthermore, to serve all the injured people waiting at the MCI site, it is more rewarding for the system to send more injured people to the Civic campus. Finally for $W^t_{(4)ij0}$ related to the state variable B^t_{ijc}, it is rewarding for the system to have available ambulances at the MCI site (B^t_{ij0}) across all the decision epochs. Thus the cost parameter is negative in this case.

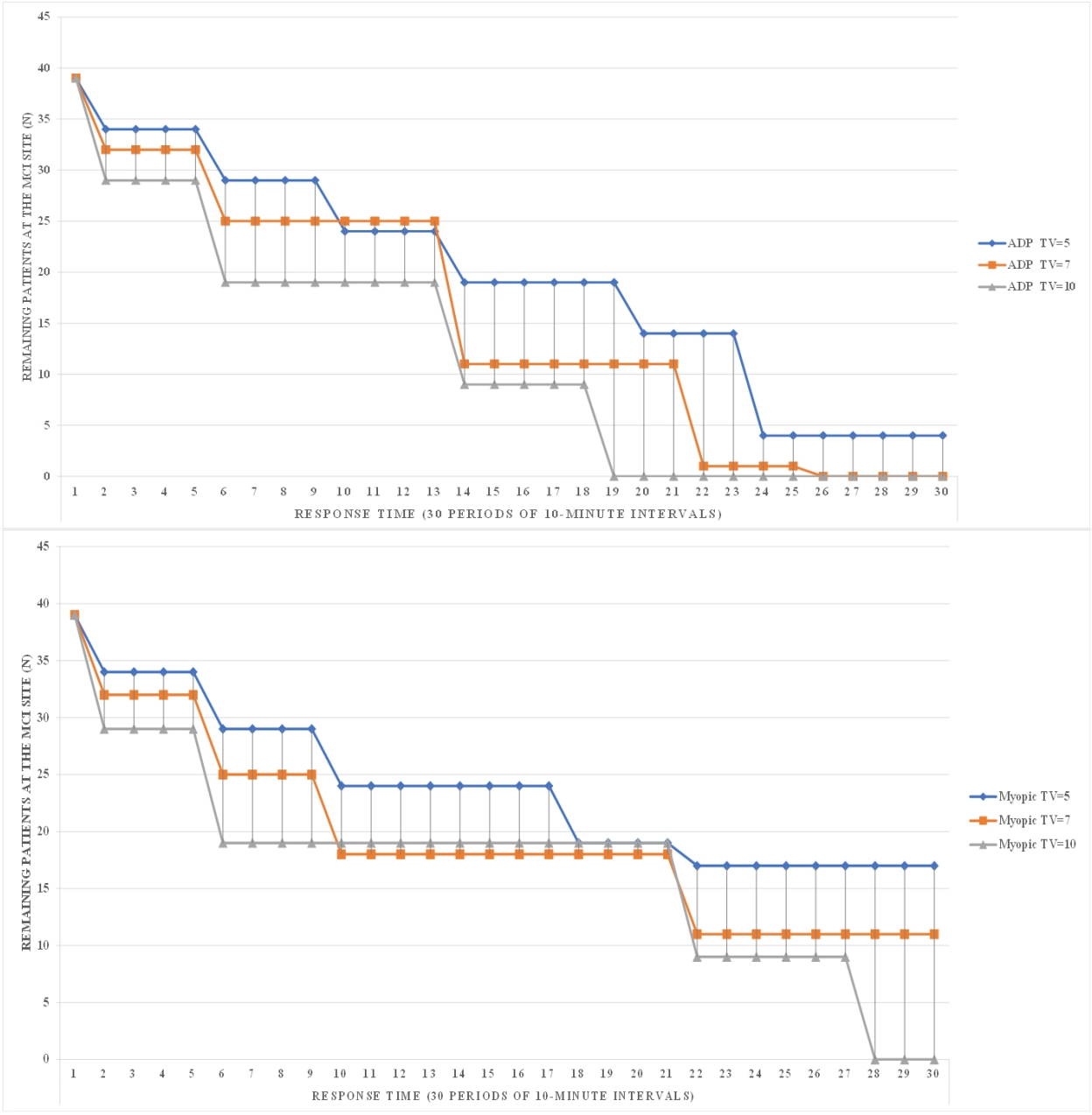

Figure 4.4: The response time (the amount of time it takes to transport all remaining patients from the MCI site) vs availability of vehicles for the congested system

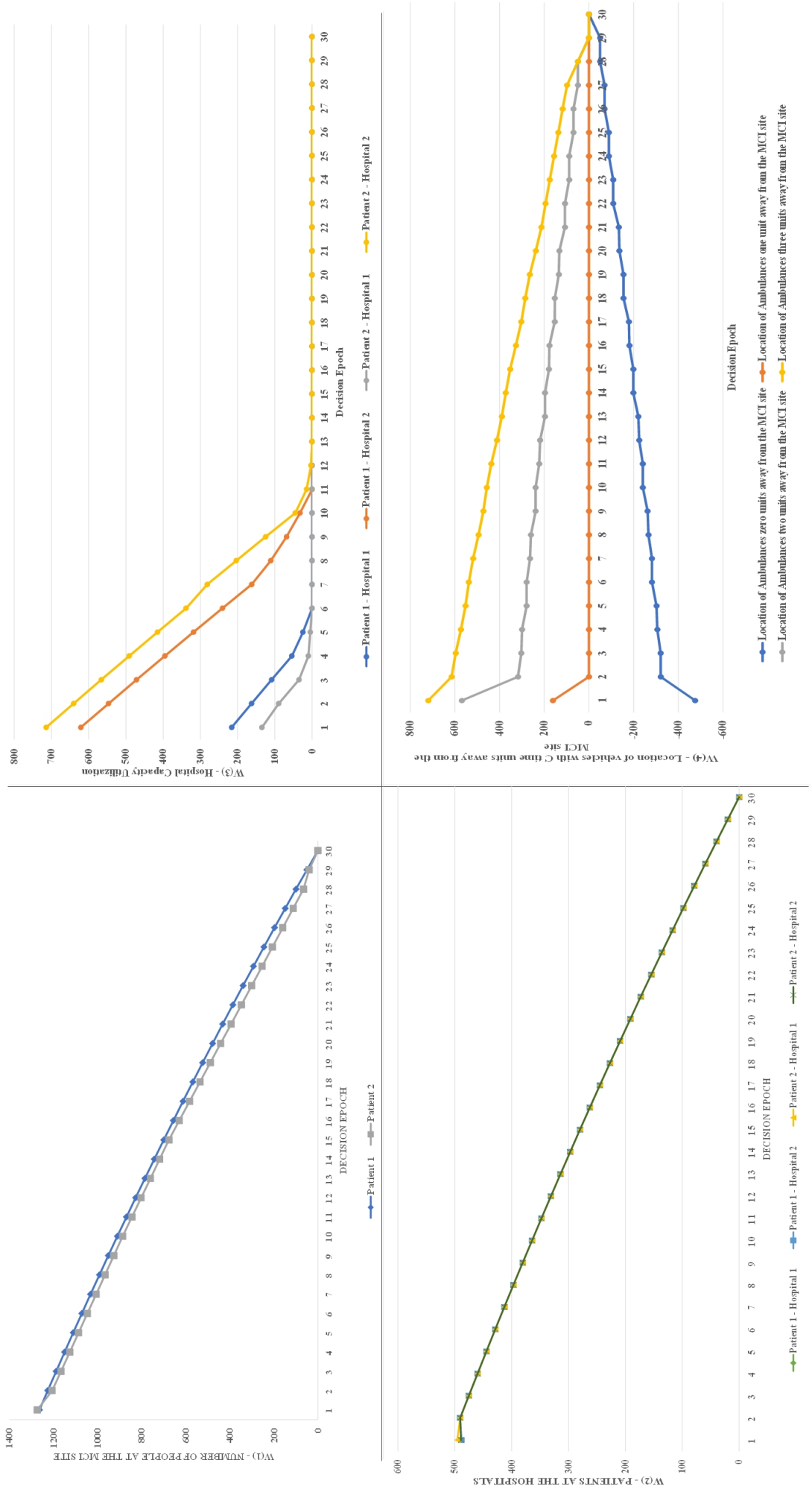

Figure 4.5: The location of ambulances with C time units away from the MCI site.

4.6.4 Computational results (a numerical example) - sensitivity analysis

In this section, we report the results of using simulation to investigate the behaviour of the ADP and Myopic policy in a variety of scenarios (scenarios A to F below). Such scenarios were defined based on expert opinion on potential MCI events and their impact on hospitals' care capacity and relief response operations. The results for all the scenarios are aligned with our first managerial insight provided in Section 4.7. In this section, the simulations are performed for a numerical example, which differs from the case study in the total number of vehicles operating through the network (eight vehicles), one type of patient (type 1: seriously injured patients), and $t = 20$ time periods. The basic capacity at each hospital is set to 25. The number of patients already at the hospital at the start is 15. The number of patients waiting at the MCI site ranges from 10 to 25 across scenarios A and B. Finally, a third capacity increase level has been added along with its associated cost.

Updated Myopic Policy: In the previously described Myopic policy, seriously injured patients (type 1) are the first to be transferred to the nearest hospital, while type 2 patients are sent to the farthest hospital after all type 1 patients are served. Here, with only one patient type, we simply send patients to the nearest hospital with available capacity.

For the following scenarios with a planning horizon with 20 time periods, one patient type, eight paramedic ambulances and two hospitals, the time to the solution was less than ten minutes for all scenarios. The simulation of the proposed MDP system was also done in GAMS/Java because it involves solving a mixed-integer program. Each scenario was run 30 times, with the resulting 95 % confidence interval provided for each statistic. The run time for a simulation was approximately ten minutes on the same laptop with the previously mentioned system requirements. The discount factor is set at 0.99 for all simulation scenarios.

Scenarios A and B: When λ and μ are set to zero (a system with no uncertainty). A system with 10 patients (scenario A) at the MCI site that increases with steps of size five from 10 to 25 patients (scenario B).

Scenario C: When λ is a positive decreasing function and μ is set to zero (a system with uncertainty in the number of new patients at the MCI site at each decision epoch). Scenario C repeats under the same condition as scenarios A and B again.

Scenario D: When λ is set to zero, and μ gets positive values ($\mu > 0$) (a system with uncertainty in the number of new patients at each hospital at each decision epoch). Scenario D repeats under the same condition as scenarios A and B again.

Scenario E: When λ and μ get positive values ($\mu > 0$ and $\lambda > 0$) (a system with uncertainty in the number of new patients at the MCI site and each hospital at each decision epoch). Scenario E

Table 4.7: The performance of the model under scenarios A and B.

Scenarios	Steps	Policy	State Variables			Actions	
			N (last period)	P (last period)	AC (last period)	a1 (total)	a2 (total)
Scenarios A and B	Scenario A	ADP	0 patients	3±0.61 at Hospital 1 5±1.24 at Hospital 2	25 at Hospital 1 25 at Hospital 2	0	10 MCI to Hospital 2
		Myopic	0 patients	9±0.37 at Hospital 2	25 at Hospital 2	0	10 MCI to Hospital 2
	Scenario B 15 Patients	ADP	0 patients	2.3±0.91 at Hospital 1 7.2±1.45 at Hospital 2	25 at Hospital 1 25 at Hospital 2	0	15 MCI to Hospital 2
		Myopic	0 patients	7.9±1.13 at Hospital 2	25 at Hospital 2	0	15 MCI to Hospital 2
	Scenario B 20 Patients	ADP	0 patient	0 at Hospital 1 10±0.77 at Hospital 2	25 at Hospital 1 25 at Hospital 2	0	20 MCI to Hospital 2
		Myopic	0 patient	11±1.80 at Hospital 2	25 at Hospital 2	0	20 MCI to Hospital 2
	Scenario B 25 Patients	ADP	0 patients	7.3±1.56 at Hospital 1 8.1±0.95 at Hospital 2	25 at Hospital 1 25 at Hospital 2	0	25 24 MCI to Hospital 2 and 1 MCI to Hospital 1
		Myopic	0 patients	13±0.16 at Hospital 2	30 at Hospital 2	5	25 MCI to Hospital 2

repeats under the same condition as scenarios A and B again.

Scenario F: When λ and μ get positive values ($\mu > 0$ and $\lambda > 0$) (a system with uncertainty in the number of new patients at the MCI site and each hospital at each decision epoch). In this scenario, one hospital is more congested than the other hospital (for instance, the $\mu_{hospital2}$ is higher than the $\mu_{hospital1}$ ($\mu_{hospital2} > \mu_{hospital1}$). Scenario F repeats under the same condition as scenarios A and B again.

4.6.4.1 The output of the model under scenarios A and B

As depicted in Table 4.7, there is no capacity increase for both scenarios A and B at both campuses, indicating a sufficient amount of capacity at each hospital for seriously injured patients (type 1). As the number of patients that are required to be sent to each hospital is lower than the capacity available and there is no uncertainty ($\mu = 0$ and $\lambda = 0$), the hospitals are not overwhelmed beyond their capacity. Under scenarios A and B, no patient remains unserved at the MCI site as all the patients are transferred to either hospital 1 or 2. As hospital 2 is closer to the MCI region, most patients (24 patients) are sent to this hospital, which does not overwhelm the hospital due to the availability of capacity.

4.6.4.2 The output of the model under scenarios C

Under scenario C (Table 4.8), no capacity increase is seen at either hospital indicating each hospital's capability to provide the incoming patients from the MCI site with enough capacity.

Table 4.8: The performance of the mode under Scenario C.

Scenario	Steps	Policy	State Variables			Actions	
			N (last period)	P (last period)	AC (last period)	a1 (total)	a2 (total)
Scenario C	Scenario A	ADP	0 patients	5±1.52 at Hospital 1 and 6.1±0.66 at Hospital 2	25 at Hospital 1 25 at Hospital 2	0	12±1.34 MCI to Hospital 2 Periods (1,5)
		Myopic	0 patients	6±1.35 at Hospital 1 and 6±1.86 at Hospital 2	25 at Hospital 1 25 at Hospital 2	0	13±1.98 MCI to Hospital 2 Periods (1,5)
	Scenario B 15 patients	ADP	0 patients	7.5±1.90 at Hospital 1 9.5±1.08 at Hospital 2	25 at Hospital 1 25 at Hospital 2	0	21±1.81 MCI to Hospital 2 Periods (1,5,9)
		Myopic	0 patients	7±0.36 at Hospital 1 8±1.09 at Hospital 2	25 at Hospital 1 25 at Hospital 2	0	20±1.33 MCI to Hospital 2 Periods (1,5,9)
	Scenario B 20 patients	ADP	0 patients	7.2±1.72 at Hospital 1 10±1.21 at Hospital 2	25 at Hospital 1 25 at Hospital 2	0	22±3.85 MCI to Hospital 2 Periods (1,5,9) 4 Patients MCI to Hospital 1 Period (9)
		Myopic	0 patients	8.2±1.43 at Hospital 1 10±1.79 at Hospital 2	25 at Hospital 1 33 at Hospital 2	8	20±0.94 MCI to Hospital 2 Periods (1,5,9)
	Scenario B 25 patients	ADP	0 patients	7±1.53 at Hospital 1 6.1±0.40 at Hospital 2	25 at Hospital 1 26 at Hospital 2	1	27±0.75 MCI to Hospital 2 Periods (1,5,9) 5 Patients MCI to Hospital 1 Period (13)
		Myopic	5 patients	10±0.49 at Hospital 1 8.2±1.03 at Hospital 2	25 at Hospital 1 32 at Hospital 2	7	20±1.01 MCI to Hospital 2 Periods (1,5,9)

However, due to the uncertainty in the arrivals of injured people at the MCI site ($\lambda > 0$), the pattern of patients being transported to both hospitals is different for scenario C compared with scenarios A and B. An interesting result here is that the patients are transferred first to hospital two instead of having a pattern of equal transfer of patients to both hospitals. The reason is that hospital 2 is closer to the MCI site, and not transporting patients from the MCI site incurs the system more cost than when patients have to wait to receive care at each hospital. Under scenario C, no patient remains unserved at the MCI site, the same as in scenarios A and B, due to the availability of vehicles (eight vehicles available at each decision epoch) to cover the needs of all patients at the MCI site. Notably, by increasing the number of patients at the MCI site from 10 to 25, hospital one is also involved in admitting patients due to the limited capacity of hospital two and the higher cost of capacity increase at hospital 2 compared to the cost of transferring patients to hospital 1.

4.6.4.3 The output of the model under scenario D

In this scenario, we redo scenarios A and B when the new arrivals at each decision epoch at each hospital are uncertain and positive ($\mu > 0$). As shown in Table 4.9, the patient transportation pattern is very different from the previous scenarios. In this case, both hospitals are involved in admitting patients, while hospital 2 still has the highest patient admission due to its proximity to the MCI site. Under scenario D, no patient remains unserved at the MCI site since the number of vehicles suffices for the transportation of all 25 patients from the MCI site while no new patients arrive at the MCI site at different decision epochs ($\lambda = 0$). Unlike previous scenarios, an increased capacity at different decision epochs is seen for both hospitals. This indicates the need for both hospitals to assign more capacity to accommodate both regular demand and the influx from the MCI site. As the system is moving from a noncongested system ($\mu = 0$) to a more congested system ($\mu > 0$) different patterns of casualty transportation to both hospitals from the MCI site, capacity increases at both hospitals, and patient transfers between hospitals result.

4.6.4.4 The output of the model under scenario E

In this scenario, the system is regarded as a fully congested system where the new arrivals at each decision epoch at each hospital and the new arrivals at the MCI site are both uncertain and positive ($\mu > 0$ and $\lambda > 0$). As Table 4.10 presents, by moving from the non-congested (scenario A) to the congested system (scenario E), we see more collaboration between hospitals through patient transfers. Increased uncertainty also leads to the need to create additional capacity. Compared to scenario, we now see some unseen patients at the MCI site by the end of the planning horizon due to the uncertainty in the number of patients at the MCI site ($\lambda > 0$), the limited finite-time

Table 4.9: The performance of the model under scenario D.

Scenario	Steps	Policy	State Variables			Actions	
			N (last period)	P (last period)	AC (last period)	a1 (total)	a2 (total)
Scenario D	Scenario A	ADP	0 patients	16±0.98 at Hospital 1 20±1.35 at Hospital 2	26±1.66 at Hospital 1 26±0.77 at Hospital 2	2±0.81 Hospital 2 (period 15) 1±1.02,1±1.25 Hospital 1 (periods 16 and 18, respectively)	8 MCI to Hospital 2 Period (1) 2 MCI to Hospital 1 Period (5)
		Myopic	0 patients	20±0.13 at Hospital 1 20±1.25 at Hospital 2	25 at Hospital 1 30±0.19 at Hospital 2	3±1.78 Hospital 2 (period 13)	10 MCI to Hospital 2 Periods (1,5)
	Scenario B 15 patients	ADP	0 patients	18±0.93 at Hospital 1 20±1.55 at Hospital 2	30±1.16 at Hospital 1 30±3.08 at Hospital 2	7±1.01,2±1.81 Hospital 2 (periods 12, 13, respectively) 4±1.19 Hospital 1 (period 16)	12 MCI to Hospital 2 Periods (1,5) 3 MCI to Hospital 1 Period (5)
		Myopic	0 patients	20±1.1 at Hospital 1 29±1.32 at Hospital 2	25 at Hospital 1 29±3.91 at Hospital 2	9±2.33,4±0.97 Hospital 2 (periods 11, 17, respectively)	15 MCI to Hospital 2 Periods (1,5)
	Scenario B 20 patients	ADP	0 patients	20±1.75 at Hospital 1 24±0.53 at Hospital 2	29±1.49 at Hospital 1 31±0.47 at Hospital 2	3±0.28,3±1.42,1±1.58,2±0.66 Hospital 2 (periods 12,15,16,17, respectively) 2±1.23,3±0.15 Hospital 1 (periods 15 and 17, respectively)	16 MCI to Hospital 2 Periods (1,5) 4 MCI to Hospital 1 Period (9)
		Myopic	0 patients	20±1.22 at Hospital 1 30±0.88 at Hospital 2	25 at Hospital 1 41±0.28 at Hospital 2	7±1.14,6±1.21,2±1.24 Hospital 2 (periods 13,16,17, respectively)	20 MCI to Hospital 2 Periods (1,5,9)
	Scenario B 25 patients	ADP	0 patients	27.1±1.12 at Hospital 1 21±1.55 at Hospital 2	28±2.40 at Hospital 1 33±3.01 at Hospital 2	3±1.06,5±1.09,3±0.18 Hospital 2 (periods 7,15,19, respectively) 2±1.37,3±1.03 Hospital 1 (periods 9 and 15, respectively)	17 MCI to Hospital 2 Periods (1,5,13) 8 MCI to Hospital 1 Period (9) 2±0.56 Hospital 1 to Hospital 2 periods (17 and 19) 1±0.41 Hospital 2 to Hospital 1 period (17)
		Myopic	5 patients	26.2±1.57 at Hospital 1 35±1.98 at Hospital 2	25 at Hospital 1 39±0.23 at Hospital 2	7±0.36,5±0.9,1±2.51 Hospital 2 (periods 13,16,17, respectively)	20 MCI to Hospital 2 Periods (1,5,9)

planning horizon, and limited vehicles. Moreover, due to the uncertainty in the number of patients at the hospitals ($\mu > 0$), the number of patients waiting to receive care at each hospital (p) and the required increases in capacity, this scenario results in substantially higher costs to the system.

4.6.4.5 The output of the model under scenario F

In this scenario, hospital 2 is considered to be a more congested hospital compared to hospital 1 ($\mu_{hospital2} > \mu_{hospital1}$). Due to the high level of congestion in this scenario, some of the actions look similar to scenario E. However, more patients are transferred from hospital 2 to hospital 1 due to the higher congestion at hospital 2 coupled with the closer proximity of hospital 2 to the MCI site. Moving patients from the MCI site to hospital 2 and allocating extra capacity to hospital 2 is less costly for the system compared to when patients are sent to hospital 1. It is also interesting to see that the resulting strategies include increasing the capacity of both hospitals as well as patient transfers between hospitals when we compare scenario F to the earlier scenarios.
In conclusion, moving from a low-congested system (Scenario A) to a fully congested system (Scenarios E and F) with a high level of uncertainty in the parameters mentioned above of the proposed MDP model, a number of changes to the derived policies are observed demonstrating the value of a model driven approach to help mitigate the impact of an MCI event.

4.6.5 Managerial insights

In the high stress of an MCI, with multiple types of patients, numerous potential destination hospitals and costly interventions that can be implemented to increase capacity, it is often quite complex to determine the best means of serving the MCI patients while still attempting to serve the rest of the population. Uncertainty in terms of demand further exacerbates the difficulties. We developed an ADP model in an attempt to derive good policies for the integrated casualty transportation and hospital capacity planning problem in the presence of multiple sources of uncertainty. The results demonstrate that the performance of the ADP can provide timely policies for the casualty transportation and hospital capacity planning problem that ensures timely access to care as well as a robust capacity plan. It would be beneficial for relief response managers to apply the proposed model and its derived policies compared with currently implemented policies such as the myopic policy in the current study.
Overall, the following are potential uses of our model for managers of an MCI event:
- importance of pre-planning for an MCI as the optimal decisions are not obvious.
- allocation and capacity decisions are highly dependent on the size and uncertainty surrounding the MCI event.
- the more uncertainty that can be resolved early on in the event, the easier it is to plan.

Table 4.10: The performance of the model under Scenario E.

Scenario	Steps	Policy	State Variables			Actions	
			N (last period)	P (last period)	AC (last period)	a1 (total)	a2 (total)
Scenario E	Scenario A	ADP	1±0.95 patient	12±2.43 Hospital 1 25±1.79 Hospital 2	27±2.02 Hospital 1 35±1.53 Hospital 2	5±1.06,5.1±0.92 Hospital 2 (periods 10,17, respectively) 2±2.73 Hospital 1 (period 9)	10±2.35 MCI to Hospital 2 Period (1,9) 3±0.56 MCI to Hospital 1 Period (5)
		Myopic	2±2.77 patient	15±0.71 Hospital 1 33±1.92 Hospital 2	25 Hospital 1 43±0.03 Hospital 2	8±0.87,10±1.06 Hospital 2 (periods 13,17, respectively)	19±1.73 MCI to Hospital 2 Period (1,5,9)
	Scenario B 15 patients	ADP	2.2±0.55 patients	15.8±1.65 Hospital 1 24.5±2.05 Hospital 2	26±2.54 Hospital 1 36±1.69 Hospital 2	4±1.76,3±1.68,3±0.04 Hospital 2 (periods 5,9,13, respectively) 3±1.34 Hospital 1 (period 16)	14.6±0.97 MCI to Hospital 2 Periods (1,5) 8±0.78 MCI to Hospital 1 Period (9)
		Myopic	8±0.45 patients	17.3±1.04 Hospital 1 36.6±1.51 Hospital 2	25 Hospital 1 43±3.09 Hospital 2	11±2.47,11±2.46 Hospital 2 (periods 9,17, respectively)	19±3.77 MCI to Hospital 2 Periods (1,5,9)
	Scenario B 20 patients	ADP	6.9±1.65 patients	21±1.23 Hospital 1 30±1.53 Hospital 2	30.9±1.11 Hospital 1 36±1.04 Hospital 2	5.7±1.9,3±1.15,1±1.25 Hospital 2 (periods 15,16,18, respectively) 4±1.72,2±0.93 Hospital 1 (periods 17,18, respectively)	22.8±0.83 MCI to Hospital 2 Periods (1,5,9) 6.3±1.31 MCI to Hospital 1 Period (13) 2±0.43 Hospital 2 to Hospital 1 Period (13) 2±0.9 Hospital 1 to Hospital 2 period (17)
		Myopic	13±2.88 patients	23±1.45 Hospital 1 42±4.01 Hospital 2	30±1.65 Hospital 1 49±0.14 Hospital 2	10±1.45,7±1.31,7.5±1.57 Hospital 2 (periods 13,17,19, respectively) 3±1.43,3±1.54 Hospital 1 (periods 13,17, respectively)	20±6.73 MCI to Hospital 2 Periods (1,5,9)
	Scenario B 25 patients	ADP	7.9±0.56 patients	23±3.21 Hospital 1 34±1.48 Hospital 2	35±1.32 Hospital 1 42±1.71 Hospital 2	7±1.67,10±0.43 Hospital 1 (periods 15 and 18, respectively) 4±1.23,6±1.56 Hospital 2 (period 13,17, respectively)	24.7±0.97 MCI to Hospital 2 Periods (1,5,9) 12±1.10 MCI to Hospital 1 Period (13,17) 3±1.69 Hospital 1 to Hospital 2 Period (17) 2±1.26 Hospital 2 to Hospital1 period (19)
		Myopic	18±0.66 patients	25±1.71 Hospital 1 40±0.55 Hospital 2	30±2.74 Hospital 1 45±3.28 Hospital 2	10±1.15,10±1.92,4±1.6 Hospital 2 (periods 11,17,19, respectively) 4±1.21,2±2.75 Hospital 1 (periods 13,17, respectively)	21.2±7.1 MCI to Hospital 2 Periods (1,5,9)

Table 4.11: The performance of the model under Scenario F.

Scenario	Steps	Policy	State Variables			Actions	
			N (last period)	P (last period)	AC (last period)	a1 (total)	a2 (total)
Scenario F	Scenario A	ADP	0 patient	9.6±2.45 Hospital 1 18±2.38 Hospital 2	25±1.32 Hospital 1 31±0.98 Hospital 2	1±1.38,4±1.57 Hospital 2 (periods 9,13, respectively)	8 MCI to Hospital 2 period (1) 8 MCI to Hospital 1 period (5)
		Myopic	4 patient	16±1.31 Hospital 1 29±1.55 Hospital 2	25 Hospital 1 39±0.66 Hospital 2	6±1.58,6.7±1.40 Hospital 2 (periods 13,17, respectively)	16 MCI to Hospital 2 period (1,5)
	Scenario B 15 patients	ADP	1.2±1.97 patients	11±2.59 Hospital 1 20±1.32 Hospital 2	29±1.32 Hospital 1 39±1.53 Hospital 2	6.8±1.03,6±1.52,3±1.07 Hospital 2 (periods 5,9,13, respectively) 3±0.55 Hospital 1 (period 17)	16±0.53 MCI to Hospital 2 periods (1,9) 8±1.65 MCI to Hospital 1 period (5) 2±1.68 Hospital 2 to Hospital 1
		Myopic	3.7±1.76 patients	15±1.97 Hospital 1 21±2.3 Hospital 2	25±1.57 Hospital 1 39±1.75 Hospital 2	9±0.72,5±0.48 Hospital 2 (periods 9,13, respectively)	12±1.51 MCI to Hospital 2 periods (1,5) 6±1.95 MCI to Hospital 1 period (9)
	Scenario B 20 patients	ADP	6±2.8 patients	21±0.88 Hospital 1 31±1.59 Hospital 2	32±1.45 Hospital 1 36±0.73 Hospital 2	7±0.32,3±0.67,1±1.14 Hospital 2 (periods 15,16,18, respectively) 4±0.73,2±1.20 Hospital 1 (periods 17,18, respectively)	22±2.06 MCI to Hospital 2 periods (1,5,9, respectively) 6±0.73 MCI to Hospital 1 period (13) 2±0.95 Hospital 2 to Hospital 1 period (13) 2±0.54 Hospital 1 to Hospital 2 1±0.90 period (17)
		Myopic	11±1.76 patients	21±2.04 Hospital 1 38±1.45 Hospital 2	30±1.57 Hospital 1 45±0.55 Hospital 2	10±1.35,4±1.38,4±0.75 Hospital 2 (periods 15,16,18, respectively) 6±1.34 Hospital 1 (periods 13 respectively)	16±4.01 MCI to Hospital 2 periods (1,5, respectively) 1±5.34 MCI to Hospital 1 period (9)
	Scenario B 25 patients	ADP	9±2.45 patients	25±1.65 Hospital 1 34±1.34 Hospital 2	35±1.05 Hospital 1 42±1.60 Hospital 2	9±1.43,9±1.92 Hospital 2 (periods 15 and 18, respectively) 4±1.06,7.3±1.65 Hospital 1 (periods 13,17, respectively)	25±0.54 MCI to Hospital 2 periods (1,5,9) 12±1.04 MCI to Hospital 1 period (13,17) 3±1.53 Hospital 1 to Hospital 2 period (17) 2±1.90 Hospital 2 to Hospital 1 period (19)
		Myopic	14±1.75 patients	30±0.40 Hospital 1 36±0.57 Hospital 2	43±1.35 Hospital 1 46±2.55 Hospital 2	10±1.67,6±1.5,6±1.72 Hospital 2 (periods 9,13,17, respectively) 8±1.43,10±1.76 Hospital 1 (periods 13,17 respectively)	15±2.58 MCI to Hospital 2 periods (1,5) 8±0.50 MCI to Hospital 1 period (9,13)

- ignoring the current congestion in the hospitals significantly impacts the ability of the network to quickly resolve the MCI.
- transferring patients between hospitals may be part of the optimal solution in situations where hospitals differ in available capacity.

4.7 Conclusions and recommendations

Although we have endeavoured to ensure that the model is as realistic as possible, there are inevitably enhancements that could potentially lead to interesting results. In this research, an MDP model for an MCI site and multiple hospitals with different levels of care capability is developed. The goal is to efficiently manage the transportation of injured people from the MCI site to hospitals or within hospitals and to decrease total cost, response time and unserved demand. To manage the proposed network effectively, we proposed an MDP model and its equivalent approximate linear programming formulation under an ADP policy. The proposed model is studied under multiple sources of uncertainty related to the new arrivals at the MCI site, new daily arrivals at the hospitals and the number of patients staying at each hospital at each decision epoch (period). To demonstrate the effectiveness of the proposed MDP model, we present an example including an MCI site, two hospitals, two types of patients (seriously; type 1 and critically; type 2 injured patients). A two-phase column generation algorithm is employed to derive the ADP policy which is compared to a Myopic policy that attempts to mimic current practice. Finally, sensitivity analysis is performed under six scenarios to ascertain the impact of several key parameters.

Although what we have presented here is adapted primarily to a dynamic finite-horizon MCI response, any situation where multiple patients with different injury levels are waiting at the MCI scene to be transferred to and receive care at multiple hospitals with different levels of care capability would be a potential application of the model.

Future research in this area could address incorporating more sophisticated myopic approaches and studying large-scale cases for other types of MCIs with various sources of uncertainty (such as reducing road capacity and unavailability of hospital capacities of multiple treatment types). Finally, future research may examine the possibility of integrating detailed vehicle routing and hospital treatment processes with various dependent and inter-locking treatment types. We believe that hospitals can use this model as a tool to determine policies in a given scenario. It is more policy-making than exact planning on real-time planning. However, as potential future research, we suggest considering a lag between when a DM make the decision and when that decision happens to align the tactical and operational decisions (capacity allocation and patient transportation) more aligned with real-settings.

4.8 Bibliography

[1] Daniel Adelman. A price-directed approach to stochastic inventory/routing. *Operations Research*, 52(4):499–514, 2004.

[2] Tabitha Beaton and Katherine Severson. A whole city approach to mass casualty planning. *Journal of Business Continuity & Emergency Planning*, 14(2):122–135, 2020.

[3] Steven L Bernstein, Dominik Aronsky, Reena Duseja, Stephen Epstein, Dan Handel, Ula Hwang, Melissa McCarthy, K John McConnell, Jesse M Pines, Niels Rathlev, et al. The effect of emergency department crowding on clinically oriented outcomes. *Academic Emergency Medicine*, 16(1):1–10, 2009.

[4] Arnab Bhattacharya and Jeffrey P Kharoufeh. Linear programming formulation for non-stationary, finite-horizon markov decision process models. *Operations Research Letters*, 45(6): 570–574, 2017.

[5] Daniela Pucci De Farias and Benjamin Van Roy. The linear programming approach to approximate dynamic programming. *Operations research*, 51(6):850–865, 2003.

[6] Daniela Pucci De Farias and Benjamin Van Roy. On constraint sampling in the linear programming approach to approximate dynamic programming. *Mathematics of operations research*, 29(3):462–478, 2004.

[7] Matthew D. Dean and Suresh K. Nair. Mass-casualty triage: Distribution of victims to multiple hospitals using the save model. *European Journal of Operational Research*, 238(1): 363–373, 2014.

[8] Xuan Vinh Doan and Duncan Shaw. Resource allocation when planning for simultaneous disasters. *European Journal of Operational Research*, 274(2):687–709, 2019.

[9] Eric DuBois and Laura A Albert. Dispatching policies during prolonged mass casualty incidents. *Journal of the Operational Research Society*, pages 1–15, 2021.

[10] A. Duffy. Code orange: Behind the ottawa hospital's response to the oc transpo bus crash. *Ottawa Citizen*, 2019.

[11] José Holguín-Veras, Noel Pérez, Miguel Jaller, Luk N Van Wassenhove, and Felipe Aros-Vera. On the appropriate objective function for post-disaster humanitarian logistics models. *Journal of Operations Management*, 31(5):262–280, 2013.

[12] Armin Jabbarzadeh, Behnam Fahimnia, and Stefan Seuring. Dynamic supply chain network design for the supply of blood in disasters: A robust model with real world application. *Transportation Research Part E: Logistics and Transportation Review*, 70:225–244, 2014.

[13] Evin Uzun Jacobson, Nilay Tanık Argon, and Serhan Ziya. Priority assignment in emergency response. *Operations Research*, 60(4):813–832, 2012.

[14] Phillip R Jenkins, Matthew J Robbins, and Brian J Lunday. Approximate dynamic programming for the military aeromedical evacuation dispatching, preemption-rerouting, and redeployment problem. *European Journal of Operational Research*, 290(1):132–143, 2021.

[15] Sukho Jin, Sukjae Jeong, Jangyeop Kim, and Kim Kyungsup. A logistics model for the transport of disaster victims with various injuries and survival probabilities. *Annals of Operations Research*, 230:17–33, 2015.

[16] Arun Jotshi, Qiang Gong, and Rajan Batta. Dispatching and routing of emergency vehicles in disaster mitigation using data fusion. *Socio-Economic Planning Sciences*, 43(1):1–24, 2009.

[17] Afshin Kamyabniya, MM Lotfi, Mohsen Naderpour, and Yuehwern Yih. Robust platelet logistics planning in disaster relief operations under uncertainty: a coordinated approach. *Information Systems Frontiers*, 20(4):759–782, 2018.

[18] Hyun-Rok Lee and Taesik Lee. Markov decision process model for patient admission decision at an emergency department under a surge demand. *Flexible Services and Manufacturing Journal*, 30(1):98–122, 2018.

[19] Dong Li and Kevin D Glazebrook. An approximate dynamic programing approach to the development of heuristics for the scheduling of impatient jobs in a clearing system. *Naval Research Logistics (NRL)*, 57(3):225–236, 2010.

[20] Yajie Liu, Hongtao Lei, Dezhi Zhang, and Zhiyong Wu. Robust optimization for relief logistics planning under uncertainties in demand and transportation time. *Applied Mathematical Modelling*, 55:262–280, 2018.

[21] Huseyin Onur Mete and Zelda B Zabinsky. Stochastic optimization of medical supply location and distribution in disaster management. *International Journal of Production Economics*, 126 (1):76–84, 2010.

[22] Alex F Mills, Nilay Tanık Argon, and Serhan Ziya. Dynamic distribution of patients to medical facilities in the aftermath of a disaster. *Operations Research*, 66(3):716–732, 2018.

[23] Alfredo Moreno, Douglas Alem, and Deisemara Ferreira. Heuristic approaches for the multi-period location-transportation problem with reuse of vehicles in emergency logistics. *Computers & Operations Research*, 69:79–96, 2016.

[24] Mehdi Najafi, Kourosh Eshghi, and Sander de Leeuw. A dynamic dispatching and routing model to plan/re-plan logistics activities in response to an earthquake. *OR spectrum*, 36(2): 323–356, 2014.

[25] Jonathan Patrick, Martin L Puterman, and Maurice Queyranne. Dynamic multipriority patient scheduling for a diagnostic resource. *Operations research*, 56(6):1507–1525, 2008.

[26] Jomon A Paul and Minjiao Zhang. Supply location and transportation planning for hurricanes: A two-stage stochastic programming framework. *European Journal of Operational Research*, 274(1):108–125, 2019.

[27] Jomon Aliyas Paul and Leo MacDonald. Location and capacity allocations decisions to mitigate the impacts of unexpected disasters. *European Journal of Operational Research*, 251(1): 252–263, 2016.

[28] Iris Perelman, Dean Fergusson, Jacinthe Lampron, Johnathan Mack, Fraser Rubens, Antonio Giulivi, Melanie Tokessy, Risa Shorr, and Alan Tinmouth. Exploring peaks in hospital blood component utilization: A 10-year retrospective study at a large multisite academic centre. *Transfusion Medicine Reviews*, 35(1):37–45, 2021.

[29] Adrian Ramirez-Nafarrate, A Baykal Hafizoglu, Esma S Gel, and John W Fowler. Optimal control policies for ambulance diversion. *European Journal of Operational Research*, 236(1): 298–312, 2014.

[30] Panagiotis P Repoussis, Dimitris C Paraskevopoulos, Alkiviadis Vazacopoulos, and Nathaniel Hupert. Optimizing emergency preparedness and resource utilization in mass-casualty incidents. *European Journal of Operational Research*, 255(2):531–544, 2016.

[31] F Sibel Salman and Sezer Gül. Deployment of field hospitals in mass casualty incidents. *Computers & industrial engineering*, 74:37–51, 2014.

[32] Antoine Sauré, Jonathan Patrick, and Martin L Puterman. Simulation-based approximate policy iteration with generalized logistic functions. *INFORMS Journal on Computing*, 27(3): 579–595, 2015.

[33] Paul J Schweitzer and Abraham Seidmann. Generalized polynomial approximations in markovian decision processes. *Journal of mathematical analysis and applications*, 110(2):568–582, 1985.

[34] Kyohong Shin and Taesik Lee. Emergency medical service resource allocation in a mass casualty incident by integrating patient prioritization and hospital selection problems. *IISE Transactions*, 52(10):1141–1155, 2020.

[35] Inkyung Sung and Taesik Lee. Optimal allocation of emergency medical resources in a mass casualty incident: Patient prioritization by column generation. *European Journal of Operational Research*, 252(2):623–634, 2016.

[36] Ke-Ming Wang and Zu-Jun Ma. Age-based policy for blood transshipment during blood shortage. *Transportation Research Part E: Logistics and Transportation Review*, 80:166–183, 2015.

[37] Duncan T Wilson, Glenn I Hawe, Graham Coates, and Roger S Crouch. A multi-objective combinatorial model of casualty processing in major incident response. *European Journal of Operational Research*, 230(3):643–655, 2013.

[38] Lina Yu, Canrong Zhang, Huasheng Yang, and Lixin Miao. Novel methods for resource allocation in humanitarian logistics considering human suffering. *Computers & Industrial Engineering*, 119:1–20, 2018.

[39] Gabriel Zayas-Cabán, Mark E Lewis, Matthew Olson, and Samuel Schmitz. Emergency medical service allocation in response to large-scale events. *IIE Transactions on Healthcare Systems Engineering*, 3(1):57–68, 2013.

[40] Jianghua Zhang, Haiyue Liu, Guodong Yu, Junhu Ruan, and Felix TS Chan. A three-stage and multi-objective stochastic programming model to improve the sustainable rescue ability by considering secondary disasters in emergency logistics. *Computers & Industrial Engineering*, 135:1145–1154, 2019.

[41] Li Zhu, Yeming Gong, Yishui Xu, and Jun Gu. Emergency relief routing models for injured victims considering equity and priority. *Annals of Operations Research*, pages 1–34, 2018.

[42] Shiva Zokaee, Ali Bozorgi-Amiri, and Seyed Jafar Sadjadi. A robust optimization model for humanitarian relief chain design under uncertainty. *Applied Mathematical Modelling*, 40 (17-18):7996–8016, 2016.

5 Concluding Remarks

In this thesis, we take an in-depth look at three practical healthcare problems focusing on humanitarian relief operations. All three chapters of the thesis make a modelling contribution to the healthcare and humanitarian relief operations research analytics community. Also, the models and numerical results have the potential to impact health and emergency practice by informing policy and patient care-related decisions. We use various analytical tools to solve these three practical problems using prescriptive methods such as linear program, mixed integer program, simulation, Markov decision process, Approximate Dynamic Programming, and multi-criteria decision analysis.

The coordination of relief logistics networks through vertical and horizontal resource sharing forms in a centralized structure is crucial for achieving a timely and cost-effective supply of short shelflife blood-derived platelets to the affected people in times of disasters. By developing, implementing and utilizing advanced analytics methodologies, the first topic in the thesis provides a robust integrated model for coordinating the relief entities for efficient distribution of blood-derived platelets of multiple types to the injured people with different urgency levels, particularly under multiple sources of uncertainty such as demand uncertainty. Such a model could be used in practice to significantly reduce shortage and wastage levels of perishable relief resources for health care services in emergencies and thus potentially decrease the impact of such shortage and wastage on patients' health. This research has the potential to provide valuable insights into the logistics planning in pre/post disaster operations for relief entities with independent resources and operations in a decentralized decision-making structure. Thus, it can help administrators make crucial decisions that will ensure timely access to perishable resources for patients and more cost-effective care delivery for health care and relief organizations.

The second topic provides a flexible robust approach to transportation decisions of a patient with different injury levels. Such a model ensures a full coordinated evacuation of the injured people from different evacuation assembly points to multiple medical centres under limited time windows and multiple sources of uncertainty. By applying various integration mechanisms for coordinating the evacuation assembly points and medical centres, such a model could be used in practice to reduce the total evacuation response time significantly. Applying this model could utilize fewer paramedic vehicles and increase the number of transferred injured people by sending the patients of specific injury levels to the most relevant medical centres.

The last topic provides a dynamic model for managing and controlling the casualty flow and the amount of capacity utilization of hospitals under a finite-time horizon and multiple sources of uncertainties. Such a dynamic model could be used in practice to reduce the overutilization of paramedic vehicles and the capacity of each hospital which ultimately result in a significant decline in the number of patients waiting at the MCI site and hospitals. This research also can provide valuable insights for relief organizations to coordinate their transportation fleet and share resources or patients between themselves in a dynamic fashion.

The practical challenges we faced when modelling and solving the three abovementioned problems were inevitable parts of any study. The most challenging part was how and from where to obtain the valid data for a real-case study, as the DROs'data are classified as very sensitive data in many organizations, particularly when the patient's information, such as the number of injuries of different types, are required. Another practical challenge for each research topic was implementing a new modelling approach different from each other. Compared to the first topic, in which we developed an optimization model in a multi-objective mixed integer programming model, the last chapter was modelled differently using a complicated MDP approach and solved using an approximate linear programming method. One of the other most important challenges for the studied topics was the tactical and operational decision-making structures. For instance, the decision was made at the tactical level for the first topic. In contrast, for the wildfire evacuation topic, the second topic, a detailed operational decision-making structure concerning the routing of paramedic vehicles, was employed. Last but not least, developing different complicated algorithms to solve the model for each topic was highly challenging. The algorithms used for three topics ranged from exact, meta-heuristics, and heuristics algorithms for the first, second, and last chapters. Matching the structure of existing algorithms and revising them to fit into each topic's modelling structure was a very demanding task, particularly for each topic with a different context, decision-making level, problem sizes, etc.